STRUCTURAL STUDIES OF SOME SILYL AND GERMYL ACETYLENES

by

Anthony R. Green

A Thesis presented for the Degree of Doctor of Philosophy,
University of Edinburgh, September 1976.

To My Parents

This dissertation has not been submitted, in whole or in any part, for any degree at this or any other University. As far as I am aware, this research is original and my own work; when this is not so, credit has been given.

Anthony R. Green.

Acknowledgements

I am most grateful to all those who have helped me in the course of this work. In particular, I would like to thank my supervisor, Professor E.A.V. Ebsworth, for his continual help and encouragement over the three years.

I would also like to thank Dr S. Cradock for recording the photoelectron spectra and for his invaluable assistance in the analysis of the infra red and p.e. spectra. My thanks also to Dr D.W.H. Rankin for recording the electron diffraction data and for his assistance in the refining processes.

In addition I would like to thank Dr A.J. Hinchcliffe for his help with matrix isolation techniques, Dr A. Lane at the University of Glasgow for recording some of the raman spectra, and the University of Manchester Institute of Science and Technology for the use of the gas diffraction apparatus.

I would also like to thank the Science Research Council for my support grant and the University of Edinburgh for provision of laboratory facilities.

Finally, I would like to thank my wife, Joyce, for photographing some spectra, for typing the tables and for her continual help and encouragement during the past few years and to Janet Carbone for typing the script.

Summary

This dissertation is concerned with the applications of infra red, photoelectron, ultra violet spectroscopy and electron diffraction techniques to the investigation of the structures of some silyl and germyl acetylenes.

Chapter 1 is concerned with the preparation and characterization of the acetylenes MH_3CCX where M = Si, Ge and X = Cl, Br, MH_3, CF_3.

Chapter 2 is concerned with the He I photoelectron spectra of MH_3CCX when M = Si, Ge and X = H, Cl, Br, MH_3. These spectra are compared and discussed in relation to their ultra violet spectra and with respect to the halogen and group IV elements present.

Chapter 3 is concerned with the electron diffraction studies of silyl chloro-, germyl chloro-acetylenes, disilyl and digermyl acetylenes. Their structures are discussed with respect to microwave and electron diffraction studies of related compounds. The limitations of microwave and electron diffraction studies are also discussed.

Chapter 4 is concerned with the assignment of the infra red and raman spectra of MH_3CCX when M = Si, Ge and X = Cl, Br, MH_3 and CF_3. The infra red and raman spectra of silyl and germyl perfluoromethyl acetylenes are reassigned with the aid of the spectra of the fully deuterated compounds.

Chapter 5 is concerned with the theory of rotation-vibration interaction, with respect to the infra red spectra, of symmetric top molecules. The effect of coriolis coupling and centrifugal distortion on the rotational spectrum of a rigid rotor is discussed. The effect of free internal rotation in a symmetric top molecule is also discussed.

Chapter 6 is concerned with the analysis of perpendicular bands of the symmetric top molecules, MH_3CCX when M = Si, Ge and X = Cl, Br, MH_3, CF_3. Several perturbations are analysed and explained in terms of Fermi and coriolis rotational interactions. The structures and zeta constants are compared with those of other acetylenes.

Contents

Page

INTRODUCTION

Introduction

The explanation for all chemical phenomena lies in molecular structure and geometry. In the 18th and 19th centuries, molecules were found to have definite compositions, which led to theories of structure and bonding. Classical analysis and intuition slowly built up a picture of structures within molecules; for example, concepts of tetrahedral carbon atoms and the ring structure of aromatic compounds.

At the turn of this century, advances in physics, together with the realisation of quantum effects by such people as Plank, Bohr and Rutherford paved the way for the development of quantum mechanics by Schroedinger, Dirac and Born in the 1920's. These developments have shown how molecular geometry and bonding are related. Since that time many rapid spectroscopic and diffraction methods have become available to the modern chemist for the elucidation of molecular structure; among these are infra red, raman and photo-electron spectroscopy and electron diffraction.

Low resolution infra red spectra often act as "finger-prints" for particular functional groups and, with the help of raman spectra, can identify the symmetry of small molecules. For example, carbon tetrachloride has only two active infra red bands, but three active raman bands, suggesting the tetrahedral nature of this molecule. In a similar way, the point group of a particular molecule can often be established from vibrational spectra.

Medium resolution infra red and raman spectra reveal band shapes which can indicate whether the molecule is linear, a symmetric top, a

spherical top or an asymmetric top. At sufficiently high resolution and under favourable circumstances, a band can be resolved into a number of components. Analysis of these bands yields information concerning the moments of inertia within the molecule and the way in which they change from vibration to vibration.

Force constant calculations can be made, using the observed vibrational frequencies, to determine the contribution of each "equivalent atom pair" vibration in a particular normal vibration. In favourable circumstances, anharmonicities and coriolis constants can also be calculated.

Electron diffraction is a good method for determining the distances between atoms within a molecule. The molecular parameters so derived, unlike those obtained from infra red data, are averaged over all populated vibrational states within the molecule. Comparisons with data obtained from infra red or microwave spectroscopy give valuable information about changes in molecular structure between different vibrational states. In some circumstances information concerning the shape of vibronic potentials is obtained. For example, electron diffraction studies of silyl isocyanate suggested that there was a maximum in the potential well for the torsional vibration about the nitrogen atom even though there was no evidence for this occurring in the infra red isothiocyanate spectrum. The "shrinkage" effects occurring between the bonded and nonbonded distances can be studied in terms of the excited deformations present and the magnitude of amplitudes of vibration within the molecules.

Ultra violet photoelectron spectroscopy yields information about the electronic structure and the interactions between different atomic

orbitals present. Fine structure on the bands, when present, shows how the molecular geometry changes between the ground state and the molecular ion. Ultra violet spectra can sometimes show how the molecular geometry changes in excited states. Assignments of these spectra can be facilitated by a knowledge of the photoelectron spectra.

This dissertation is concerned with the applications of these techniques to the investigation of the structures of some silyl and germyl acetylenes. Before the work described here was started, silyl and germyl perfluoromethyl acetylene were prepared[1]. The structure of the silyl compound was determined by electron diffraction while tentative assignments of the infra red spectra of the two compounds were also given. Rotational fine structure was observed on three fundamental modes, suggesting that these molecules were free internal rotors. At this time the only similar compounds that had been reported were silyl acetylene[2], germyl acetylene[3], disilyl acetylene[4] and silyl methyl acetylene[5], of which the last two appeared to be internal rotors. Although the infra red spectrum of disilyl acetylene had been reported the rotational fine structure had not been studied in detail and so no structural information was available for direct comparison with that of the other acetylenes.

In this work four novel acetylenes of type MH_3CCX where M = Si, Ge; X = halogen, MH_3 are synthesed and their rotational fine structure analysed to see whether internal rotation had any noticeable effect on the structure of the MH_3 group.

CHAPTER 1

Preparation and Characterization of Some Silyl and Germyl Acetylenes

1.1 Preparation of Silyl and Germyl Acetylenes

The mono[5], dihalo[6] acetylenes and the methyl halo-acetylenes[7] are all extremely well known. The majority of them are prepared in high yields by "halide exchange" with a suitable lithium salt[8] in ether or liquid ammonia. For example,

$$LiC \equiv C - X \xrightarrow{HY} LiY + HC \equiv CX$$

$$LiC \equiv C - X \xrightarrow{Y_2} LiY + YC \equiv CX$$

where X, Y are halogens. The latter solvent cannot be used with silyl or germyl compounds without destroying, sometimes violently, the M-H bonds. Ether can be used with these compounds, though its use as a bulk solvent does lead to difficulties in the separation of the products from the solvent.

The most suitable method for the preparation of these acetylenes involved evaporation of the solvent under reduced pressure before adding silyl or germyl halide to the lithium salt.

Preparation of silyl chloro-acetylene

Silyl chloro-acetylene was prepared by "halide exchange" above with lithium chloro-acetylene. The lithium salt was prepared in the absence of air and water by allowing methyl lithium to react with cis or trans dichloroethylene in an ether medium.

$$2\ LiMe + C_2H_2Cl_2 \xrightarrow{Et_2O} LiCl + LiC \equiv C - Cl + 2\ MeH$$

Addition of silyl halide yielded the product

$$LiC \equiv C - Cl + SiH_3Br \rightarrow LiBr + SiH_3C \equiv C - Cl$$

In a typical experiment, methyl lithium (12 m moles) in ether solution, was placed in a greaseless tap ampoule. Dichloroethylene (6 m moles) was condensed into the ampoule and the mixture warmed to room temperature. Effervescence was immediate and rapid. The methane produced and the ether were taken from the mixture after effervescence had ceased, leaving a white solid residue. The vessel was "pumped" under vacuum for about an hour to remove the majority of the residual ether.

Silyl bromide (6 m moles) was then condensed into the vessel and allowed to vapourise. After five minutes the volatile products were removed to a liquid nitrogen trap.

The products were passed through a trap held at -120^{o}C into a trap cooled by liquid nitrogen. Silane ($\simeq$ 1 m mole) condensed in the liquid nitrogen trap. The contents of the -120^{o}C trap were fractionated through a -96^{o}C trap. The required product, together with a trace of ether, condensed at this temperature while the major byproduct, chloro-acetylene, passed through. The trace of ether could not be removed efficiently from the silyl chloro-acetylene by fractional condensation.

Boron trifluoride did not react with silyl chloro-acetylene although it is known to form a complex of relatively low volatility with ether. An excess of boron trifluoride was added to the impure silyl chloro-acetylene using the apparatus shown in figure 1.1. Boron trifluoride was condensed into bulb A. Tap C was closed and the contents of A allowed to evaporate. The sample of silyl chloro-acetylene was condensed into bulb B and allowed to warm. Tap C was opened and closed with care until the pressures in A and B were

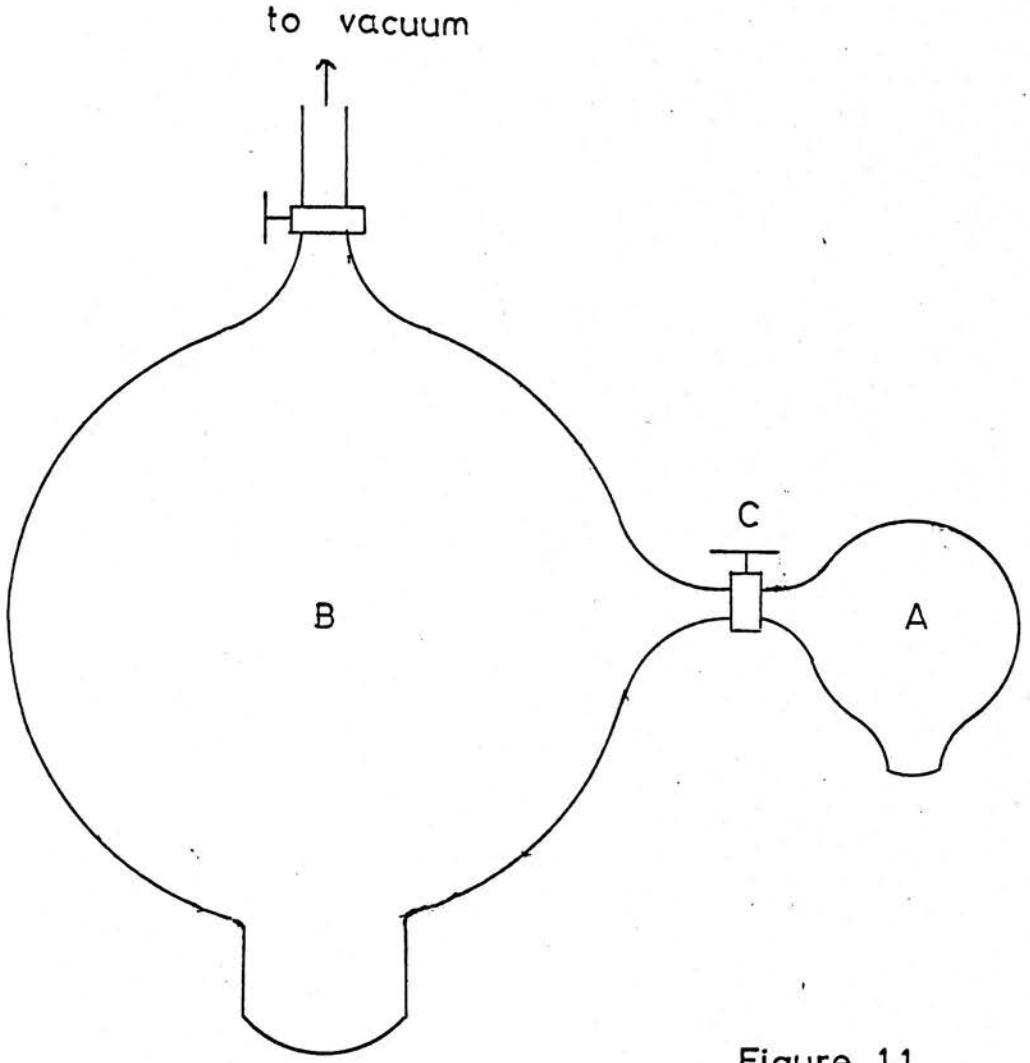

Figure 1.1

the same. The mixture was left to equilibrate for fifteen minutes.

The products were removed to a liquid nitrogen trap and then fractionated through a -45°C trap. The ether-BF_3 complex condensed at this temperature; excess of boron trifluoride and the silyl chloro-acetylene passed through. Fractionation at -120°C removed the boron trifluoride from the silyl chloro-acetylene.

Silyl chloro-acetylene (4.1 m moles) was obtained from the above method. The yield, based on the quantity of silyl halide added, varied from 60% to 70%.

It was discovered that silyl chloride and silyl fluoride could also be used to prepare this acetylene. The deuterated species was made in a similar manner using deuterated silyl bromide.

Preparation of germyl chloro-acetylene

Germyl chloro-acetylene was prepared by the same method as that described for silyl chloro-acetylene.

In a typical reaction, methyl lithium (10 m moles) was allowed to react with dichloroethylene (5 m moles) in ether solution. The ether and methane produced were removed from the reaction mixture after effervescence had ceased and the residue was "pumped" under vacuum for about an hour. Germyl chloride (5 m moles) was condensed into the reaction vessel and allowed to react for five minutes, before the products were condensed into the trap cooled by liquid nitrogen. The products were fractionated at -120°C and -96°C. The sample, in a trap held at -96°C, was "pumped" under vacuum for three hours to remove the remaining ether. The sample was then fractionated at -46°C to remove some involatile impurities.

Germyl chloro-acetylene (3 m moles) was obtained. The yield,

based on the quantity of germyl halide used, varied from 50%-60%.

Preparation of disilyl acetylene

Disilyl acetylene was prepared from dilithium acetylene although it has been prepared previously by halide exchange with the magnesium grinard[4]. The reaction of tetra-bromo ethane with a threefold excess of methyl lithium at -40°C did not give the expected product, lithium bromo-acetylene, but a mixture of dilithium and monolithium acetylene.

$$HBr_2CCBr_2H + LiMe \xrightarrow{Et_2O} LiBr + Br_2C = CBrH + MeH$$

$$Br_2CCBrH + LiMe \xrightarrow{Et_2O} LiBr + BrC \equiv CH + MeH$$

$$BrC \equiv CH + LiMe \begin{cases} \nearrow & LiCCH + MeBr \\ \not\searrow & LiCCBr + MeH \end{cases}$$

$$LiCCH + LiMe \xrightarrow{Et_2O} LiCCLi.$$

Clearly the relative strength of the $(C \equiv C) - X$, $CH_3 - X$, $(C \equiv C) - H$ and $CH_3 - H$ bonds play an important role in deciding which reaction course is followed.

This reaction scheme was modified, by using a fourfold excess of methyl lithium, to give a maximum yield of disilyl acetylene.

In a typical reaction methyl lithium (20 m moles) was allowed to react with tetra-bromo ethane (5 m moles) at room temperature in an ether medium. The ether and gaseous products were removed under

reduced pressure after completion of the reaction. The remaining solid was "pumped" under vacuum for about an hour. Silyl bromide (10 m moles) was condensed into the vessel and allowed to react for five minutes. The products were removed to a trap cooled by liquid nitrogen and then fractionated at -120°C. Silane and silyl acetylene passed through the trap at -120°C. The remaining ether was removed by continuously "pumping" the sample for several hours while it was held at -78°C.

Disilyl acetylene (3.5 m moles) was produced. The yield, based on the quantity of silyl halid added, varied from 63% to 70%.

Preparation of digermyl acetylene

Digermyl acetylene was prepared in an analogous manner. In a typical experiment methyl lithium (15 m moles) and tetra-bromo ethane (3.7 m moles) were allowed to react together at room temperature. The ether and gaseous products were removed after completion of the reaction. Germyl chloride (6.2 m moles) was added to the solid and reacted for five minutes. The products were removed to a trap cooled by liquid nitrogen, and then fractionated through a trap at -64°C. The required product, digermyl acetylene, condensed at this temperature but any remaining ether or starting material in the sample passed into a liquid nitrogen trap.

Digermyl acetylene (1.6 m moles) was obtained. The yield, based on the quantity of germyl halide reacted, varied between 45% and 50%.

Preparation of silyl bromo-acetylene

The attempted preparation of lithium bromo-acetylene from methyl lithium and tetra-bromo ethane was not successful. The sodium salt

was prepared, in an attempt to make silyl bromo-acetylene, by dissolving sodium in liquid ammonia and then treating this solution with dibromoethylene at -64°C until the blue colouration had been discharged. The ammonia was removed under vacuum and the salt was left under vacuum for several hours to ensure that the last traces of ammonia had been removed. Extreme care was needed in handling the dried salt because shock of any sort could cause detonation of the solid.

Silyl fluoride was carefully added to this salt and then left to react for a few minutes. The products were removed and fractionated at -120°C to remove any silane that had been produced. Fractionation at -96°C separated some disiloxane impurity from the sample of silyl bromo-acetylene. Silyl bromo-acetylene was purified by "pumping" on the sample, while it was held at -78°C, for several hours to remove bromo-acetylene. The reactions involved in this system are set out below.

$$Na + NH_3 \xrightarrow[NH_3]{liq} NaNH_2$$

$$NaNH_2 + HBrCCBrH \xrightarrow[NH_3]{liq} HCCBr + NaBr$$

$$HCCBr + NaNH_2 \xrightarrow[NH_3]{liq} NaCCBr + NH_3$$

$$NaCCBr + SiH_3F \longrightarrow NaF + SiH_3CCBr.$$

Silyl bromo-acetylene was not produced when silyl bromide was reacted instead of silyl fluoride: slight decomposition of silyl bromide was the only reaction.

Preparation of silyl perfluoromethyl acetylene

Silyl perfluoromethyl acetylene was prepared using the same method described by Anderson[1] in which silyl halide was exchanged with the perfluoromethyl acetylene grinard reagent.

In a typical experiment, magnesium (0.3 gm) was allowed to react with methyl iodide (1.2 mls) in an an ether solution for two hours. Perfluoromethyl acetylene (10 m moles) was condensed into the reaction vessel and reacted until effervescence ceased. The solvent and excess of starting materials were removed under reduced pressure. Silyl bromide (10 m moles) was condensed into the reaction vessel after the solid had been dried under vacuum. The reaction was stopped after 10 minutes by condensing the volatile contents of the vessel into a trap cooled by liquid nitrogen. If the reaction was left too long, the quantity of silyl product tended to decrease. The products were fractionated through a trap at -130°C to remove silane and perfluoromethyl acetylene. Fractionation at -120°C removed any remaining ether and unreacted silyl bromide from the required product. The yield varied from 40% to 50% based on the quantity of silyl bromide added. The deuterated analogue was prepared in a similar manner using deuterated silyl bromide.

Preparation of germyl perfluoromethyl acetylene

Germyl perfluoromethyl acetylene was prepared using the same method as described for the preparation of silyl perfluoromethyl

acetylene. Germyl chloride was used as the exchange agent, deutero germyl chloride being used to prepare the deuterated acetylene.

1.2 Mass Spectra of Silyl and Germyl Acetylenes

The mass spectra of the two perfluoromethyl acetylenes have been described elsewhere[1]. The mass spectra of the other acetylenes were obtained although a complete breakdown pattern could not be given due to the presence of inseparable impurities. The mass spectra did show, however, consistent breakdown patterns for the two series of compounds. For example, a range of peaks was observed which corresponded to proton loss from the parent ion.

Mass spectra of the silyl and germyl halo acetylenes

The major breakdown path appeared to be loss of halogen followed by cleavage of the M-C single bond

$$MH_n\ C \equiv C - X^+ \rightarrow MH_n\ C \equiv C^+ \rightarrow MH_n^+$$

The other route involved the production of a metastable ion with the formation of the group IV halide.

$$MH_n\ C \equiv C - X^+ \rightarrow C_2 + MH_nX^+$$

The base peak in silyl chloro-acetylene was at mass number 63. This peak together with another half as intense at mass number 65 corresponded to a chlorine isotopic pattern. These lines could therefore be attributed to the species $SiCl^+$. The $^{35}Cl, ^{37}Cl$ isotopic pattern is also evident at mass numbers 89, 91 and 90,92;

Table I.I Accurate Masses Of Some Silyl and Germyl Acetylenes

Species	Mass Observed	Mass Calculated	Error
$^{28}SiH_2C_2{}^{35}Cl^+$	88.96I575	88.96I43I	2p.p.m.
$^{28}SiH_2C_2{}^{37}Cl^+$	90.958755	90.958482	3p.p.m.
$^{28}SiH_2C_2{}^{8I}Br^+$	I34.908802	I34.908998	2p.p.m.
$^{74}GeH_2C_2{}^{35}Cl^+$	I34.905527	I34.905702	2p.p.m.
$^{73}GeH_3C_2{}^{35}Cl^+$	I34.888236	I34.887I04	9p.p.m.
$^{74}GeC_2{}^{37}Cl^+$	I34.9I5089	I34.9I5726	5p.p.m.
$^{28}Si_2H_4C_2{}^+$	83.9853I0	83.985I56	2p.p.m.
$^{72}Ge^{74}GeHC_2{}^+$	I70.852095	I70.850725	8p.p.m.[a]
$^{74}Ge^{70}GeH_3C_2{}^+$	I70.868780	I70.868974	Ip.p.m.
$^{72}Ge^{70}GeH_5C_2{}^+$	I70.884979	I70.885I23	Ip.p.m.
$^{70}Ge^{76}Ge^+$	I45.845I30	I45.845700	4p.p.m.
$^{72}Ge^{72}GeH_2{}^+$	I45.859429	I45.859050	3p.p.m.

a Peak was not properly resolved.

the former pair was 95% of the height of the base peak and the latter pair 30%.

Reduction of the ionizing voltage from 70 eV to 12 eV moved the base peak to mass 90. This observation is consistent with the parent ion being SiH_3CCCl^+ which readily loses a hydrogen atom at higher ionizing voltages.

The base peak in the mass spectrum of silyl bromo-acetylene is at mass number 53 corresponding to the species $SiHCC^+$. A bromine isotopic pattern is observed with two sets of peaks at mass numbers 133, 135 and 134,136 respectively. The peak at 134 mass units was 95% of the base peak height. The two sets of peaks could be attributed to the species $SiH_2C_2Br^+$ and $SiH_3C_2Br^+$ respectively.

A similar isotopic pattern was observed at mass numbers 108, 110 and 107,109 corresponding to the species SiH_3Br^+ and $SiH_2{}^+Br$ respectively.

The base peak in the mass spectrum of germyl chloro-acetylene occurred at mass number 135 in the midst of a series of lines extending from mass number 131 to 138. This series of lines corresponds to the ions of $GeH_nC_2Cl^+$ where n = 0, 1, 2, 3. Another peak similar in intensity to the base peak occurred at mass number 109, in the midst of a 'GeCl' isotopic pattern. This series of lines could be attributed to the ions GeH_nCl^+. The germanium isotopic pattern was observed at mass numbers 95 to 101 and can be attributed to the ions $GeH_nC_2^+$.

Accurate masses were measured for selected peaks of each compound. The results are tabulated in table 1.1.

Mass spectra of disilyl and digermyl acetylene

One breakdown route was cleavage of a M-C bond

$$MH_nC_2MH_m^+ \rightarrow MH_nC_2^+$$

A second route must occur involving a metastable ion leading to the formation of a M-M bond

$$MH_nC_2MH_m^+ \rightarrow MH_nHM_m^+$$

The base peak in disilyl acetylene occurred at mass number 84: one of a number of peaks over the range m/e 80 to 86 corresponding to the series of ions $SiH_nC_2SiH_m^+$. Another series of peaks at mass numbers 53-55 corresponding to the ions $SiH_nC_2^+$ was observed. Two peaks at 58 and 60 mass units respectively could be due to the species $Si_2H_2^+$ and $Si_2H_4^+$.

Peaks between mass numbers 167 and 178 were observed in the spectrum of digermyl acetylene. These corresponded to the species $GeH_nC_2GeH_m^+$.

A similar pattern was observed between mass numbers 142 and 150 which corresponded to the ions $Ge_2H_n^+$, n = 1, 2, . . . , 6. The germanium isotopic pattern occurred between mass numbers 95 and 101 corresponding to the ions $GeH_nC_2^+$.

Accurate mass measurements on selected peaks of both compounds are included in table 1.1. The presence of the ions of type $Ge_2H_n^+$ was confirmed by accurate mass measurements.

1.3 Vapour Pressures, Boiling and Melting Points

The vapour pressure of silyl chloro-acetylene was measured over the temperature range 210 to 280K. The temperature range used for

silyl bromo-, germyl chloro- and digermyl acetylene was 220 to 280K. The vapour pressure data gave a linear relationship with slope a and intercept b when $\log_{10}P$ was plotted against $\frac{1}{T}$, where P is the vapour pressure and T is the temperature in degrees Kelvin. These graphs are shown in figure 1.2. Extrapolation of each graph to atmospheric pressure gave an estimate of the boiling points of each compound.

The values of a and b found, the estimated boiling points and measured melting points are tabulated in table 1.2.

The vapour pressure curve of digermyl acetylene deviates from the linear relationship at high temperature. Measurement of the mass of compound recovered and examination of the apparatus after completing the vapour pressure determination showed that considerable polymerisation had occurred.

The melting points of all the compounds were measured using the "slip point" method. The material was condensed halfway along a vertical glass tube. A glass indicator that would just slide along this tube was rested on the solid compound. A bath whose temperature was lower than the melting point was placed around the vertical tube. As the "slip point" of the solid is reached, the indicator falls to the bottom of the tube: this temperature is recorded as the melting point of the solid. Several observations were necessary for one compound so that consistent results were obtained. Inspection after 30 seconds showed whether the sample melted sharply or not.

Disilyl acetylene had been prepared previously[4] and vapour pressure data was available from the literature. Two vapour pressures of the sample were measured at widely spaced temperatures

Table 1.2. Vapour Pressure Constants, Melting and Boiling Points and Molecular Weights

Compound	a[a]	b[a]	B.P. (°C)	M.P. (°C)	M. Wt.
SiH_3CCCl	-1645	8.263	32	-86	90±3
SiH_3CCBr	-1763	8.194	59	-39	135±3
GeH_3CCCl	-1761	8.232	56	-156	139±4
GeH_3CCGeH_3	-1824	8.078	78	-18	173±5
SiH_3CCSiH_3[b]	-1434	7.417	43	-59	90±3

	$P_{obs.}$	$T_{obs.}$	$T_{calc.}$
SiH_3CCSiH_3	11.0	229.7K	224.9K
	57.0	256.5K	253.4K

a. From $\log_{10} P = \frac{a}{T} + b$.

b. Values from reference 4.

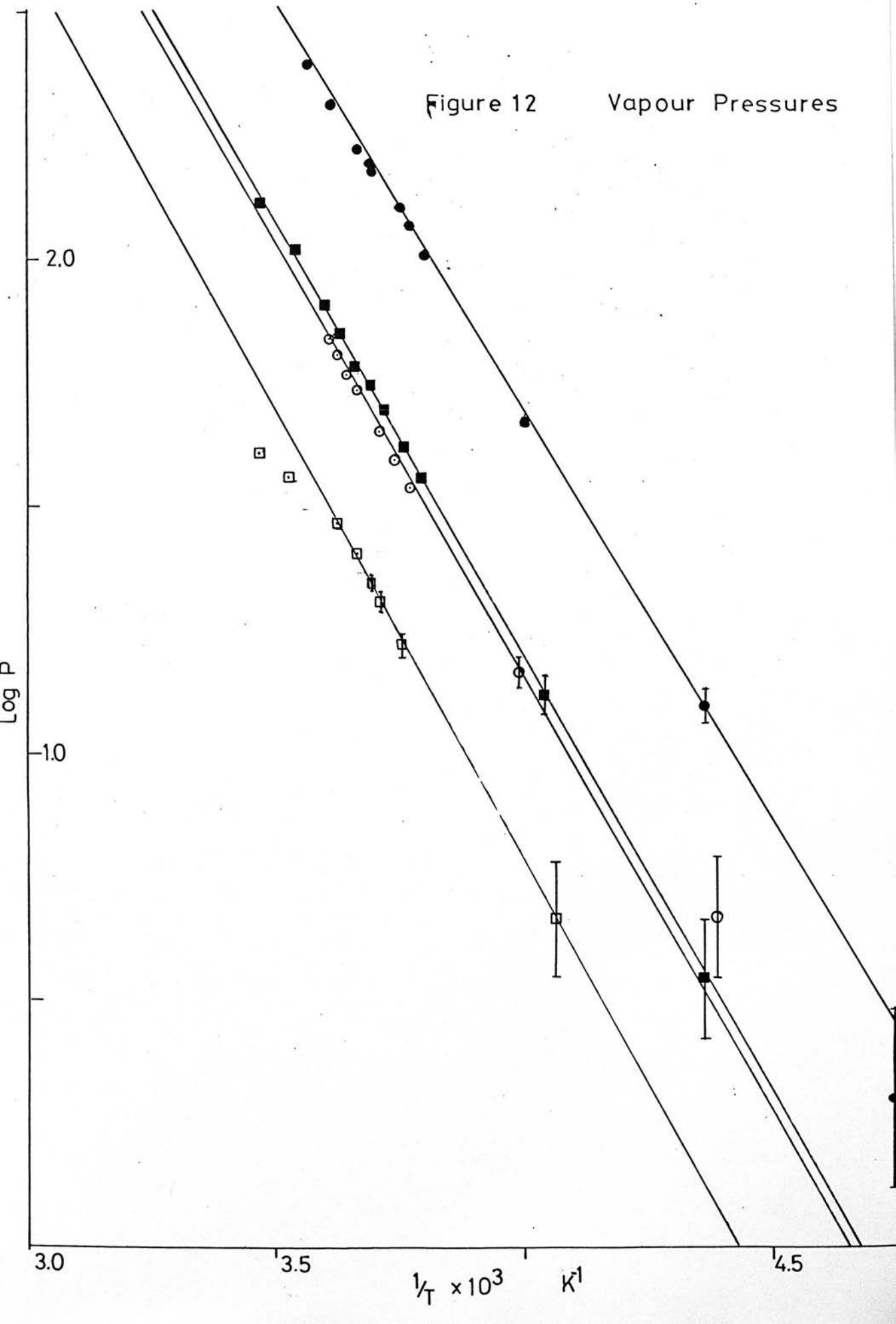
Figure 12 Vapour Pressures
2.0
1.0
Log P
3.0
3.5
4.5
1/T x10^3 K^-1

and compared with the literature values. The calculated temperatures are in close agreement: a 1% error in the intercept value b quoted leads to about a 3 degree error on the calculated temperature.

The molecular weights of the compounds were checked by weighing a known pressure of gas in a small bulb of known volume. The molecular weights determined are given in table 1.2. The estimated molecular weights of the pure gases are all within the experimental errors.

1.4 N.m.r. Spectra of Some Silyl and Germyl Acetylenes

The ^{1}H n.m.r. spectra of silyl chloro- and bromo-acetylenes, germyl chloro-acetylene and disilyl acetylene were recorded in either T.M.S. or chloroform solutions.

The spectra of three silyl compounds consisted of a singlet with ^{29}Si satellites. That of germyl chloro-acetylene consisted of a singlet.

^{13}C spectra were recorded on a Fourier Transform spectrometer but, due to very long relaxation times and relatively weak solutions, peaks were only observed in the case of silyl bromo-acetylene. In this spectrum, two peaks were observed: one for each carbon atom.

The n.m.r. parameters of these compounds are given in table 1.3. All p.p.m. were measured relative to T.M.S.

Table 1.3. N.M.R. Parameters

Compound	Solvent	$\tau(H_m)$ (±0.02)	$\delta(^{13}C)$ ppm(±0.1)	$^1J(Si-H)$ Hz(±1)
SiH_3CCCl	TMS	6.18		217
SiH_3CCBr	$CDCl_3$	6.10	6.62,74.95	220
SiH_3CCSiH_3	TMS	6.19		216
GeH_3CCCl	TMS	6.00		-
GeH_3CCGeH_3	$CDCl_3$	5.91		-

+ve ppm to high frequency of TMS.

CHAPTER 2

Photoelectron and Ultra-Violet Spectra of Some Silyl and Germyl Acetylenes

2.1 Photoelectron Spectra of Some Group IV Acetylenes

The photoelectron (p.e.) spectra of monohalo[9], dihalo[10], and silyl[11] acetylenes have been reported. The spectra have been assigned on the basis of linear combinations of bonding orbitals (l.c.b.o.) and using calculations involving semi-empirical methods such as complete neglect of differential overlap (CNDO) or intermediate neglect of differential overlap (INDO)[12,13].

The p.e. spectra of silyl chloro- and bromo-acetylenes, germyl chloro-acetylene, germyl, disilyl and digermyl acetylenes have been recorded. The spectrum of disilyl acetylene was reported in the literature during the course of this study. The spectrum has been included as it has similar features to the spectrum of digermyl acetylene.

The validity of Koopmans' theorem[14] is accepted throughout. Thus the observed ionization potential (i.p.) is equated with minus the corresponding molecular orbital energy.

2.2 P.e. Spectra of the Haloacetylenes MH_3CCX(M = Si,Ge; X = Cl, Br, H)

Basis set orbitals

The basis set molecular orbitals (m.o.'s) are formed from a combination of valence shell atomic orbitals (a.o.'s). These a.o.'s are of a_1 and e symmetry classes because these acetylenes belong to the C_{3V} point group. The a.o.'s are

M_{ns} a_1

M_{np} a_1 M_{np} e

H_{1s}	a_1	H_{1s}	e
C_{2s}	a_1		
C_{2p}	a_1	C_{2p}	e
$X_{n's}$	a_1		
$X_{n'p}$	a_1	$X_{n'p}$	e

The nine a_1 a.o.'s combine to give nine a_1 m.o.'s which can be represented as

$9a_1$ ⎤	
$8a_1$ ⎥	antibonding MH, MC, CC, CX
$7a_1$ ⎥	
$6a_1$ ⎦	
$5a_1$	MC/MH bonding (M_{np})
$4a_1$	CX bonding
$3a_1$	MC/MH bonding (M_{ns})
$2a_1$	CC bonding
$1a_1$	X_{ns} "lone pair"

The s a.o.'s tend to be of much higher energy than the p a.o.'s; this s/p separation dominates the a_1 bonding scheme.

The five e a.o.'s will combine to give five e m.o.'s which can be described as

5e, 4e	antibonding
3e	CC "π" bonding
2e	MH σ bonding
1e	$X_{n'p}$ "lone pairs"

There is strong evidence for extensive mixing of at least the 1e and 3e m.o.'s and it is likely that the 2e level interacts as well.

The highest levels that are expected to be occupied are $5a_1$ and 3e requiring 22 electrons (supplied as 7 from X, 4 from M, 4 from each of two C's and 1 from each of three H's). In the case of X being replaced by hydrogen, the levels corresponding to the $X_{n'p}$ atomic orbitals disappear so that the highest occupied levels are $4a_1$ and 2e.

Assignments of the p.e. spectra

The p.e. spectra of the three haloacetylenes are shown in figures 2.1 to 2.3, and that of germyl acetylene in 2.4. The ionization potentials of these and some related compounds are given in table 2.1.

Integrated band intensities for bands occurring below 15 eV can be used tentatively as a basis for assignment, although this is not always a safe guide if the m.o.'s in question are composed of different types of a.o.'s.

The p.e. spectrum of germyl acetylene consists of three bands below 18 eV. The first two bands are of roughly equal intensity. This would be expected if each corresponded with ionization from each of the two occupied m.o.'s of e symmetry; however, there is a

Table 2.1. Ionization Potentials of Acetylenes of Type MH_3CCX; M = Si, Ge; X = H, Cl, Br, MH_3

Band	M / X	Si			Ge		Band	Si	Ge
		H[a]	Cl	Br	H	Cl		SiH_3	GeH_3
3e (2e)[b]		10.73	10.22[c]	10.17[c]	10.61	10.19[c]	$2e_g$	10.48	10.13
$5a_1$ ($4a_1$)[b]		12.53	12.54[c]	12.52[c]	12.46[c]	12.45	$3a_{1g}$	12.54	12.1
2e (1e)[b]		13.05; 13.85	12.68; 13.2	13.18	12.87; 13.73	12.75	$1e_u$		
1e		-	13.92	13.8	-	13.83	$1e_g$	13.0	12.6
$4a_1$ ($3a_1$)[b]		17.4	17.2	16.36	17.2	17.10	$2a_{2u}$	14.53	14.03
$3a_1$ ($2a_1$)[b]		18.9	18.7	18.6	-	18.8	$2a_{1g}$	18.06	18.57
$2a_1$ ($1a_1$)[b]		20.4	20.4	19.2	-	19.2	$1a_{2u}$	19.1	19.23
$1a_1$		-	23.4[d]	20.3	-	20.1	$1a_{1g}$	-	20.4

a) reference 11.

b) levels in MH_3CCH.

c) fine structure observed on bands.

d) He II spectrum.

Figure 2.1 P.e. Spectrum of $SiH_3C{\equiv}CCl$

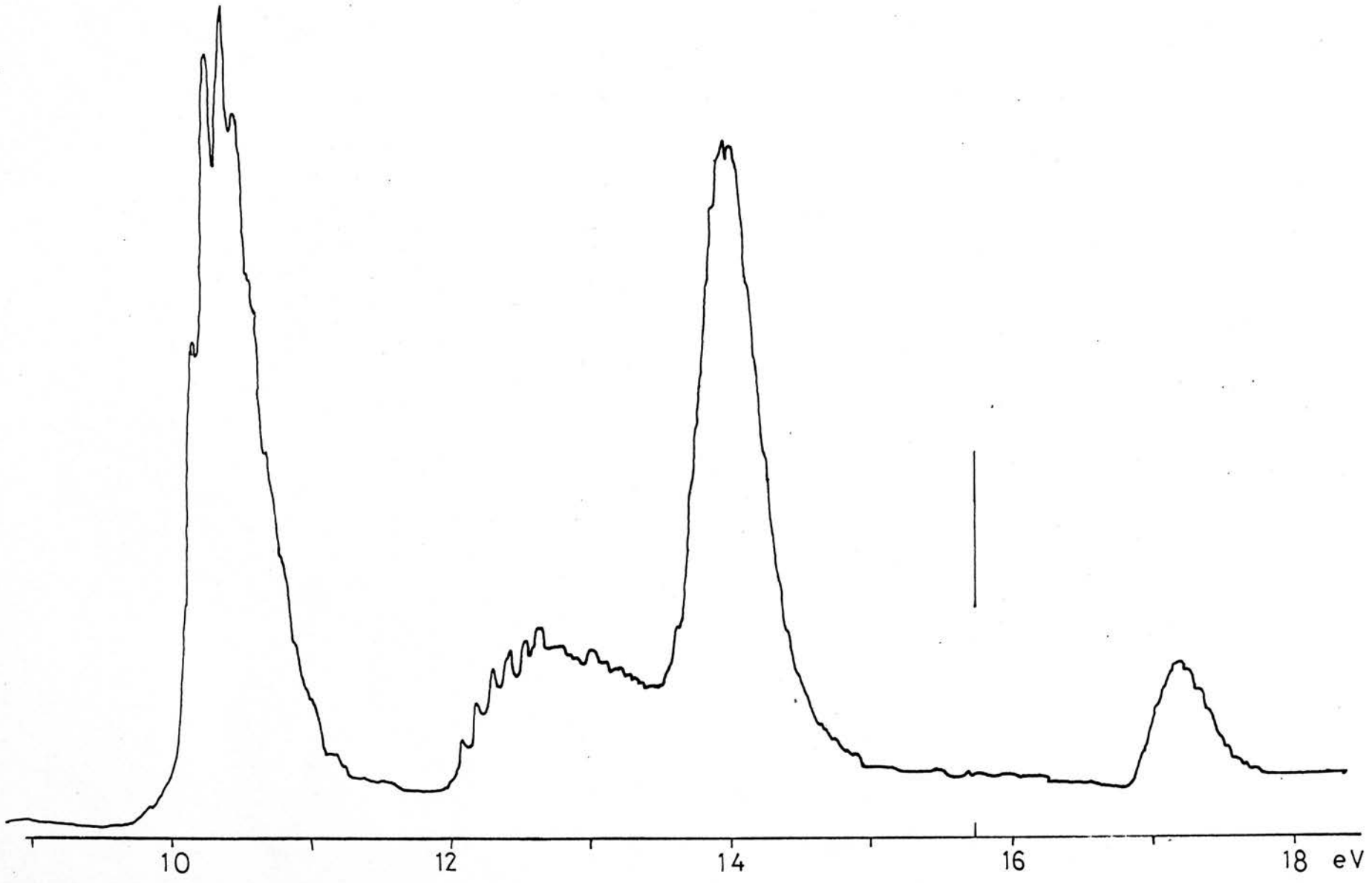

Figure 2.2 P.e. Spectrum of $SiH_3C{\equiv}CBr$

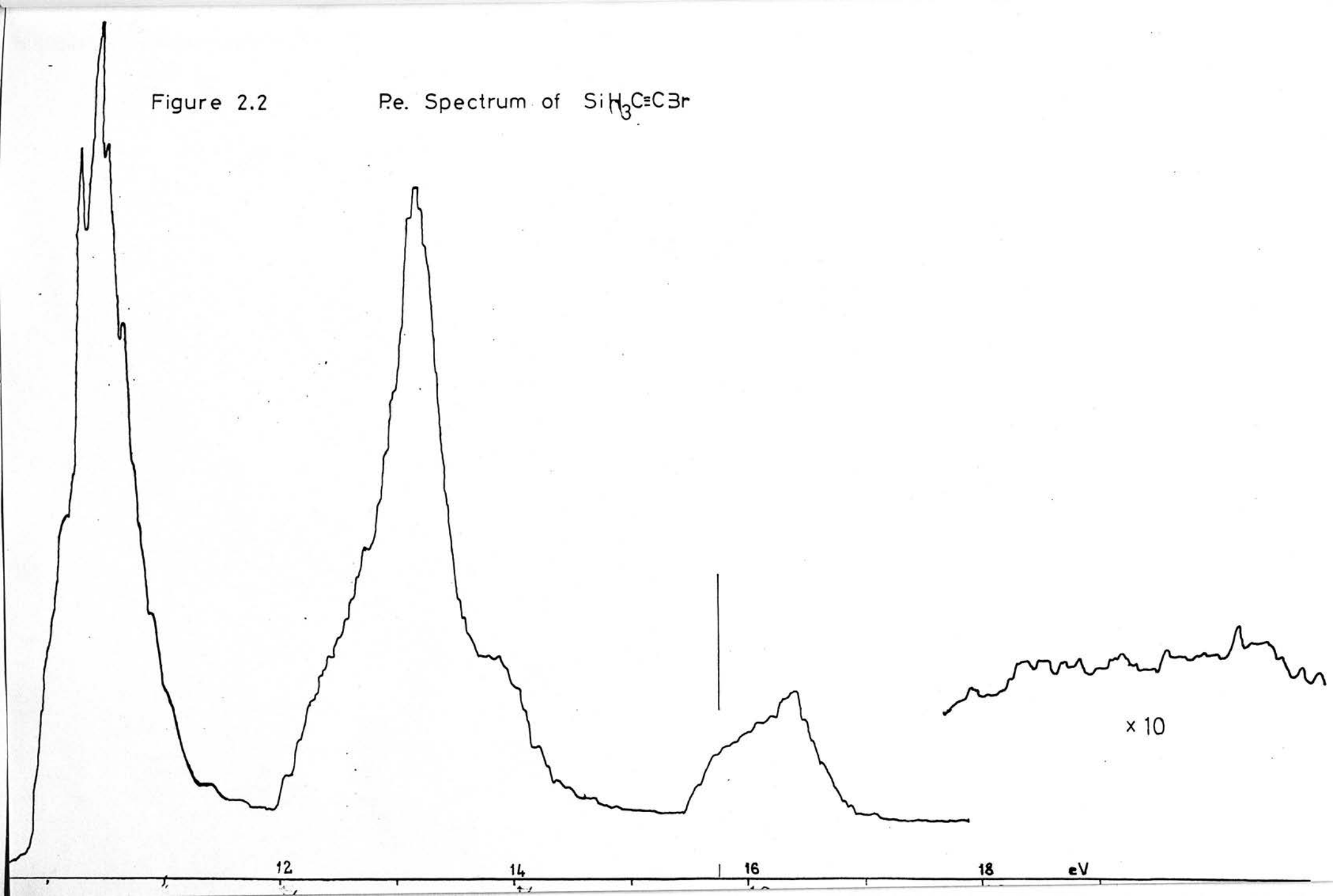

Figure 2.3 P.e. Spectrum of $GeH_3C{\equiv}CCl$

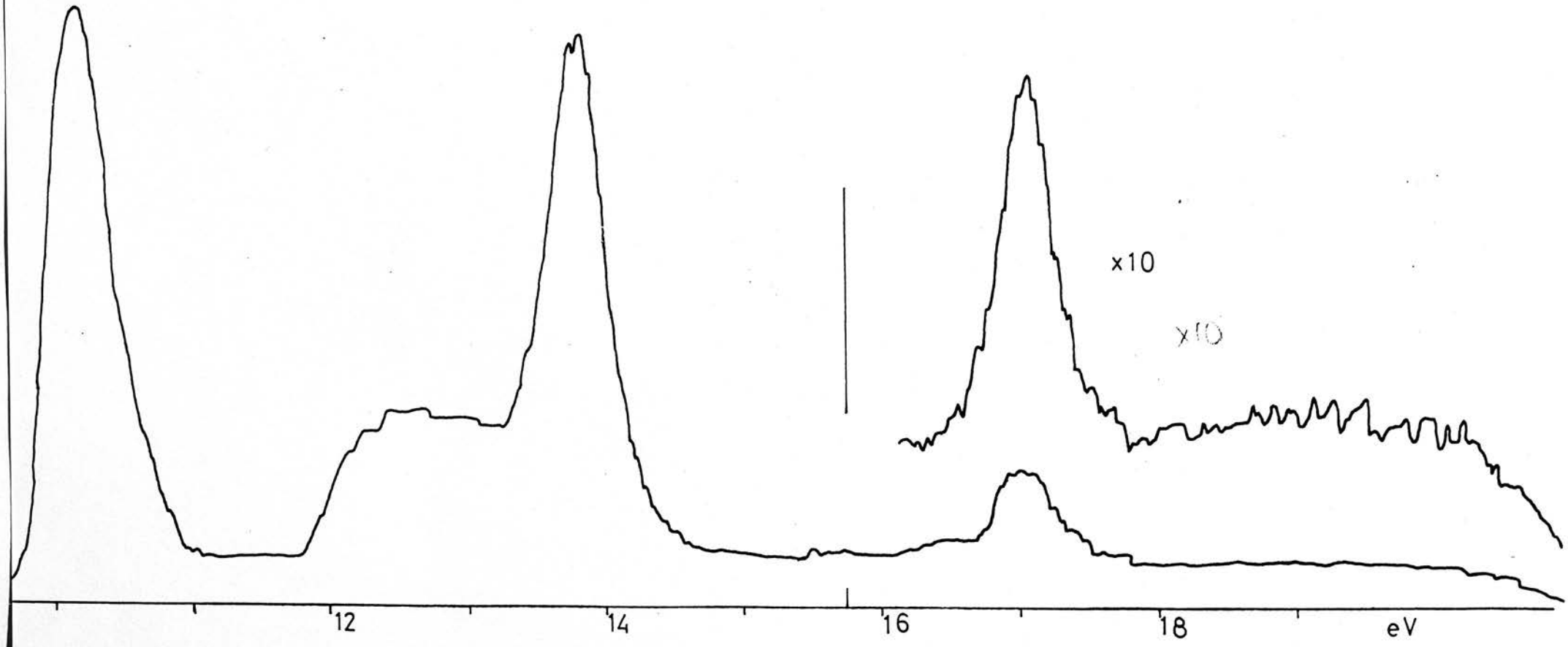

Figure 2.4 P.e. Spectrum of $GeH_3C{\equiv}CH$

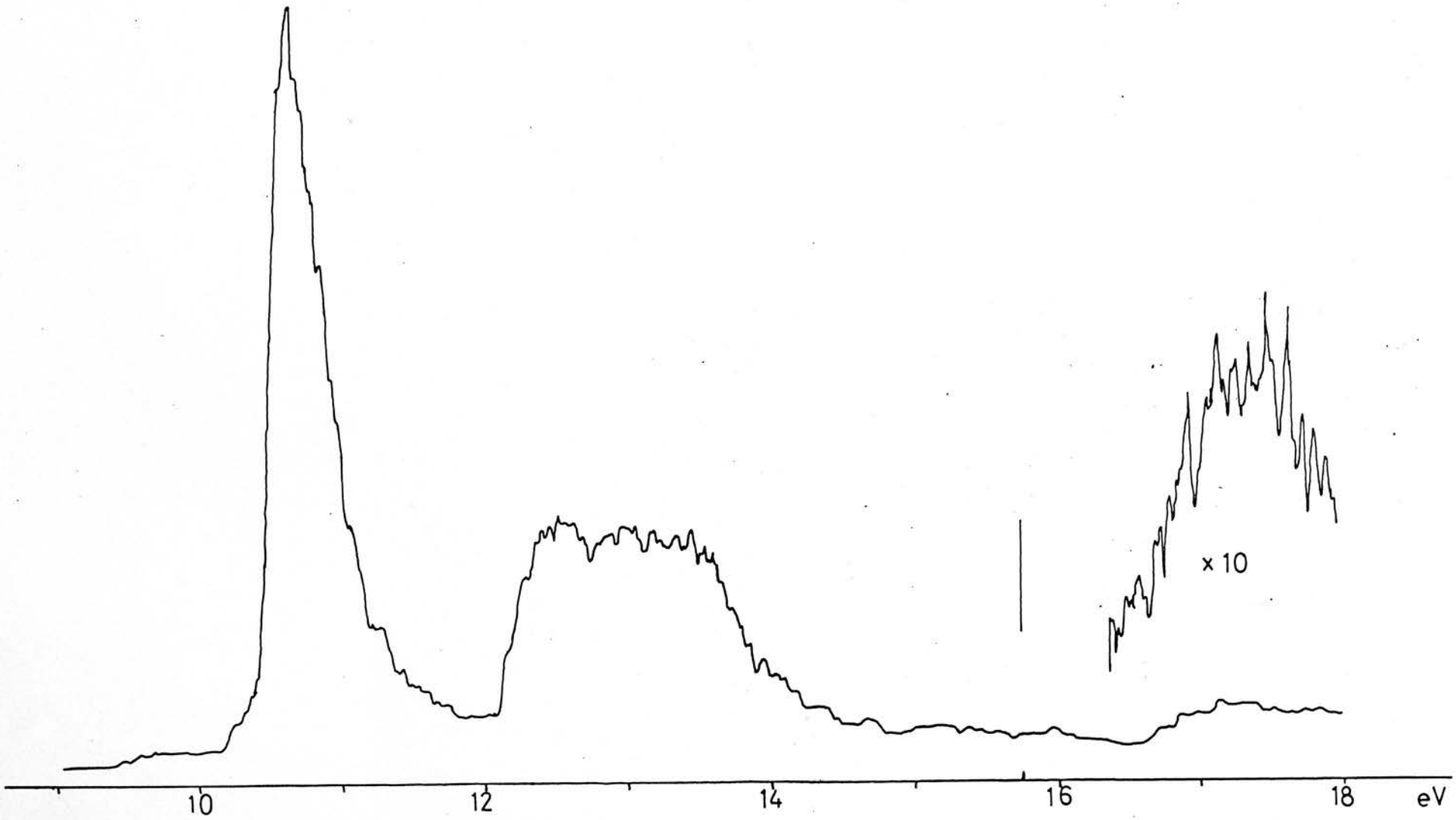

vibrational progression at the low i.p. end of the second band; implying that this band may cover ionization from the $4a_1$ as well as the 1e level. The first band (band I) will be the 2e m.o. which will be mainly of 'π' CC bonding character. The 1e m.o. occurring in the second band (band II) will be of σ_{GeH_3} bonding character. It is expected that Jahn-Teller distortion in the ion corresponding to this band will be comparable in size to that found in silyl and methyl acetylene[19]. Band II in fact has three distinct maxima: the first, being the top of the vibrational progression, is almost certainly the vertical i.p. associated with the $4a_1$ m.o.. This m.o. is mainly σ_{GeC} bonding; the vibrational spacing is consistent with this assignment. The second and third maxima can be assigned to the two Jahn-Teller components of the 1e m.o. The spacing between these levels is 0.60 eV, slightly smaller than that found in silyl and methyl acetylenes[1].

The third band (band III) at 17.2 eV will be the $3a_1$ m.o., of mainly σ_{CH} bonding character. The binding energy of this level is close to that of the equivalent level in both silyl and methyl acetylene.

The first three bands of the silyl and germyl haloacetylenes have intensity ratios between 2:3:2 and 2:2:2 (in the case of silyl bromo-acetylene the second two bands overlap, giving an intensity ratio of 2:5). This indicates the presence of the three e m.o.'s and one a_1 m.o. below 14 eV. The first band (3e) and third band (1e) in silyl and germyl chloro-acetylene are sharper and more intense than the second band (2e + $5a_1$) which is very broad. Band I will be mainly 'π' CC bonding and band III mainly the 'p_π' chlorine

lone pair although there will be extensive mixing between the two. The second band will consist of the e σ_{MH_3} orbitals. It is expected to be broad due to a large vibrational envelope and Jahn-Teller splitting. Another complication is due to the presence of the σ_{MC} bonding orbital ($^5a_1$) which is expected in this region. The Jahn-Teller splitting in silyl acetylene is very large for the e σ_{MH_3} band (0.8 eV) while for disilane it is about half this value. Since this effect is dependent on reduced mass, Jahn-Teller distortion is expected in the 2e m.o.'s of both silyl and germyl chloro-acetylene. Furthermore, it will be much stronger than any spin orbit coupling present (ΔE for spin orbit coupling in Si atoms is 0.019 eV[15]). The broad peaks with maxima at 12.7 eV and 13.2 eV in silyl chloro-acetylene could be assigned to the two Jahn-Teller components of 2e. No distinct maxima can be observed in the corresponding region of germyl chloro-acetylene. Vibrational structure on the beginning of band II is consistent with the $^4a_1$ levels being present. The maxima of this band occurs at about 12.5 eV in all three spectra.

The i.p.'s of the free chlorine and bromine atoms for the transitions $X(^2P_{3/2}) \rightarrow X^+(^3P_2) + e^-$ are I(Cl) = 13.01 eV and I(Br) = 11.84 eV. The shift to lower i.p. on going from chlorine to bromine should be, and indeed is, reflected in the p.e. spectra of silyl chloro- and bromo-acetylenes. The peak corresponding to the bromine p electron level occurs at 13.18 eV, in the midst of the 5 a_1 and 2e (e σ_{MH_3}) m.o.'s. The corresponding level in silyl chloro-acetylene is at 13.92 eV. The Jahn-Teller distortion of the 2e m.o. in silyl bromo-acetylene will be of the same order as that in silyl chloro-acetylene. The shoulder at 13.8 eV could be

one component of this level: the other coming under the 'pπ' bromine lone pair.

Bands at 17.2 eV and 17.1 eV in silyl and germyl chloro-acetylenes respectively can be attributed to the CX bonding ($4a_1$) m.o. The corresponding band in silyl bromo-acetylene is at 16.36 eV, a shift to lower i.p. of 0.8 eV. This is comparable to the change in energy of the 'pπ' m.o.'s of silyl chloro- and bromo-acetylenes, suggesting that this band also involves the p electron character of the halogens.

The a_1 σ_{SiH_3} level has been assigned to the band occurring at 17.5 eV in silyl acetylene on the basis of simple self consistent field calculations[11]. The band occurs at about 18 eV in the silyl halides[17] and silane[18]; silane being assigned on the basis of observed vibrational structure. It seems likely, however, that this band in silyl acetylene is mainly σ_{CH} bonding character because similar levels occur in both germyl and methyl acetylene. The band at 18.9 eV would then be mainly σ_{SiH_3} bonding character.

The bands occurring between 18.5 eV and 18.8 eV in the three haloacetylenes could be assigned to this a_1 m.o. The bands are too diffuse to see vibrational structure. Interaction with other orbitals would excite vibrations other than the expected MH stretching frequency and so cause broadening of the band.

The band at 20 eV in silyl acetylene has been assigned to the mainly σ_{CC} bonding level. Bands in this region occur in all three haloacetylenes. The band in silyl and germyl chloro-acetylenes are probably due to this bonding level because the chlorine 3s level is not expected below the limit of the He I spectrum. Indeed the

He II spectrum of silyl chloro-acetylene shows a band at 23.4 eV which should be this 3s level. Silyl bromo-acetylene has bands at 19.2 eV and 20.2 eV which should be mainly σ_{CC} bonding and bromine 4s in character. It is not clear, however, which is which.

Vibrational Fine Structure

Fine structure corresponding to vibrations of the ion have been observed in six bands: in the three bands assigned to the 3e levels of the halo acetylenes, $5a_1$ m.o.'s of silyl chloro- and bromo-acetylenes and the $4a_1$ band of germyl acetylene. The molecular and ion frequencies are tabulated in table 2.2.

The $5a_1$ band of silyl chloro-acetylene has a progression of six members with a band frequency of 900 cm^{-1} $\pm$ 40 cm^{-1}: consistent with the reduced skeletal stretching frequency expected with removal of a SiC bonding electron. The two skeletal modes corresponding to the SiC and CX stretches appear to be heavily mixed because they occur outside the normal ranges of the CX and SiC stretches.

The corresponding progression in silyl bromo-acetylene is more diffuse but the band frequency lies between 800 cm^{-1} and 850 cm^{-1}. This is again consistent with removal of a SiC bonding electron. This vibration could be assigned alternatively to a reduced SiH deformation indicating a sizable contribution of the SiH bonding level to that of the SiC bonding level. Since the positions of the vibronic levels in silyl bromo-acetylene could not be accurately measured, it is difficult to distinguish between these two assignments.

Table 2.2 Molecular and Ion Frequencies

			X(A_1) (cm^{-1})	A(E) (cm^{-1})	B(A_1) (cm^{-1})
SiH_3CCCl	ν_2	ν_{CC}	2164	1860	
	ν_3	ν_{SiH_3}	939		
	ν_4	$\nu_{skel\ asym}$	917	930	900
	ν_5	$\nu_{skel\ sym}$	436		
	ν_{10}	δ_{skel}	124	150[a]	
SiH_3CCBr	ν_3	δ_{SiH_3}	932		
	ν_4	ν_{skel}	832	870	800-850
	ν_5	ν_{skel}	361		
GeH_3CCH	ν_3	δ_{GeH_3}	844[b]		
	ν_4	ν_{GeC}	530		
GeH_3CCCl	ν_3	δ_{GeH_3}	833	920[a]	
	ν_4	ν_{skel}	888		
	ν_5	ν_{skel}	348		
	ν_{10}	δ_{skel}	110	140[a]	

a from U.V. spectra

b reference 62

The $4a_1$ band of germyl acetylene shows five maxima which appear to form a double progression. The larger progression is in the order of 900 cm^{-1} while the smaller is in the order of 600 cm^{-1}. The smaller progression is consistent with removal of a GeC bonding electron. The larger progression is due to mixing of the σ_{GeC} level with the σ_{MH} level.

The 3e band of silyl chloro-acetylene shows a distinct progression of about six members having band frequencies separated by 930 cm^{-1} corresponding to either a skeletal stretch or a SiH deformation. In most halo acetylenes[9,10], the frequency that is excited is a reduced C ≡ C stretching frequency corresponding to loss of a bonding electron from the 'π' CC m.o. Mixing of this 'π' orbital with either the 2e or 1e orbitals will cause any totally symmetric vibrations associated with these orbitals to become active in the p.e. spectrum. Here it appears that the vibrational mode corresponding to the skeletal stretch on the silyl deformation has become the dominant feature of the spectrum. It is not inconceivable that the reduced C ≡ C stretch is approximately double this band frequency at about 1860 cm^{-1}. This order of frequency is observed in comparable compounds[9,10].

The 3e band of silyl bromo-acetylene shows a progression of five members, the frequency separation being about 870 cm^{-1}. This is consistent with an increased skeletal stretching frequency. The structure of the 3e band of germyl chloro-acetylene is very diffuse, the bands overlapping, such that a reliable frequency cannot be given, although it does appear to lie between 600 cm^{-1} and 850 cm^{-1}.

Removal of a 3e orbital electron is expected to increase the C ≡ C equilibrium bond length thus decreasing the frequency of the C ≡ C stretch. The C-X bond length will decrease because there is less repulsion between the halogen "lone pair" electron and the C ≡ C bonding electron, with the result that the frequency of the skeletal stretch in the ion should increase.

It is possible that spin orbit coupling could affect the p.e. spectrum of silyl bromo-acetylene. If the molecular orbital involved in spin orbit coupling is expressed as a linear combination of atomic orbitals with coefficients c_μ, then the effective splitting z is given by

$$z = \sum_\mu c_\mu^2 \, z_\mu$$

where z_μ are the characteristic splittings of the component atomic orbitals. In acetylenes, c_μ can be approximately determined using the method used in the monohalo- and dihalo-acetylenes[9,10]. Using this method and a z value for bromine of 0.31 eV[15], the spin orbit couplings for the 3e and 2e levels in silyl bromo-acetylene are approximately 0.11 eV and 0.19 eV respectively.

The splitting for the 3e band is the same order as the vibrational splitting such that the effect is obscured by the vibronic progression. The splitting on the 2e band is obscured by overlap of the $5a_1$ and 1e bands, the latter being split by Jahn-Teller distortion.

2.3 P.e. Spectra of Disilyl and Digermyl Acetylene

The symmetry configuration of these two diacetylenes can be taken as D_{3d}, D_{3h} or D_3 where the two MH_3 groups are staggered,

eclipsed or intermediate between the two. It is easier to expand the basis set orbitals in terms of one of the higher symmetry classes i.e. D_{3d} or D_{3h}. Both these groups have the same characters although they belong to different symmetry species. In this section, the D_{3d} point group is used but whatever is said can equally be applied to the D_{3h} point group.

Basis set orbitals

The basis set m.o.'s are formed from a combination of valence shell a.o.'s. These a.o.'s belong to the a_{1g}, a_{2u}, e_g and e_u symmetry classes. The a.o.'s are

M_{ns}	a_{1g}	M_{ns}	a_{2u}				
M_{np}	a_{1g}	M_{np}	a_{2u}	M_{np}	e_g	M_{np}	e_u
H_{1s}	a_{1g}	H_{1s}	a_{2u}	H_{1s}	e_g	M_{1s}	e_u
C_{2p}	a_{1g}	C_{2p}	a_{2u}	C_{2p}	e_g	C_{2p}	e_u
C_{2s}	a_{1g}	C_{2s}	a_{2u}				

The five a_{1g} a.o.'s will combine to give five a_{1g} m.o.'s which can be represented as

$5a_{1g}$, $4a_{1g}$ — antibonding SiC, SiH

$3a_{1g}$, $2a_{1g}$, $1a_{1g}$ — bonding SiC, SiH, CC

The five a_{2u} a.o.'s combine to give five a_{2u} m.o.'s which are represented as

$5a_{2u}$]
$4a_{2u}$] antibonding SiC, SiH, CC

$3a_{2u}$]
$2a_{2u}$] bonding SiC, SiH
$1a_{2u}$]

The six e a.o.'s combine to give six e m.o.'s represented as

$3e_u$]
$2e_u$] antibonding π_{CC} and σ_{SiH}
$3e_g$]

$2e_g$]
$1e_u$] bonding π_{CC} and σ_{SiH}
$1e_g$]

The expected occupied m.o.'s are $3a_{1g} + 2a_{2u} + e_u + 2e_g$ requiring 22 electrons (supplied as 4 from each of two M, 4 from each of two C and 1 from each of six H).

If the molecule is considered to belong to the D_3 point group then the classes change as; $a_{1g} \rightarrow a_1$; $a_{2u} \rightarrow a_2$; $e_u, e_g \rightarrow e$, so that the occupied m.o.'s are $3a_1 + 2a_2 + 3e$ (levels for the D_3 symmetry molecule will be shown in brackets).

Assignments of p.e. spectra

The p.e. spectra of disilyl and digermyl acetylene are shown in figures 2.5 and 2.6 respectively. The i.p.'s are given in table 2.1.

Both spectra have six bands in them. The shape and relative intensities of these bands are similar in the two spectra. The first band (band I) is the $2e_g$(3e) band of mainly 'π_{CC}' bonding character similar to band I of other acetylenes. The second band (band II) is expected to contain both of the remaining e orbitals, $1e_g$ and $1e_u$ (2e + 1e). Both m.o.'s will be similar in energy as the interaction between them will be smaller than for the corresponding levels in disilane[11] and digermane[16]. The expected energy for these two m.o.'s will be the energy of the $e\sigma_{SiH_3}$ m.o. in other silyl and germyl acetylenes. Jahn-Teller distortion of the ion will broaden both m.o.'s, the magnitude of which should be similar to that found in disilane and digermane.

Band II should also contain the $3a_{1g}$ ($3a_1$) level just as the $5a_1$ level was present in this band of the silyl and germyl haloacetylenes. This m.o. will be one of the σ_{MC} bonding levels. No vibrational fine structure is found at the onset of band II suggesting that the $3a_{1g}$ band must be obscured by one of the e bands.

The third band (band III) occurs at about 14 eV in both molecules. This band is probably the $2a_{2u}$ ($2a_2$) level being either of σ_{MH} or σ_{MC} bonding character. The recent assignment of disilyl acetylene using CNDO/2 calculations suggest that the $2a_{2u}$ level is mainly σ_{MH} bonding and overlaps with one Jahn-Teller component of the $1e_g$ level. The last band (band VI) at around 20 eV is most likely to correspond to the $1a_{1g}$ ($1a_1$) m.o. which is of mainly

Figure 2.5 P.e. Spectrum of SiH_3CCSiH_3

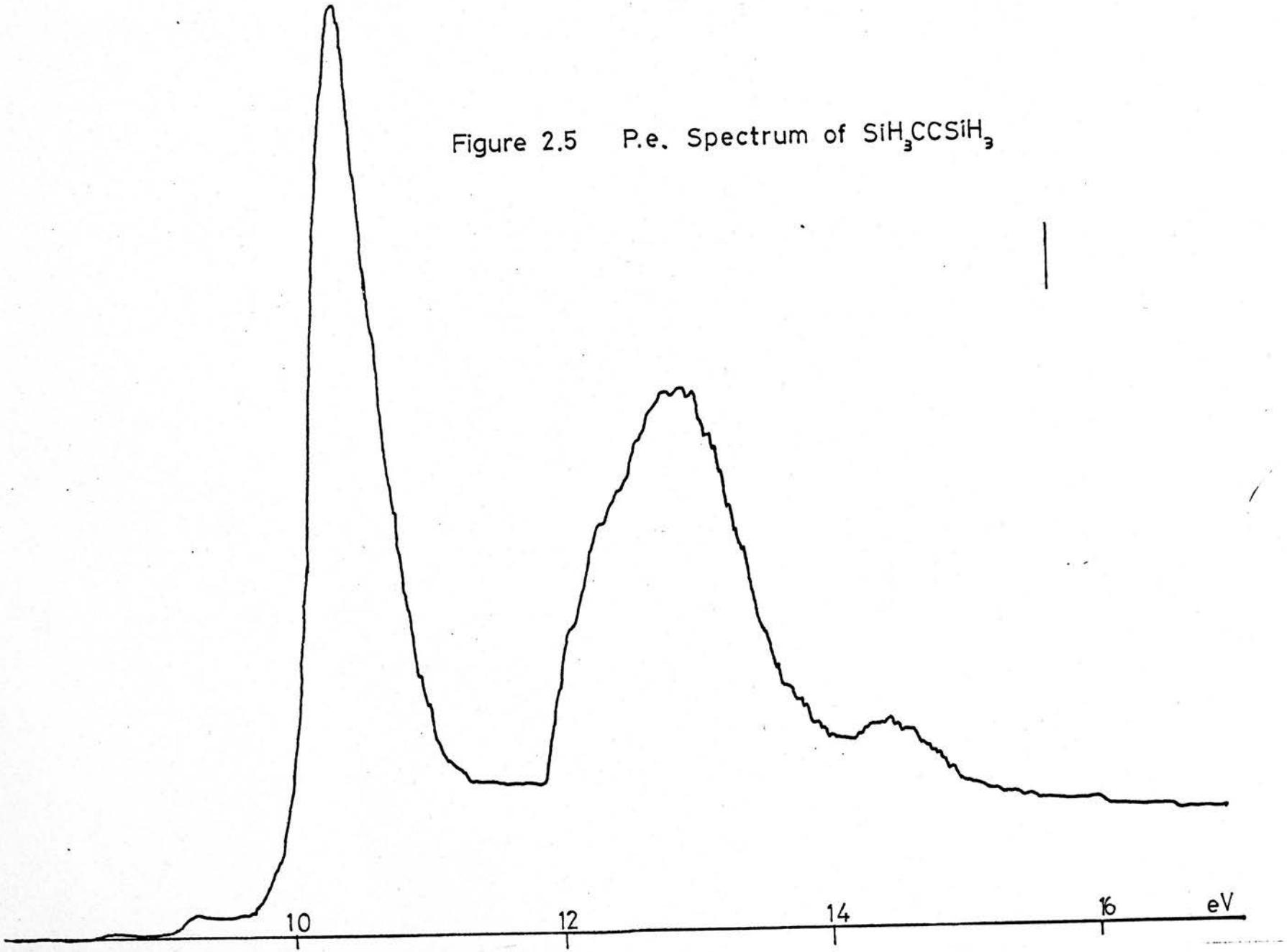

Figure 2.6 P.e. Spectrum of $GeH_3C{\equiv}CGeH_3$

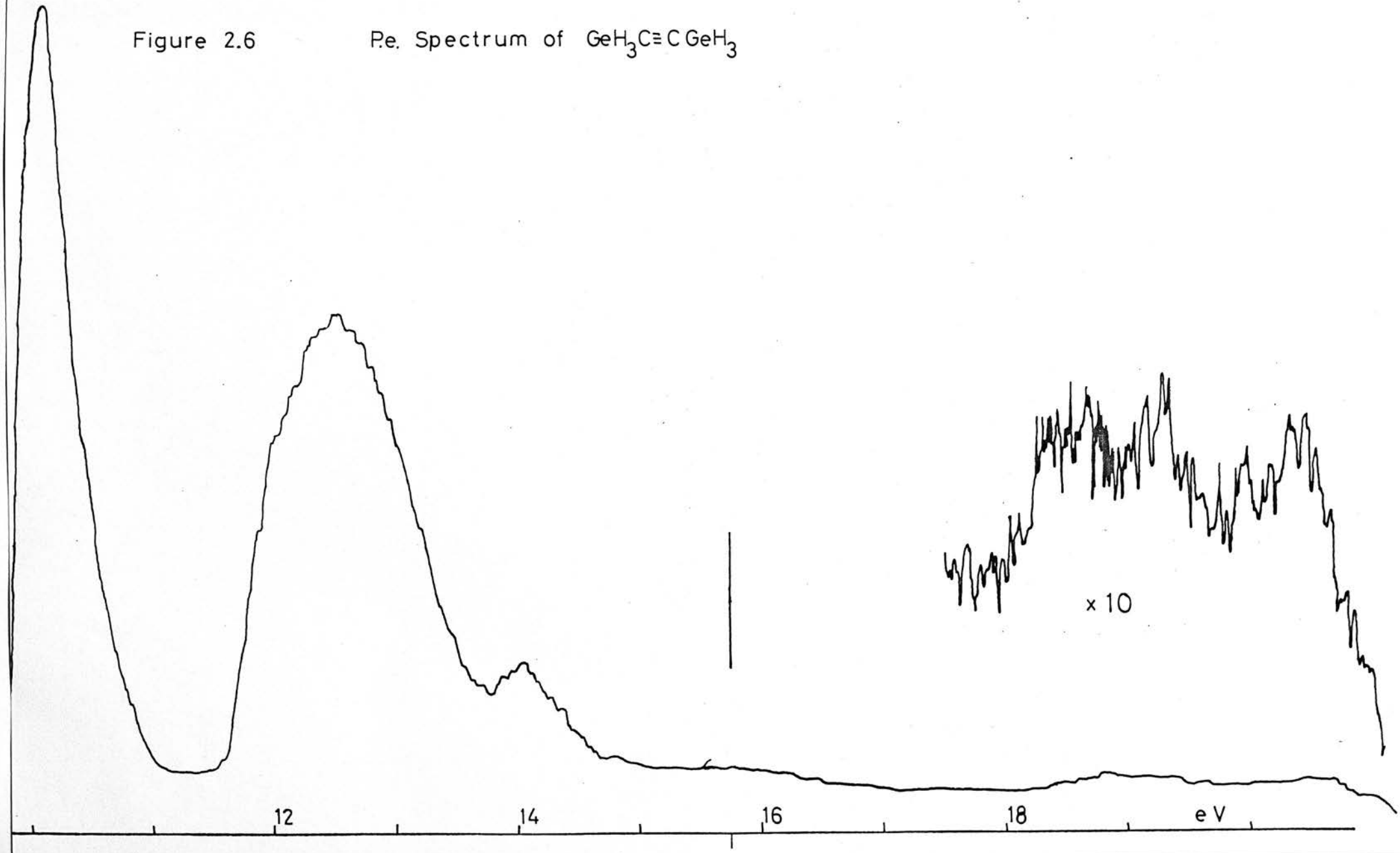

σ_{CC} bonding character. The energy of this level is consistent with that found in other acetylenes.

The two remaining bands are the $2a_{1g}$ ($2a_1$) and $1a_{2u}$ ($1a_2$) m.o.'s being mainly σ_{MH_3} and σ_{MC} bonding respectively. It is difficult to predict in which order of energy they will come although the CNDO/2 investigation suggest the order is $2a_{1g} < 1a_2$ in binding energy.

2.4 Trends in Ionization Potentials

The energy levels in germyl acetylene are similar to those in silyl acetylene. This is not surprising because the electronegativities of the silyl and germyl groups are approximately the same. Those levels involving either σ_{MH_3} or σ_{MC} bonding are shifted to lower i.p.'s by about 2 eV in the silyl and germyl compounds relative to those in the methyl compounds. This reflects the drop in the first atomic i.p. corresponding to loss of a np electron down the group IV elements. These are 11.3 eV for carbon, 8.15 eV for silicon and 7.88 eV for germanium. This suggests that the $4a_1$ and 1e m.o.'s in the acetylenes contain similar contributions from the np atomic orbitals. A similar, although less pronounced, effect is observed for the $3a_{1g}$, $2a_u$, $1e_u$ and $1e_g$ levels of disilyl and digermyl acetylene.

The order of the first i.p. in mono- and di- group IV acetylenes is C < Si > Ge. This order is that found in other group IV compounds[17,18]. This order has been explained in terms of p → d 'π' bonding between the 'π_{CC}' electrons and the vacant d_m orbital on the M atom. Since the strength of the interaction is determined by the efficiency of overlap between the orbitals, the 'π' electrons will be harder to remove in the case of silicon than either carbon or germanium.

The energy levels in silyl and germyl chloro-acetylene are also similar in energy. The i.p. of the halogen np electron falls by 1.2 eV on going from chlorine to bromine. A similar drop is expected for those m.o.'s having mainly halogen np character. This is found in the 1e and $4a_1$ levels of the silyl halo-acetylenes (2e in silyl bromo-acetylene). Unfortunately there is no data at present on the i.p.'s of the methyl halo-acetylenes and no comparison with the silyl and germyl compounds is therefore possible.

The p.e. spectra of monohalo-[9] and dihalo-acetylenes[10], however, reflect the drop in i.p.'s of the halogens, not only in those levels directly associated with the np electrons but also the π_{CC} bonding level. This has been interpreted in terms of extensive mixing of the π m.o.'s in these molecules. Similar trends are found in halo di- and tri-acetylenes[19]. The π_{CC} level in silyl chloro- and bromo-acetylenes do not differ significantly from each other suggesting either that there is little mixing in these molecules or that the σ_{SiH_3} m.o. has a significant effect, in the opposite direction from the X_{np} level, or the π_{CC} level. The former is unlikely considering that the fine structure observed in band I is in keeping with heavy mixing of at least the X_{np} m.o. with the π_{CC} m.o.

The energy of the m.o.'s of conjugated acetylenes are heavily mixed forming extensive delocalized systems. To a lesser extent the 'π' systems of hetero-acetylenes form these systems. The extent of conjugation, hypoconjugation, p → d 'π' bonding within such molecules cannot be differentiated, at present, by the use of semi-empirical or "ab initio" calculations. Such calculations are not

precise enough to allow anything other than a semi-quantitative analysis of the photoelectron spectra, because they have to predict both the ground state energy levels and the ionic state energy levels.

2.5 U.v. Spectra

The u.v. spectra of disilyl and digermyl acetylene, silyl chloro- and bromo-acetylenes, and germyl chloro-acetylene were recorded in the region 52,500 cm^{-1} to 32,500 cm^{-1} (190 nm to 310 nm). The band frequencies are given in table 2.3 along with those of the corresponding halo-acetylenes.

All the spectra have two bands above 190 nm although some of these overlap extensively making the position of the band centres unclear. The spectra of silyl and germyl halo-acetylenes are very similar to those of the parent halo-acetylenes in position and intensity. Silyl and germyl chloro-acetylenes possess a double progression of bands on the absorption peak at 264 nm (38,000 cm^{-1}). The frequencies, listed in table 2.4, are excited approximately every 160 cm^{-1} and 940 cm^{-1} in silyl chloro-acetylene and 145 cm^{-1} and 925 cm^{-1} in germyl chloro-acetylene which corresponds with the ground state skeletal stretch ν_3 and skeletal deformation ν_{10}. The activation of a bending vibration would suggest that the upper state is bent. The corresponding band in chloro-acetylene has been assigned to a 'π' $\rightarrow$ 'π^*' transition[20] as have the absorptions at 225 nm in chloro- and bromo-acetylene[21]. It seems reasonable that the bands in silyl and germyl chloro-acetylenes are also 'π' $\rightarrow$ 'π^*' transitions. The absorption visable beyond 190 nm (52,500 cm^{-1}) in silyl bromo-acetylene corresponds to a similar band in bromo-

Table 2.3. U.V. Spectra

Species	Band I			Band II		
	(cm^{-1})		(nm)	(cm^{-1})		(nm)
HCCCl[a]	40000-43000	v.w.	250-230	45000-50000	s.[c]	220-200
HCCBr[b]	45000-52000	s.	220-190	∿55000	v.s.	~180
SiH_3CCCl	38000-42000	v.w.[c]	265-240	43000-50000	s.	230-200
SiH_3CCBr	41000-48000	s.	235-210	50000-∿60000	v.s.	200-165
GeH_3CCCl	38000-42000	v.w.[c]	265-240	44000-50000	s.	225-200
GeH_3CCGeH_3	46000-49500	s.	215-200	49500-55000	v.s.	200-180

a) reference 20.

b) reference 21.

c) bands show vibronic progressions.

v.w. very weak

s. strong

v.s. very strong

Table 2.4 Vibronic Transition in Silyl and Germyl Chloro-Acetylenes

a) SiH_3CCCl

ν (cm^{-1})	Relative Intensity	ΔE Progression 1	ΔE Progression 2
38260	1	160	950
38420	2	140	940
38560	4	-	970
39050	1	160	950
39210	1	150	950
39360	2	170	920
39530	4	-	920
40000	1	160	-
40160	1	160	-
40280	2	170	950
40450	4	-	930
41230	2	150	-
41380	4		920
42300	4		

b) GeH_3CCCl

ν (cm^{-1})	Relative Intensity	ΔE Progression 1	ΔE Progression 2
38440	1	160	950
38600	2	170	930
38770	1	-	910
39390	1	140	920
39530	2	150	920
39680	1	-	890
40310	1	140	
40450	2	120	
40570	1		

acetylene that has been assigned to a 'π' $\rightarrow$ σ^* transition.

The absorptions in digermyl acetylene are 'π' $\rightarrow$ 'π^*' and 'π' $\rightarrow$ σ^* transitions for the 210 nm and 190 nm bands respectively corresponding to transitions from the π_{CC} bonding level.

All of the observed transitions must come from the π_{CC} level because excitation from other levels would give rise to transitions of much lower energy which are not observed. The p.e. spectra can be used, in conjunction with the u.v. spectra, to determine the energies of the upper state levels from the transition energies. These are given in table 2.5. The assignment of other bands in u.v. spectra (especially the vacuum u.v.), can be facilitated by knowledge of upper state energies. Transition frequencies to these upper states from more tightly bound m.o.'s can be predicted and compared with those bands occurring at higher energies in the u.v. spectra.

Substituent effects, such as the extent of mixing of the 'π' m.o.'s in similar molecules, affect the u.v. spectra in a similar manner to the photoelectron spectra. For example the lowest energy transition of chloro-acetylene[20] and bromo-acetylene[21] occur at a higher energy than the corresponding transitions in the silyl halo-acetylenes and at a lower energy than the corresponding transition in acetylene itself. This shift towards longer wavelengths as the number of 'π' electrons increases in corresponding molecules appears to be a common feature of many unsaturated systems. This change in wavelength as the number of 'π' electrons increases, however, is not uniform suggesting several effects are occurring.

Table 2.5. Binding Energies of Excited Electronic States.

Species	I.P.(eV)	Transition Energies (eV)		Upper Level I.P.'s (eV)	
		Band (I)	Band (II)	I	II
SiH_3CCCl	10.27	4.7	5.3	5.5	4.9
GeH_3CCCl	10.19	4.7	5.4	5.5	4.8
SiH_3CCBr	10.17	5.1	6.2	5.1	4.0
GeH_3CCGeH_3	10.1	5.7	6.1	4.4	4.0

CHAPTER 3

Electron Diffraction Studies of Some Silyl and Germyl Acetylenes

3.1 Introduction

Gas phase electron diffraction data for silyl chloro-, disilyl, germyl chloro- and digermyl acetylene were obtained using the Balzer's K.D.G.2 apparatus at the University of Manchester Institute of Science and Technology. The analysis of the data is presented in this chapter.

Electron diffraction studies of these compounds were undertaken to give accurate structures from which reliable values of the rotational constants B could be computed. Analysis of the perpendicular bands in the infra red spectra of these molecules requires knowledge of these rotational constants.

It has been found, mainly from microwave studies, that the C - C and C ≡ C bond distances in a series of methyl acetylenes do not change significantly even though some assumptions were made in determining their structures. On the other hand, electron diffraction studies of two silyl acetylenes by Anderson[1] have shown significant variation in the C - Si and C ≡ C bond lengths. The C ≡ C bond length was longer and the C - Si bond length shorter in silyl acetylene than in silyl perfluoromethyl acetylene in which a CF_3 group replaced the hydrogen atom.

Similarly no difference has been observed in the C - C bond lengths of methyl cyanide and methyl acetylene[22], but in both silyl and germyl cyanide, the M - C bond is considerably longer than in the corresponding acetylenes[1,25]. This has been interpreted in terms of electron withdrawal from the p → d 'π' component of the M - C bond by the electron withdrawing group, explaining why the methyl analogues do not show the same effect.

Studies of silyl chloro-, germyl chloro-, disilyl and digermyl acetylenes were undertaken to see whether this trend was continued.

3.2 The Structures of Silyl and Germyl Chloro-Acetylenes

During exposure, the sample of silyl chloro-acetylene was maintained at 250 K and germyl chloro-acetylene at 273 K with nozzle temperatures of 296 K. Nozzle to plate distances of 250 mm, 500 mm and 1000 mm were used: these gave ranges in the scattering variables of 6 - 30 Å^{-1}, 2 - 16 Å^{-1} and 1 - 8 Å^{-1} respectively. The electron beam had a wavelength of 0.05660 $\pm$ 0.00005 nm.

The weighting function, correlation parameters and scale factors are given in table 3.1. The intensity and final weighted difference curves are shown in figures 3.1 and 3.2 respectively.

Both acetylenes were assumed to possess linear skeletons with overall C_{3V} symmetry in the vibrational ground state. The electron diffraction pattern, however, represents a time average structure of all occupied states so that the average structure is no longer linear.

In a molecule of type

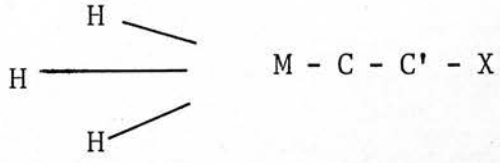

the MH, MC, CC' and C' bonded distances, together with the HMC angle, define the geometry of the ground state. If the M - C - C' and C - C' - X angles are fixed at 180^{o} then the M . . . C, C . . . X and M . . . X nonbonded distances must be independently refined to take account of the average structure. The HMC angle can be defined

Table 3.1. Weighting Functions, Correlation Parameters and Scale Factors

Compound	Camera Height (mm)	Δ S	S_{min}	S_1	S_2	S_{max}	P/h	Scale Factor
SiH_3CCCl	250	4	68	160	280	300	0.2251	0.450±0.023
	500	2	26	40	140	152	0.4575	0.694±0.014
	1000	1	11	20	70	77	0.4330	0.502±0.014
SiH_3CCSiH_3	250	4	68	100	285	302	0.4065	0.618±0.020
	500	2	22	35	140	152	0.4924	0.697±0.014
	1000	1	11	18	69	77	0.4968	0.735±0.022
GeH_3CCCl	250	4	64	100	284	304	0.3788	0.313±0.031
	500	2	22	36	140	156	0.4811	0.371±0.018
	1000	1	11	20	70	79	0.4962	0.560±0.028
GeH_3CCGeH_3	250	4	72	120	280	300	0.3995	0.681±0.031
	500	2	26	40	130	156	0.4881	0.667±0.019
	1000	1	11	22	64	79	0.4926	0.629±0.030

Figure 3.1 Intensity Data for SiH_3CCCl

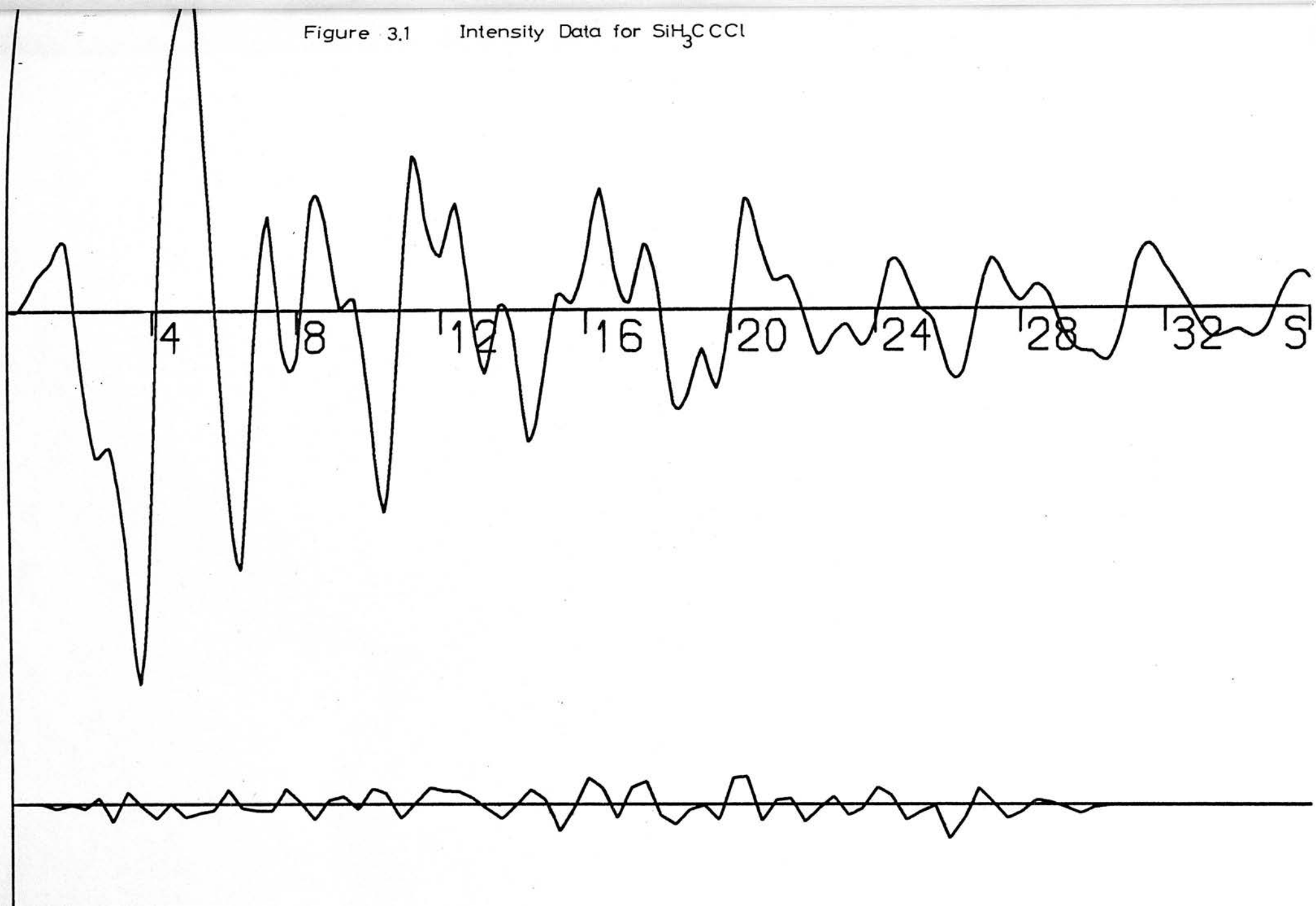

Figure 3.2 Intensity Data for GeH_3CCCl

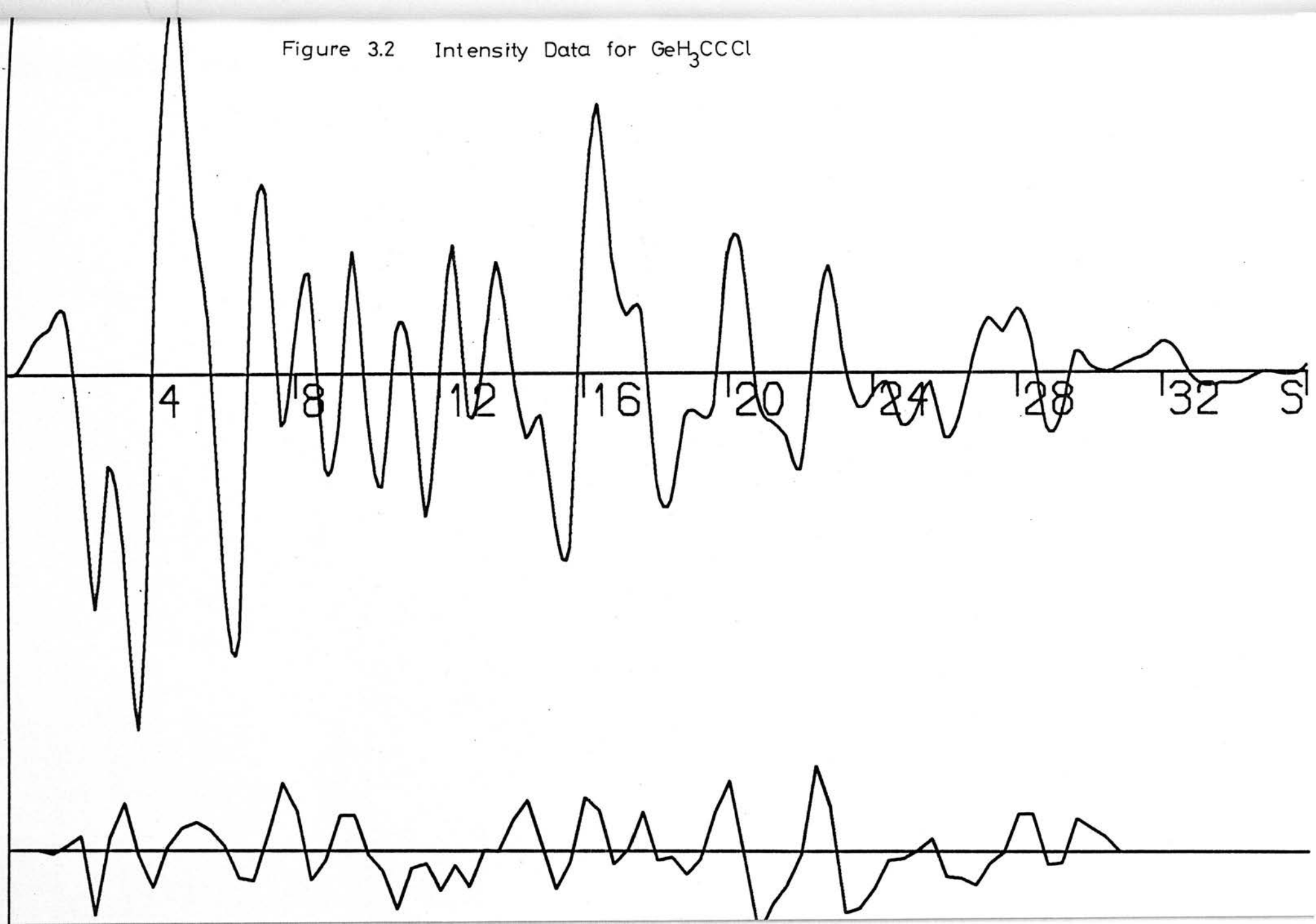

in terms of the H . . . C, H . . . C' or H . . . X nonbonded distances and the HM bonded distances. Electron diffraction studies do not generally give the position of the H atoms very well except when scattering from the hydrogens is similar in intensity to that from other atoms present. In silyl chloro-acetylene, the positions of the H . . . C, H . . . C' and H . . . X nonbonded distances were determined well enough to define the HSiC angle in terms of these distances rather than fix the value of the HSiC angle and define the three nonbonded distances in terms of this angle and the MH bonded distance. These three peaks in germyl chloro-acetylene were not well defined. As a result, a reasonable value of the HGeC angle was chosen and the three H . . . nonbonded distances were defined from this angle.

The radial distribution curves, P(r)/r were calculated after each refinement and made the process of refinement easier. Since in silyl and germyl chloro-acetylenes few overlapping peaks are expected in the radial distribution curves, the peaks can be readily assigned. As a result each bonded and nonbonded distance and most amplitudes of vibration can be refined successfully.

Silyl chloro-acetylene refinements

The radial distribution curve is shown in figure 3.3. The strongest peak corresponds to the Si . . . Cl nonbonded atom pair distance at 4.6 Å. The other two major peaks are the C . . . Cl nonbonded atom pair distance at 2.8 Å and the C' . . . Cl bonded atom pair distance at 1.6 Å. The peaks at a distance greater than 2 Å correspond to various nonbonded atom pairs. The positions of the majority of these peaks depend on the independent distances that define the structure.

Figure 3.3 P(R)/R – SiH_3CCCl

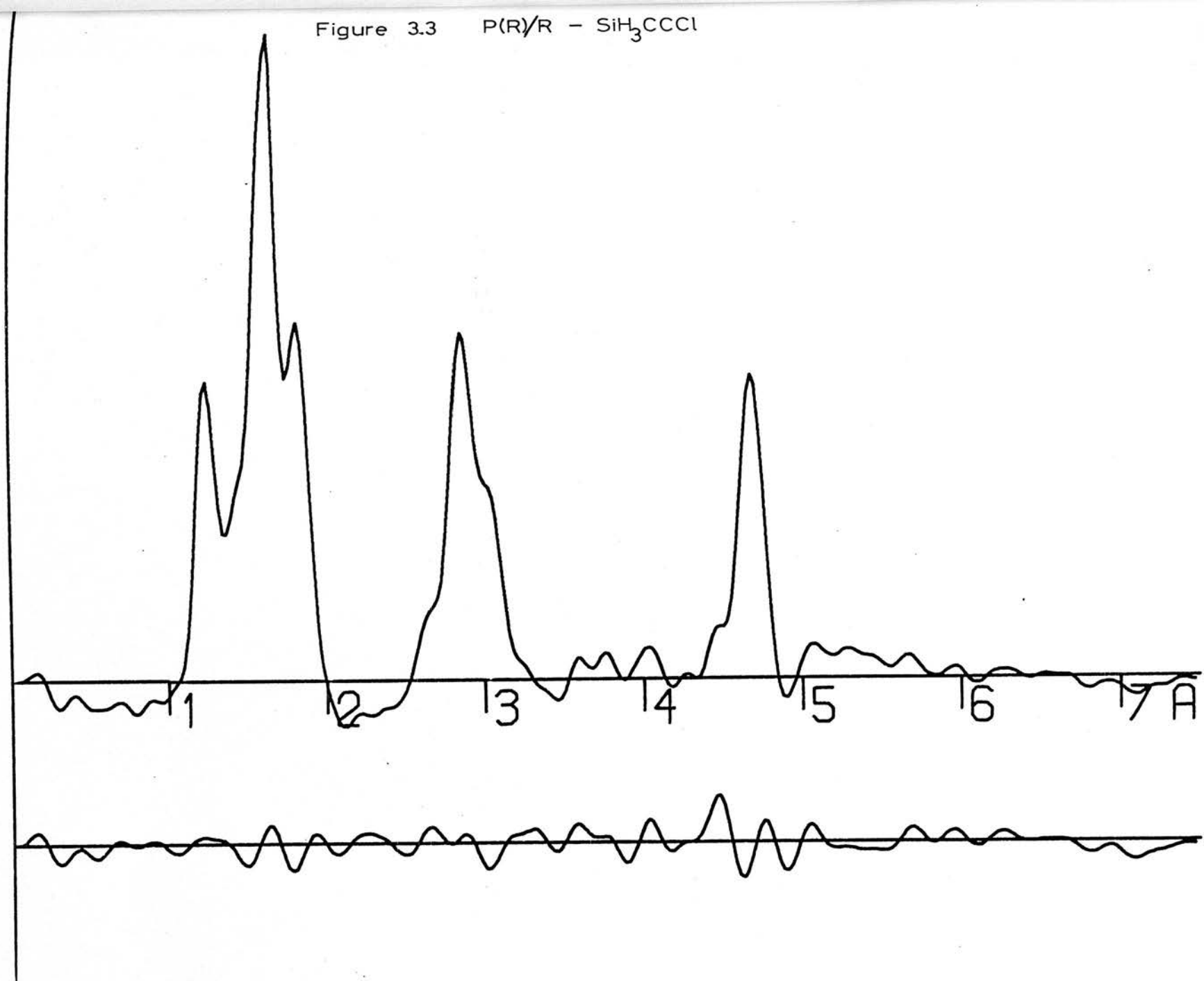

Satisfactory refinements were carried out on the SiH, SiC, CC', C'Cl bonded distances, the Si . . . C', C . . . Cl, Si . . . Cl, H . . . C, H . . . C', H . . . Cl nonbonded distances and the amplitudes of vibrations of the SiC, CC', C'Cl bonded and Si . . . C', C . . . Cl', Si . . . Cl' nonbonded atom pairs.

The amplitude of vibrations of the SiH bonded atom pair would not refine while the amplitudes of the CC' and C'Cl bonded atom pairs were refined. The amplitudes of vibration of the H . . . C, H . . . C', and H . . . Cl nonbonded atom pairs were not refined but fixed at suitable values[26]. The HSiC angle, and hence the HSiH angle, was defined in terms of the three H . . . nonbonded distances.

Germyl chloro-acetylene refinements

Attempts at refinement of the data for germyl chloro-acetylene were not successful at first. It was discovered from the radial distribution curve that germyl bromide was present and no account of this had been made in refinement of the data. The quantity of impurity was calculated for each camera height and the theoretical scattering curve for each height was subtracted from the experimental data. Although this operation leads to a reduction in the scale factor for each camera height and hence larger errors than are normal, a reasonable structure could be calculated.

The radial distribution curve, P(r)/r is shown in figure 3.4. The major peaks correspond to the C' - Cl bonded atom pair, the Ge - C bonded atom pair and the Ge . . . Cl nonbonded atom pair distances at 1.6 Å, 1.9 Å and 4.7 Å respectively. The outer peaks are due to the various nonbonded atom pairs, the majority of which

Figure 3.4 P(R)/R — GeH_3CCCl

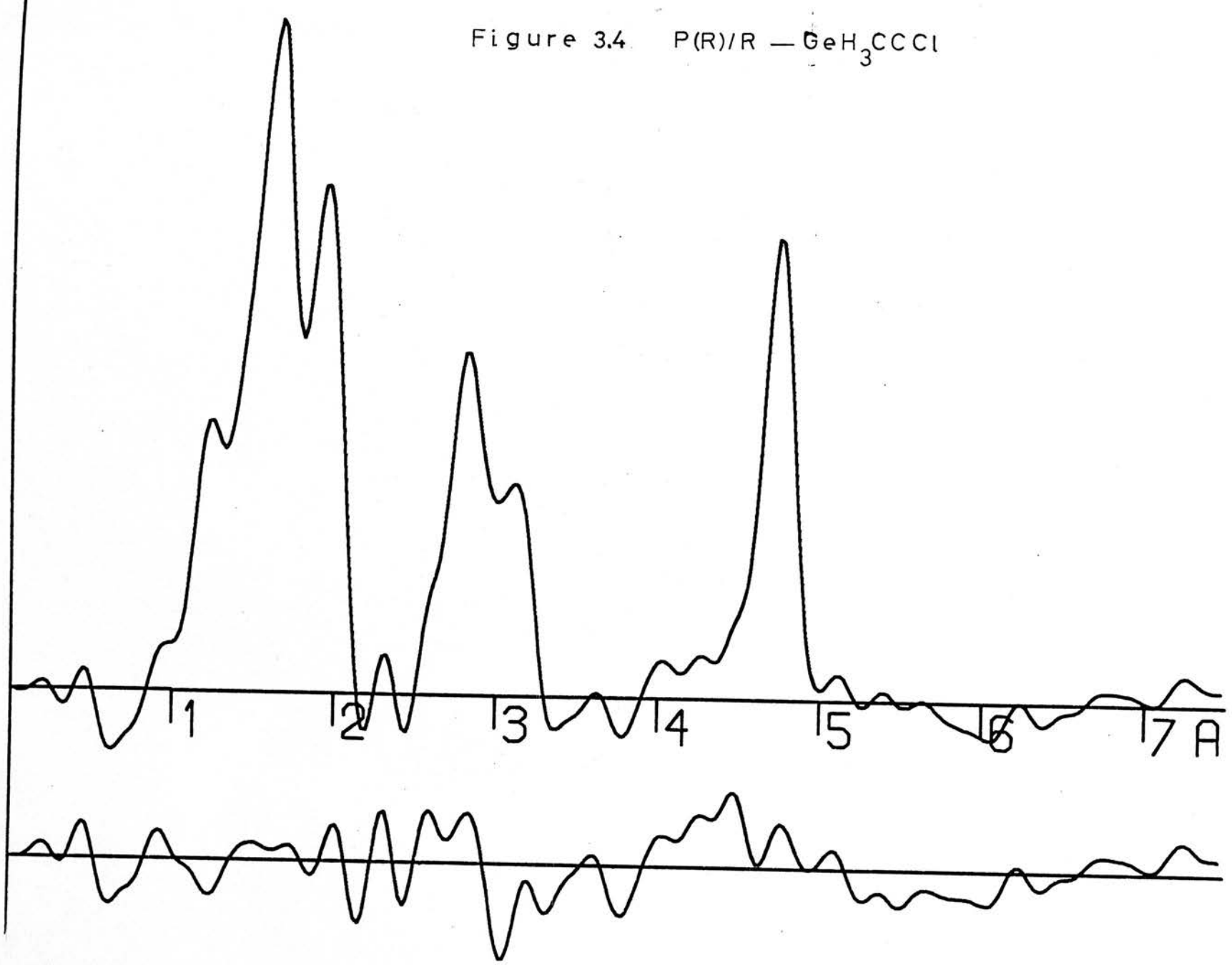

are defined in terms of the seven independent distances and the HGeC angle.

Satisfactory refinements were carried out on the GeH, GeC, CC', C'Cl bonded distances, the Ge . . . C', C . . . Cl, and Ge . . . Cl nonbonded distances and the amplitudes of vibration of the GeC bonded and Ge . . . Cl nonbonded atom pairs. The remaining amplitudes of vibration were all set to reasonable values[27]. They did not refine properly because information was lost when the theoretical scattering curves for germyl bromide were subtracted from the data.

The HGeC angle in this compound was fixed at a value in keeping with other germyl compounds. The H . . . C, H . . . C' and H . . . Cl nonbonded distances were defined in terms of this angle since they do not contribute significantly to the overall scattered intensity unlike the silyl analogue.

The final parameters and least squares correlation matrices obtained for both chloro-acetylenes are given in tables 3.2, 3.3 and 3.4. The lowest R factor obtained for silyl chloro-acetylene was 0.14 and for germyl chloro-acetylene, 0.35. The high value for the germyl acetylene reflects the poor quality of data obtained from the photographic plates.

3.3 The Structures of Disilyl and Digermyl Acetylene

During exposure, the sample of disilyl acetylene was maintained at 250 K and digermyl acetylene at 273 K. The nozzle temperature, nozzle to plate distances and electron wavelength were the same as those used for silyl and germyl chloro-acetylenes.

Table 3.2a. Molecular Parameters for SiH_3CCCl

A. Independent Distances:

		Distance (Å)	Amplitude
R1	Si H	1.502±0.012	0.088 (fixed)
R2	Si C	1.811±0.006	0.051±0.008
R3	C C'	1.232±0.006	0.040±0.011
R4	C' Cl	1.620±0.004	0.044±0.008
R5	Si C'	2.998±0.009	0.060±0.012
R6	Si Cl	4.641±0.007	0.059±0.005
R7	C Cl	2.831±0.007	0.045±0.009
R8	H C	2.643±0.037	0.12 (fixed)
R9	H C'	3.786±0.052	0.18 (fixed)
R10	H Cl	5.278±0.034	0.21 (fixed)

D. Dependent Angles

1	(C-Si-H)	107.4±1.2
2	(H-Si-H)	111.4±1.0

Table 3.2b. Molecular Parameters for GeH_3CCCl

A. Independent Distances:

		Distance (Å)	Amplitude
R1	Ge H	1.528±0.026	0.088 (fixed)
R2	Ge C	1.926±0.010	0.038±0.027
R3	C C'	1.211±0.020	0.040 (fixed)
R4	C' Cl	1.635±0.013	0.043 (fixed)
R5	Ge C'	3.072±0.015	0.060 (fixed)
R6	Ge Cl	4.701±0.009	0.070±0.011
R7	C Cl	2.789±0.016	0.047 (fixed)

B. Dependent Distances:

R1	H C	2.838±0.024	0.12 (fixed)
R2	H C'	3.873±0.023	0.16 (fixed)
R3	H Cl	5.426±0.020	0.19 (fixed)
R4	H H'	2.518±0.042	0.20 (fixed)

C. Independent Angles

1	(C-Ge-H)	109.0 (fixed)

D. Dependent Angles

2	(H-Ge-H)	109.9

TABLE 3.3. LEAST SQUARES CORRELATION MATRIX MULTIPLIED BY 1000

SILYL CHLORO ACETYLENE

R 1	R 2	R 3	R 4	R 5	R 6	R 7	R 8	R 9	R10	U 2	U 3	U 4	U 5	U 6	U 7	K 1	K 2	K 3
1000	324	339	-77	-58	4	-42	-31	41	5	91	55	412	-24	-89	-23	-125	-115	-66
324	1000	150	395	-35	5	-118	-274	58	-30	112	113	338	124	189	132	171	370	302
339	150	1000	91	-44	0	5	46	5	13	37	-29	83	-22	-40	-6	-27	-99	-170
-77	395	91	1000	-49	-2	-55	-198	42	-16	7	134	69	90	156	88	200	207	189
-58	-35	-44	-49	1000	19	339	261	-35	26	-8	6	-28	-41	11	-115	23	43	-3
4	3	0	-2	19	1000	-17	8	-8	119	-1	8	7	15	-13	7	3	1	-4
-42	-118	5	-55	339	-17	1000	237	-66	32	-61	-52	-96	200	-67	50	-71	-141	-85
-31	-274	46	-198	261	8	237	1000	-170	48	-44	-91	-160	-19	-186	107	-135	-447	-428
41	58	5	42	-35	-8	-66	-170	1000	-86	-4	12	26	57	-12	18	0	61	69
5	-30	13	-16	26	119	32	48	-86	1000	-3	-1	-8	-7	19	-3	0	-68	-23
91	112	37	7	-8	-1	-61	-44	-4	-3	1000	272	505	156	238	197	346	226	110
55	113	-29	134	6	8	-52	-91	12	-1	272	1000	389	94	283	170	449	233	87
412	338	83	69	-28	7	-96	-160	26	-8	505	389	1000	148	332	239	488	326	168
-24	124	-22	90	-41	15	200	-19	57	-7	136	94	148	1000	189	620	229	242	122
-89	189	-40	156	11	-13	-67	-186	-12	19	238	285	332	189	1000	233	613	485	191
-23	132	-6	88	-115	7	50	107	18	-3	197	170	239	620	233	1000	357	238	81
-125	171	-27	200	23	3	-71	-135	0	0	346	449	488	229	613	357	1000	451	163
-115	370	-99	207	43	1	-141	-447	61	-68	226	233	326	242	485	238	451	1000	355
-66	302	-170	189	-3	-4	-85	-428	69	-23	110	87	168	122	191	81	163	355	1000

TABLE 3.4- LEAST SQUARES CORRELATION MATRIX MULTIPLIED BY 1000

GERMYL CHORO ACETYLENE

R 1	R 2	R 3	R 4	R 5	R 6	R 7	U 2	U 6	K 1	K 2	K 3
1000	255	403	-381	6	11	-144	-309	-268	-321	-281	-225
255	1000	156	177	11	0	-153	-176	-58	-141	7	55
403	156	1000	-79	-21	2	-47	-115	-96	-80	-129	-140
-381	177	-79	1000	-3	-6	23	63	162	211	153	87
6	11	-21	-3	1000	16	336	1	-16	-32	46	131
11	0	2	-6	16	1000	-1	-17	-52	-17	-10	-14
-144	-153	-47	23	336	-1	1000	122	21	84	-56	-72
-309	-176	-115	63	1	-17	122	1000	281	418	194	135
-268	-58	-96	162	-16	-52	21	281	1000	608	488	193
-321	-141	-80	211	-52	-17	84	418	608	1000	314	135
-281	7	-129	153	46	-10	-56	194	488	314	1000	152
-225	55	-140	87	131	-14	-72	135	193	135	152	1000

The weighting functions, correlation parameters and scale factors are given in table 3.1. Intensity and final weighted difference curves are shown in figures 3.5 and 3.6.

Both acetylenes were assumed to have a vibrational ground state of D_{3d} symmetry in which the hydrogen atoms of each end group were staggered. Although the MH, MC and CC' bonded distances and the HSiC angle completely define the ground state in a molecule of type

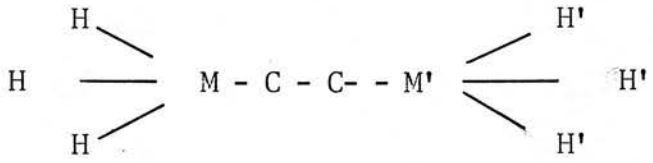

the M . . . C' and M . . . M' nonbonded distances are also required to refine independently so that a time average structure is obtained. The HSiC angle in disilyl acetylene could be defined in terms of the three H-skeletal nonbonded distances in the same way as the corresponding angle in silyl chloro-acetylene was defined. The HGeC angle in digermyl acetylene determined the three H . . . nonbonded distances because they were not well defined from the scattering data.

The radial distribution curve was calculated after each refinement to assist with further refinement.

Disilyl acetylene refinements

The radial distribution curve, P(r)/r is shown in figure 3.7. The major peaks belong to the Si - C bonded, the Si . . . C' nonbonded atom pair and the Si . . . Si' nonbonded atom pair distances at 1.8 Å, 3.0 Å and 4.8 Å respectively.

Figure 3.5 Intensity Data For SiH_3CCSiH_3

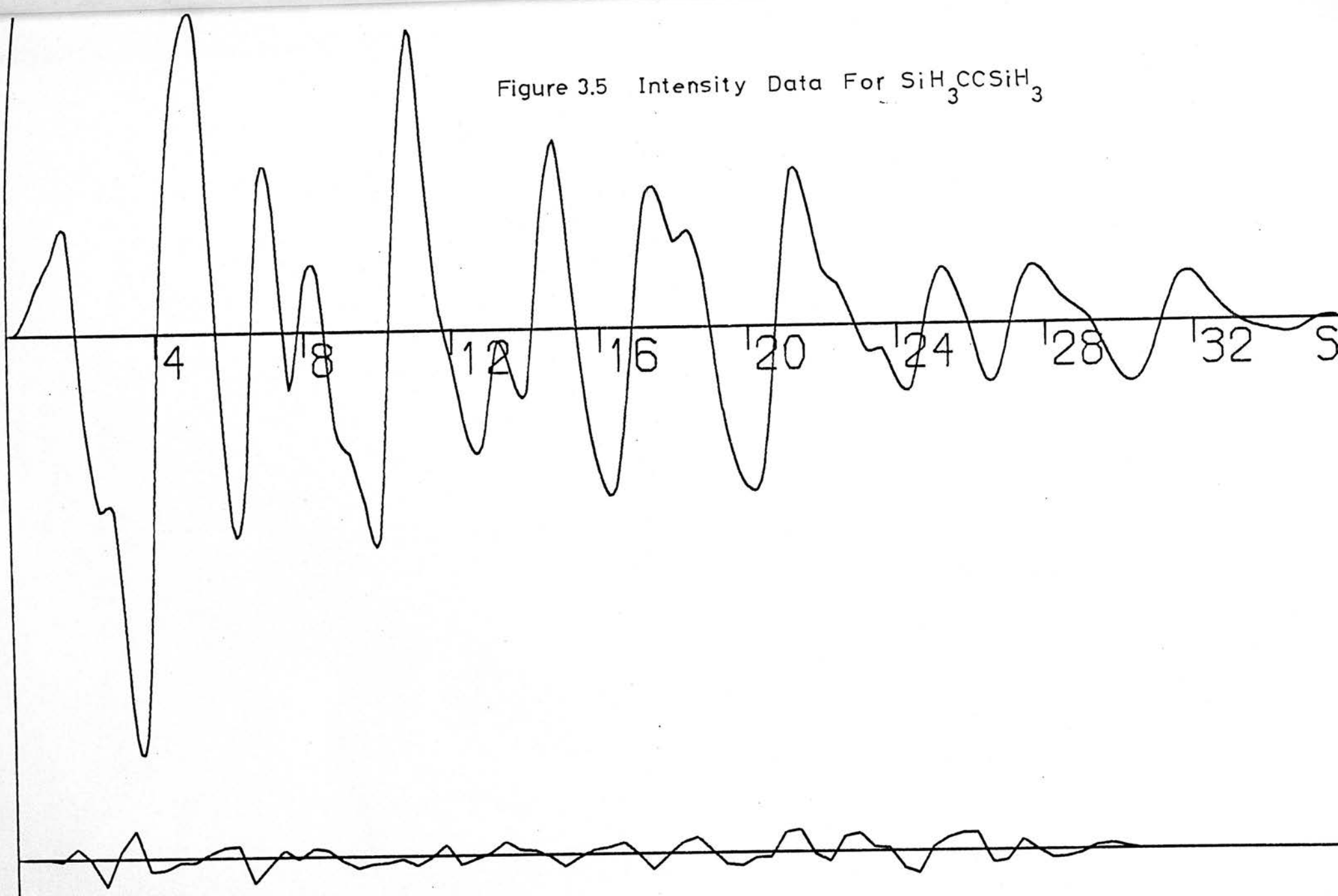

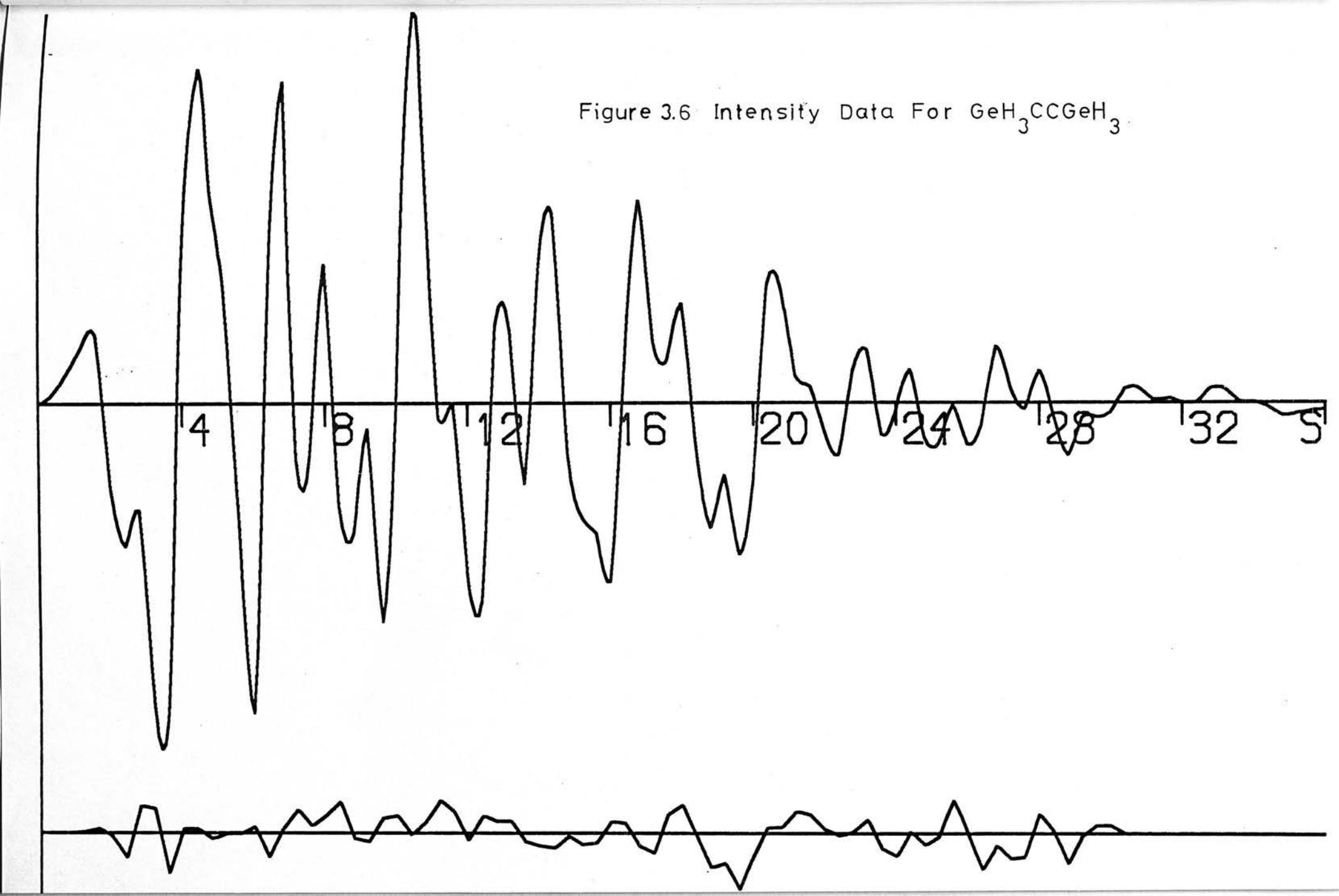

Figure 3.6 Intensity Data For GeH_3CCGeH_3

Figure 3.7 P(R)/R — $SiH_3CC SiH_3$

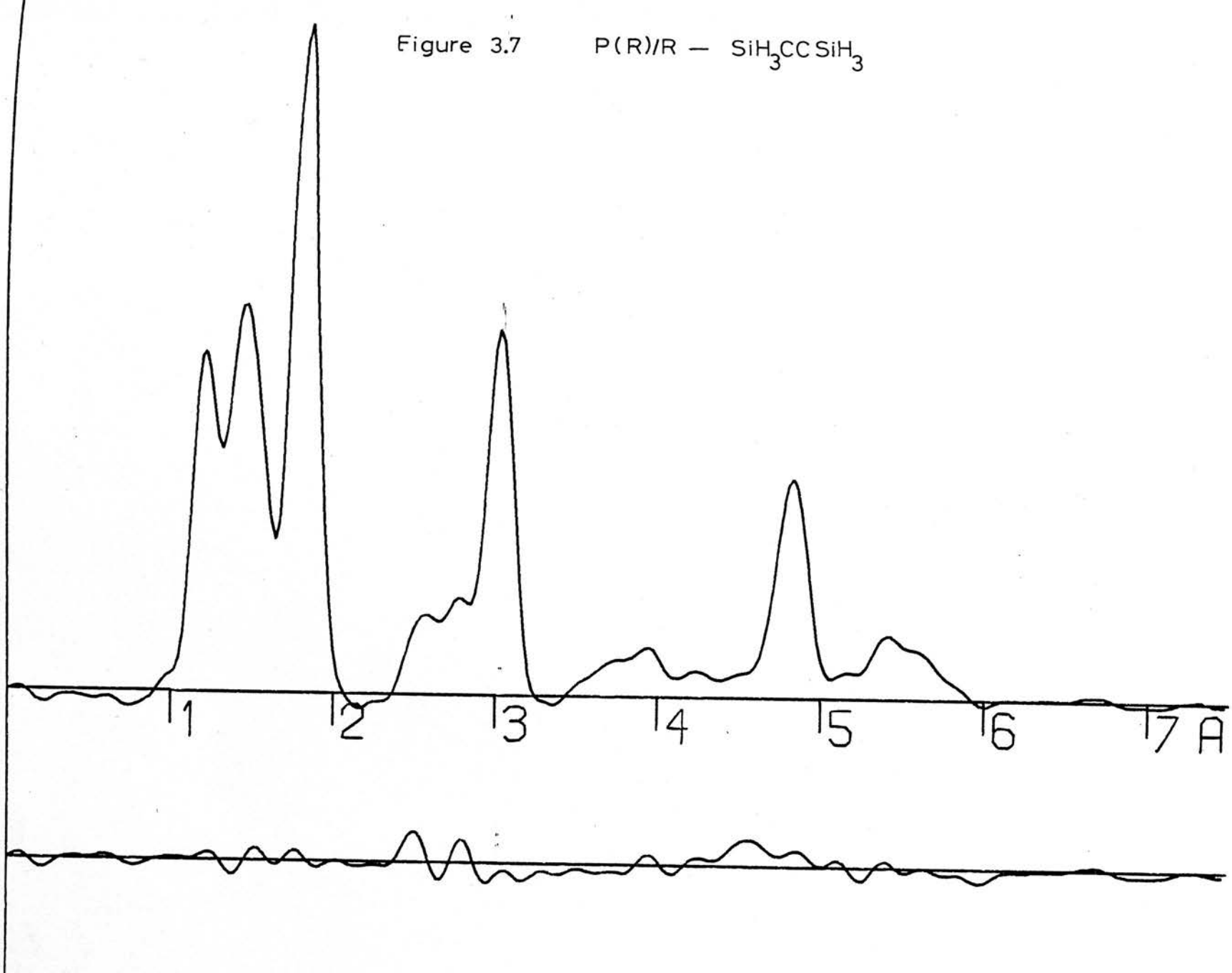

Satisfactory refinements were carried out on the SiH, SiC, CC' bonded distances, the Si . . . C', Si . . . Si', H . . . C, H . . . C', H . . . Si' nonbonded distances and the amplitudes of vibration of the SiH, SiC, CC' bonded and Si . . . C', Si . . . Si', H . . . C, H . . . C', H . . . Si' nonbonded atom pairs. The H . . . H amplitudes of vibration were fixed at suitable values because the peaks corresponding to the H . . . H nonbonded distances do not contribute significantly to the overall intensity.

The HSiC angle was taken as the average of the three triangles defined by the SiH, SiC, and HC atom pairs, the SiH, SiC' and HC' atom pairs and the SiH, SiSi' and HSi' atom pairs respectively.

Digermyl acetylene refinements

The radial distribution curve, P(r)/r is shown in figure 3.8. The major peaks belong to the Ge-C bonded, the Ge . . . C' nonbonded atom pairs and the Ge . . . Ge nonbonded atom pair distances at 1.9 Å, 3.1 Å and 5.0 Å respectively.

Satisfactory refinements were carried out on the GeH, GeC, CC' bonded distances, the Ge . . . C', Ge . . . Ge' nonbonded distances and the amplitudes of vibration of the GeH, GeC bonded and Ge . . . C', Ge . . . Ge', H . . . Ge' nonbonded atom pairs.

The amplitude of vibration of the CC' bonded distance would not refine, tending to vanish if refined. This amplitude was fixed at a reasonable value[27]. The H . . . H, H . . . H', H . . . C and H . . . C' nonbonded amplitudes of vibration were fixed to suitable values. The H . . . Ge' nonbonded amplitude refined to a reasonable value.

Figure 3.8 $P(R)/R - GeH_3CCGeH_3$

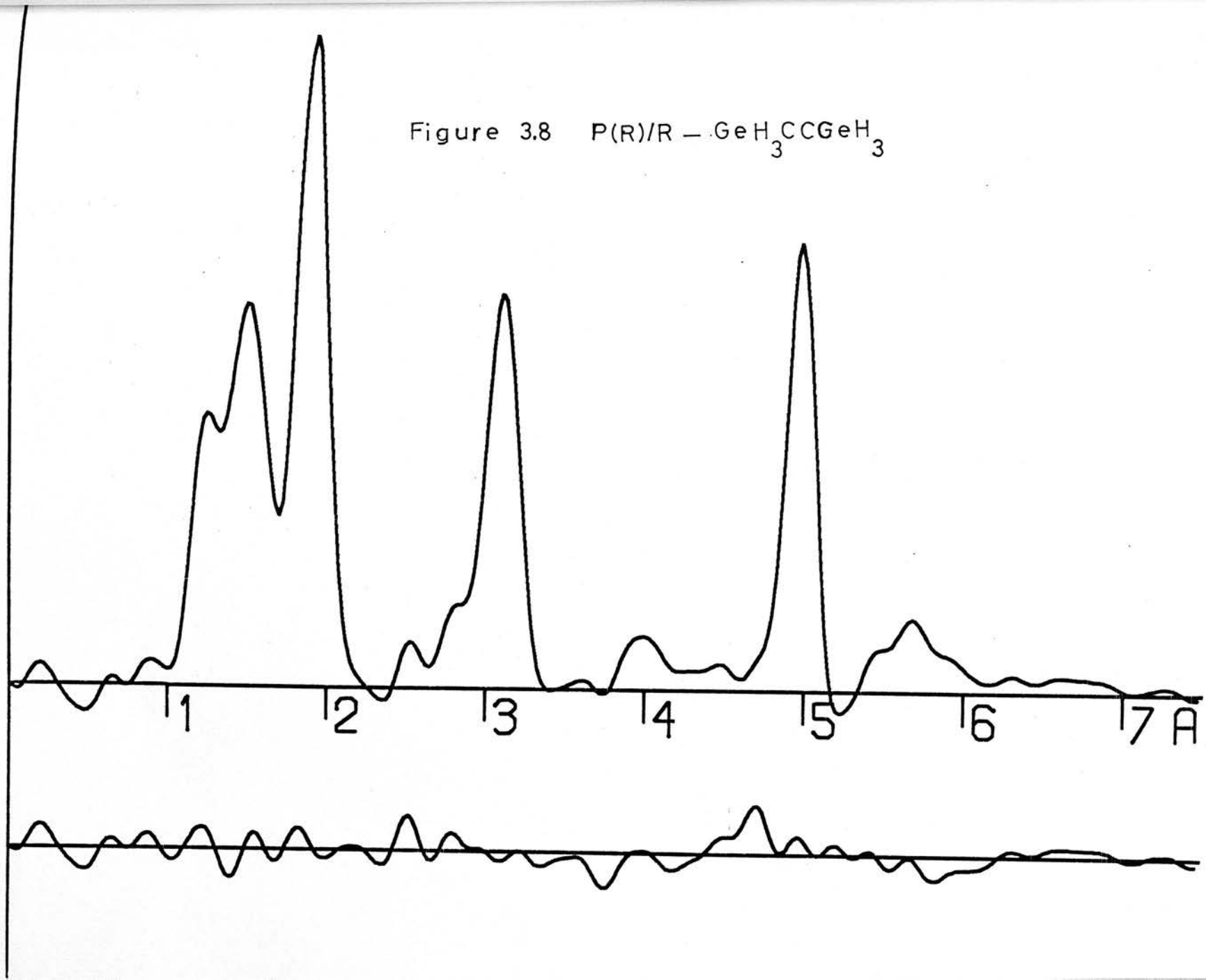

The Ge . . . Ge' nonbonded peak was very asymmetric in the radial distribution curve. One reason is the magnitude of the relative populations in the ground state and states involving the two skeletal bending deformations. Since the lowest of the excited states is that state having an excited symmetric bending deformation and an energy of about $\frac{1}{2}$ KT above the ground state, the relative population is approximately 60% of the ground state population. The larger wing of this asymmetric peak will be to shorter distances.

Asymmetric peaks also appear because of large amplitudes of vibrations occurring for atoms associated with the bending mode. This is illustrated in figure 3.9. Consider the amplitude of vibration in a linear molecule XYZ. The amplitude moves the atom Z from Z' to Z'' and back. When Z is at Z', the effective nonbonded X . . . Z distance has been shortened to XQ as shown in figure 3.9a. The distribution of the XZ distance r(XZ) is shown in figure 3.9b. Each point on the distribution curve is broadened by the skeletal vibrations so that the overall distribution curve is as shown in figure 3.9c: an asymmetric peak. The asymmetry is more pronounced when the bonds are associated with excited vibrational states because excited states have larger amplitudes of vibration than ground state vibrations.

Use of a negative anharmonicity with the Ge . . . Ge' distance will predict some of the asymmetry of the peak, even though no physical significance can be attached to this anharmonicity. More reliable distances and hence shrinkages for the Ge - C - C - Ge chain are obtained if negative anharmonicities are used in such

figure 3.9 The Effect of the Amplitude of Vibration on the XZ Non-bonded Distance

a

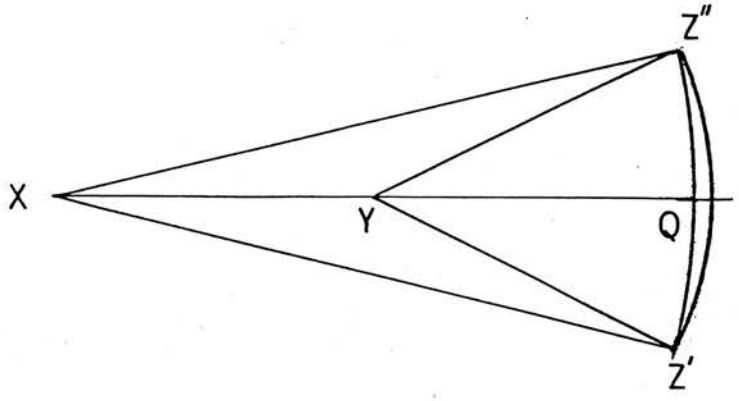

b

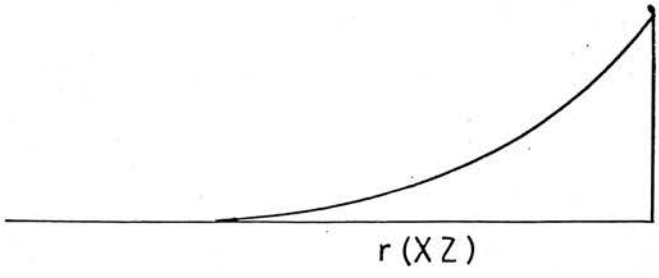

c

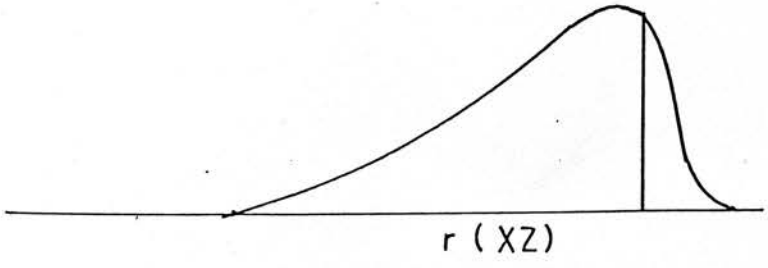

circumstances. The best fit to the peak was obtained by refining the stable parameters at different anharmonicities and then plotting the Ge . . . Ge distance, the amplitude and the overall R factor (RG) against the anharmonic constant (figure 3.10). The minimum in the RG curve gave the value of the anharmonic constant with the best overall fit to the data. The Ge . . . Ge distance and amplitude of vibration could then be read directly from the graph.

The final parameters and least squares correlation matrices obtained for disilyl and digermyl acetylenes are given in tables 3.5, 3.6 and 3.7. The lowest R factor obtained for disilyl acetylene was 0.15 and for digermyl acetylene, 0.21.

3.4 Results and Discussion

Disilyl and silyl chloro-acetylene have SiC bond lengths of 1.825 Å and 1.811 Å respectively. These are similar to those observed in the electron diffraction studies of silyl acetylene (1.813 Å)[1], trimethyl silyl acetylene (1.827 Å) and trimethyl silyl chloro-acetylene (1.827 Å)[28]. All of these SiC bond lengths are (0.05-0.06) Å shorter than the SiC bond lengths of the methyl silanes[29]. Digermyl and germyl chloro-acetylene have GeC bond lengths of 1.906 Å and 1.926 Å respectively. These values agree with the GeC bond lengths of other germyl acetylenes determined by electron diffraction[28] and microwave studies[25] and are (0.05-0.07) Å shorter than the GeC bond lengths in methyl germanes. The shortening of the M - C bond length in acetylenes has been attributed to an increased 's' character contributed from the M atom.

The range of the C ≡ C bond lengths observed for the four molecules is wider than the range in other acetylenes. In silyl

Table 3.5a. Molecular Parameters for SiH_3CCSiH_3

A. Independent Distances

		Distance (Å)	Amplitude
R1	Si H	1.462±0.006	0.087±0.006
R2	Si C	1.825±0.003	0.049±0.006
R3	C C'	1.206±0.005	0.024±0.012
R4	Si C'	3.028±0.005	0.060±0.004
R5	Si Si'	4.817±0.008	0.081±0.004
R6	H C	2.658±0.017	0.115±0.018
R7	H C'	3.768±0.031	0.219±0.036
R8	H Si'	5.475±0.025	0.223±0.022

B. Dependent Distances

1	H H	1.642±0.008	0.21 (fixed)
2	H H'	4.151±0.032	0.2 (fixed)
3	H H'	4.862±0.029	0.2 (fixed)

D. Dependent Angles

1	(C-Si-H)	108.58±(0.6)
2	(H-Si-H)	110.35±(0.6)

Table 3.5b. Molecular Parameters for GeH_3CCGeH_3

A. Independent Distances

		Distance (Å)	Amplitude
R1	Ge H	1.494±0.012	0.095±0.010
R2	Ge C	1.907±0.005	0.037±0.007
R3	C C'	1.216±0.013	0.034 (fixed)
R4	Ge C'	3.107±0.007	0.044±0.007
R5	Ge Ge'	4.959±0.007	0.077±0.003

B. Dependent Distances

1	H C	2.844±0.019	0.12 (fixed)
2	H C'	3.937±0.021	0.16 (fixed)
3	H Ge'	5.709±0.025	0.195±0.026
4	H H	1.595±0.009	0.2 (fixed)
5	H H'	4.079±0.029	0.2 (fixed)
6	H H'	4.830±0.022	0.2 (fixed)

C. Independent Angle

<1	(H-Ge-C)	112.92±0.25

D. Dependent Angle

<2	(H-Ge-H)	105.81±0.69

TABLE 3.6- LEAST SQUARES CORRELATION MATRIX MULTIPLIED BY 1000

DISTLYL ACETYLENE

R 1	R 2	R 3	R 4	R 5	R 6	R 7	R 8	U 1	U 2	U 3	U 4	U 5	U 6	U 7	U 8	K 1	K 2	K 3
1000	164	342	-1	-19	28	48	25	-44	18	131	118	86	-18	-25	29	197	58	-81
164	1000	41	-1	-2	0	6	0	231	-85	25	-18	-15	-27	6	-3	-39	21	31
342	41	1000	5	-4	22	13	9	-129	-64	-46	-6	-24	23	-20	0	-1	-82	-73
-1	-1	5	1000	-15	284	28	8	-8	-41	-23	-103	-49	281	-84	-13	-54	-109	-61
-19	-2	-4	-15	1000	14	2	87	-3	-13	-10	-13	-50	-1	11	-112	-23	-20	-7
28	0	22	284	14	1000	-83	15	36	71	43	-109	8	12	-50	20	127	-212	-336
48	6	-13	28	2	-83	1000	-119	15	-5	7	36	-5	39	-1	44	15	-22	-9
25	0	9	8	87	15	-119	1000	7	0	12	-3	49	2	7	-71	9	-35	-13
-44	231	-129	-8	-3	36	15	7	1000	111	152	109	79	-18	11	20	168	20	28
18	-85	-64	-41	-13	71	-5	0	111	1000	282	457	369	-44	12	83	718	290	35
131	25	-46	-23	-10	43	7	12	152	282	1000	212	174	-28	0	43	358	107	0
118	-18	-6	-103	-13	-109	36	-3	109	457	212	1000	310	-19	3	72	597	334	94
86	-15	-24	-49	-30	8	-5	49	79	369	174	310	1000	-58	10	5	489	334	58
-18	-27	23	281	-1	12	39	2	-18	-44	-28	-19	-58	1000	-65	-15	-75	-121	-10
-25	6	-20	-84	11	-50	-1	7	11	12	0	3	10	-65	1000	9	11	56	54
29	-3	0	-13	-112	20	44	-71	20	83	43	72	3	-15	9	1000	117	54	-49
197	-39	-1	-54	-23	127	15	9	168	718	358	597	489	-75	11	117	1000	293	2
58	21	-82	-109	-20	-212	-22	-35	20	290	107	334	334	-121	56	54	293	1000	108
-81	31	-73	-61	-7	-336	-9	-13	23	35	0	94	58	-10	54	-49	2	108	1000

TABLE 3.7- LEAST SQUARES CORRELATION MATRIX MULTIPLIED BY 1000

DIGERNYL ACETYLENE

R 1	R 2	R 3	R 4	R 5	< 1	U 1	U 2	U 3	U 4	U 5	U 8	K 1	K 2	K 3
1000	116	309	32	-45	-218	97	-79	99	67	82	9	126	9	-102
116	1000	-5	22	3	-69	326	-68	59	12	-5	-6	-4	-19	12
309	-5	1000	13	13	-74	-147	-46	-59	-21	-30	-8	-25	-51	-54
32	22	13	1000	-11	184	3	-19	1	-50	-8	-16	-1	-33	-20
-45	3	13	-11	1000	-40	-50	-233	-51	-198	-513	-50	-367	-212	-33
-218	-69	-74	184	-40	1000	-11	15	-16	-14	-51	-66	-2	-237	-224
97	326	-147	3	-50	-11	1000	-12	197	78	97	6	148	11	-3
-79	-68	-46	-19	-233	15	-12	1000	38	334	454	75	608	315	80
99	59	-59	1	-51	-16	197	38	1000	80	100	10	150	30	-3
67	12	-21	-30	-198	-14	78	334	80	1000	390	67	516	293	73
82	-5	-30	-8	-513	-51	97	454	100	390	1000	101	711	447	88
9	-6	-8	-16	-50	-66	6	75	10	67	101	1000	101	167	0
126	-4	-25	-1	-367	-2	148	608	150	516	711	101	1000	365	61
9	-19	-51	-33	-212	-237	11	315	30	293	447	167	365	1000	101
-102	12	-54	-20	-33	-224	-3	80	-3	73	88	0	61	101	1000

figure 3.10

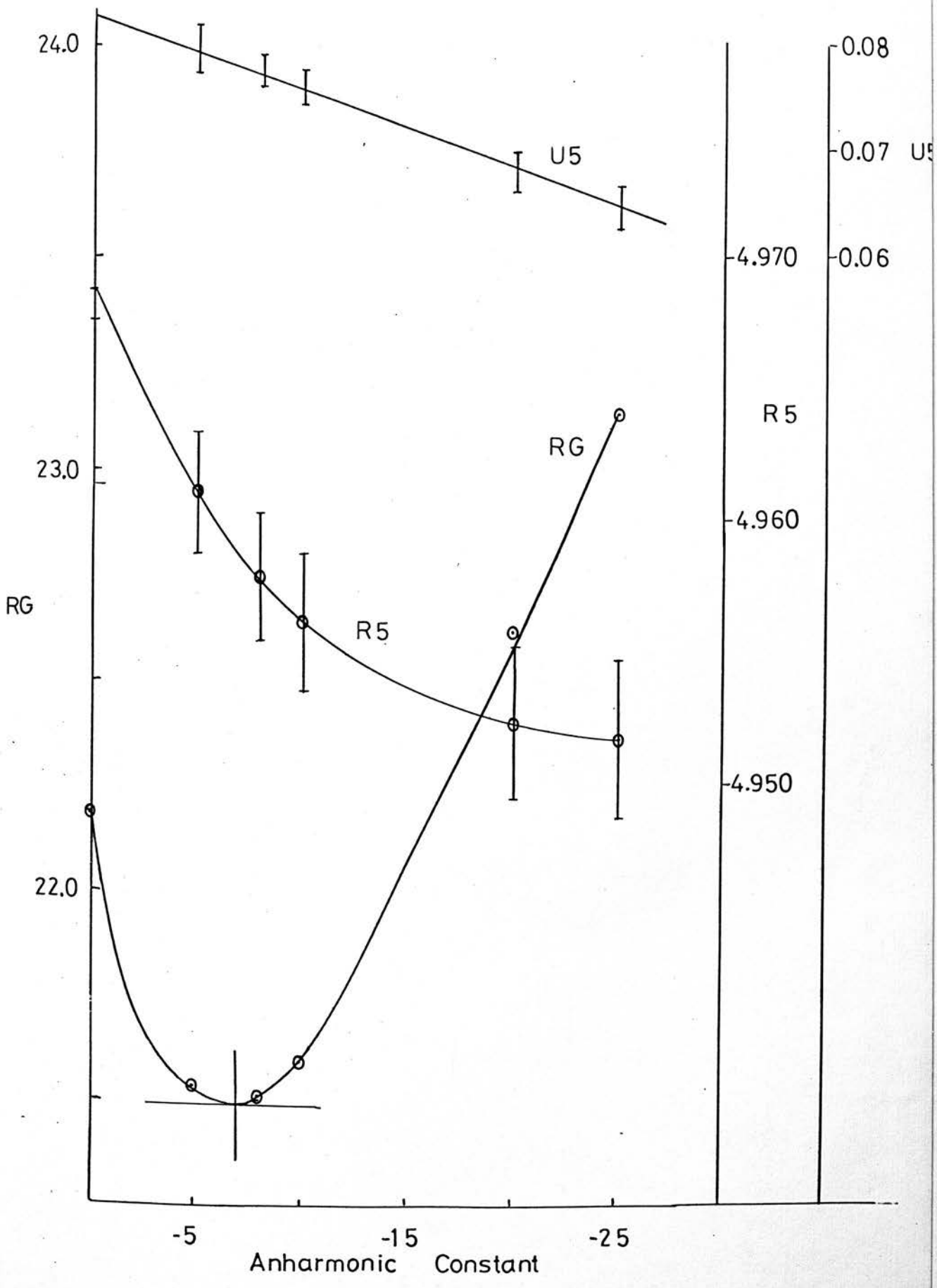
24.0
23.0
22.0
RG
U5
R5
RG
0.08
0.07
0.06
4.970
4.960
4.950
R5
-5
-15
-25
Anharmonic Constant

chloro-acetylene, the value of 1.232 Å for the C ≡ C bond length is exceptionally long compared to the normal range of 1.205 Å to 1.212 Å. The C - Cl bond length in this molecule, however, is shorter than the average value: 1.602 Å instead of (1.630 - 1.637) Å. These variations suggest considerable rearrangement in the electron density within the molecule. Germyl chloro-acetylene, on the other hand, seems to have more reasonable values for the C ≡ C and C - Cl bond lengths (1.211 Å and 1.635 Å respectively) even though the uncertainties in these parameters are much larger than in silyl chloro-acetylene.

In digermyl acetylene, the C ≡ C bond length (1.216 Å) is long compared to the normal range for this bond, whereas the value in disilyl acetylene (1.206 Å) is well within the normal range.

These acetylenes, as expected, have shrinkages associated with distances greater than a single bond length along the linear chain. The shrinkages are given in table 3.8. The shrinkages are larger in magnitude for the germyl acetylenes than the silyl acetylenes. This is due to the larger mass of germanium causing larger amplitudes of vibration, which in turn make the germanium atom spend more time, on average, away from the equilibrium structure.

Within the experimental limits, the two bond shrinkages are similar in size to the three bond shrinkages in the two chloro-acetylenes. In the disubstituted acetylenes, however, they are significantly smaller than the three bond shrinkages. This suggests that the vibrational modes mainly responsible for the shrinkages are different in the two cases. Care is needed in such an interpretation because observed shrinkages are subject to large errors.

Table 3.8. Bond Shrinkages

Compound	Bond	Bond Length	2 Bond Shrinkage	3 Bond Shrinkage
SiH_3CCCl	R5	2.998	0.045(20)	-
	R6	4.641	-	0.022(20)
	R7	2.831	0.021(15)	-
GeH_3CCCl	R5	3.072	0.065(45)	-
	R6	4.701	-	0.071(50)
	R7	2.789	0.057(50)	-
SiH_3CCSiH_3	R4	3.028	0.003(13)	-
	R5	4.817	-	0.038(20)
GeH_3CCGeH_3	R4	3.107	0.014(25)	-
	R5	4.959	-	0.071(30)

Generally, the data obtained for these four acetylenes are not particularly good. It should be possible, with care, to obtain more reliable sets of parameters. Use of electron diffraction with microwave determinations enable a higher accuracy to be obtained than by each technique individually by eliminating many of the faults inherent in each method.

Over the last few years a number of acetylenes have been studied by microwave and electron diffraction techniques in the hope of elucidating effects such as hyperconjugation and p → d 'π' bonding[37,38,39]. These effects have been implied by variations in bond lengths at the present limits of experimental observation. Often comparison of bond lengths is not very satisfactory because the bond length observed is dependent on the technique employed.

In addition to variations in bond lengths caused by the techniques employed, there are other problems associated with the determination of structures. Unless sufficient isotopic species are analysed in microwave studies only partial structures can be deduced. This inevitably means that assumptions are made concerning the lengths of some bonds; for example, the C ≡ C bond distance in methyl bromoacetylene was assumed to be 1.207 $\pm$ 0.004 Å even though an electron diffraction study of bromo-acetylene suggested that the bond length could have been outside of this range.

If one of the atoms lies near the centre of mass of the molecule, for example the C_F atom in fluoro-acetylene, the individual bond distances to that atom are not well defined even though the overall chain distance may be accurately known. Isotopic substitution causes a change in the bond length . Sometimes, neglect of this change can

cause large errors to occur in the determination of other bond lengths; for example in the determination of the structure of vanadyl (V) chloride[32], the rotational constant B_{α}^{o} calculated from electron diffraction studies and the rotational constant, B_Z determined from microwave studies differ significantly. When, however, the isotopic variation of the V - Cl bond length (6×10^{-5} Å) was taken into account, the rotational constants became compatible within the experimental limits.

On the other hand, electron diffraction techniques give accurate ratios of different bond lengths as long as the peaks are well defined on the radial distribution curve. The absolute value of each bond length depends on correct scaling of the radial distribution curve, which is dependent on the accuracy of the electron wavelength employed and the measurement of camera height.

The structure of the four acetylenes studied along with those of related compounds are shown in table 3.9. The type of bond length determined is quoted together with the reference. A description of each type of bond length has been given by Robiette[30].

The results obtained indicate that there appears to be little correlation between the C ≡ C bond lengths and the substituent attached to the acetylene. The C ≡ C bond lengths vary more than the 0.008 Å spread assumed from microwave studies (r_g values range from 1.200 Å to 1.232 Å). The CH bond lengths are fairly constant (1.050 Å to 1.060 Å) as are the C-halogen bond lengths except in silyl chloro-acetylene where the value found was shorter than the normal range.

The C - C acetylenic bond lengths, however, vary considerably. Both methyl acetylene and methyl chloro-acetylene have bond lengths

Table 3.9. Structure of Some Related Acetylenes

Molecule	Distance Type	$r_{C\equiv C}$	$r_{\equiv C-X}$	$r_{\equiv C-M}$	Ref.
$HC\equiv CH$	r_g	1.2120(4)			83
$CH_3C\equiv CH$	r_o	1.2073	1.0582	1.4577	52,55
$(CH_3)_2CHC\equiv CH$	r_s	1.200(5)	1.050(4)	1.495(11)	57
$(CH_3)_3CC\equiv CH$	r_s	1.209(1)	1.055(1)	1.50(est.)	76
$CF_3C\equiv CH$	r_g	1.211(5)		1.500(5)	77
$CH_3C\equiv CCH_3$	r_g	1.2135(6)	-	1.4675(5)	83
$(CH_3C\equiv C)_2$	r_g	1.210(2)		1.434	78
$HC\equiv CCl$	r_s	1.204	1.637	1.055	79
$CH_3C\equiv CCl$	r_o	1.2069(5)	1.6371(5)	1.458(5)	80
$(CH_3)_3CC\equiv CCl$	r_g	1.210(5)	1.637(5)	1.468(5)	81
$CF_3C\equiv CCl$	r_o	1.199(5)	1.627(9)	1.453(2)	82
$SiH_3C\equiv CH$	r_g	1.221(5)	1.075(19)	1.813(4)	1
$(CH_3)_3SiC\equiv CH$	r_g	1.200(8)	1.050(5)	1.825(6)	28
$SiH_3C\equiv CSiH_3$	r_g	1.206(5)	-	1.825(3)	-
$SiH_3C\equiv CCl$	r_g	1.232(6)	1.620(4)	1.811(6)	-
$(CH_3)_3SiC\equiv Cl$	r_g	1.210(8)	1.630(5)	1.825(8)	28

...continued

Table 3.9 (Continued)

Molecule	Distance Type	$r_{C\equiv C}$	$r_{\equiv C-X}$	$r_{\equiv C-M}$	Ref.
SiH_3CCCF_3	r_g	1.207(9)	1.472(11)	1.825(6)	1
$GeH_3C\equiv CH$	r_o	1.208(1)	1.056	1.896(1)	25
$GeH_3C\equiv CGeH_3$	r_g	1.216(13)	-	1.907(5)	-
$GeH_3C\equiv CCl$	r_g	1.211(20)	1.635(13)	1.926(10)	-
$(CH_3)_3GeC\equiv CCl$	r_g	1.215(5)	1.630(5)	1.930(7)	28
$HC\equiv CBr$	r_o	1.216	1.784	1.051	58
$CH_3C\equiv CBr$	r_s	1.207(4)	1.793(5)	1.46(2)	59
$ClC\equiv CBr$	r_o	1.209(8)	1.790(5)	1.628(5)	84
$HC\equiv CF$	r_s	1.198	1.279	1.053	79

of 1.458 Å, which is shorter than in t-butyl acetylene (1.500 Å), t-butyl chloro-acetylene (1.466 Å) and i-propyl acetylene (1.495 Å). The C_{methyl} - $C_{tert.}$ bond length in the t-butyl acetylenes are also shorter than the corresponding bond length in t-butane[31].

A similar effect is observed in the corresponding silicon compounds. Electron diffraction studies show that the Si - C bond lengths in silyl acetylene (1.813 Å) and silyl chloro-acetylene (1.811 Å) are shorter than in trimethyl silyl acetylene (1.827 Å) and trimethyl silyl chloro-acetylene (1.827 Å). Similarly the C_{methyl} - Si bond lengths are shorter than those in trimethyl silane[29].

The lengths, however, of the Ge - C bonds in germyl chloro-acetylene (1.926 Å) and trimethyl germyl chloro-acetylene (1.930 Å) do not show the shortening observed in the methyl and silyl analogues, although it should be pointed out that the value in germyl chloro-acetylene is subject to a large standard deviation. In germyl acetylene, this bond length is shorter at 1.90 Å. The C - C, Si - C, and Ge - C bond lengths in dimethyl acetylene (1.4675 Å), disilyl acetylene (1.825 Å) and digermyl acetylene (1.907 Å) do not fit very well in the above scheme because although the bond lengths in dimethyl and digermyl acetylenes are shortened, the disilyl acetylene has a long Si - C bond compared to the other silyl acetylenes.

Trends in bond lengths are not readily observed even when the standard deviations are of the order 0.005 Å. This suggests that bond lengths are fairly insensitive to changes in bonding energy of the molecular orbitals and substituent effects about the bond.

It is now possible by combining microwave spectroscopy with electron diffraction studies to overcome many of the problems

inherent in each separate technique. It is possible to reduce the standard deviation to less than 0.001 Å. The spread in bond lengths of these acetylenes suggests that this order of standard deviation would be enough to distinguish trends among related compounds.

CHAPTER 4

The Infra Red and Raman Spectra of Some Silyl and Germyl Acetylenes

4.1 Introduction

The gas phase infra red spectra of silyl chloro-acetylene and its deuterated analogue, silyl bromo-acetylene, germyl chloro-acetylene, disilyl acetylene and digermyl acetylene have been recorded over the range 40 cm^{-1} to 4500 cm^{-1}. The infra red spectra of silyl and germyl perfluoromethyl acetylenes were reassigned with the help of the spectra of their deuterated analogues.

The raman spectra of these acetylenes in the liquid phase were recorded and preliminary studies were made on silyl chloro- and disilyl acetylene in the gas phase.

Overtone and combination bands have been assigned on the basis that the band frequency does not differ significantly from the sum of the fundamental frequencies involved. Often more than one combination or overtone can be assigned to a given frequency. If some of these combinations cannot be eliminated by comparison with similar molecules or from their band shape, then all plausible assignments are given.

Analysis of the Q branch fine structure is dealt with in chapters 5 and 6. Any frequencies quoted for the band centres of such perpendicular bands are derived from that analysis.

The vibrational spectrum of disilyl acetylene has been recorded by Lord[4] although the lowest fundamental frequency was not observed. The analysis of the rotational fine structure associated with the perpendicular silyl bands only showed that the spacing was consistent with a very low barrier to internal rotation. In the present work, the lowest frequency has been observed and the fine structure reanalysed with additional data.

Anderson[1] has assigned the infra red spectra of the silyl and the germyl perfluoromethyl acetylenes, but the asssignments did not

take account of a low bending vibration at about 100 cm^{-1}. The spectra have been reassigned with the help of data for the fully deuterated species.

4.2 The Vibrational Spectra of MH_3CCX; M = Si, Ge; X = Cl, Br

Molecules of the type MH_3CCX where M = Si, Ge and X = Cl, Br have overall C_{3V} symmetry. They have $5a_1$ and 5e normal modes of vibration, each mode being infra red and raman active. These modes with the approximate description of the vibration concerned are listed in table 4.1.

Usually the assignment of these spectra are straightforward. The three bands that show rotational fine structure can be assigned to the perpendicular modes; the MH stretch, ν_6; the MH deformation, ν_7; and the MH_3 rock, ν_8. The band occurring near to the centre of ν_6 will be the parallel mode of the MH stretch, ν_1, and the band near to the centre of ν_7 will be the MH deformation, ν_3. The acetylenic stretch, ν_2 is expected in the 2100 cm^{-1} to 2200 cm^{-1} region and could be close enough to ν_1 to mix extensively with this band.

The two remaining a_1 modes, ν_4 and ν_5, correspond to the M - C and C - X stretching vibrations, though they are not well described as purely one type or the other, generally occurring outside the normal range of values for such modes in acetylenes[33,34]. This suggests extensive interaction of the "group vibrations" due to the proximity in frequency and substantial mechanical coupling in the molecules. Similarly, the two remaining e modes, ν_9 and ν_{10} are not well described as purely M - C ≡ C or X - C ≡ C bending vibrations.

Table 4.1. The Fundamental Modes of MH_3CCX

Description of mode	a_1 symmetry	e symmetry
MH stretch, ν_{MH}	ν_1	ν_6
C≡C stretch, ν_{CC}	ν_2	
MH deformation, δ_{MH}	ν_3	ν_7
MC stretch[a], ν_{MC}	ν_4	
CX stretch[a], ν_{CX}	ν_5	
MH_3 rock, ρ_{MH_3}		ν_8
M-C≡C deformation, δ_{MCC}		ν_9
C≡C-X deformation[b], δ_{CCX}		ν_{10}

a) These skeletal stretches are heavily coupled.

b) These skeletal deformations are heavily coupled.

The vibrational spectra of silyl chloro-acetylene and its deuterated analogue

The infra red spectra of silyl chloro-acetylene and the fully deuterated analogue are shown in figure 4.1. The fundamental frequencies given by the infra red and raman spectra are listed in table 4.2. The assignments of frequencies to overtone and combination bands are given in tables 4.3 and 4.4.

The gas phase raman and infra red frequencies of the fundamental bands are in good agreement. The position of the silyl stretch, ν_6, in the raman spectrum is not known with any degree of accuracy because it is a weak shoulder on the side of the other silyl stretch, ν_1. The higher frequency in the raman of the acetylenic stretch, ν_2, appears somewhat anomalous although this shift can be explained by a series of "hot" bands altering the band shape in the two spectra.

The discrepancy between the frequencies of the silyl deformation, ν_7, is due to the different mechanisms involved in infra red and raman spectroscopy. The infra red gives strong ^{P}Q and ^{R}Q branches while the raman effect produces strong ^{O}Q and ^{S}Q branches. The position of the centres of the Q branch progressions depends on the moments of inertia, the coriolis constant and the band origin, with the result that the $^{R}Q_o$ and $^{S}Q_o$ branches are in different positions. The values shown are consistent with this pattern.

The $^{R}Q_o$ branch of the silyl rock could be at one of two frequencies, 683.4 cm^{-1} or 694.7 cm^{-1}. Analysis of the rotational structure did not help in clarifying the problem, although the raman frequency and that of the overtone, $2\nu_8$ at 1365 cm^{-1} in the infra red

Table 4.2. The Fundamental Frequencies of SiH_3CCCl and SiD_3CCCl (Gas Phase).

Mode	SiH_3CCCl		SiD_3CCCl
	IR(cm^{-1})	Raman (cm^{-1})	IR (cm^{-1})
ν_1	2193.1	2199	1574.8
ν_2	2164.3	2171	2166.7
ν_3	938.9	941	691.2
ν_4	917.1	917	922.5
ν_5	436	434	420
ν_6	2192.4	2196	1603.5
ν_7	946.6	936	676.5 or 665.8
ν_8	693.7 or 682.4	685	535
ν_9	351	349	344
ν_{10}	124	119	116

Table 4.3a Assignments of i.r. Frequencies of SiH_3CCCl (gas phase)

$\nu(cm^{-1})$	Strength	Structure	Assignment
4390.7 4383.0	vw	PR	$2\nu_2$
4354	vw		
4319.2	vw	centre of 'Q' branch	$2\nu_6$ (e)
4317.6 4310.8	vw	PR	$2\nu_6$ (a_1)
3128.6	vw	centre of 'Q' branch[a]	$\nu_3 + \nu_6$
3111.7 3102.2	vw	PR	$\nu_1 + \nu_4$
2970	w	-	$\nu_1 + \nu_5 + \nu_9$
2935	vw	-	$\nu_2 + \nu_5 + \nu_9$
2876	vw	-	$\nu_6 + \nu_8$, $\nu_1 + \nu_8$
2621	vw	-	$\nu_1 + \nu_5$, $\nu_5 + \nu_6$
2590	w	PR	$\nu_2 + \nu_5$
2195.1	vs	centre of 'Q' branch	ν_6
2198.3 2188.0	vs	PR	ν_1
2169.7 2159.0	vs	PR	ν_2
1889.2	vw	centre of 'Q' branch	$2\nu_7$
1890 1881	vw	PR	$2\nu_3$
1875 1867	w	PR	$\nu_3 + \nu_4$
1824	w	-	$2\nu_4$
1652	vw	-	
1620	vw	-	$\nu_3 + \nu_8$
1460	vw	-	$\nu_5 + \nu_8 + \nu_9$
1374.2	vw	centre of 'Q' branch	$2\nu_8$ (e)
1365	w	-	$2\nu_8$ (a_1)

continued/....

Table 4.3a continued

ν (cm^{-1})	Strength	Structure	Assignment
1264 1259	vw	PR	$\nu_4 + \nu_9$
1206	vw	-	
1195	vw	-	$\nu_6 + 2\nu_{10}$
1171	vw	-	
1157	vw	-	$\nu_8 + \nu_9 + \nu_{10}$
1142	vw	-	
1095	vw	-	
1050	vw	-	$\nu_3 + \nu_{10}$
992.2	vw	centre of 'Q' branch[a]	
950.7	s	centre of 'Q' branch	ν_7
943.3 938.9 934.6	vs	PQR	ν_3
921.2 913.0	m	PR	ν_4
810	w	-	$\nu_8 + \nu_{10}$
694.7 or 683.3	s	centre of 'Q' branch	ν_8
476 464	w	PR?	$\nu_9 + \nu_{10}$
436	s	-	ν_5
351	w	-	ν_9
310	vw	-	
230	w	-	$2\nu_{10}$
124	m	-	ν_{10}

a see text

Table 4.3b Assignments of Raman Frequencies of SiH_3CCCl (gas phase)

ν (cm^{-I})	Strength	Structure	Assignment
2I99	vs	-	ν_1
2I96	w	br sh	ν_6
2I7I	m	br	ν_2
2I62		br	$\nu_2 + \nu_9 - \nu_9$
2I52		br	$\nu_2 + 2\nu_9 - 2\nu_9$
2I42		br	$\nu_2 + 3\nu_9 - 3\nu_9$
2I33		br	$\nu_2 + 4\nu_9 - 4\nu_9$
2I2I 2II5	w	PR/SO	
994	sp	sp	
990		sp	
955		sp	
947		sp	
94I	s	Q	ν_3
936		br	ν_7 ???
9I7	m	Q	ν_4
900		sp	
685	w	-	ν_8
670	m	-	
434	s	-	ν_5
354 345	s	PR/SO	ν_9
243 235	w	PR/SO	$2\nu_{10}$
I24 II4	s	PR/SO	ν_{10}

Key to Symbols

vw - very weak

w - weak

m - medium

s -strong

vs - very strong

br - broad

sh - shoulder

sp - spike

DP - depolarised

P - polarised

SD - standard deviation

Bond lengths are quoted in Angstroms and I.R. band frequencies and energy levels are quoted in cm^{-I} unless otherwise stated

Table 4.4a Assignments of i.r. Frequencies of SiD_3CCCl (gas phase)

ν (cm^{-1})	Strength	Structure	Assignment
2580	w.	–	$\nu_2+\nu_5$
2170.7 2162.7	vs	v. asym: PR	ν_2
1603.5	s	centre of 'Q'	ν_6
1578.9 1574.8 1570.3	vs	PQR	ν_1
1265	w	-	$\nu_4+\nu_9$
926.6 918.5	m	PR	ν_4
695.8 682.2	vs	PR	ν_3
676.5 or 665.8	s	centre of 'Q'	ν_7
535	m	'C' type band	ν_8
420	m	-	ν_5
344	vw	-	ν_9
116	m	-	ν_{10}

Table 4.4 b Assignments of Raman Frequencies of SiD_3CCCl (liq.)

ν (cm^{-I})	Strength	Polarization	Assignment
2I65	m	60%	ν_2
I600	m	DP	ν_6
I570	vs	70%	ν_1
680	s	30%	ν_3, ν_7
423	m	60%	ν_5
343	s	DP	ν_9
II6	m	DP	ν_{10}

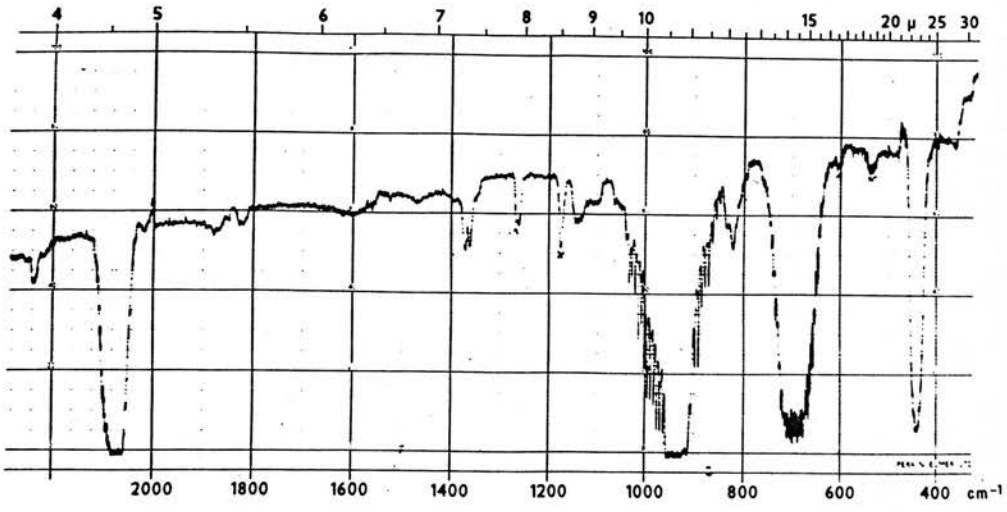

Figure 4.I a) IR Spectrum of SiH_3CCCl

b) IR Specrtum of SiD_3CCCl

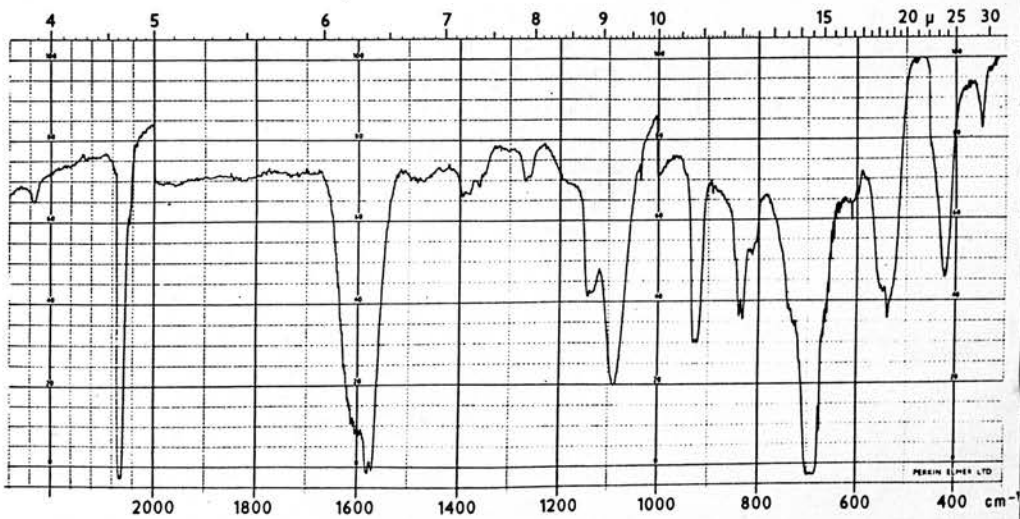

spectrum suggests that the former frequency is more likely: small anharmonicities being observed for this overtone in other silyl compounds.

Substitution of hydrogen by deuterium affects the vibrational frequencies as expected, with the greatest shift in frequency occurring for the five silyl modes. All the modes, except the skeletal stretch, ν_4, decrease in frequency on deuteration; ν_4 increases in frequency because the silyl deformation, ν_3, on deuteration is removed from the vicinity of ν_4, thus decreasing the extent of interaction between them. If the interaction is strong, ν_4 will be lower in frequency than normal. Removal of this interaction will cause ν_4 to increase in frequency.

The shift in frequencies are all consistent with the Reiner-Teller product rule[35]. The calculated and observed products for the a_1 symmetry species are 0.508 and 0.517 respectively. Those of the e symmetry species are 0.346 and 0.373. 7%!

It has been observed in molecules of the type MH_3CCX, where M is a group IV 'metal' and X = H, Halogen, that the acetylenic stretching frequency, ν_2 has several "hot" bands of the type, $\nu_2 + n\nu_{10} - n\nu_{10}$ associated with it[36]. In the infra red spectrum of silyl chloro-acetylene, this region is obscured by the overlapping bands of ν_6, although ν_2 does appear to possess a PR structure. In the gas phase raman, however, a series of Q branches with rapidly decreasing intensities occur to lower frequency of the main peak (figure 4.2a). These peaks could be attributed to such a series of "hot" bands. The separation of the peaks is constant at between 9 cm^{-1} to 10 cm^{-1}. The relative intensities would fit a frequency

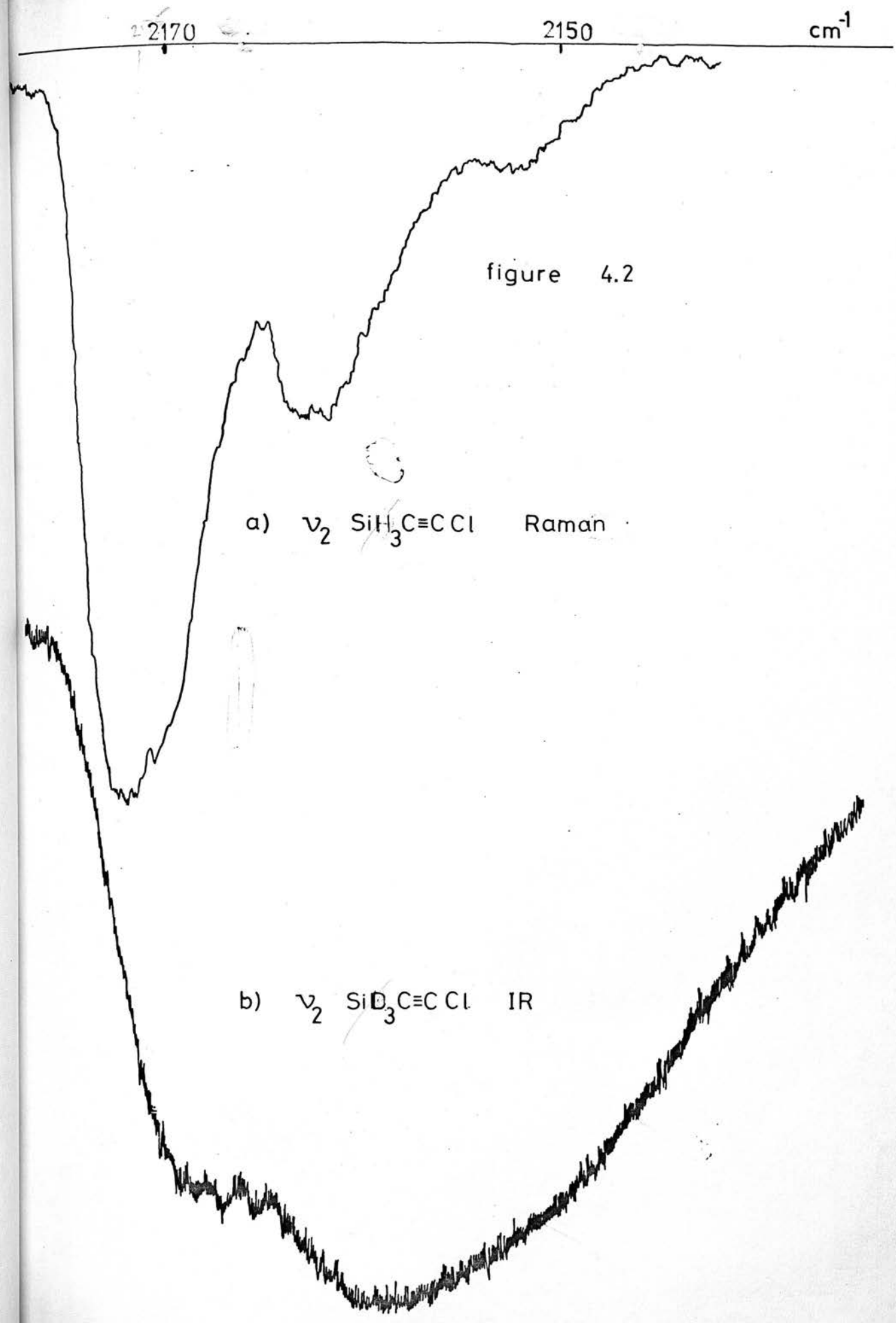

figure 4.2

of between 100 cm^{-1} to 140 cm^{-1} assuming a Boltzman distribution for the states; G.S., ν_{10}, $2\nu_{10}$, $3\nu_{10}$, . . . respectively. This value agrees well with the observed raman frequency of 118 cm^{-1} for ν_{10}.

In the infra red spectrum of deutero silyl chloro-acetylene, ν_2 should possess a similar pattern of "hot" bands.

As is shown in figure 4.2b, this band has a different band shape from the expected PR curve. This can be explained by the overlap of the PR envelopes of ν_2 with those of the series $\nu_2 + n\nu_{10} - n\nu_{10}$ as illustrated in figure 4.3.

The peak occurring at about 430 cm^{-1} in silyl chloro- and deutero silyl chloro-acetylenes, assigned to the skeletal stretch, ν_5, has no apparent structure. Raman polarization studies in the liquid phase show that this band is polarized. One explanation is that "hot" bands similar to those associated with ν_2 are present, with the result that the expected minimum in the band is obscured. Similar band shapes, although more asymmetric, are observed for ν_5 in germyl chloro- and silyl bromo-acetylene.

The gas phase raman spectrum of silyl chloro-acetylene contained some curious peaks in the 900 cm^{-1} to 1000 cm^{-1} region. There were several sharp spikes on either side of the silyl deformations, ν_3 and ν_7. These peaks are probably ^{O}Q and ^{S}Q branches of ν_7. The structure of this band was not studied in detail because the laser of the raman spectrometer was operating at reduced power. Similar structure was not observed in the ν_6 or ν_8 region of the spectrum because the bands were too weak.

ν_9 and ν_{10} have PR envelopes in the gas phase raman spectrum, consistent with the selection rules.

Figure 4.3 Theoretical IR Bandshape of the Bands $\nu_x + n(\nu_y - \nu_y)$

a) anharmonicity = 2 × PR separation : $\nu_y \simeq 120\ cm^{-1}$

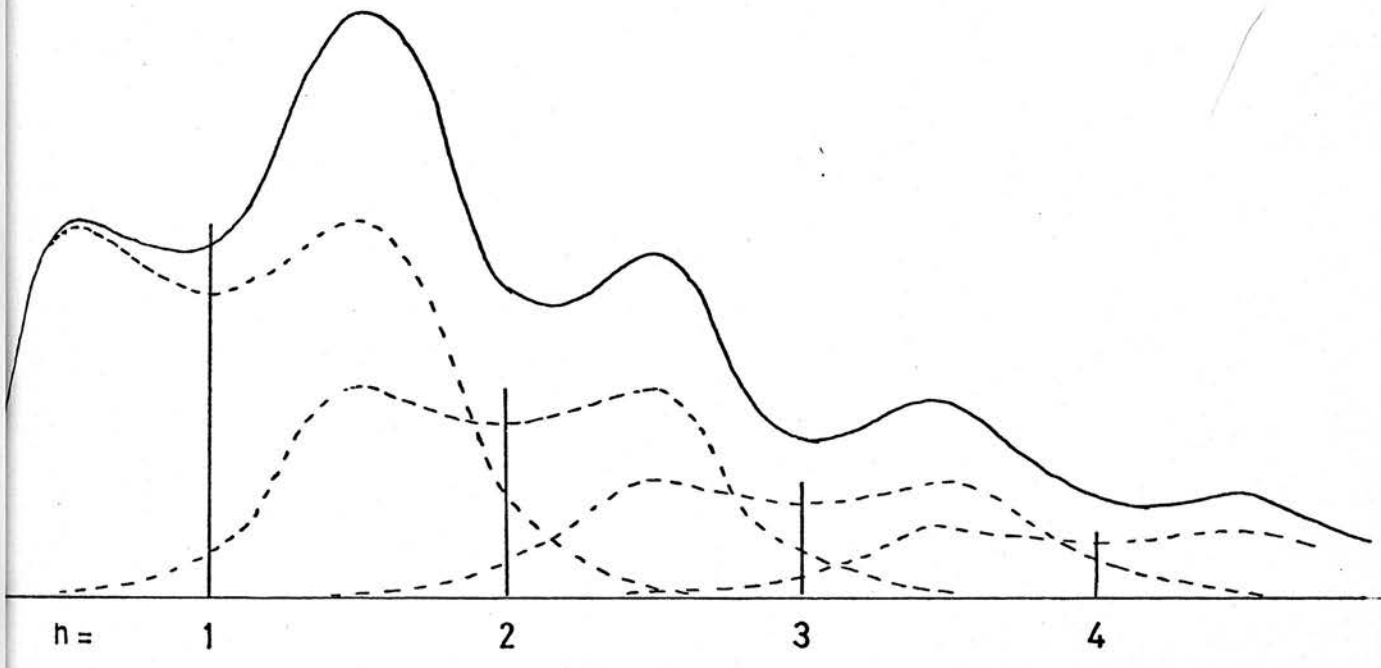

b) anharmonicity = PR separation : $\nu_y \simeq 120\ cm^{-1}$

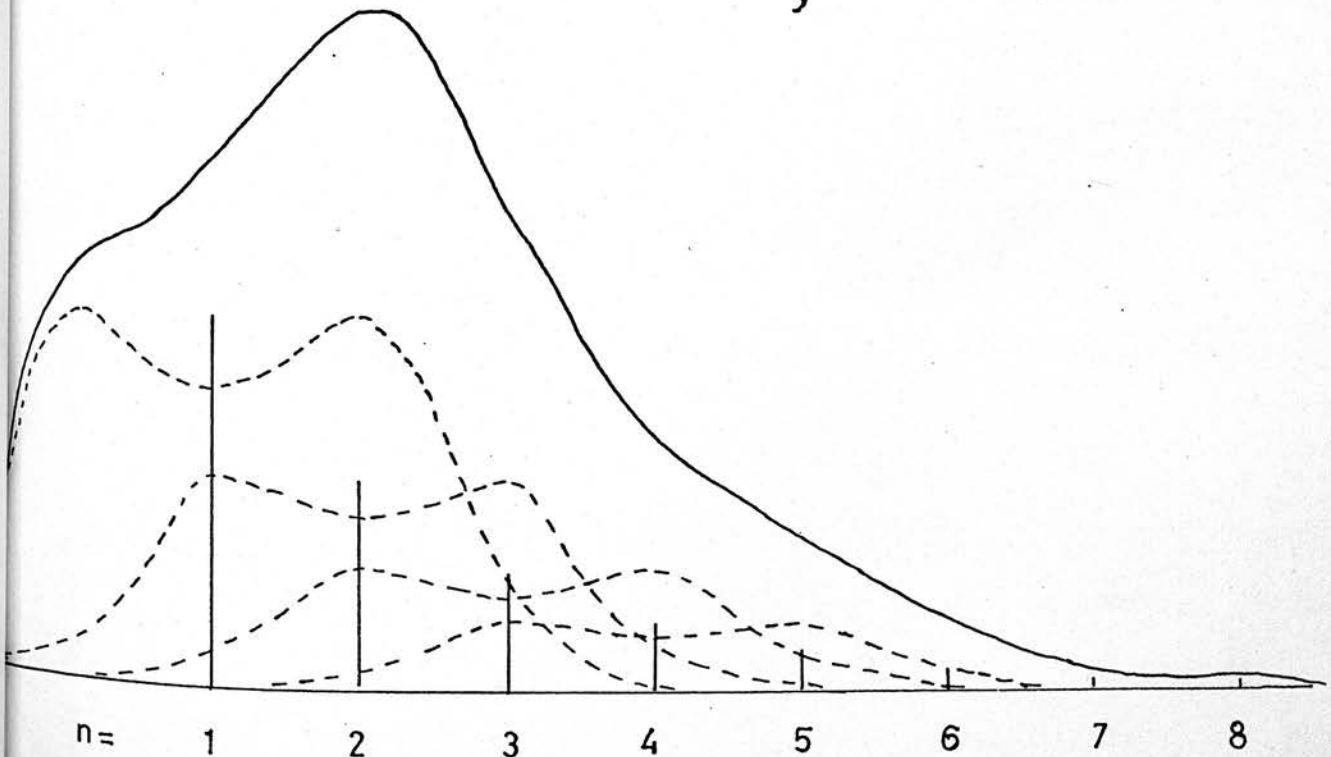

The vibrational spectra of germyl chloro-acetylene

The infra red spectrum of germyl chloro-acetylene is shown in figure 4.4. The fundamental frequencies are listed in table 4.5. The assignments of overtone and combination bands to the infra red and raman frequencies are given in table 4.6.

The acetylenic stretch, ν_2, is similar to the corresponding band in silyl chloro-acetylene (figure 4.5) being partially hidden by the overlapping Q branches of the germyl stretch, ν_6. This band does not appear to have a simple PR structure suggesting that it has "hot" bands affecting the shape of the band envelope.

Rotational structure occurs, as expected, with the germyl stretch, ν_6, the germyl deformation, ν_7 and the germyl rock, ν_8. No rotational fine structure is observed on the other two e modes, ν_9 and ν_{10}.

In germyl chloro-acetylene, ν_4, has moved to low frequency compared to the silyl analogue, reflecting the much heavier mass of the germanium atom. The band shape of ν_4 is difficult to discern due to the Q branches of ν_7 overlapping with this band. The envelope should consist of a PR structure but, as is shown in figure 4.6, it is possible that associated "hot" bands obscure the central minimum.

The infra red spectrum has a strong asymmetric band at 347 cm^{-1}, having what could be PR branches, and a medium intensity band at 219 cm^{-1} possessing no structure. These bands could be assigned to the skeletal stretch, ν_5 and skeletal deformation, ν_9 respectively.

The assignment of the 347 cm^{-1} band to ν_5 is supported by the relatively strong combination, $\nu_2 + \nu_5$ at 2512 cm^{-1} which is also

Table 4.5. The Fundamental Frequencies of GeH_3CCCl

Mode	IR	Raman[a]
ν_1	2116	2111
ν_2	2172	2166
ν_3	832.9	824
ν_4	888	880
ν_5	348	-
ν_6	2117.5	2113
ν_7	884.1	880
ν_8	624.3	622
ν_9	-	339
ν_{10}	116	123

a) liquid phase.

Table 4.6a Assignments of i.r. Frequencies of GeH_3CCCl (gas phase)

$\nu(cm^{-1})$	Strength	Structure	Assignment
4283	vw	-	$2\nu_2$, $\nu_2 + \nu_6$
4169.0	vw	centre of 'Q' branch	$2\nu_6$ (e)
4168.2 4160.3	vw	PR	$2\nu_6$ (a_1)
3060.3	vw	centre of 'Q' branch	$\nu_2 + \nu_7$
3058	vw	-	$\nu_2 + \nu_3$
2975	vw	-	
2967	vw	-	
2949 2939	vw	PR[a]	$\nu_1 + \nu_3$, $\nu_3 + \nu_6$
2867	vw	-	$\nu_2 + 2\nu_5$, $\nu_2 + \nu_9 + \nu_5$
2512	w	-	$\nu_2 + \nu_5$, $\nu_2 + \nu_9$
2172	vs	PR[b]	ν_2
2120.6	vs	centre of 'Q' branch	ν_6
2116	vs	PR[b]	ν_1
1845	vw	-	$\nu_4 + \nu_5 + \nu_8$, $\nu_5 + \nu_7 + \nu_8$
1760	vw	centre of 'Q' branch[c]	$2\nu_7$, $\nu_4 + \nu_7$
1765 1758	vw	PR	$2\nu_4$
1719	vw	br	$\nu_4 + \nu_3$, $\nu_3 + \nu_7$
1658	vw	br	$2\nu_3$
1526	vw	br	$\nu_4 + \nu_8$
1450	vw	br	$\nu_3 + \nu_8$
1366	vw	-	$\nu_5 + \nu_9 + \nu_{10}$
1248.7 1241.5	w	PR	$2\nu_8$
888	s	b	ν_4
887.6	s	centre of 'Q' branch	ν_7
836.7 829.2	vs	PR	ν_3

continued/....

Table 4.6a continued

$\nu(cm^{-1})$	Strength	Structure	Assignment
688.2	m		$2\nu_5$, $\nu_5+\nu_9$
624.9	s	centre of 'Q' branch	ν_8
352 344	s	PR?	ν_5, $(\nu_9)^d$
219	m	-	$2\nu_{10}$
116	m	-	ν_{10}

a PR structure is obscured by 'Q' branches of the overlapping GeH_3 mode.

b 'Q' branches observed but too weak to measure.

c this could be two separate bands.

d see text.

Table 4.6b Assignments of Raman Frequencies of GeH_3CCCl (liq.)

ν (cm^{-1})	Structure	Polarization	Assignment
2166	m	60%	ν_2
2158	w	-	
2113[a]	w	DP	ν_6
2111	vs	70%	ν_1
880	s	30%	ν_4, ν_7
843	m	-	
824	s	60%	ν_3
684	vw	P	$2\nu_9$
622	vw	DP	ν_8
339	vs	DP	ν_9 ν_5
123	s	DP	ν_{10}

a suggests that ν_6 is to high frequency of ν_1

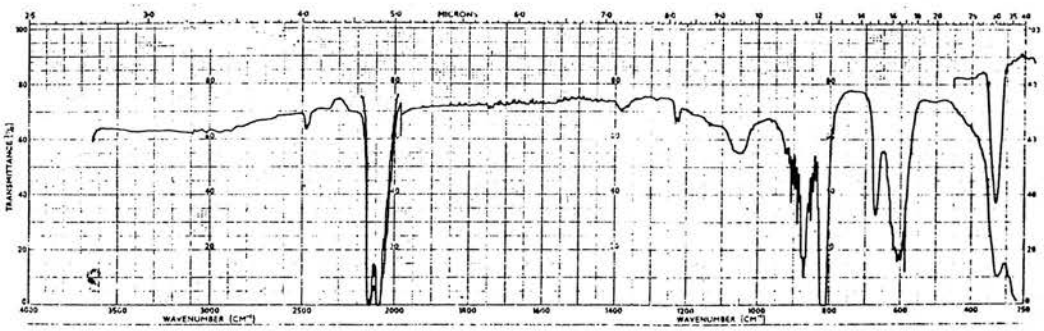

Figure 4.4 IR Spectrum of GeH_3CCCl

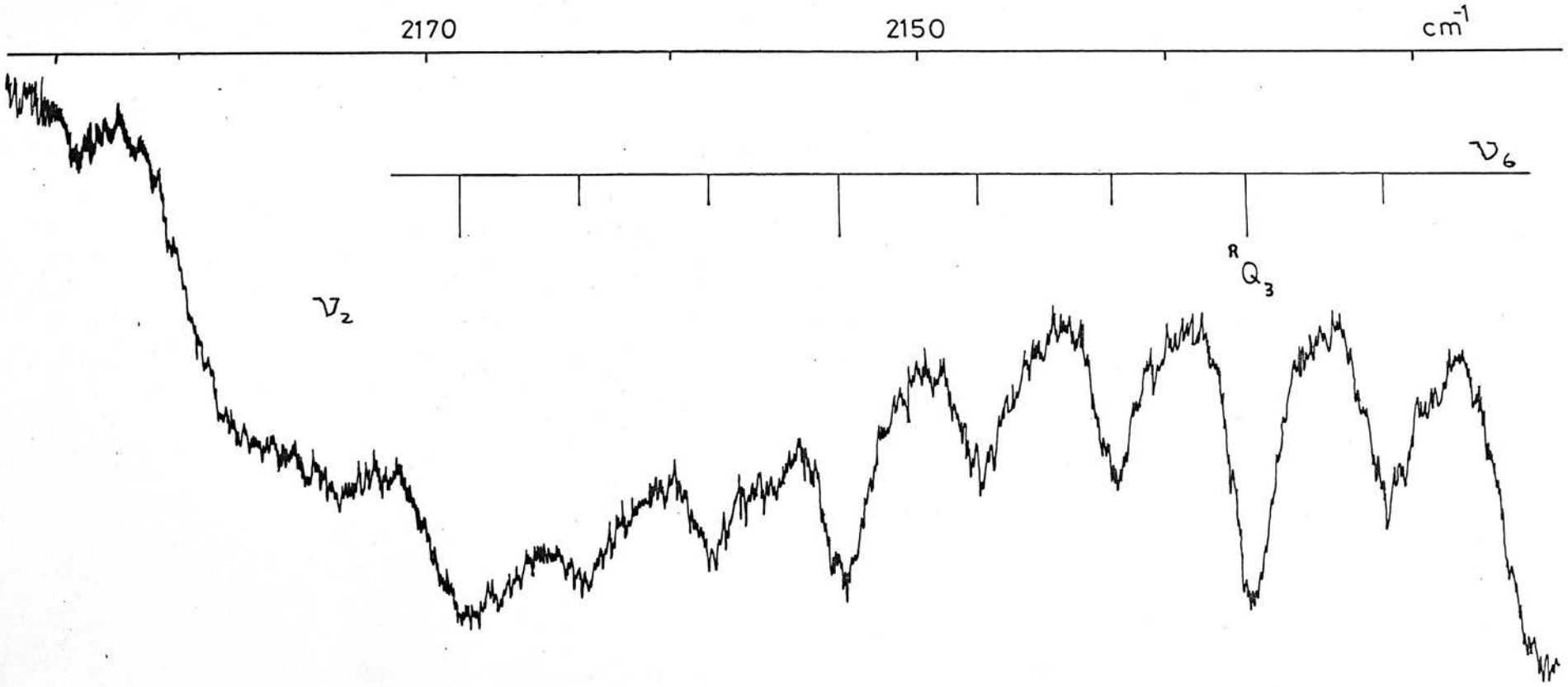

figure 4.5 ν_2 $GeH_3C{\equiv}CCl$ IR

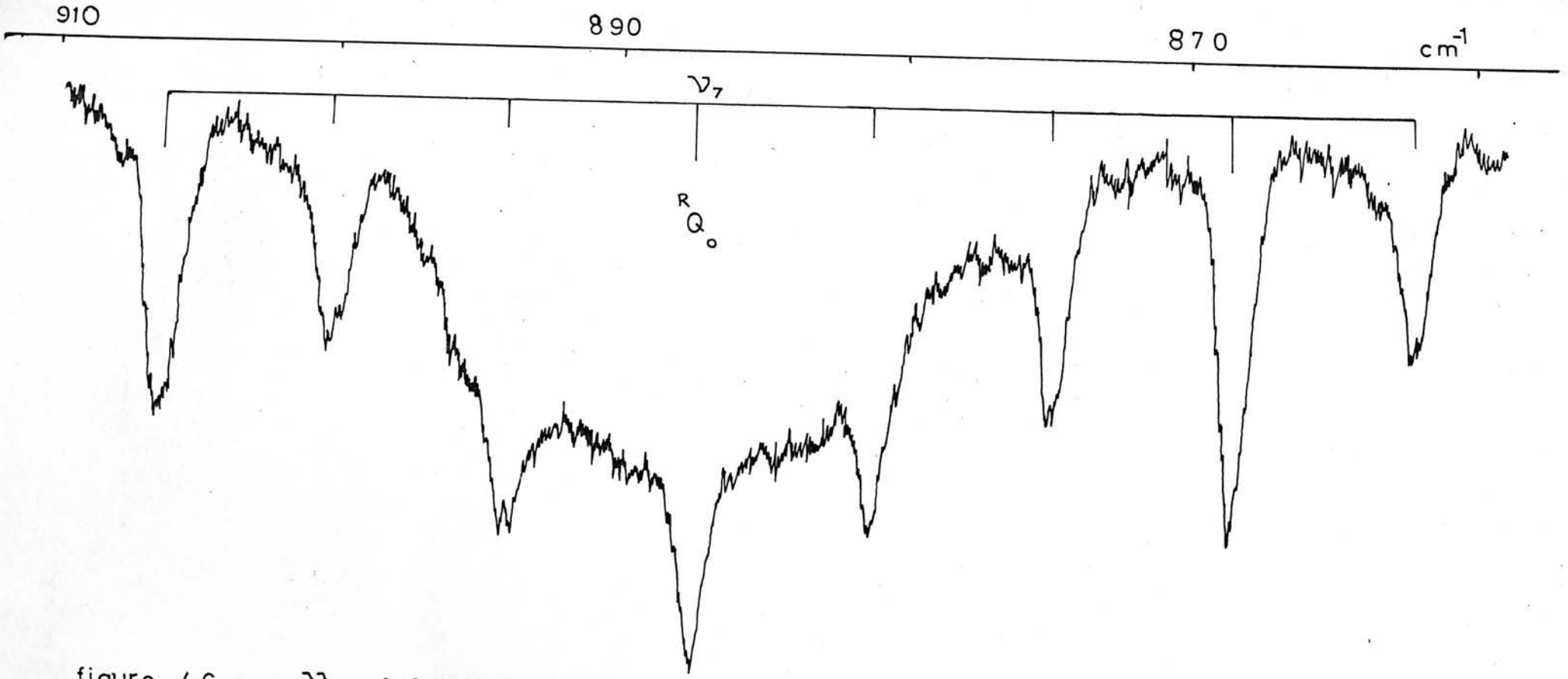

figure 4.6 ν_4 of $GeH_3C{\equiv}CCl$ - IR

observed at 2590 cm^{-1} in silyl chloro-acetylene and deutero silyl chloro-acetylene. The 2512 cm^{-1} band, however, does not possess a similar PR envelope to the 2590 cm^{-1} band.

The liquid phase raman spectrum has a very strong, depolarised line at 339 cm^{-1} and no band in the 220 cm^{-1} region. This suggests that ν_5 and ν_9 occur in the same region of the spectrum and that the 219 cm^{-1} band corresponds to $2\nu_{10}$ rather than ν_9. This conclusion is supported by the fact that polarization measurements on the 339 cm^{-1} raman band show a greater difference between the two normal planes of polarized light than expected for a depolarized band. This indicates the presence of a weakly polarized band around 339 cm^{-1} as well as ν_9. ν_9 is a weak band in the infra red spectrum of silyl chloro-acetylene. It is quite conceivable that ν_9 is hidden under ν_5 in germyl chloro-acetylene, being too weak to be observed. Loss of structure in the band at 2512 cm^{-1} could result from the combination, $\nu_2 + \nu_9$ occurring with the much stronger band, $\nu_2 + \nu_5$.

The vibrational spectra of silyl bromo-acetylene

The infra red spectrum of silyl bromo-acetylene is shown in figure 4.7. The fundamental frequencies are listed in table 4.7 and the assignments of the infra red and raman spectra are given in table 4.8.

There is good agreement between the fundamental frequencies observed in the infra red and raman spectra. Rotational structure is observed on the three silyl bands, ν_6, ν_7 and ν_8. The acetylenic stretch, ν_2 has moved to lower frequency relative to that found in the two chloro-acetylenes and the silyl stretch, ν_1 occurs to the

Table 4.7. The Fundamental Frequencies of SiH_3CCBr

Mode	IR	Raman[a]
ν_1	2192.8	2195
ν_2	2148.2	2145
ν_3	932.4	927
ν_4	832.2	830
ν_5	360.7	360
ν_6	2192.2	2195
ν_7	952.7 or 936.0	943
ν_8	681.7	-
ν_9	325.5	325
ν_{10}	114	118

a) liquid phase.

Table 4.8a Assignments of i.r. Frequencies of SiH_3CCBr (gas phase)

ν (cm^{-1})	Strength	Structure	Assignment
3140	vw	-	$\nu_1 + \nu_7$, $\nu_6 + \nu_7$
3120	vw	-	$\nu_1 + \nu_3$, $\nu_3 + \nu_7$
2913	vw	-	
2850	vw	-	
2780	vw	-	$\nu_1 + \nu_8$, $\nu_6 + \nu_8$
2507	w		$\nu_2 + \nu_5$
2195.0	s	centre of 'Q' branch	ν_6
2196.1 2188.5	vs	PR	ν_1
2152.9 2143.6	vs	PR	ν_2
1885	vw	PR	$2\nu_7$
1858	vw	-	$\nu_3 + \nu_7$
1365 1357	w	PR	$2\nu_8$
1260	vw	-	$\nu_3 + \nu_9$
1190	vw	-	$\nu_4 + \nu_5$
1175	w	-	
956.8 or 936.0	s	centre of 'Q' branch	ν_7
935.9 929.0	vs	PR	ν_3
835.3 829.2	s	PR	ν_4
682.7	s	centre of 'Q' branch	ν_8
440	w		$\nu_9 + \nu_{10}$
360.7	m	asym. band	ν_5
325.5	w	-	ν_9
114	m	-	ν_{10}

Table 4.8b Assignments of Raman Frequencies of SiH_3CCBr (liq.)

ν (cm^{-I})	Strength	Polarization	Assignment
2I95	vs	60%	ν_1 and ν_6
2I45	vs	60%	ν_2
943	s	?	ν_7
927	s	?	ν_3
830	vw	90%	ν_4
360	m	70%	ν_5
325	vs	DP	ν_9
II8	m	DP	ν_{10}

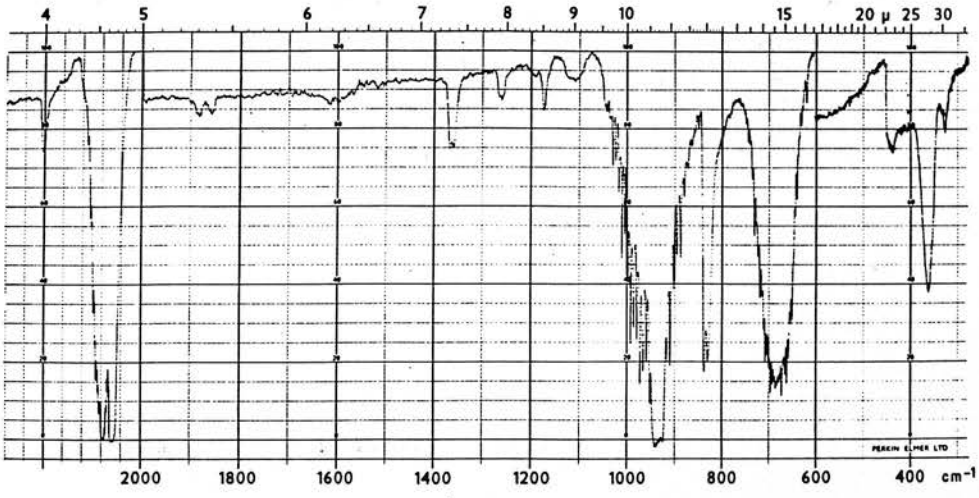

Figure 4.7 IR Spectrum of SiH_3CCBr

high frequency side of ν_2. This shift in frequency is similar in magnitude to that found in other series of halo-acetylenes[46]. The PR structure of ν_1 is just discernable between the overlapping Q branches of the other silyl stretch, ν_6.

The structure of the acetylenic stretch, ν_2 is obscured by weak Q branches of ν_6, but two distinct maxima of unequal intensity, belonging to ν_2, have a separation of 10.5 cm^{-1}. This is much larger than other PR separations on a_1 modes, which are in keeping with that predicted from Gerhart and Dennison[37]. This suggests that the band shape is similar to ν_2 in deutero silyl chloro-acetylene and arises from overlap of ν_2 with the "hot" band series $\nu_2 + n\nu_{10} - n\nu_{10}$.

Substitution of the chlorine atom by a bromine atom has lowered the frequencies of both skeletal stretches, ν_4 and ν_5. They now occur in the same region as the skeletal stretching modes of dibromo-acetylene[38]. As with silyl chloro-acetylene and germyl chloro-acetylene, ν_5 is asymmetric with no PR band envelope. ν_5 is much stronger in the infra red spectrum but in the raman spectrum the relative intensities are reversed. This pattern adds weight to the assignments of ν_5 and ν_9 in germyl chloro-acetylene. A strong combination, corresponding to $\nu_2 + \nu_5$ occurs at 2507 cm^{-1}, similar to the other halo-acetylenes studied.

The relative behaviour of the skeletal frequencies in these three compounds is similar to that found in the dihalo-acetylenes (figure 4.8). It is interesting that the silyl and germyl groups behave in a similar manner to chlorine and bromine atoms respectively when attached to the acetylenic group. Perhaps this is not surprising in view of their similar masses.

Figure 4.8 Skel tal Frequencies of some Halo-acetylenes

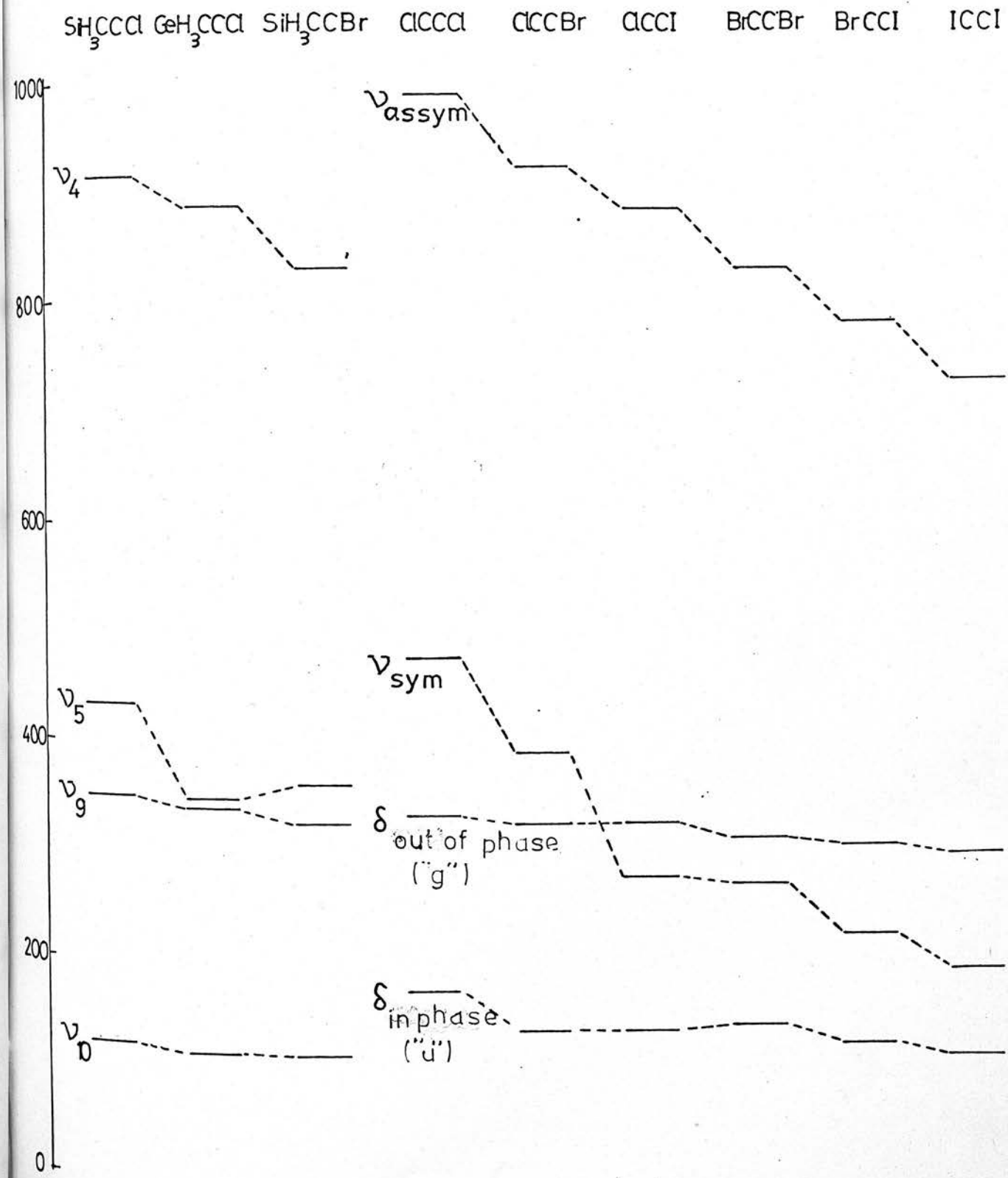

The two skeletal bending modes remain practically constant in frequency in both series of compounds. The gradual drop in frequency with increasing mass is not nearly as marked as the drop in frequency of the skeletal stretches. This trend strongly suggests that ν_9 in germyl chloro-acetylene is at 339 cm^{-1} rather than 220 cm^{-1}.

4.3 The Vibrational Spectra of Molecules of Type MH_3CCMH_3;M = Si,Ge

Molecules of type MH_3CCMH_3, where M = Si or Ge, can be considered as possessing overall D_{3d} symmetry although they are free internal rotors and should be described by a more flexible point group such as those described by Longuet-Higgins[39]. These molecules have 4 x a_{1g}, 3 x a_{2u}, 4 x e_g and 4 x e_u normal modes of vibration. Due to the mutual exclusion principle, only the g modes are raman active and only the u modes are infra red active. This makes assignments of the bands relatively straightforward.

The eleven modes, with the approximate description of the vibrations concerned, are listed in table 4.9. The MH stretches, ν_1, ν_5, ν_8 and ν_{12} occur within 20 cm^{-1} of one another while the acetylenic stretch, ν_2 occurs in the same region of the spectrum but is separated from the former group of frequencies. Similarly the MH_3 deformations, ν_3, ν_6, ν_9 and ν_{13} and the MH_3 rocks, ν_{10} and ν_{14}, occur in the expected regions of the spectra. The symmetric and asymmetric stretches, ν_4 and ν_7, occur outside the "normal" region associated with the M - C stretching frequencies. The reason is similar to that evoked for the silyl and germyl halo-acetylenes, namely that the "group vibrations" have interacted extensively due to strong mechanical coupling and their proximity

Table 4.9. The Fundamental Modes of MH_3CCMH_3

Description	a_{1g}	a_{2u}	e_g	e_u
	Raman active	IR active	Raman active	IR active
MH stretch, ν_{MH}	ν_1	ν_5	ν_8	ν_{12}
Acetylinic stretch, ν_{CC}	ν_2	-	-	-
MH deformation, δ_{MH}	ν_3	ν_6	ν_9	ν_{13}
Symetric skeletal stretch, $\nu_{MC\ sym}$	ν_4	-	-	-
Asymmetric Skeletal stretch, $\nu_{MC\ asym}$	-	ν_7	-	-
MH_3 rock, ρ_{MH_3}	-	-	ν_{10}	ν_{14}
Symmetric skeletal deformation, $\delta_{MCC\ sym}$	-	-	ν_{11}	-
Asymmetric skeletal deformation, $\delta_{MCC\ asym}$	-	-	-	ν_{15}

in frequency within the molecules. The skeletal deformation frequencies, ν_{11} and ν_{15}, are similarly outside their "normal" frequencies.

The vibrational spectrum of disilyl acetylene

The infra red spectrum and raman spectrum of disilyl acetylene are shown in figure 4.9 and the fundamental frequencies with those observed by Lord[4], are given in table 4.10. The liquid phase raman frequencies observed by Lord are shifted up to 10 cm^{-1} from those observed in the gas phase. This shift is adequately explained by phase differences between the gas and liquid states. The spectral assignments of the observed bands are listed in table 4.11.

The highest fundamentals in the infra red spectrum are the two overlapping silyl modes, ν_5 and ν_{12} corresponding to the a_{2u} and e_u silyl stretches. The PR branches of ν_5 are partially obscured by the Q branches of ν_{12}.

The asymmetric silyl deformation, ν_6 occurs at 913 cm^{-1} and possesses a distinct PQR band envelope although the Q branch is weak compared to the R and P branches. As Lord has pointed out, the bending mode, ν_{15}, does not form a series of "hot" bands with this mode otherwise the Q branch would be obscured by the overlapping envelopes of the "hot" bands.

The structure of the asymmetric M - C stretch, ν_7 is very similar to that of the acetylenic stretch, ν_2 in deutero silyl chloro-acetylene, which has been assigned to "hot" bands overlapping with the fundamental mode. It seems plausible that the structure of ν_7 is due to the series of bands $\nu_7 + n\nu_{15} - n\nu_{15}$.

Table 4.10. The Fundamental Frequencies of SiH_3CCSiH_3 (gas phase)

Mode	This work IR(cm^{-1})	This work Raman(cm^{-1})	Lord[a]
ν_1	-	2198	2187[b]
ν_2	-	2140	2132
ν_3	-	946	(930)[b]
ν_4	-	411	420[b]
ν_5	2189.0	-	2170
ν_6	913.4	-	912
ν_7	809.3	-	807
ν_8	-	2194	2187[b]
ν_9	-	947	946[b]
ν_{10}	-	[672 or 684[c]]	607[b]
ν_{11}	-	293	297[b]
ν_{12}	2194.9	-	2190
ν_{13}	943.8	-	946
ν_{14}	693.6 or 681.8	-	682
ν_{15}	102	-	-

a) reference 4.

b) liquid phase.

c) from $\nu_{10} + \nu_{14}$ assuming no anharmonicity.

Table 4.IIa Assignments of i.r. Frequencies of SiH_3CCSiH_3 (gas phase)

ν (cm^{-1})	Strength	Structure	Assignment
4389.1 4384.7 4380.5	vw	PQR	$\nu_1 + \nu_5$, $\nu_5 + \nu_8$
4318.9	vw	centre of 'Q' branch	$\nu_8 + \nu_{12}$ (e_u)
4322.4 4313.0	vw	PR	$\nu_8 + \nu_{12}$ (a_{2u})
3166	vw	-	$\nu_{10} + \nu_{11} + \nu_{12}$
3142.0	vw	centre of 'Q' branch[a]	
3136.5 3126.8	w	PR	$\nu_3 + \nu_5$
3108.5 3100.5	w	PR	$\nu_1 + \nu_6$, $\nu_6 + \nu_8$
3045	w	-	$\nu_2 + \nu_6$
3015	w	-	$\nu_1 + \nu_7$, $\nu_7 + \nu_8$
2971	w	-	$\nu_1 + \nu_{10} + \nu_{15}$
2937	w	-	$\nu_2 + \nu_{14} + \nu_{15}$
2871	w	-	$\nu_{10} + \nu_{12}$, $\nu_5 + \nu_{12}$
2786	vw	-	$\nu_8 + \nu_{14}$
2495	vw	-	$\nu_5 + \nu_{11}$
2380	vw	-	
2194.9	vs	centre of 'Q' branch	ν_{12}
2184.8 2193.2	vs	PR	ν_5
1879	w	PR?	$\nu_3 + \nu_{13}$, $\nu_9 + \nu_{13}$
1857.5 1850.0	w	PR	$\nu_3 + \nu_6$
1625	vw	br	$\nu_{10} + \nu_{13}$
1501	vw	-	
1373.0	vw	centre of 'Q' branch	$\nu_{10} + \nu_{14}$ (e_u)
1366.5 1358.4	m	PR	$\nu_{10} + \nu_{14}$ (a_{2u})

continued/...

Table 4.IIa continued

ν (cm^{-1})	Strength	Structure	Assignment
1251	vw	-	$\nu_{11} + \nu_{13}$
1217	m	-	$\nu_4 + \nu_7$, $\nu_6 + \nu_{11}$
948.2	vs	centre of 'Q' branch	ν_{13}
942.8 934.4	m	PR	$2\nu_4 + \nu_{15}$
917.5 913.4 908.8	vs	PQR	ν_6
817 809.3 800	vs	sh central max. sh	ν_7
694.1 or 682.7	vs	centre of 'Q' branch	ν_{14}
397.1 389.2	w	PR?	$\nu_{15} + \nu_{11}$
360	vw	-	
102	m	-	ν_{15}

a see chapter 6

Table 4.IIb Assignments of Raman Frequencies of SiH_3CCSiH_3 (gas phase)

ν (cm^{-1})	Strength	Structure	Assignment
2198	vs	-	ν_1
2194	w	sh	ν_8
2152	vw	br	
2140	s	-	ν_2
2136	m	-	$\nu_2 + \nu_{15} - \nu_{15}$
2131	w	sh	$\nu_2 + 2\nu_{15} - 2\nu_{15}$
2124	vw	sh	$\nu_2 + 3\nu_{15} - 3\nu_{15}$
994	vw	sp	
947[a]	m	br	ν_9
946	s	Q	ν_3
943	w	b	
921			
411	m	v. asym.	ν_4
293	m	br	ν_{11}

a centre of broad band

b series of peaks - see text.

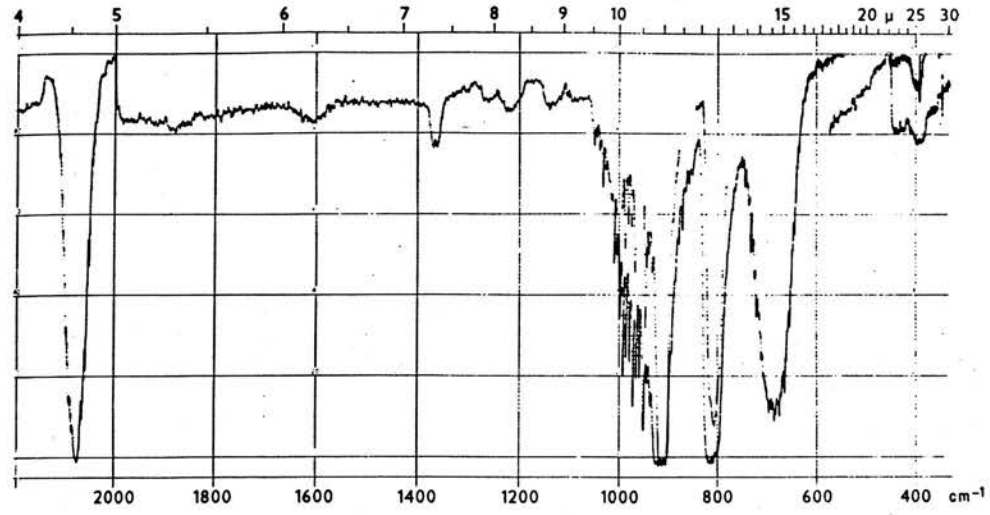

Figure 4.9 a) IR Spectrum of SiH_3CCSiH_3

b) Raman Spectrum of SiH_3CCSiH_3

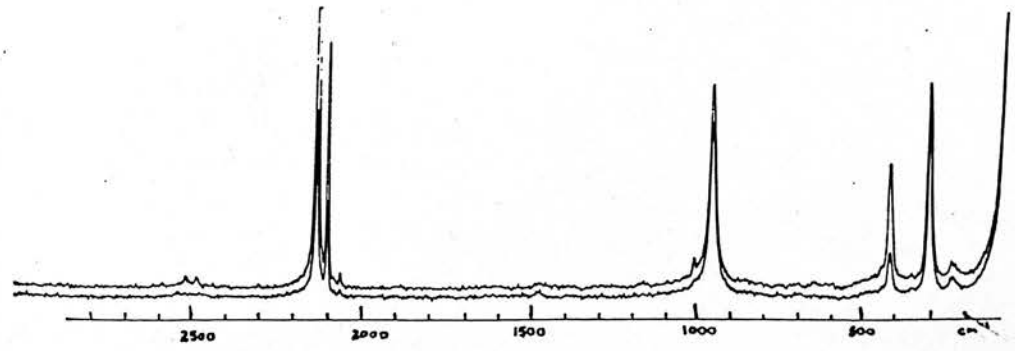

The silyl deformation, ν_6, occurs, as expected, about 30 cm^{-1} below the perpendicular mode, ν_{13}. The silyl rock, ν_{14}, occurs at either 693.0 cm^{-1} or 681.8 cm^{-1}. The exact centre of the Q branch sequence is difficult to determine but a perturbation of some of the rotational energy levels suggests that the former frequency is the more likely centre although the latter frequency cannot be ruled out.

The skeletal deformation, ν_{15}, is observed at 102 cm^{-1}. This frequency is low enough to enable "hot" band phenomena to occur. "Hot" band sequences involving this frequency could move the PR branches by 3 cm^{-1} or 4 cm^{-1} due to changes in bonding in the excited molecule. This movement is large enough to obscure the central minimum of a PR branch of about 8 cm^{-1} separation as occurs in ν_7.

In the raman spectrum, the non-degenerate symmetrical silyl stretch, ν_1, is very much stronger than the corresponding degenerate mode, ν_8; the latter band appearing as a shoulder on the former. It is therefore difficult to determine the precise position of ν_8 because the Q branches will be very weak and spread over a large region of the spectrum.

The acetylenic stretch, ν_2, occurs to lower frequency of ν_1 and, like the corresponding band in the gas phase raman spectrum of silyl chloro-acetylene, possesses a progression of bands to lower frequency of the main band. These bands are assigned to the series of combination bands $\nu_2 + n\nu_{15} - n\nu_{15}$; the average separation of each band is about 5 cm^{-1} which is consistent with this assignment.

The silyl deformation, ν_3, appears as a strong sharp Q branch in the gas phase, in contrast to the spectrum of the liquid compound,

where Lord has described ν_3 as being weaker than the other silyl deformation, ν_9. ν_3 at 946 cm^{-1} is on top of a broad band whose maximum occurs at 947 cm^{-1}. This broad band has been assigned to the degenerate silyl deformation, ν_9. A series of badly resolved peaks (whose amplitude was greater than the background noise) occur between 943 cm^{-1} and 921 cm^{-1} and is probably due to the $^{P,R}Q$ and $^{S,O}Q$ branches of ν_9.

The band at 411 cm^{-1} is assigned to the symmetric skeletal stretch, ν_{14}. The Q branch of this mode is asymmetric towards higher frequencies. The occurrence of "hot" bands of excited bending modes is probably responsible for the shape of this band.

The remaining band at 293 cm^{-1} is assigned to the symmetrical skeletal deformation, ν_{11}. This is a broad band having evidence for a PR type of band shape.

The symmetric silyl rock, ν_{10}, was not observed, being too weak to be seen. However, the position of several combination bands would suggest that this frequency is around 670 cm^{-1}. The infra red bands at 1362 cm^{-1} and 1372 cm^{-1} are probably due to the combination $\nu_{10} + \nu_{14}$, the two frequencies being the a_{2u} and e_u components respectively. This combination band is analogous to the strong combination occurring in digermyl acetylene and the strong overtone in silyl and germyl halo acetylenes. If ν_{14} is taken as occurring at 693 cm^{-1} then ν_{10} will be about 670 cm^{-1}.

The vibrational spectra of digermyl acetylene

The infra red and raman spectra of digermyl acetylene are shown in figure 4.10; the fundamental frequencies are given in table 4.12 and the infra red and raman frequencies are given in table 4.13.

Table 4.12. The Fundamental Frequencies of GeH_3CCGeH_3

Mode	IR(cm^{-1})	Raman(cm^{-1})[a]
ν_1	-	2105
ν_2	-	2127
ν_3	-	844
ν_4	-	339
ν_5	2113.1	-
ν_6	842.3	-
ν_7	688.6	-
ν_8	-	2105
ν_9	-	876
ν_{10}	-	624
ν_{11}	-	278
ν_{12}	2113.6	-
ν_{13}	902.6 or 883.2	-
ν_{14}	623.4	-
ν_{15}	91	-

a) liquid phase.

Table 4.I3a Assignments of i.r. Frequencies of GeH_3CCGeH_3 (gas phase)

ν (cm^{-1})	Strength	Structure	Assignment
4246	vw	br	$\nu_2 + \nu_{12}$, $\nu_2 + \nu_5$
4I62.8	vw	centre of 'Q' branch	$\nu_8 + \nu_{12}$ (e_u)
4I6I.7 4I55.5	vw	PR	$\nu_8 + \nu_{12}$ (a_{2u})
30I5	w	br	$\nu_9 + \nu_{12}$
2986	w	br	$\nu_1 + \nu_{14}$, $\nu_5 + \nu_8$, $\nu_8 + \nu_{14}$
2966	w	br	$\nu_2 + \nu_6$
2957	w	br	$\nu_3 + \nu_9$
2953.9	w	centre of 'Q' branch	$\nu_3 + \nu_{12}$, $\nu_8 + \nu_6$
2II6.5	vs	centre of 'Q branch	ν_{12}
2II6.5 2II0.8	vs	PR	ν_5
I84I	vw	-	$\nu_4 + \nu_9 + \nu_{14}$
I760	vw	centre of 'Q' branch?	$\nu_9 + \nu_{13}$ (e_u)
I756.4 I747.5	vw	PR	$\nu_9 + \nu_{13}$ (a_{2u})
I5I0	vw	sh	$\nu_{10} + \nu_{13}$
I480	vw	br	$\nu_9 + \nu_{14}$, $\nu_3 + \nu_{14}$
I430	vw	sh	$\nu_6 + \nu_{14}$
I3I0	vw	-	$\nu_4 + \nu_9 + \nu_{15}$
I255.5	vw	centre of 'Q' branch	$\nu_{10} + \nu_{14}$ (e_u)
I247.8 I242.7	w	PR	$\nu_{10} + \nu_{14}$ (a_{2u})
II35	vw	PR?	$\nu_{11} + \nu_6$
905.8 886.2	vs	centre of 'Q' branch	ν_{13}
838.9 844.7	vs	PR	ν_6
758.I 754.4	w	PR	
688.6	vs	-	ν_7

continued/...

Table 4.I3a continued

ν (cm^{-I})	Strength	Structure	Assignment
623.9	vs	centre of 'Q' branch	ν_{14}
426	vw	br	$\nu_4 + \nu_{15}$
356	w	-	$\nu_{11} + \nu_{15}$
9I	m	-	ν_{15}

Table 4.I3b Assignments of Raman Frequencies of GeH_3CCGeH_3 (liq.)

ν (cm^{-I})	Strength	Polarization	Assignment
2I27	w	70%	ν_2
2I05	vs	90%	ν_1, ν_8
876	vs	60%	ν_9
844	vs	80%	ν_3
624	vw	70%	ν_{10}
569	vw	80%	$2\nu_{11}$
339	vw	-	ν_4
278	vs	60%	ν_{11}

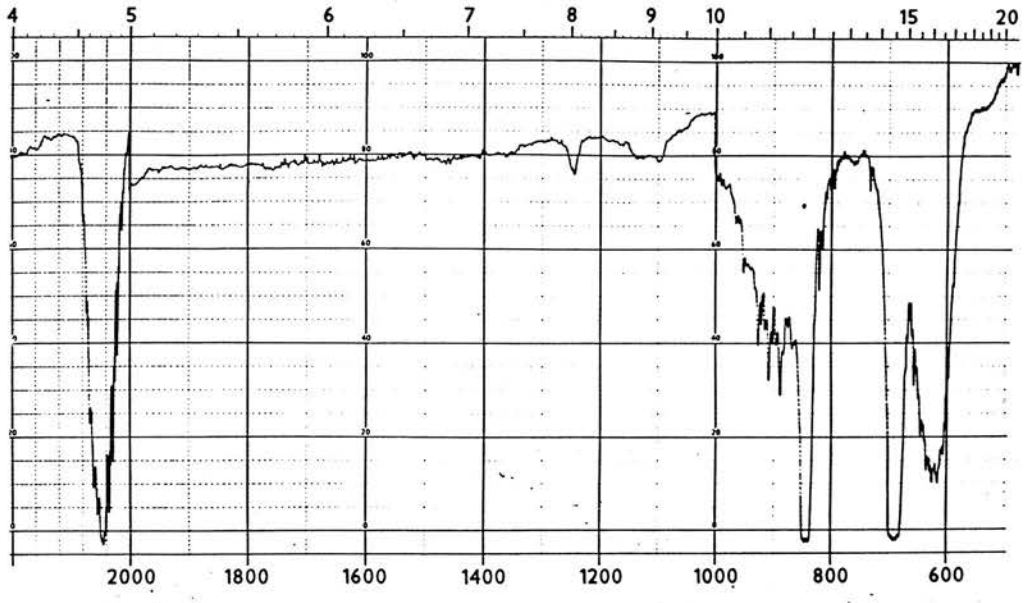

Figure 4.IO a) IR Spectrum of GeH_3CCGeH_3

b) Raman Spectrum of GeH_3CCGeH_3

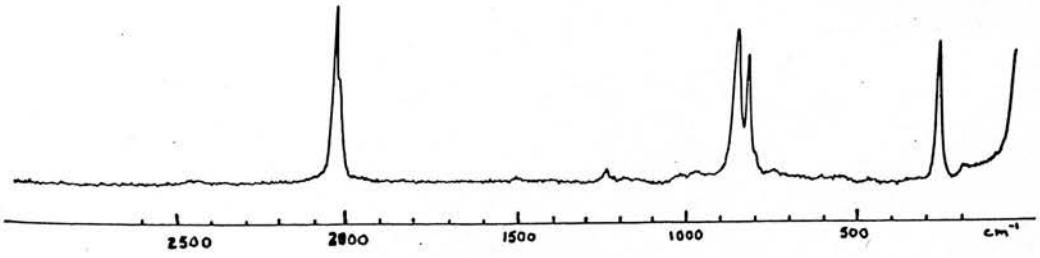

The highest fundamentals in the infra red spectrum are the two germyl stretches, ν_5 and ν_{12}. The PR envelope of ν_5 is clearly visible amongst the Q branches of ν_{12}.

The germyl deformation, ν_6, like its silyl analogue exhibits a PR band shape, again suggesting that "hot" bands do not occur with this mode.

The centre of the rotational progression of the germyl deformation, ν_{13}, is not well defined although perturbation of the rotational energy levels suggest that this band is at 886.0 cm^{-1} rather than 905.0 cm^{-1}.

The asymmetric stretching mode, ν_7, occurs as a very strong band at 689 cm^{-1}. This frequency is considerably lower than the corresponding mode in disilyl acetylene.

From consideration of the disilyl acetylene spectrum, the other skeletal stretch, ν_4 is expected at 260 cm^{-1}. It is therefore likely that the band at 278 cm^{-1} belongs to this mode. ν_7 has no PR structure as in disilyl acetylene. "Hot" bands arising from the low bending vibration, ν_{15} at 91 cm^{-1} would cause this loss of structure.

The raman frequencies were determined from liquid phase spectra. The acetylenic stretch, ν_2 occurs as a weak shoulder to high frequency of the very strong germyl stretch, ν_1. The other germyl stretch, ν_8 is not visible but is hidden under ν_1.

The two germyl deformations, ν_3 and ν_9, are very strong bands occurring at 844 cm^{-1} and 876 cm^{-1} respectively. The germyl rock, ν_{10} is a very weak band at 624 cm^{-1}. The symmetric deformation, ν_{11}, at 278 cm^{-1}, is another extremely strong band.

4.4 The Vibrational Frequencies of Molecules of Type MX_3CCCF_3; M = Si, Ge; X = H, D

Molecules of the type MX_3CCCF_3 where M = Si, Ge and X = H, D can be described as belonging to the C_{3V} symmetry point group although a more flexible group should be used. These molecules have $7a_1$ and 8e normal modes of vibration and $1a_2$ internal rotational degrees of freedom.

The vibrational modes, with an approximate description of the vibrations are listed in table 4.14. The simple description of these modes breaks down when considering many of the lower frequency modes due to strong mechanical coupling causing extensive interaction between many of the "group vibrations".

The MX_3 group retains the group frequencies with the result that these frequencies are easily assigned. Similarly the CF_3 group stretches have a very characteristic pattern and these too are easily assigned. It is, however, extremely difficult to assign many of the other bands in the spectrum. As an aid to the assignment of the spectra, use was made of the fully deuterated species.

The vibrational spectra of silyl and deutero silyl perfluoromethyl acetylene

The infra red spectra of silyl perfluoromethyl acetylene and its deuterated analogue are shown in figure 4.11. The fundamental frequencies are given in table 4.15, and the assignments of overtones and combinations for the hydrogen and deuterium compounds respectively are listed in tables 4.16 and 4.17.

There is generally good agreement between the infra red and raman fundamental frequencies although a few bands show a moderate

Table 4.14. The Fundamental Modes of MH_3CCCF_3

Description	a_1	e
Acetylenic stretch, $\nu_{C\equiv C}$	ν_1	-
MH stretch, ν_{MH}	ν_2	ν_8
CF stretch, ν_{CF}	ν_3	ν_9
MH deformation, δ_{MH}	ν_4	ν_{10}
C-C skeletal stretch, ν_{CC}	ν_5	-
MH_3 rock, ρ_{MH_3}		ν_{11}
CF deformation, δ_{CF}	ν_6	ν_{12}
M-C skeletal stretch, ν_{MC}	ν_7	-
CF_3 rock, ρ_{CF_3}	-	ν_{13}
Skeletal deformation	-	ν_{14}
Skeletal deformation	-	ν_{15}

Table 4.15. The Fundamental Frequencies of SiH_3CCCF_3 and SiD_3CCCF_3

Mode	SiH_3CCCF_3 (cm^{-1})	SiD_3CCCF_3 (cm^{-1})
ν_1	2228[a]	2219
ν_2	2202.0	1583
ν_3	1275.0	1264
ν_4	926.2	712
ν_5	878[a]	874
ν_6	690	660
ν_7	349	340
ν_8	2206.8	1606
ν_9	1175	1176
ν_{10}	945.2	685
ν_{11}	690.0 or 680.5	536
ν_{12}	617	620[a]
ν_{13}	464	458
ν_{14}	240	230
ν_{15}	87	93[a]

a) liquid phase Raman.

Table 4.I6a Assignments of i.r. Frequencies of SiH_3CCCF_3 (gas phase)

ν (cm^{-1})	Strength	Structure	Assignment
4405	vw	-	$2\nu_2$, $\nu_1 + \nu_2$
4360	vw	-	$\nu_1 + \nu_8$, $\nu_2 + \nu_8$
4345.I	vw	centre of 'Q' branch	$2\nu_8$ (e)
4340	vw	PR?	$2\nu_8$ (a_1)
3482	vw	-	$\nu_3 + \nu_8$
3I43.5	vwc	centre of 'Q' branch	$\nu_8 + \nu_{10}$
3I26.0 3I22.0 3II8.3	vw	PQR	$\nu_2 + \nu_4$
2962	vw	-	$\nu_4 + \nu_5 + \nu_9$
2880	vw	-	$\nu_2 + \nu_{11}$
257I	vw	-	$\nu_1 + \nu_7$
2523	vw	-	$2\nu_3$
248I	vw	-	$\nu_3 + \nu_5 + \nu_7$
2439	w	-	$\nu_3 + \nu_9$
23I6.4	m	-	$\nu_1 + \nu_{15}$
2209.5	vs	centre of 'Q' branch	ν_8
2205.4 2202.0 2I97.5	vs	PQR	ν_2
2045.2	w	-	$\nu_3 + \nu_5$
I953	vw	-	$\nu_3 + \nu_{11}$
I883.5 I879.0 I875.4	vw	PQR	$\nu_3 + \nu_{12}$
I87I or I86I	vw	centre of 'Q' branch	$2\nu_{10}$ (e)
I86I.0	vw	-	$2\nu_{10}$ (a_1)
I785	vw	-	$\nu_4 + \nu_5$, $\nu_5 + \nu_{10}$, $\nu_9 + \nu_{12}$
I745	vw	-	
I7I6	w	-	$2\nu_5$

continued/...

Table 4.I6a continued

ν (cm^{-I})	Strength	Structure	Assignment
I6I8	w	PQR?	$\nu_4 + \nu_6$, $\nu_{10} + \nu_{11}$
I478	w	PQR?	$\nu_5 + \nu_{12}$
I4II	vw	-	$\nu_9 + \nu_{14}$
I378 I373 I368	w	PQR	$2\nu_6$, $\nu_6 + \nu_{11}$
I355	w	-	$2\nu_{11}$
I278.3 I275.0 I27I.5	vs	PQR	ν_3
I220.2 I2I4.0	s	PR	$\nu_5 + \nu_7$
II75	vs	-	ν_9
II46	m	-	$\nu_{11} + \nu_{13}$
III5	w	-	$\nu_4 + 2\nu_{15}$, $\nu_{10} + 2\nu_{15}$
952	m	-	$\nu_5 + \nu_{15}$, $\nu_7 + \nu_{12}$
949.2	vs	centre of 'Q' branch	ν_{10}
930.I 926.2 92I.7	vs	PQR	ν_4
858.3	m	-	
806	w	-	$\nu_7 + \nu_{13}$
690	s	-	ν_6
692.7 or 68I.4	s	centre of 'Q' branch	ν_{11}
6I7	m		ν_{12}
543 536 528 523	m	PQQ'R	
464	vw	PQR?	ν_{13}
374	w	-	$\nu_{14} + 2\nu_{15}$

continued/....

Table 4.I6a continued

ν (cm^{-1})	Strength	Structure	Assignment
349	m	-	ν_7
319	w	-	$\nu_{14} + \nu_{15}$
240	w	-	ν_{14}
87	vw	-	ν_{15}

Table 4.I6b Assignments of Raman Frequencies of SiH_3CCCF_3 (liq.)

ν (cm^{-1})	Strength	Polarization	Assignment
2228	vs	-	ν_1
2206	vs	90%	ν_2, ν_8
1265	w	60%	ν_3
1170	w	DP	ν_9
946	s	DP	ν_{10}
924	s	50%	ν_4
878	vs	90%	ν_5
695	s	90%	ν_6
620	w	DP	ν_{12}
465	m	DP	ν_{13}
358	s	80%	ν_7
340	w	P?	
250	vs	DP	ν_{14}
98	vs	DP	ν_{15}

Table 4.I7a Assignments of i.r. Frequencies of SiD_3CCCF_3 (gas phase)

ν (cm^{-1})	Strength	Structure	Assignment
3108	vw	-	
3088	vw	-	$\nu_1 + \nu_5$
3058	vw	-	
2990	vw	-	
2982	w	-	
2870	vw	-	$\nu_1 + \nu_6$, $\nu_3 + \nu_8$
2436	w	-	$\nu_3 + \nu_9$
2359	w	-	$2\nu_9$
2329	w	-	$\nu_4 + \nu_8$
2219	m	-	ν_1
2045	w	-	$\nu_2 + \nu_{13}$, $\nu_5 + \nu_9$
1984	vw	-	$\nu_3 + \nu_4$
1885	vw	-	$\nu_3 + \nu_{12}$, $\nu_4 + \nu_9$
1820	vw	-	$\nu_2 + \nu_{14}$
1805	vww	-	$\nu_3 + \nu_{11}$
1606	s	-	ν_8
1583	s	-	ν_2
1495	vw	PQR?	
1482	w	-	
1472	w	-	
1418	w	PQR?	$2\nu_4$, $\nu_9 + \nu_{14}$
1395	w	-	
1363 1353	w	PR	$\nu_3 + \nu_{15}$
1348	w	-	$\nu_6 + \nu_{10}$
1268 1264 1260	vs	PQR	ν_3
1253		Q?	

continued/....

Table 4.I7a continued

ν (cm^{-1})	Strength	Structure	Assignment
I245	s	-	$\nu_4 + \nu_{11}$
I23I	s	-	$2\nu_{12}$
I223	s	-	$\nu_{10} + \nu_{11}$
I206	s	-	$\nu_5 + \nu_7$, $\nu_6 + \nu_{12}$
II76	vs	-	ν_9
II40	m	-	$\nu_{10} + \nu_{13}$, $2\nu_7 + \nu_{13}$
I092	m	-	
944	w	-	$\nu_4 + \nu_{14}$
932	w	-	
9I0	w	-	$2\nu_3$
878 874 870	vs	PQR	ν_5
846	w	-	$\nu_{12} + \nu_{14}$
832 828 824	m	PQR	
7I5 7I2 708	vs	PQR	ν_4
685	s	centre of 'Q' branch	ν_{10}
664 660 656	vs	PQR	ν_6
628	vw	-	$\nu_{11} + \nu_{15}$
598	m	-	ν_{12}
536	vs	-	ν_{11}
458	w	-	ν_{13}
375	w	-	$\nu_{14} + 2\nu_{15}$
340	s	-	ν_7
305	w	-	$\nu_{14} + \nu_{15}$
230	w	-	ν_{14}

Table 4.I7b Assignments of Raman Frequencies of SiD_3CCCF_3 (liq.)

ν (cm^{-1})	Strength	Polarization	Assignment
2225	m	70%	ν_1
I6I8	m	50%	ν_8
I587	vs	90%	ν_2
I265	w	P	ν_3
II60	w	DP	ν_9
877	m	90%	ν_5
7I2	m	60%	ν_4
688	m	DP	ν_{10}
663	m	70%	ν_6
620	w	DP	ν_{12}
538	w	70%	ν_{11}
462	w	DP	ν_{13}
348	m	70%	ν_7
3I2	vw	P	$\nu_{14} + \nu_{15}$
238	vs	DP	ν_{14}
I70	w		$2\nu_{15}$
93	s	DP	ν_{15}

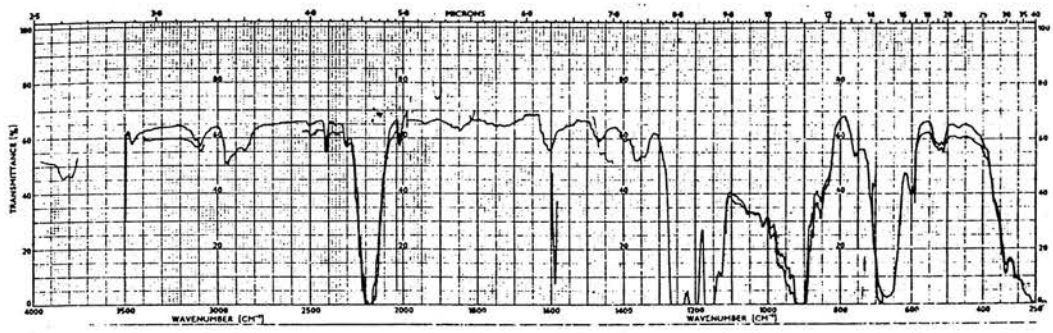

Figure 4.II a) IR Spectrum of SiH_3CCCF_3

b) IR Spectrum of SiD_3CCCF_3

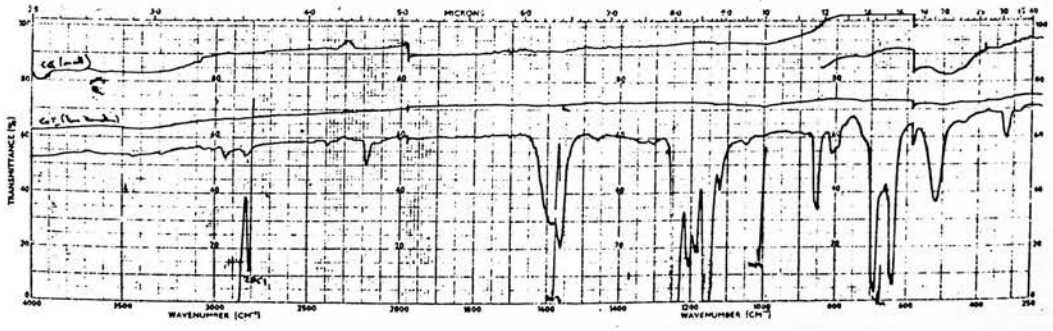

phase shift. Q branch frequencies, where visible, were taken as the vibrational frequency otherwise the centre of the band was used.

In the raman spectrum of the liquid, the acetylenic stretch, ν_1 of silyl perfluoromethyl acetylene occurs at 2228 cm^{-1}, appearing as a distinct shoulder on the very strong silyl stretch, ν_2. ν_1 is not visible in the gas phase infra red spectrum because it is hidden under the rotational fine structure of the perpendicular silyl stretch, ν_6. In the deuterated species, ν_1 occurs at 2219 cm^{-1} in the infra red and at 2225 cm^{-1} in the raman spectrum, implying that the hidden band in the gas phase infra red should occur at about 2220 cm^{-1}. This frequency is also implied by the position of the equivalent band in germyl and deutero germyl perfluoromethyl acetylene. Interaction with the silyl stretch, ν_2 in the silyl acetylene, however, would increase this frequency compared to the deuterated silyl acetylene or either of the germyl compounds. Such an interaction is suggested by the shift of about 5 cm^{-1} in ν_1 between silyl perfluoromethyl acetylene and its deuterated analogue when matrix isolated in argon at a ratio of 1:900. In deutero silyl perfluoromethyl acetylene and in the germyl compounds, ν_2 occurs at much lower frequency than ν_1 with the result that interaction between the two modes will be much reduced.

The silyl stretch ν_2 occurs at 2202 cm^{-1} with the other silyl stretch, ν_8 which possesses rotational structure. Both bands have a large isotopic shift on deuteration, moving both bands to around 1600 cm^{-1}.

The CF_3 stretch, ν_3 occurs at 1275 cm^{-1}. This mode appears around this frequency as a very strong band in all molecules of type

$R - C \equiv C - CF_3$ where $R = CH_3$ H, SiH_3, GeH_3, CF_3. Deuteration of the silyl group does not alter the frequency significantly.

The silyl deformation, ν_4 occurs at 926.2 cm^{-1} overlapping with the fine structure of the other silyl deformation, ν_{10}. These two bands move by a considerable amount on deuteration. There are bands in the deuterated compound at 712 cm^{-1} and 660 cm^{-1}, either of which could be assigned to ν_4 or the CF_3 deformation, ν_6. In the infra red spectrum of silyl perfluoromethyl acetylene, ν_6 is hidden under the rotational structure of the silyl rock, ν_{11}. The raman spectrum suggests that this band is at 690 cm^{-1}. ν_6 should not be greatly affected by deuterium substitution within the molecule. The only a_1 bands, however, are at 712 cm^{-1} and 660 cm^{-1}. It would appear that deuteration causes mixing of these two vibrations. As a result, one vibrational mode increases in energy while the other mode decreases. It is difficult to determine how much mixing has occurred because the respective bands have similar intensities in the silyl and germyl species.

The skeletal stretch, ν_5 is not a strong band in the infra red spectrum of silyl perfluoromethyl acetylene and is consequently hidden under the Q branch envelope of the silyl deformation, ν_{10}. A weak band is present at 858 cm^{-1} which could be assigned to this mode, although the raman spectrum indicates that this band is at 875 cm^{-1}, some 17 cm^{-1} higher. In the deuterated compound this band is clearly visible at 874 cm^{-1} in the infra red spectrum and is at a similar frequency in the raman spectrum.

The other skeletal stretch, ν_7 occurs at 351 cm^{-1} in silyl perfluoromethyl acetylene and 340 cm^{-1} in the deuterated compound.

The low frequency of the SiC stretch and the high value of ν_5, the C-C stretch, suggest that these two modes are heavily coupled, as observed in the other acetylenes studied.

The silyl rock, ν_{11} occurs in silyl perfluoromethyl acetylene at 681.4 cm^{-1} or 692.6 cm^{-1} depending on which Q branch is taken as the band centre. The spacing of the Q branches in this band and in the other two degenerate silyl modes, ν_8 and ν_{10} are similar to that found in the silyl halides. As the rotational constant, A is half as large as the value in the silyl halides, silyl perfluoromethyl acetylene must possess a free internal mode of rotation. This subject is dealt with in detail in chapters 5 and 6.

Deuteration causes the bands, ν_8, ν_{10} and ν_{11} to shift to low frequency with a change in the Q branch separation. Q branches in the deuterated compound were only resolved for ν_{10} although they were visible but not well resolved for ν_8.

The CF stretch, ν_9 occurs characteristically about 100 cm^{-1} to lower frequency of the other CF stretch, ν_3. This frequency does not change significantly on deuterium substitution.

The CF_3 deformation, ν_{12} occurs at 617 cm^{-1}, a frequency similar to that of the equivalent mode in methyl perfluoromethyl acetylene[40]. ν_{12} decreases in frequency by about 20 cm^{-1} on deuteration.

The band at 464 cm^{-1} in silyl perfluoromethyl acetylene has been assigned to the CF_3 rock, ν_{13}, an assignment consistent with those for other CF_3 acetylenes[40].

The bands at 240 cm^{-1} and 87 cm^{-1} were assigned to the two skeletal deformations, ν_{14} and ν_{15}. In the infra red spectrum, ν_{15} is observed as a weak band to high frequency of the polythene band

(polythene windows were used in the far infra red region). This band, however, is an intense band at 93 cm^{-1} in the raman spectrum.

When applied to silyl perfluoromethyl acetylene, the Redlich-Teller product rule[35] suggests that the assignments are substantially correct. The observed and calculated products for the a_1 symmetry species are 0.516 and 0.506 respectively and for the e symmetry species are 0.371 and 0.364.

Although partly obscured by the Q branches of ν_8, the silyl stretch, ν_2 has a definite PQR structure (figure 4.12). This is not surprising as Gerhard and Dennison[37] have shown that the intensity of the Q branch relative to that of the R and P branches depends on the ratio of the rotational constants B and A, where B is the rotation constant about the axes perpendicular to the unique axis and A is the rotation constant about the unique axis. When $B \to A$, the intensity of the Q branch is similar to the P and R branches; when $B \ll A$, as occurs with the silyl halo-acetylenes, the intensity of the P and R branches are very much greater than the Q branch. In silyl perfluoromethyl acetylene, B = 0.0301 cm^{-1} and A = 0.178 cm^{-1} with the result that the Q branch should be visible in a_1 bands. In silyl chloro-acetylenes, where B = 0.0444 cm^{-1} and A = 2.86 cm^{-1}, no Q branch should be visible in a_1 bands.

The CF stretch, ν_3 and the silyl deformation, ν_4, have the PQR structure as is shown in figure 4.12. The C - C stretch, ν_5 and the CF_3 deformation, ν_6, however, are hidden under the Q branches of ν_{10} and ν_{11} respectively in the infra red spectrum. In the infra red spectrum of the deuterated compound, ν_5 and ν_6 are visible and both possess PQR structures.

Figure 4.12 IR Bandshapes in SiH_3CCCF_3 (H) and SiD_3CCCF_3 (D)

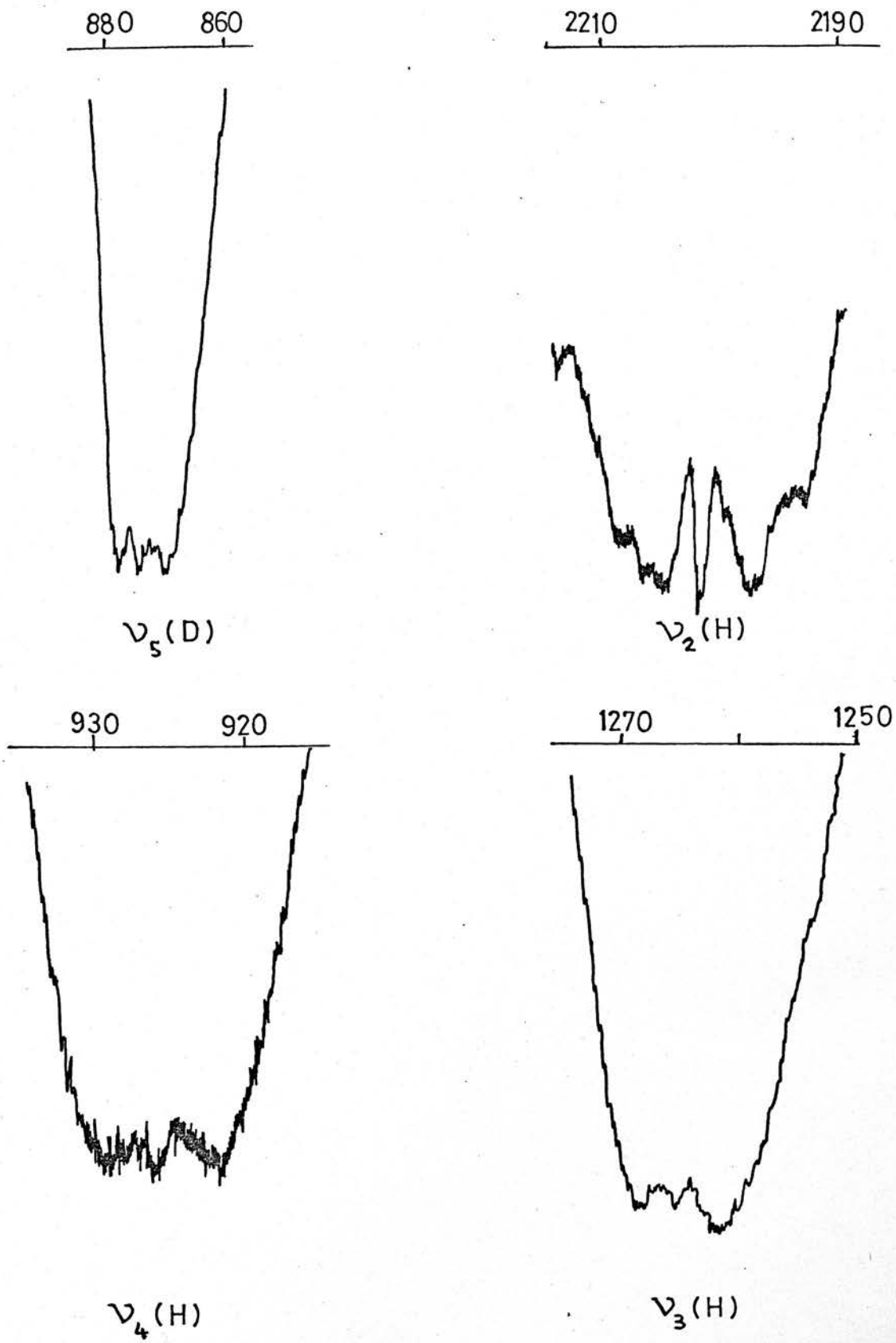

In both species, the SiC stretch, ν_7 does not have a convincing PQR strucutre although both bands have what appears to be a weak series of Q branches over the band (figure 4.13). A similar band shape is observed on the acetylenic stretch, ν_1 of the deuterated species. Such a series of bands is consistent with a series of "hot" bands of type $\nu_i + n\nu_{15} - n\nu_{15}$ occurring with the fundamental ν_i.

The degenerate CF stretch, ν_9 appears as a 'C' type band in both compounds (figure 4.13). This band shape is due to the zeta constant having a value close to unity as is found in the trifluoromethanes[41] where the zeta constant ranges from 0.70 to 0.98. The spacing of the Q branches in such bands is given by $2[A(1 - \zeta) - B]$, which tends to -2B as $\zeta \rightarrow 1$. The net result is that the central Q branch becomes more intense as the Q branches are drawn together. At the same time, the P and R branches, which are dependent on the quantum number J as well as K, are drawn in on the central Q branch giving an overall "C" type of band structure.

Rotational fine structure was resolved on the three silyl bands, ν_8, ν_{10} and ν_{11}, in silyl perfluoromethyl acetylene and on ν_{10}, but not on ν_8 or ν_{11} in the deuterated species. However, ν_{11} was very asymmetric probably due to a large positive zeta constant.

A set of strong combination and overtone bands is observed between 2000 cm^{-1} and 2600 cm^{-1} in both compounds. These bands seem to form a regular pattern centred on the acetylenic stretch, ν_1 (figure 4.14). This series of bands can be assigned in one of two ways, either in terms of combination bands involving one or other of the CF stretches (e.g. $\nu_3 + \nu_5$ is observed at 2045 cm^{-1} and $\nu_3 + \nu_9$ at 2439 cm^{-1}) or assigned to the combinations involving

Figure 4.13 IR Bandshapes in SiH_3CCCF_3 (H) and SiH_3CCCF_3 (D)

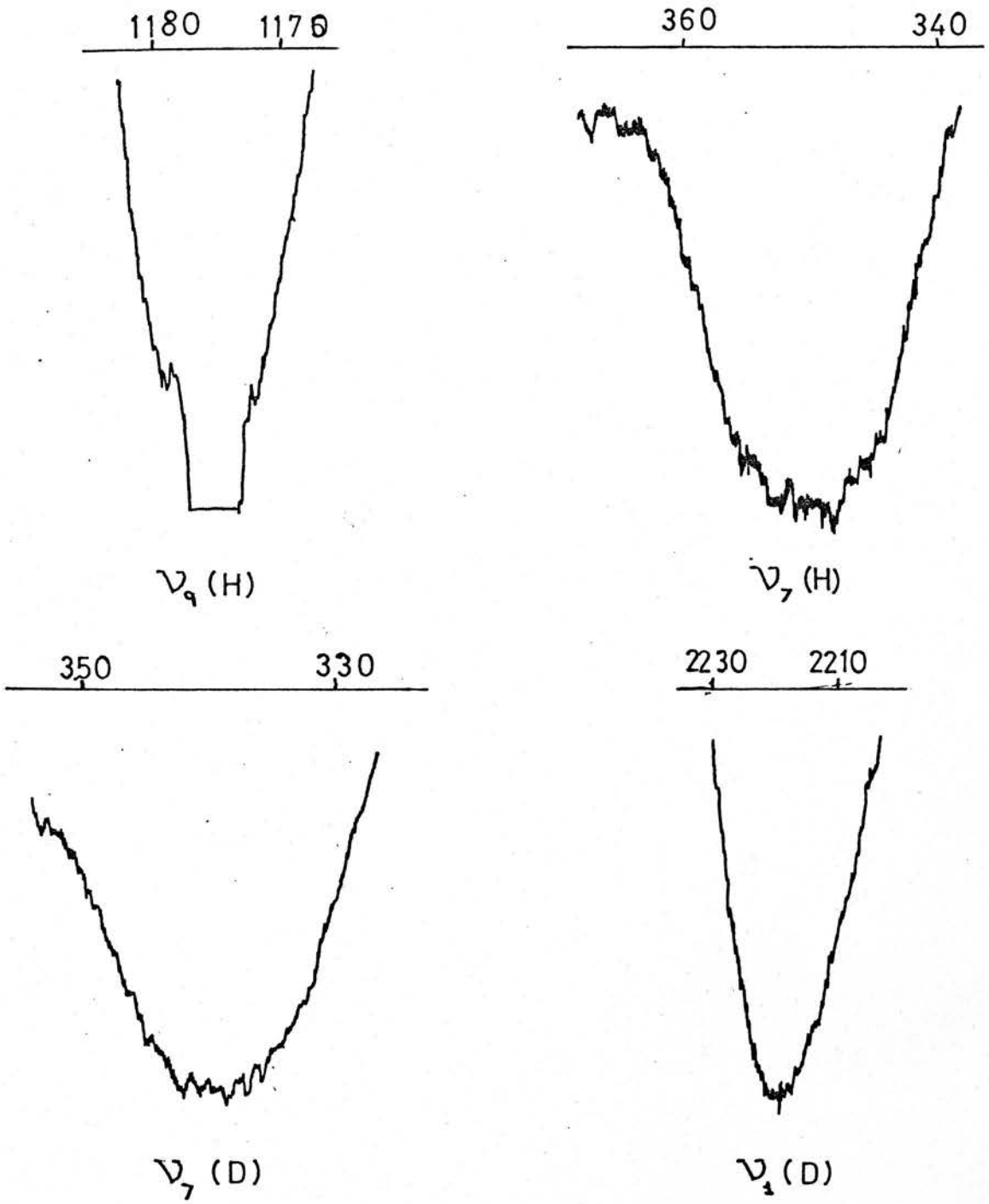

Figure 4.14 The 2300 cm^{-1} Region in the IR Spectrum of SiD_3CCCF_3

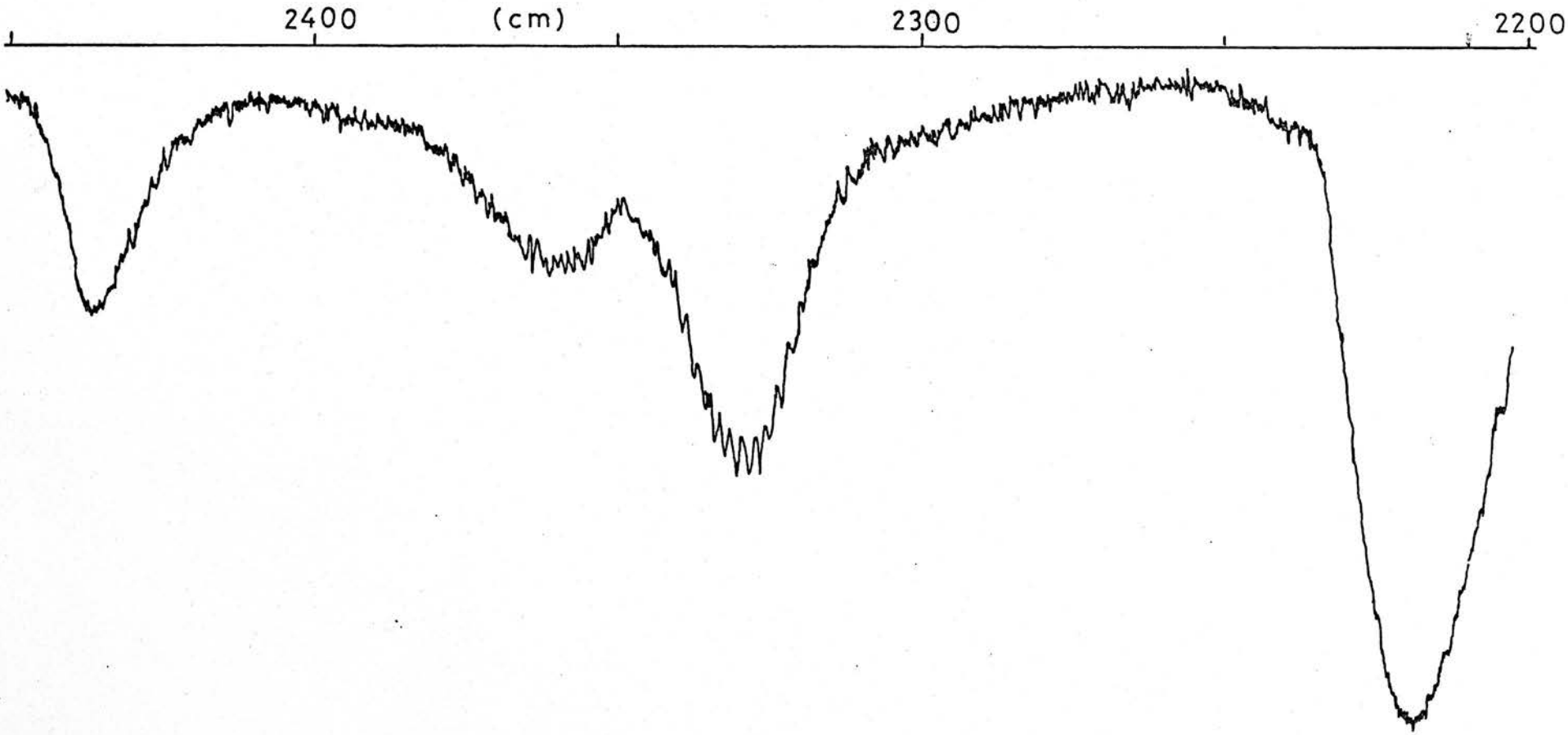

ν_1 and ν_{15} (e.g. the above frequencies could be due to $\nu_1 - 2\nu_{15}$ and $\nu_1 + 2\nu_{15}$ respectively). The latter assignment has ν_{15} at 97 cm^{-1} with an anharmonic constant of 16.5 cm^{-1} and predicts $\nu_1 + \nu_{15}$ to be at 2323 cm^{-1} and $\nu_1 + 3\nu_{15}$ at 2559 cm^{-1}. There are bands at 2316 cm^{-1} and 2329 cm^{-1} in the silyl and deutero silyl acetylenes respectively which could be assigned to $\nu_1 + \nu_{15}$. A band at 2523 cm^{-1} could be assigned to $\nu_1 + 3\nu_{15}$. This would require, however, an anharmonic constant of -4 cm^{-1}. Another argument against this type of assignment to this series of bands is that $\nu_1 - \nu_{15}$ is not as intense as expected in the spectrum of the deuterated acetylene. In deutero germyl perfluoromethyl acetylene, however, $\nu_1 - \nu_{15}$ could well be present although this band could also be due to residual hydrogen in the deuterated species.

Intense combination bands also occur in the region of the CF stretches in both compounds, probably resulting from Fermi resonance with either of the fundamentals. In silyl perfluoromethyl acetylene, $\nu_5 + \nu_7$ appears to be very strong with no central Q branch. In the deuterated acetylene, several combinations involving the silyl deformations move into this region resulting in a more complicated spectrum (figure 4.15). Another band in resonance is at 1140 cm^{-1} which could be assigned to the combination $2\nu_7 + \nu_{13}$ rather than the binary combinations $\nu_{11} + \nu_{13}$ and $\nu_{10} + \nu_{13}$ for the silyl and deutero silyl acetylenes respectively. All three bands have e components which can interact with ν_9.

The vibrational spectra of germyl perfluoromethyl acetylene and its deuterated analogue

The infra red spectra of germyl and deutero germyl perfluoromethyl acetylenes are shown in figure 4.16, the fundamentals are

Figure 4.15 ν_{CF} Regions of SiH_3CCCF_3 and SiD_3CCCF_3

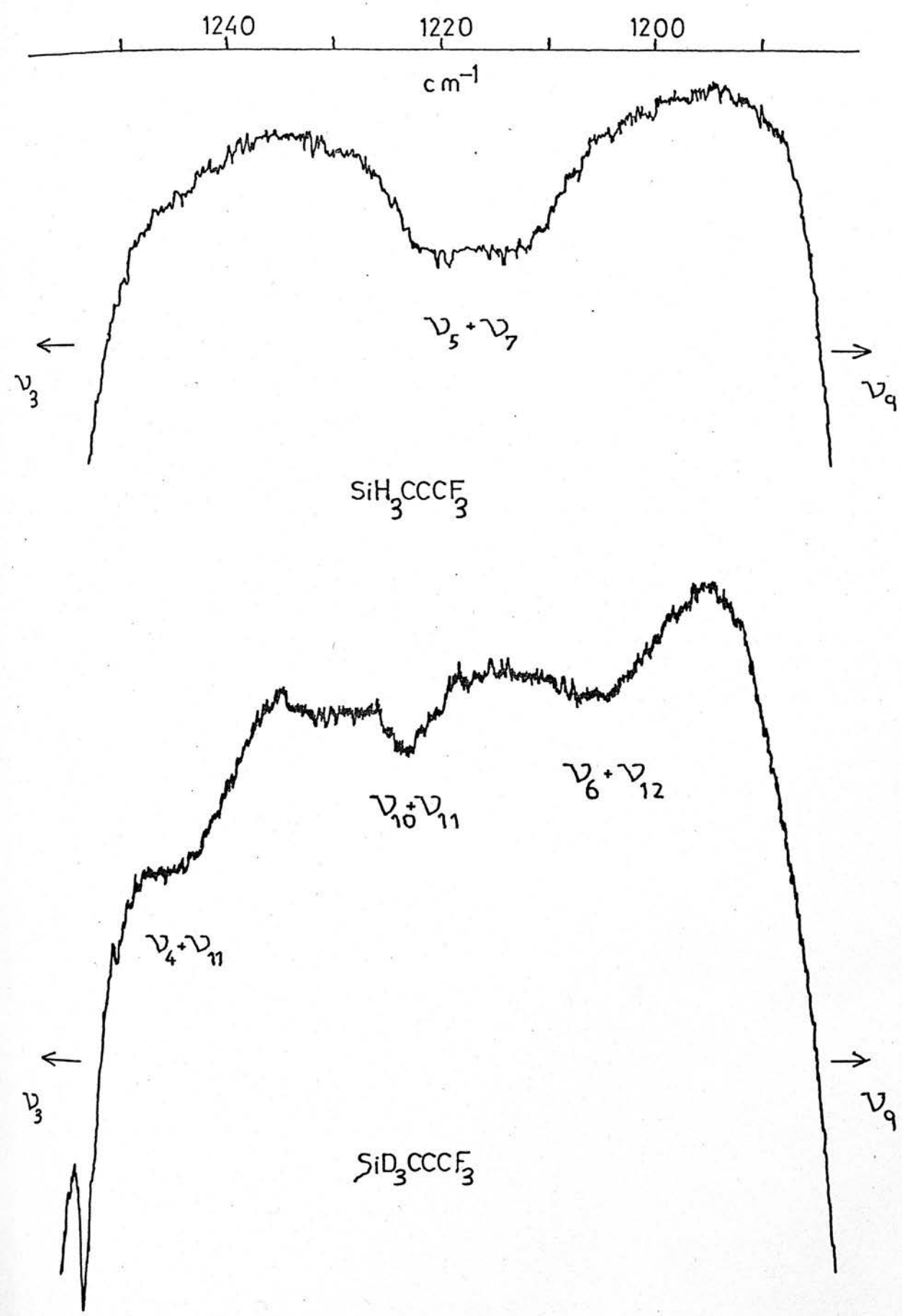

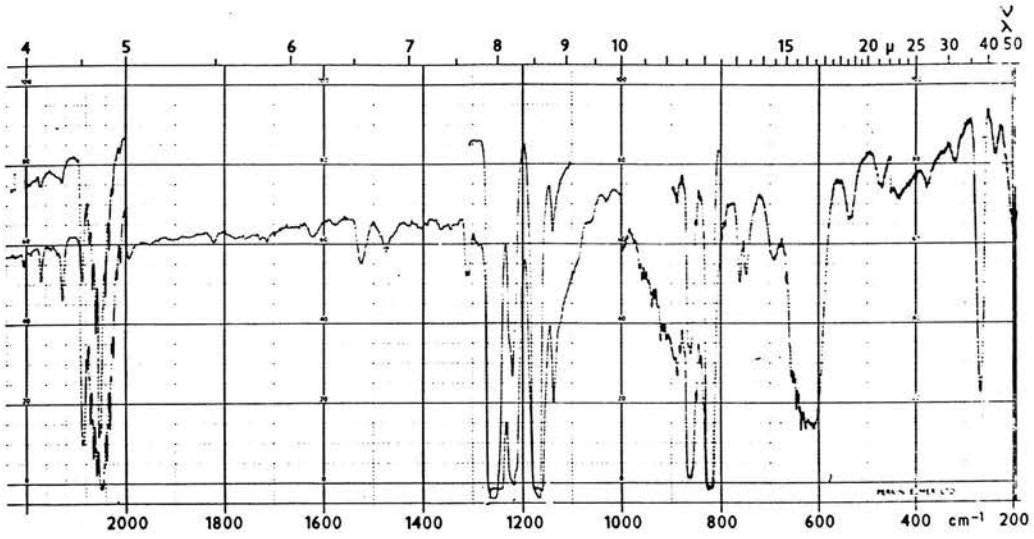

Figure 4.I6 a) IR Spectrum of GeH_3CCCF_3

b) IR Spectrum of GeD_3CCCF_3

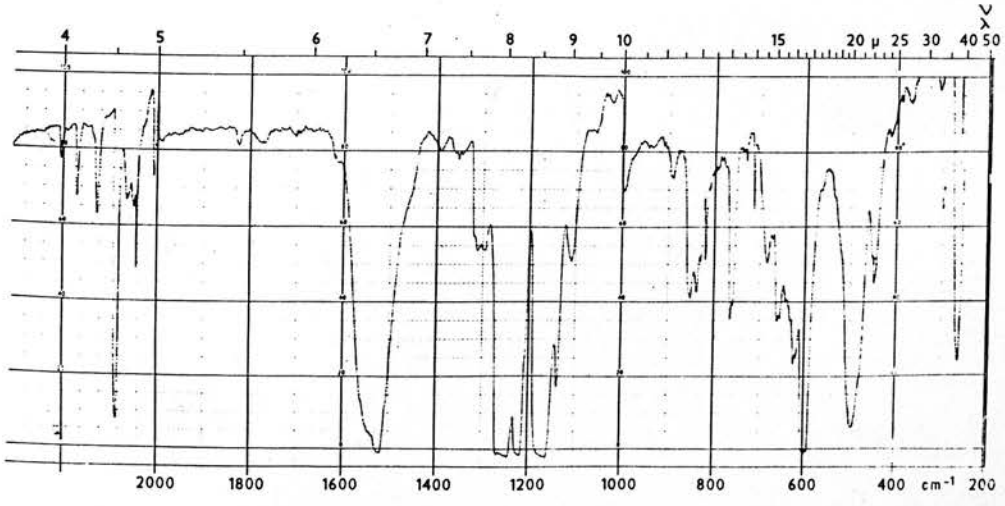

listed in table 4.18 and the assignments of the spectra in tables 4.19 and 4.20 respectively.

The main bands above 700 cm^{-1} were easily assigned to fundamental vibrations but those occurring below 700 cm^{-1} presented more of a problem because some bands although present in the raman spectrum did not appear in the infra red spectrum and vice versa. Assignment of these bands was based on comparison with the silyl and methyl analogues.

In both germyl acetylenes, the acetylenic stretch is at 2218 cm^{-1}, which is not very different from the frequency found in deutero silyl perfluoromethyl acetylene. In germyl perfluoromethyl acetylene, the germyl stretch, ν_2 occurs in the expected region at 2120 cm^{-1}. This frequency is shifted to 1528 cm^{-1} on deuterium substitution. The CF stretch, ν_3 occurs at a slightly lower frequency than the corresponding band in silyl perfluoromethyl acetylene, but this shift is not significant. The germyl deformation, ν_4 occurs at 821 cm^{-1}. There are bands in the deuterated compound at 662 cm^{-1} and 597 cm^{-1} that could be assigned to ν_4. Since the CF deformation, ν_6 occurs at 660 cm^{-1} in the germyl acetylene, it seems more plausible that ν_6 in the deutero germyl acetylene is at 662 cm^{-1} with ν_4 being assigned to the frequency at 597 cm^{-1}. There seems to be no interaction between these two bands, in contrast to the behaviour of the silyl analogue when the interaction on deuteration is in the order of 15 cm^{-1}. The C - C stretch, ν_5 in germyl perfluoromethyl acetylene is at 862 cm^{-1} approximately 10-15 cm^{-1} lower than the silyl analogue. In the deuterated acetylene ν_5 is at 853 cm^{-1}. These frequencies reflect the much lower value of the GeC stretch, ν_7 (compared with

Table 4.18. The Fundamental Frequencies of GeH_3CCCF_3 and GeD_3CCCF_3

Mode	GeH_3CCCF_3 (cm^{-1})	GeD_3CCCF_3 (cm^{-1})
ν_1	2119	2218
ν_2	2128.1	1524
ν_3	1262.5	1260.6
ν_4	821.8	597.0
ν_5	862	852
ν_6	660[a]	658
ν_7	264	261
ν_8	2131.1	1547
ν_9	1173	1172.5
ν_{10}	863.6 or 848.9	622.7
ν_{11}	626.6	489
ν_{12}	615[a]	618
ν_{13}	440	449
ν_{14}	235	221
ν_{15}	76	76

a) liquid phase Raman.

Table 4.I9a Assignments of i.r. Frequencies of GeH_3CCCF_3 (gas phase)

ν (cm^{-1})	Strength	Structure	Assignment
4I95.3	vw	centre of 'Q' branch	$2\nu_8$ (e)
4I90	vw	PR	$2\nu_8$ (a_1)
3478	w	-	$\nu_1 + \nu_3$
3390	vw	-	$\nu_1 + \nu_9$, $\nu_3 + \nu_8$
2980	w	-	$\nu_2 + \nu_5$
295I	w	-	$\nu_2 + \nu_4$, $\nu_4 + \nu_8$
2870	w	-	$\nu_1 + \nu_6$
25I7	w	-	$2\nu_3$
2486	w	-	$\nu_1 + \nu_7$
2430	m	-	$\nu_3 + \nu_9$
2382	vw	-	$\nu_2 + \nu_{14}$
2355	w	-	$2\nu_9$
2323	m	-	$\nu_1 + \nu_{15}$
22I9	m	-	ν_1
2I33.9	s	centre of 'Q' branch	ν_8
2I3I.5 2I24.7	s	PR	ν_2
I994	w	-	$\nu_4 + \nu_9$
I955	vw	-	
I827	vw	-	$\nu_6 + \nu_9$
I778	vw	-	$\nu_9 + \nu_{11}$
I7I8	vw	-	$2\nu_4$, $\nu_3 + \nu_{13}$
I624	w	-	$\nu_9 + \nu_{13}$
I580	w	-	
I527 I52I	w	PR	$\nu_3 + \nu_7$, $\nu_5 + \nu_6$
I482 I475	w	PR	$\nu_4 + \nu_6$
I435	vw	-	$\nu_4 + \nu_{11}$, $\nu_7 + \nu_9$

continued/....

Table 4.19a continued

ν (cm^{-1})	Strength	Structure	Assignment
1406	vw	-	$\nu_9 + \nu_{14}$
1361 1353	vw	PR	
1353 1346	vw	PR	
1340	m	-	$\nu_3 + \nu_{15}$
1315 1308	w	PR	
1294	vw	-	$\nu_{10} + \nu_{13}$
1265.5 1259.5	vs	PR	ν_3
1226 1220 1214	s	-	$\nu_5 + \nu_7 + \nu_{15}$, $\nu_7 + 2\nu_{13}$
1173	vs	-	ν_9
1137	m	-	$\nu_5 + \nu_7$
1059	w	-	$\nu_5 + \nu_{14}$
862	vs	-	ν_5
867.2 849.4	vs	centre of 'Q' branch	ν_{10}
825.2 818.4	vs	PR	ν_4
753 747	vw	PR	$\nu_7 + \nu_{12}$
685	m	-	
626.8	vs	centre of 'Q' branch	ν_{11}
536	vw	-	$2\nu_7$
474	w	-	$2\nu_{14}$
440	w	-	ν_{13}
382	w	-	$\nu_{14} + 2\nu_{15}$
339	vw	-	$\nu_7 + \nu_{15}$
314	w	-	$\nu_{14} + \nu_{15}$

continued/....

Table 4.I9a continued

ν (cm^{-1})	Strength	Structure	Assignment
264	m	-	ν_7
235	w	-	ν_{14}
I89	vw	-	$\nu_7 - \nu_{15}$
I50	w	-	$\nu_{14} - \nu_{15}$
II5	vw	-	$\nu_7 - 2\nu_{15}$
76	vw	-	ν_{15}

Table 4.I9b Assignments of Raman Frequencies of GeH_3CCCF_3 (liq.)

$\nu(cm^{-1})$	Strength	Polarization	Assignment
2225	m	70%	ν_1
2I35	vs	90%	ν_2, ν_8
I255	w	P	ν_3
II60	w	DP	ν_9
885	s	P	ν_4
865	m	-	ν_{10}
825	s	70%	ν_5
660	w	80%	ν_6
6I5	w	DP	ν_{12}
535	vw	P	$2\nu_7$
460	m	DP	ν_{13}
270	s	70%	ν_7
245	vs	DP	ν_{14}
I85	vw	-	$2\nu_{15}$
90	m	DP	ν_{15}

Table 4.20a Assignments of i.r. Frequencies of GeD_3CCCF_3 (gas phase)

ν (cm^{-1})	Strength	Structure	Assignment
3460	w	-	$\nu_1 + \nu_3$
2516	w	-	$2\nu_3$
2486	vw	-	$\nu_1 + \nu_7$
2429	w	-	$\nu_3 + \nu_9$
2360	vw	-	
2348	vw	-	$2\nu_9$
2321	m	-	$\nu_1 + \nu_{15}$
2218	s	-	ν_1
2160	w	-	$\nu_2 + \nu_{11}$
2125	w	fine structure	GeD_2HCCCF_3
2023	w	-	$\nu_4 + \nu_9$, $\nu_{10} + \nu_{12}$
1827	vw	-	$\nu_5 + \nu_9$
1778	vw	-	$\nu_9 + \nu_{11}$
1707	vw	-	$2\nu_4$, $\nu_3 + \nu_{13}$
1612	vw	-	$\nu_2 + \nu_{15}$, $\nu_9 + \nu_{13}$
1547	vs	-	ν_8
1524	vs	-	ν_2
1312	w	PQR?	$\nu_4 + \nu_{13}$
1301	w	-	
1263.8 1257.5	vs	PR	ν_3
1224.3 1218.2	s	PR	$\nu_{11} + \nu_{12} + \nu_{15}$
1172.5	vs	-	ν_9
1138	s	-	$\nu_4 + \nu_7$
1112	m	-	$\nu_5 + \nu_{13}$
995	w	-	
890	w	-	$\nu_5 + \nu_{14}$, $\nu_7 + \nu_{10}$

continued/....

Table 4.20a continued

ν (cm^{-1})	Strength	Structure	Assignment
855 850	m	PR	ν_5
837	m	-	$\nu_6 + \nu_{14}$
828	m	-	GeD_2HCCCF_3
763 760 757	m	PQR	$\nu_7 + \nu_{12}$
7I2	w	-	$\nu_{10} + \nu_{15}$
688	m	-	$\nu_6 + \nu_{15}$
66I 656	m	PR	ν_6
623.7	m	centre of 'Q' branch	ν_{10}
6I8	m	-	ν_{12}
600.5 594.5	vs	PR	ν_4
489	s	-	ν_{11}
449	m	-	ν_{13}
408	vw	-	$\nu_7 + 2\nu_{15}$
377	vw	-	$\nu_{14} + 2\nu_{15}$
339	vw	-	$\nu_7 + \nu_{15}$
303	w	-	$\nu_{14} + \nu_{15}$
26I	s	-	ν_7
22I	m	-	ν_{14}
I87	vw	-	$\nu_7 - \nu_{15}$
I46	vw	-	$\nu_{14} - \nu_{15}$
II4	vw	-	$\nu_7 - 2\nu_{15}$
76	vw	-	ν_{15}

Table 4.20b Assignments of Raman Frequencies of GeD_3CCCF_3 (liq.)

ν (cm^{-I})	Strength	Polarization	Assignment
2220	m	70%	ν_1
I540	s	DP	ν_8
I525	vs	P	ν_2
I260	vw	-	ν_3
II60	vw	DP	ν_9
855	m	90%	ν_5
660	m	90%	ν_6
635	s	DP	ν_{10}
620	m sh	-	ν_{12}
605	m	50%	ν_4
455	m	35%	ν_{13}
275	m	60%	ν_7
235	vs	DP	ν_{14}
I85	vw	60%	$2\nu_{15}$
90	m	DP	ν_{15}

the SiC stretch of the silyl analogue) at 266 cm^{-1} and hence the lessening of interaction between these modes; consequently these two frequencies are nearer to the frequencies of "pure" C - C stretches and "pure" Ge - C stretches respectively.

The three degenerate germyl bands, ν_8, ν_{10} and ν_{11}, all possess rotational structure in the spectrum of germyl perfluoromethyl acetylene, but only ν_{10} has a resolved structure in the deuterated acetylene. As expected, all three bands have a large isotopic shift.

The degenerate CF stretch, ν_9 occurs in the same position as this band in the silyl and methyl analogues.

The CF deformation, ν_{12} is not observed in the infra red spectrum of germyl perfluoromethyl acetylene due to overlap of the neighbouring germyl rock, ν_{11}. There is, however, a band of medium strength in the raman spectrum at 615 cm^{-1}. Comparison with other molecules shows that this is the expected region for the CF deformation. It is known from observation of germyl compounds that the germyl rock is very weak in the raman and for this reason is very rarely observed. The band at 615 cm^{-1} is almost certainly ν_{12} rather than the rock, ν_{11}.

Similarly, ν_{12} in deutero germyl perfluoromethyl acetylene is hidden by an overlapping band; this time by the germyl deformation, ν_{10}. The intensities of the bands in this region of the infra red spectrum suggest that the missing band lies between 615 cm^{-1} and 620 cm^{-1} (figure 4.17). The raman spectrum indicates that three bands are present between 600 cm^{-1} and 650 cm^{-1}; 600 cm^{-1}, 620 cm^{-1} and 635 cm^{-1} respectively. The band at 600 cm^{-1} can be assigned

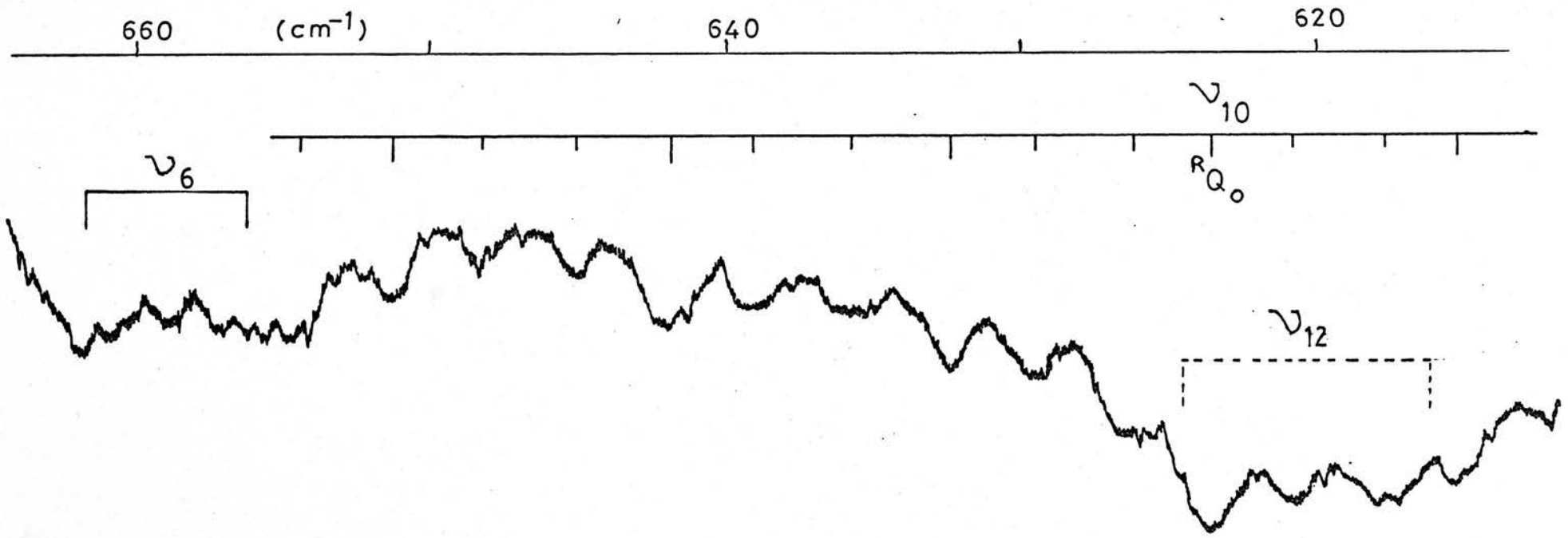

Figure 4.17 ν_{10} of GeD_3CCCF_3

to ν_4 because it is polarized, unlike the other two bands which are depolarized. The band at 620 cm^{-1} occurs as a shoulder on the 635 cm^{-1} band. Germyl deformations are usually strong in raman spectra suggesting that the deformation is at 635 cm^{-1}, leaving the band at 620 cm^{-1} to be assigned to ν_{12}.

In the infra red spectrum of germyl perfluoromethyl acetylene, the CF rock, ν_{13} can be assigned to the medium band at 474 cm^{-1}; the raman spectrum has a band at 460 cm^{-1}. The deutero acetylene has a raman band at 455 cm^{-1} and an infra red band of similar intensity to the germyl acetylene at 449 cm^{-1}. The phase shift is in the opposite direction for the two compounds. There is a shoulder, however, on the side of the germyl rock, ν_{11} in the deuterated acetylene similar in strength to the band at 449 cm^{-1}. It is not clear whether this shoulder is due to the unresolved structure of ν_{11} or is a separate band: perhaps ν_{13}. Since the Q branch separation on ν_{11} is the same order as the width of the Q branch, this band is a very broad unresolved band covering 60 cm^{-1}. There is a weak band at 440 cm^{-1} in the spectrum of the germyl acetylene but this band is more likely to be one of a series involving overtones and combinations of ν_7 and ν_{15}.

The skeletal deformation, ν_{14} at 234 cm^{-1} is a very weak band in the infra red spectrum of germyl perfluoromethyl acetylene, and is not observed in the deuterated acetylene. The raman bands, however, at 240 cm^{-1} and 230 cm^{-1} respectively, are the strongest in both spectra.

The other skeletal deformation, ν_{14} occurring at about 90 cm^{-1} is a strong band in the raman spectrum of both molecules. The far

infra red spectrum of the germyl acetylene obtained using a long path cell has a band at 76 cm^{-1}, although it could be due to a difference band, $\nu_{14} - 2\nu_{15}$.

The Redlich-Teller product ratios[34] agree with the calculated values. The a_1 calculated and observed products are 0.504 and 0.520 respectively and the e calculated and observed products are 0.374 and 0.365. The slight discrepancy is probably due to neglect of anharmonic, higher order effects and Fermi resonance between combinations and fundamentals.

The acetylenic stretch, ν_1 in both molecules is a very broad band (figure 4.18) with no PQR structure, suggesting the presence of "hot" bands similar to that discussed in other acetylenes. The skeletal stretch, ν_7 is also devoid of structure.

The four a_1 modes, ν_2, ν_3, ν_4 and ν_6 (figure 4.18) all possess PQR or PR band shapes. The Q branch is not as marked as in the spectra of the silyl molecules because of the increase in the ratio A/B which affects the Q branch intensity relative to the P and R branches.

The CF stretch, ν_9 (figure 4.19) possesses a 'C' type band shape, similar to that occurring in the silyl acetylenes, due to a zeta constant approaching to unity.

In the region between 2000 cm^{-1} and 2600 cm^{-1}, the same series of strong overtones and combinations occur as those observed in the two silyl perfluoromethyl acetylenes. This series of bands can be assigned either to a series of overtones and combinations based on ν_3 and ν_9 or to a series of combinations and difference bands based on $\nu_1 \pm n\nu_{15}$. The latter assignment gives a frequency for ν_{15} of

Figure 4.18 IR Bandshapes in GeH_3CCCF_3 and GeD_3CCCF_3

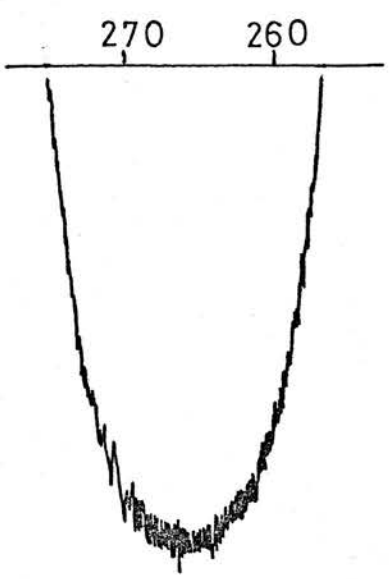

ν_7(H)

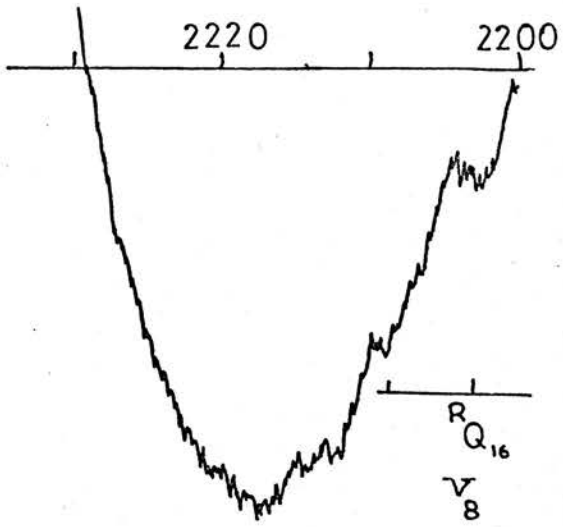

ν_1(H)

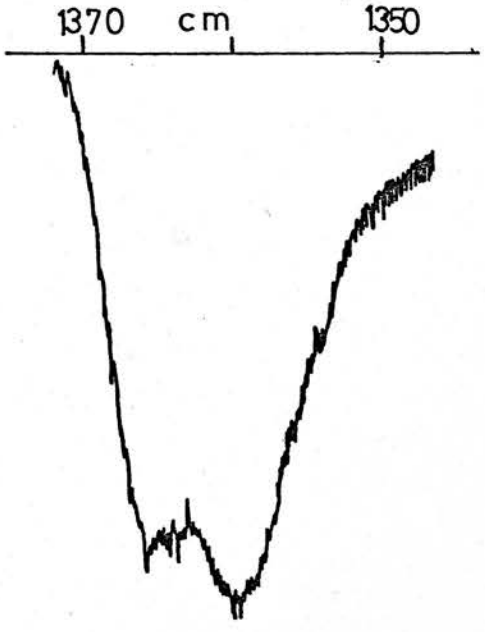

ν_3(H)

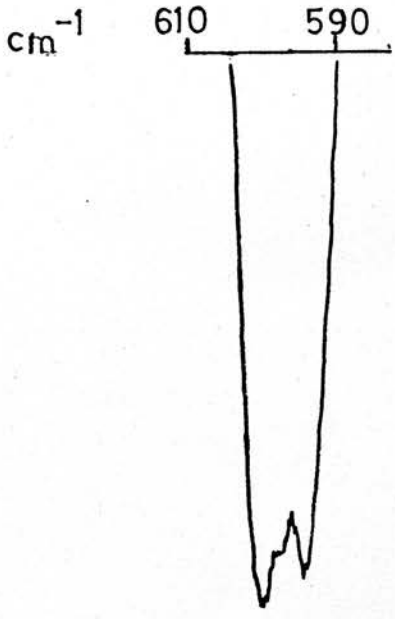

ν_4(D)

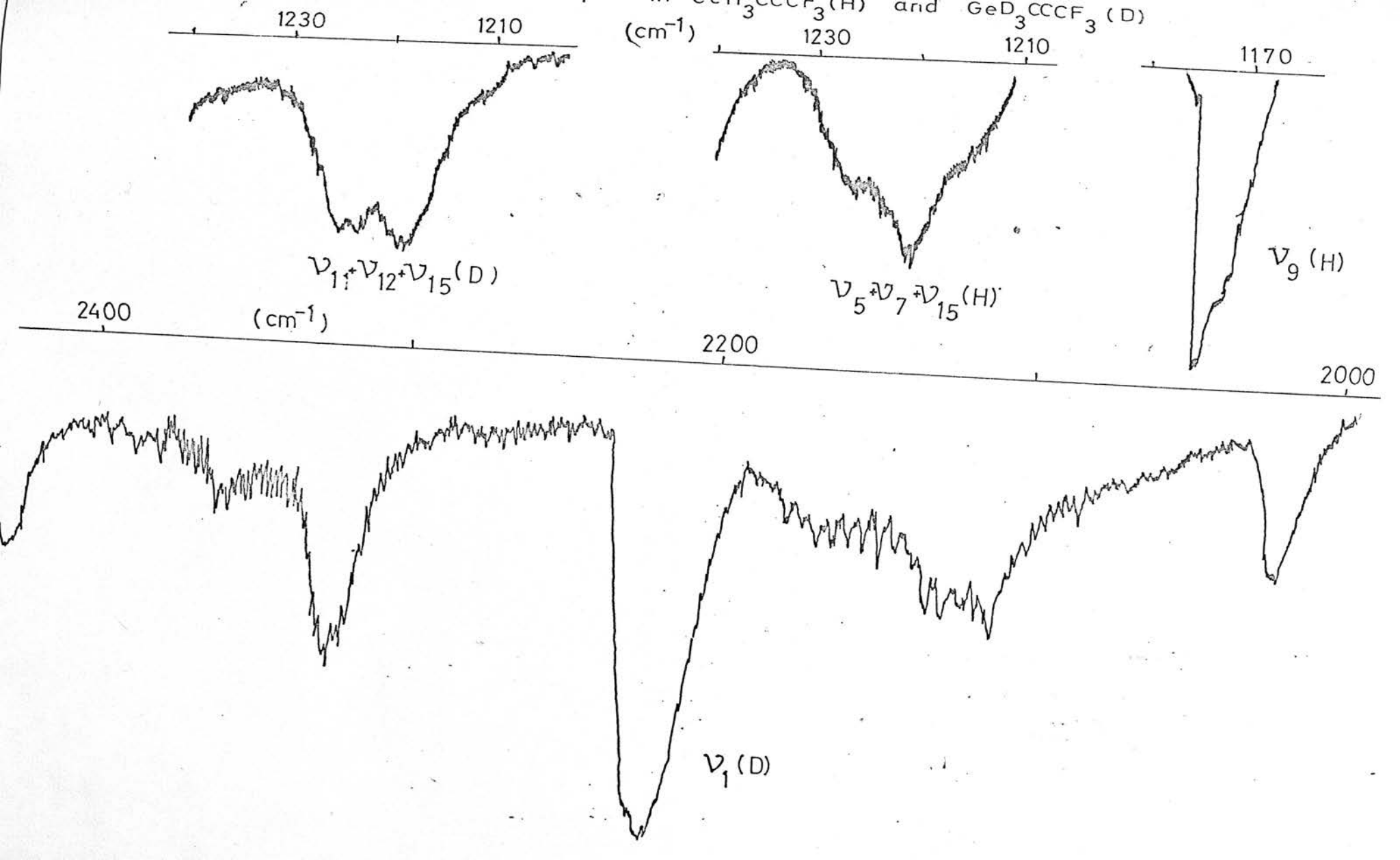
GeH3CCCF3 (H) and GeD3CCCF3 (D)
1230
1210
(cm-1)
ν11+ν12+ν15 (D)
1230
1210
ν5+ν7+ν15 (H)
1170
ν9 (H)
2400
(cm-1)
2200
2000
ν1 (D)

99.5 cm^{-1} with an anharmonic constant of 5.75 cm^{-1} from consideration of the frequencies of ν_1, $\nu_1 + 2\nu_{15}$ and $\nu_1 - 2\nu_{15}$. These values predict the frequency of $\nu_1 + \nu_{15}$ to be 2324.5 cm^{-1} and $\nu_1 + 3\nu_{15}$ at 2535.5 cm^{-1}. Bands actually occur at 2323 cm^{-1} and 2517 cm^{-1} in germyl perfluoromethyl acetylene and 2321 cm^{-1} and 2516 cm^{-1} in the deuterated analogue. This is a better fit to the frequencies than obtained with ν_1 and ν_{15} in the silyl molecules. The frequency of $\nu_1 - \nu_{15}$ is predicted at 2125 cm^{-1}, but this region is obscured by ν_2 and ν_8 in germyl perfluoromethyl acetylene. There is a band in this region in the deuterated molecule but this could well be due to the molecule $GeHD_2CCCF_3$ caused by residual hydrogen in the deuterating material (figure 4.19).

A similar progression of bands is observed in the far and middle infra red region involving ν_7, ν_{14} and ν_{15} (figure 4.20). The bands below 380 cm^{-1} were observed using a long path cell and a far infra red spectrometer. The spectrum observed confirmed the presence of weak bands associated with ν_7 and ν_{14} in both germyl compounds. A band at 76 cm^{-1} is likely to be ν_{15} although it is possible that it is due to the difference band $\nu_{14} \pm 2\nu_{15}$. The bands at 150 cm^{-1}, 314 cm^{-1} and 387 cm^{-1} are associated with the series of bands $\nu_{14} \pm n\nu_{15}$ where n = -1, +1, 2 respectively. The bands at 115 cm^{-1}, 189 cm^{-1}, 339 cm^{-1} are associated with the series of bands $\nu_7 \pm n\nu_{15}$ where n = -2, -1, +1 respectively.

Both acetylenes have a very strong combination band between the two CF stretches, ν_3 and ν_9 (figure 4.19) at 1220 cm^{-1}, but the band arises from different combinations in the two species. In germyl perfluoromethyl acetylene, this band has a prominent Q branch

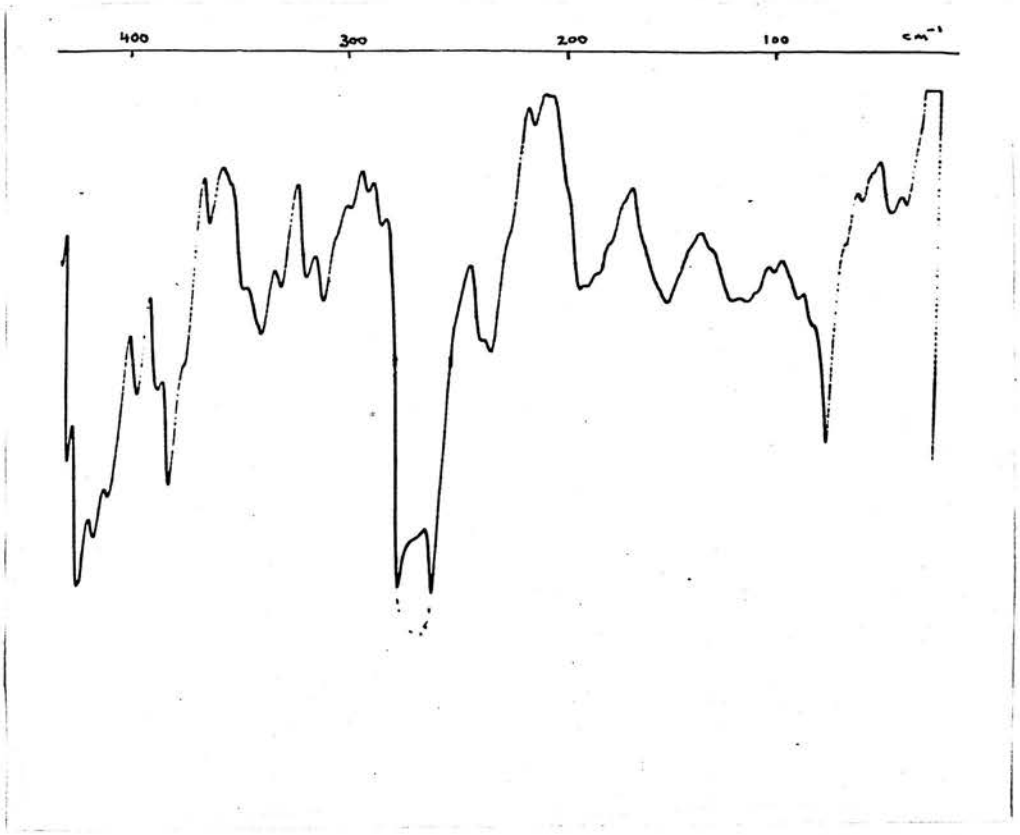

Figure 4.20 a) Far IR Spectrum of GeH_3CCCF_3

b) Far IR Spectrum of GeD_3CCCF_3

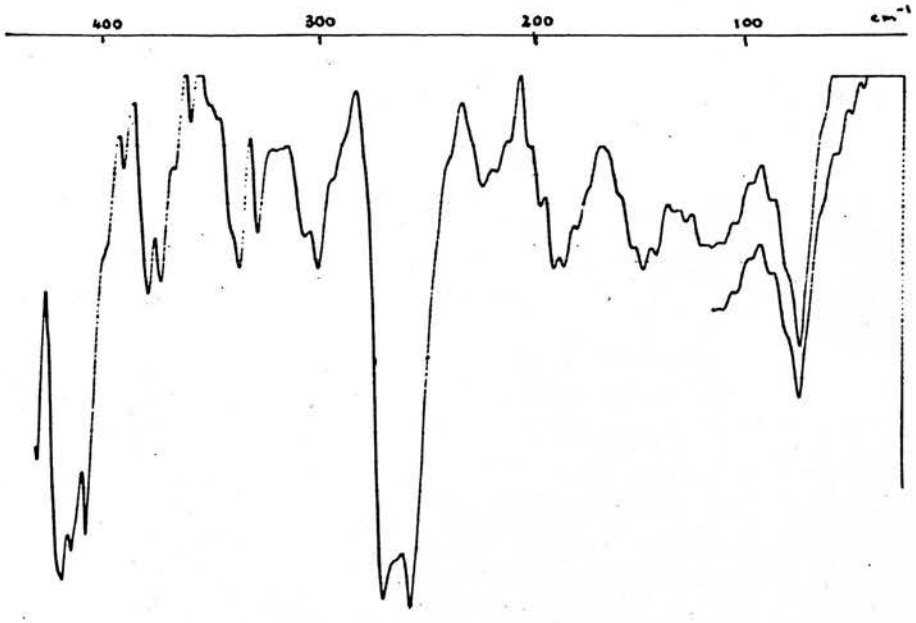

with weaker P and R branches, but in the deuterated acetylene it has P and R branches but no Q branch. Both bands are stronger in intensity than expected and thus, must be in Fermi resonance with either ν_3 or ν_9. The PQR band is most probably a perpendicular band in resonance with ν_9; the most likely candidates are $\nu_5 + \nu_7 + \nu_{15}$ and $\nu_7 + 2\nu_{13}$. The PR band is a parallel band in resonance with ν_3; the only reasonable candidate is $\nu_{12} + \nu_{11} + \nu_{15}$ due to the fact that $\nu_{10} + \nu_4$ is of the wrong symmetry.

4.5 Discussion

The acetylenic stretch in the monohalo-acetylenes, when plotted against the electronegativities of the respective halogen atoms gives a straight line[42]. A similar plot results when the electronegativities (χ) of X and Y are summed and plotted against the frequency of the acetylenic stretch for molecules of type X - C ≡ C - Y. In figure 4.21, $\chi_X + \chi_Y$ has been plotted against $\nu_{C\equiv C}$ for the mono and dihalo acetylenes, some silyl and germyl acetylenes and one or two other relevant compounds. The data is set out in table 4.21. The mono and dihalo acetylenes fit fairly well. Perfluoromethyl acetylene was fitted to the line to obtain an electronegativity for the CF_3 group; a value of 3.35 was obtained which falls between oxygen and fluorine on the electronegativity scale. This is consistent with other properties displayed by the CF_3 group. Hexafluoro dimethyl acetylene also lay on this curve when the above value was used.

In a similar manner, electronegativities were obtained for the silyl and germyl groups from this curve by using the acetylenic frequencies of disilyl and digermyl acetylenes. This gave values of 2.55 and 2.58 respectively for the silyl and germyl groups.

Table 4.21. The Electronegativities and Acetylenic Stretching Frequencies of Some Acetylenes

X	Y	$\nu_{C\equiv C}(cm^{-1})$	χ_X	χ_Y	$\chi_X + \chi_Y$
HCCCl		2110	2.10	3.00	5.20
HCCBr		2085	2.20	2.76	4.96
HCCI		2060	2.20	2.56	4.76
HCCF		2255	2.20	3.91	6.11
$HCCCF_3$		2165	2.20	3.34	5.54[a]
ClCCCl		2234	3.00	3.00	6.00
ClCCBr		2223	3.00	2.76	5.76
ClCCI		2191	3.00	2.56	5.56
BrCCBr		2185	2.76	2.76	5.52
BrCCI		2166	2.76	2.56	5.32
ICCI		2118	2.56	2.56	5.12
SiH_3CCH		2055	2.55	2.20	4.75
SiH_3CCCl		2164	2.55	3.00	5.55
SiH_3CCBr		2148	2.55	2.76	5.31
SiH_3CCSiH_3		2140	2.55	2.55	5.10[a]
SiH_3CCCF_3		2228	2.55	3.34	5.89
GeH_3CCH		2060	2.58	2.20	4.78
GeH_3CCCl		2172	2.58	3.00	5.58
GeH_3CCGeH_3		2127	2.58	2.58	5.16[a]
GeH_3CCCF_3		2218	2.58	3.34	5.92
CF_3CCCF_3		2300	3.34	3.34	6.68
HCCH		1974	2.20	2.20	4.40

a) Value found from the curve, hence electronegativities were derived for the unknown groups and subsequently used for the other compounds containing the groups.

figure 4.21 Electronegativities

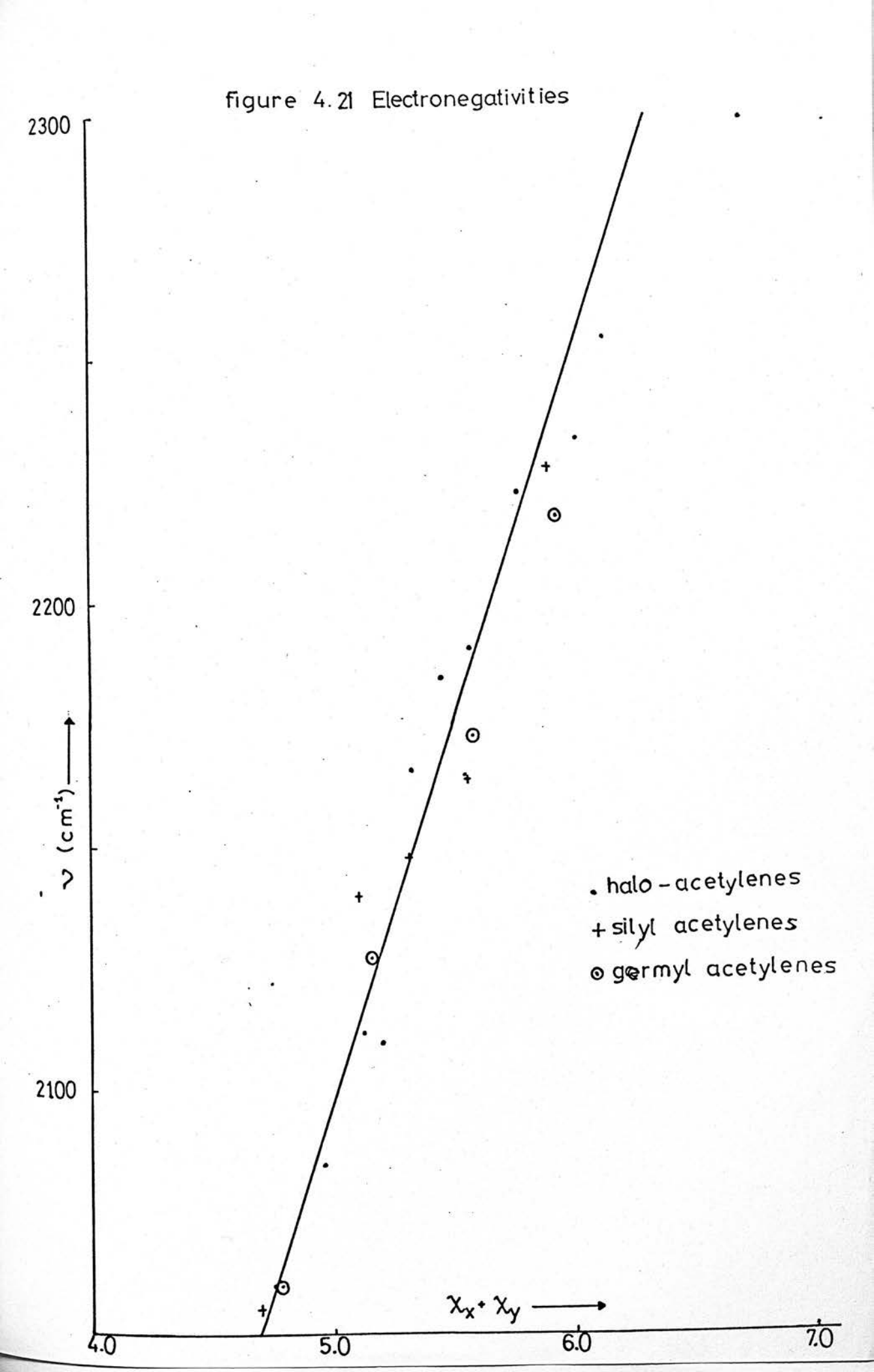

All the other silyl and germyl compounds were plotted and found to be close to this line. The electronegativities used were those obtained by the Mulliken method[43]. The values found for the silyl and germyl groups are in keeping with the Mulliken values for Si and Ge atoms which are 2.44 and ≃ 2.5 respectively.

Mulliken electronegativities are derived from ionization potentials and electron affinities of atoms or functional groups. Pauling electronegativities, however, are based on thermodynamical data of atoms and molecules. It is perhaps, not surprising that Mulliken electronegativities are preferable here because the change in frequency of the acetylenic stretch between different compounds reflects the change in energy of the π_{CC} bonding orbital and hence the ionization potentials. This effect is probably the largest factor involved in determining the position of the stretching frequency although the frequency will be modified by Fermi resonance and interaction with adjacent vibrations.

The anomalous structures on the acetylenic stretches and other parallel bands have been interpreted as evidence for overlap of a series of "hot" bands. A similar interpretation has been applied to the C ≡ C stretches and C ≡ N stretches in some other acetylenes and nitriles[44]. In many of these compounds, multiple Q branch structure had been observed which extended from a position near to the band centre towards lower frequencies. As the skeletal deformation is increasingly excited, the classical situation, where the most probable configurations are at the extremes of the vibration, is adopted. The energy of the molecular orbitals of the π_{CC} bonding level will be affected as the molecule becomes increasingly bent

with the result that the C ≡ C stretching vibration will progressively decrease or increase in frequency. In the majority of acetylenes, the stretching frequency has decreased indicating a decrease in the binding energy of the molecular orbital concerned. In methyl acetylene[45] the "hot" bands on the C - C stretching mode extends to higher frequency suggesting that the binding energy of the relevant molecular orbital has increased.

In principle it should be possible to obtain information on how the molecular orbital diagram changes as molecules become increasingly distorted from consideration of "hot" bands in the vibrational spectra of the molecules.

CHAPTER 5

Energy Levels of a Symmetric Top Vibrator

5.1 Energy Levels Within a Molecule

The energy of any molecular system can be written as the sum of the kinetic and potential energies of the nuclei and electrons

$$E = \sum_n \frac{P_n^2}{2m_n} + \sum_e \frac{P_e^2}{2m_e} + V_{nn} + V_{ee} + V_{ne} \qquad V.1$$

where P_n and P_e are the momenta of the nucleus n and electron e respectively; V_{nn}, V_{ee} and V_{ne} are the nucleus-nucleus, electron-electron, nucleus-electron interaction terms respectively.

In general, the quantum mechanical equivalent of equation V.1

$$\mathcal{H} = -\sum_n \frac{\nabla_n^2}{2m_n} - \sum_e \frac{\nabla_e^2}{2m_e} + V_{nn} + V_{ee} + V_{ne} \qquad V.2$$

may be greatly simplified by the Born-Oppenheimer approximation[46]. The approximation takes account of the fact that electrons are much lighter than nuclei and so tend to move much more rapidly. If a molecule is tumbling in space then electrons are assumed to move with the nuclear framework. If the nuclear framework is distorted, as occurs in a small amplitude vibration, the electrons are assumed to adopt instantaneously the new electronic configuration associated with the distorted framework. Thus equation V.2 becomes

$$\mathcal{H} = \mathcal{H}_n + \mathcal{H}_e$$

where $\mathcal{H}_n = -\sum_n \frac{\nabla_n^2}{2m_n} + V_{nn}$; $\mathcal{H}_e = -\sum_e \frac{\nabla_e^2}{2m_e} + V_{ee} + V_{ne}$

To a first approximation the Hamiltonian for nuclear motion can be further simplified. Motion of the nuclear framework can be separated into vibrational and rotational motion ignoring any interaction between them. A vibration between two atoms can be considered as an harmonic oscillator, the Hamiltonian of which is

$$\mathcal{H} = -\frac{\hbar^2}{2m_n}\frac{\partial^2}{\partial x} + \frac{1}{2}kx^2$$

This has eigenvalues of $E(V) = \nu(V + \frac{1}{2})$ where V is the vibrational quantum number = 0, 1, 2 . . . and ν is the vibrational frequency. The vibrational energy of a molecule is thus the sum of the 3N - 6 harmonic oscillators

$$G(V_1, V_2, \ldots, V_n) = \sum_{i}^{3n-6} \nu(V_i + \frac{d_i}{2}) \qquad V.3$$

where d_i is the degeneracy of the i^{th} normal mode.

Rotational motion can be considered as rotation of a rigid motor. In classical physics, the energy of rotation of a rigid body is determined by the moment of inertia about the rotation axis.

$$E_q = \frac{1}{2} I_{qq} \omega_q^2$$

where ω_q is the angular velocity of the body and q is one of the cartesian coordinates. Since the angular momentum P_q is given by

$$P_q = I_{qq} \omega_q$$

the Hamiltonian due to rotation becomes

$$\mathcal{H} = \frac{P_x^2}{2I_{xx}} + \frac{P_y^2}{2I_{yy}} + \frac{P_z^2}{2I_{zz}} \qquad V.4$$

In general, the solution to this equation is not exact except in a few special cases. The symmetric top rotor is one of these cases.

5.2 Energy Levels of a Symmetric Top Rotor

In a symmetric top molecule, two of the principal moments of inertia are equal in magnitude such that

$I_a < I_b = I_c$ for a prolate top or

$I_a = I_b < I_c$ for an oblate top.

Considering the prolate top only (the oblate top can be treated in a similar manner), equation V.4 can be rearranged

$$\mathcal{H} = \frac{P^2}{2I_b} + \left[\frac{1}{2I_a} - \frac{1}{2I_b}\right] P_z^2 \qquad V.5$$

where P is the total angular momentum of the rotor and is given by $P^2 = P_x^2 + P_y^2 + P_z^2$; P_z is conventionally taken as the angular momentum about the unique axis. The eigenvalues of this Hamiltonian are thus given by

$$F(J,K) = B\,J(J+1) + (A - B)\,K^2 \qquad V.6$$

where J and K are the total rotational quantum number and the component rotational quantum number about the unique axis respectively.

Since P_z is the component of angular momentum along the top axis, $P_z \leq P$, and $K \leq J$.

The energy levels of a symmetric top vibrator will be the sum of equations V.3 and V.6

$$E(V_1, V_2, \ldots V_{3n-6}, J, K) = G(V_1, V_2 \ldots V_{3N-6}) + F(J,K)$$

This gives sets of energy levels similar to that shown in figure 5.1.

The observed infra red spectrum will consist of transitions between the ground state and the upper state rotational levels.

In symmetric top molecules, vibrations occur with dipole changes either parallel or perpendicular to the unique axis. The absorptions associated with each type of vibration are known as parallel and perpendicular bands.

5.3 Parallel Bands

When the dipole change is parallel to the top axis, the selection rules for the quantum numbers V, J, K are

$$\Delta V_i = +1; \ \Delta K = 0, \ \Delta J = 0, \pm 1 \ (K \neq 0);$$

$$\Delta K = 0, \ \Delta J = \pm 1 \ (K = 0)$$

For a given value of K, the energy of the upper state is

$$E' = \nu_i(V_i' + \frac{d_i}{2}) + \sum_{\substack{j \\ j \neq i}} \nu_j(V_j' + \frac{d_j}{2}) + B\,J'\,(J' + 1) + (A - B)\,K^2 \qquad V.7$$

Figure 5.1 Rotational Energy Levels of a Symmetric Top

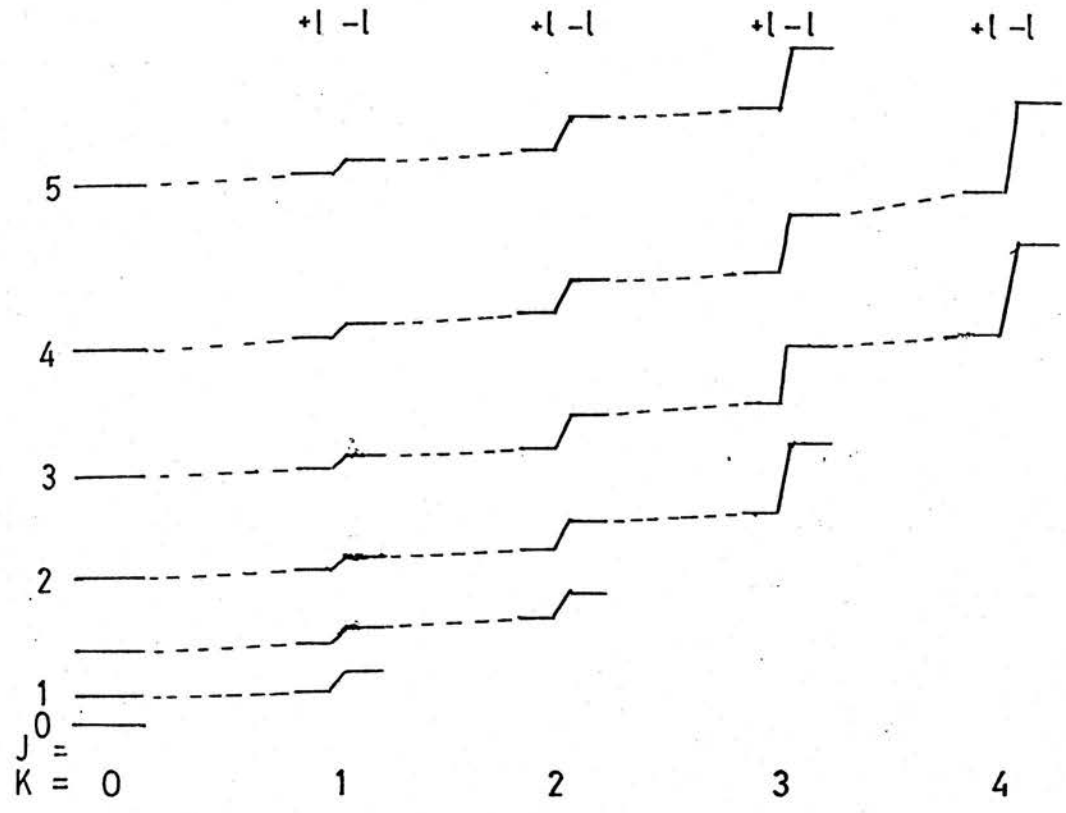

a) Degenerate State: $\zeta_i > 0$

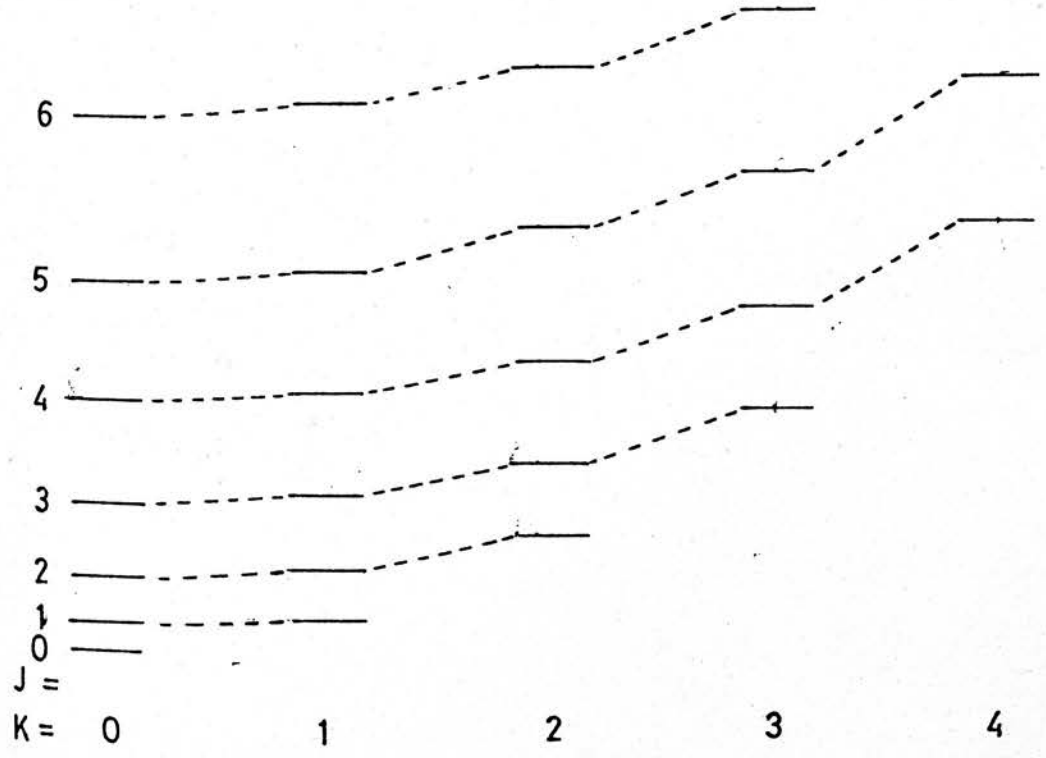

b) Non-degenerate State

and that for the lower state is

$$E'' = \nu_i(V_i'' + \frac{d_i}{2}) + \sum_{\substack{j \\ j \neq i}} \nu_j(V_j'' + \frac{d_i}{2}) + B\,J''(J''+1) + (A - B)\,K^2 \qquad V.8$$

The standard notation of single primes for the upper state values and double primes for the lower state values will always be employed.

The energy of the transition is given by

$$\nu = \nu_i + B\,J'(J'+1) - B\,J''(J''+1)$$

when $\Delta J = +1$ (R branch); $\nu = \nu_i + 2B\,(J''+1)$

when $\Delta J = 0$ (Q branch); $\nu = \nu_i$

when $\Delta J = -1$ (P branch); $\nu = \nu_i - 2\,B\,J''$

A sub-band is obtained for a given value of K with P, Q and R branches; the spacing of lines in the P and R branches is 2B. The complete band is obtained by superposition of each K sub-band.

In practice, the PQR bands for each K sub-band do not coincide, due to the rotational constants A and B having slightly different values in the upper and lower states. This is a consequence of vibration rotation interaction. The upper and lower states are now given by

$$E' = \nu_i(V_i' + \frac{d_i}{2}) + \sum_{\substack{j \\ j \neq i}} \nu_j(V_j' + \frac{d_j}{2}) + B'\,J'\,(J'+1) + (A' - B')\,K'^2 \qquad V.9$$

$$E'' = \nu_i (V_i'' + \frac{d_i}{2}) + \sum_{j \neq i} \nu_j (V_j'' + \frac{d_j}{2}) + B'' J'' (J'' + 1) + (A'' - B'') K''^2 \qquad V.10$$

The transitions occur at

$$\nu = \nu_i + B' J' (J' + 1) - B'' J'' (J'' + 1) + (\alpha_A - \alpha_B) K^2$$

where $\alpha_A = A' - A''$; $\alpha_B = B' - B''$.

The R, Q, P branches are respectively

$$\nu_R = \nu_i + (\alpha_A - \alpha_B) K^2 + \alpha_B J'' (J'' + 1) + 2B' (J'' + 1)$$

$$\nu_Q = \nu_i + (\alpha_A - \alpha_B) K^2 + \alpha_B J'' (J'' + 1)$$

$$\nu_P = \nu_i + (\alpha_A - \alpha_B) K^2 + \alpha_B J'' (J'' + 1) - 2B' J''$$

The spacing between rotational lines is 2B', but this spacing is not constant due to the quadratic term in J''. Usually α_B is small and B' < B'' with the result that the R branch converges slightly and the P branch diverges slightly at high values of J''. Since $\alpha_A + \alpha_B$ is not zero, the sub-bands of different K values are no longer coincident. As a result each "line" in the P and R branches is composed of many rotational lines which lie close together but do not quite coincide. An example of a parallel band is given in figure 5.2.

5.4 Perpendicular Bands

When the dipole change is perpendicular to the top axis, the selection rules for the quantum numbers are

figure 5.2 A Parallel Band

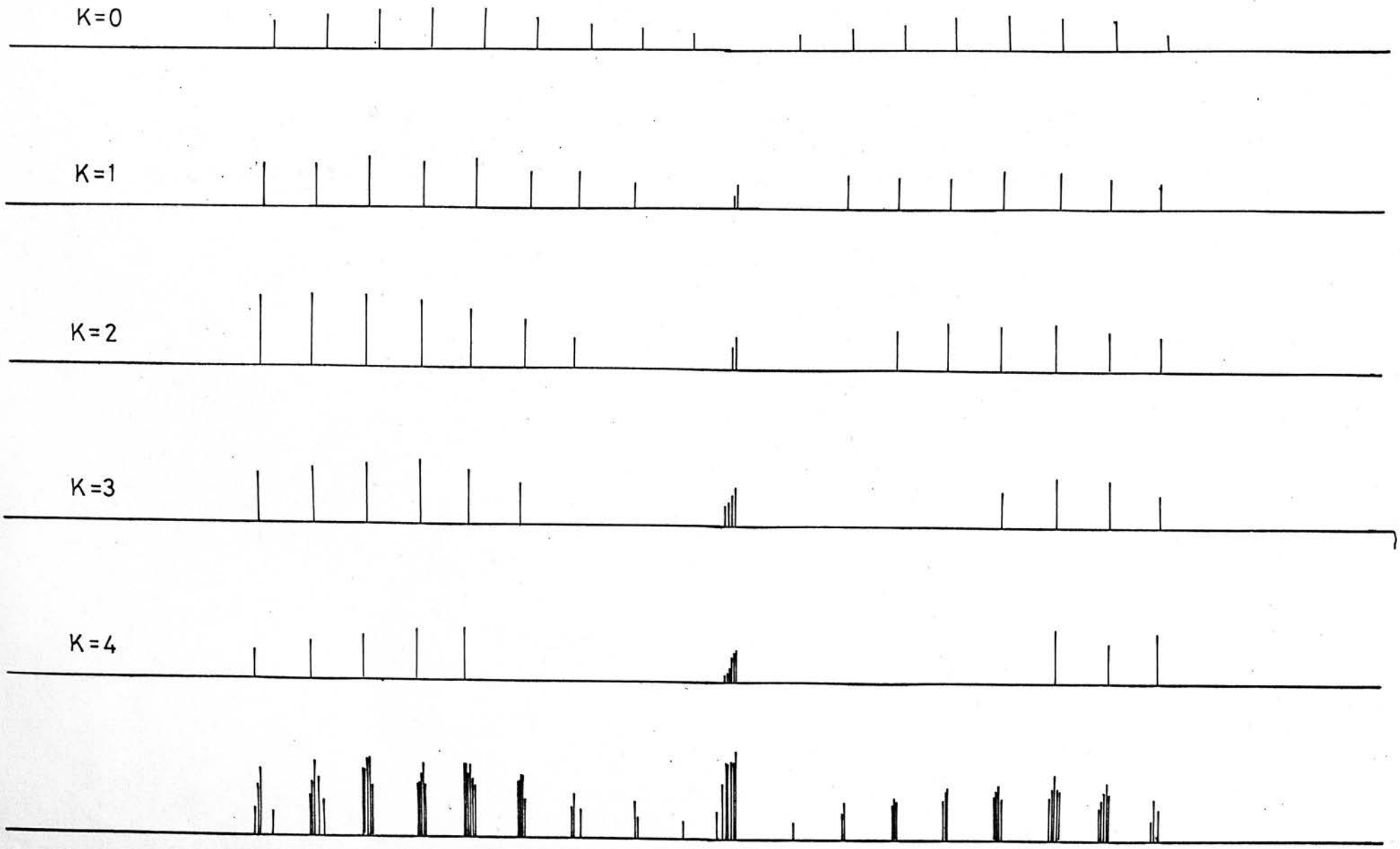

$$\Delta V_i = +1,\ \Delta J = 0, \pm 1,\ \Delta K = \pm 1.$$

It can be readily seen by comparison of these selection rules with those of a parallel band that PQ and R branches are obtained for a given value of K but that the K sub-band origin will shift according to the value of K since $\Delta K = \pm 1$.

The upper and lower state energies are still given by equations V.9 and V.10. The K sub-band origins will correspond to the position of the Q branches for each value of K and occur when $\Delta J = 0$.

The Q branch transitions are given by

$$\nu_Q = \nu_i + \alpha_B J'' (J'' + 1) + (A' - B') K'^2 - (A'' - B'') K''^2$$

because $\Delta K = \pm 1$.

$$\nu_Q = \nu_i + \alpha_B J'' (J'' + 1) + (A' - B') \pm 2(A' - B') K + (\alpha_A - \alpha_B) K^2 \qquad \text{V.11}$$

These Q branches form the most prominent features of a perpendicular band standing out from the unresolved background of the overlapping P and R branches, as shown in figure 5.3.

5.5 Coriolis Interaction and Centrifugal Distortion

According to equation V.11, the Q branch separation is the same in all perpendicular bands within the same molecule. In practice this is not so. Teller[47] was the first to explain this effect in terms of a coriolis type of coupling between a vibration and a rotation.

figure 5.3 A Perpendicular Band

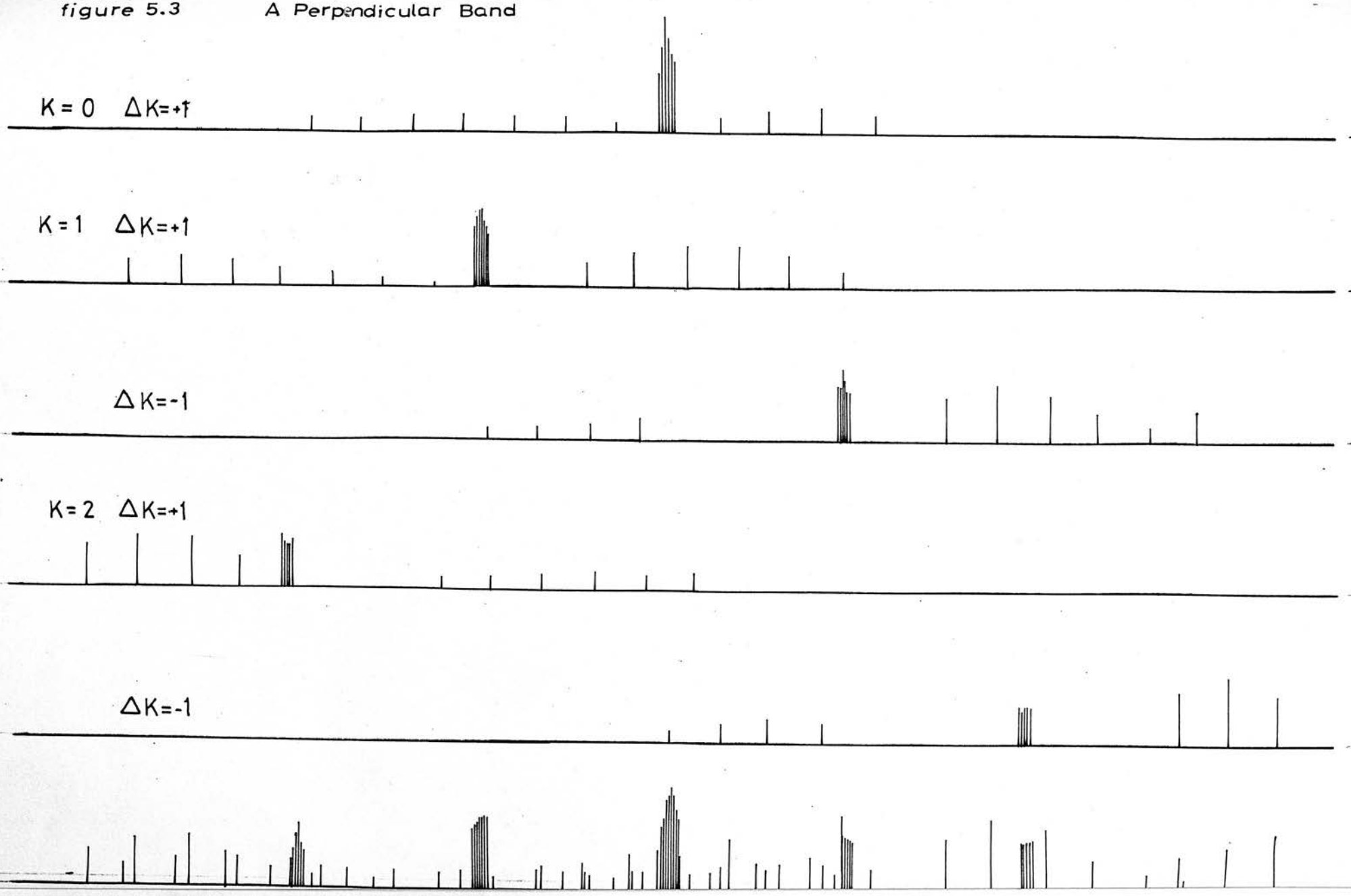

Consider a body in motion in a rotating coordinate system. In addition to the normal forces acting on the body with regard to its motion, there are two virtual forces needed to account for the actual motion of the body relative to an observer in the rotating frame, the centrifugal and coriolis forces.

Consider a wheel with a rigidly attached beam and a frictionless ball as shown in figure 5.4. As the wheel rotates, the beam imparts a tangential force to the ball and it will move in such a way that, to an observer rotating with the wheel and looking along the beam, the ball will seem to roll along the beam away from the centre of rotation. The observer would conclude that in order to maintain the ball at a constant radius, a radial force directed towards the centre of rotation must be applied.

The centrifugal distortion caused by this "force" causes a slight change to the energy levels for the rigid rotor given in equation V.6.

$$F(J,K) = B\,J(J+1) + (A-B)\,K^2 + D_J\,J^2(J+1)^2 + D_{K,J}\,J(J+1)\,K^2 + D_K\,K^4$$

where D_J is the centrifugal distortion constant for end over end rotation,

D_K is the centrifugal distortion constant along the unique axis,

D_{JK} is the interaction between these two.

The Q branch positions in a perpendicular band are now given by

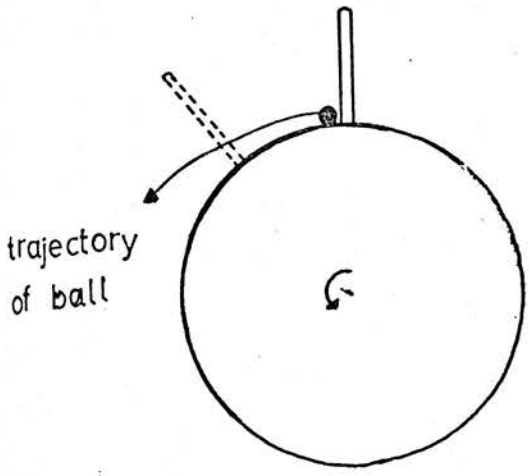

Figure 5.4 'Centrifugal' Force

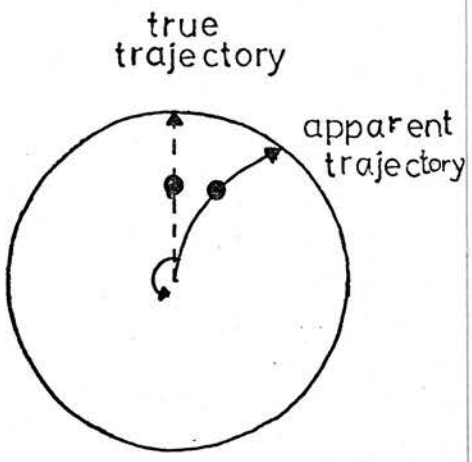

Figure 5.5 'Coriolis' Force

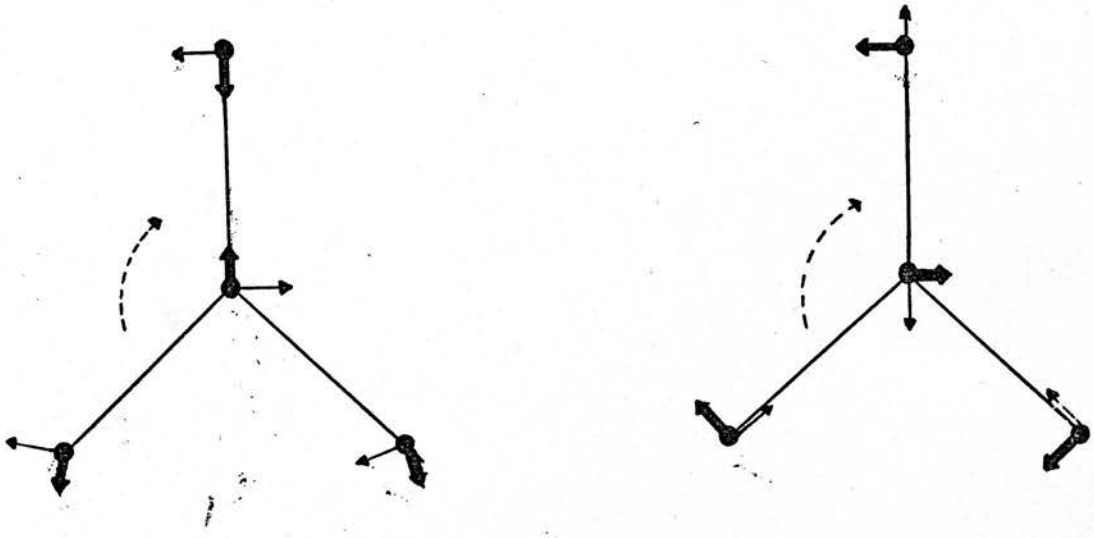

Figure 5 6 Planar XY_3 Molecule : Coriolis Interaction

$$\nu_Q = \nu_i + \alpha_B J''(J'' + 1) + (A' - B') \pm 2(A' - B') K$$

$$+ (\alpha_A - \alpha_B) K^2 \pm 4 D_K K^3$$

assuming that D_J, D_K, D_{JK} are all very small compared to A or B. In general centrifugal distortion is of little importance to infra red spectroscopy, but it will become increasingly more important with the development of spectrometers capable of at least 10^{-3} cm^{-1} resolution.

If the observer in the rotating frame were to roll balls from the centre radially (figure 5.5), the balls to him would not appear to move in a straight line. To an external observer, however, the balls would move in a straight line along the radius. The rotating observer would conclude that the ball had a tangential component of velocity and since he only applied a radial force to the ball, that a tangential force was effectively operating due to the rotation of the coordinate system. This force is the coriolis force: a standard illustration of the force is the fact that a projectile fired towards the equator from the north pole will seem to drift towards the west because the earth rotates towards the eastern horizon.

Consider the coriolis effect on the two components of a degenerate stretch in a planar XY_3 molecule as shown in figure 5.6. The motion of the atoms are represented by the black lines and the resultant coriolis accelerations by thin arrows. It is clear that each component of the degenerate vibration executes the other component. Since these components have the same frequency, the interaction is very strong.

In order to analyse the problem, two motions that do not influence each other in this way need to be considered. Appropriate linear combinations of the components can be found in which the atoms execute a clockwise and anticlockwise movement about their equilibrium positions without exciting the other component. Each of these linear combinations, however, has a resultant angular momentum associated with the vibration.

In a symmetric top molecule in a degenerate vibration, this angular momentum is with and against the angular momentum of the top axis. The Hamiltonian for any vibrating rotating molecule is a modification of equation V.4.

$$\mathcal{H} = \frac{(P_x - \rho_x)^2}{2I_{xx}} + \frac{(P_y - \rho_y)^2}{2I_{yy}} + \frac{(P_z - \rho_z)^2}{2I_{zz}}$$

$$+ \frac{1}{2}\sum_i \rho_i^2 + V \qquad \text{V.12}$$

where P_x, P_y, P_z are again the components of total angular momentum

ρ_x, ρ_y, ρ_z are the components of vibrational angular momentum

ρ_i is an operator associated with the linear momentum of the i^{th} normal mode and V is the potential energy.

Boyd and Longuet-Higgins[48] have treated this problem by perturbation theory but a semi-classical treatment[49] derives the same result.

In a degenerate vibration of a symmetric top molecule

$$I_x = I_y = I_B;\ I_z = I_A;\ \rho_x = \rho_y = 0;\ \rho_z = \pm \rho,$$

with the result that equation V.12 simplifies to

$$\mathcal{H} = \frac{P^2}{2I_b} + \frac{P_z^2}{2}\left[\frac{1}{I_a} - \frac{1}{I_b}\right] \mp \frac{2\rho P_z}{I_a} + \frac{\rho^2}{2I_a} + \frac{1}{2}\sum_i \rho_i^2 + V \qquad \text{V.13}$$

The first two terms are the same as the rigid rotor Hamiltonian of equation V.5. ρ is a function solely dependent on the normal coordinates of the molecule and so the term $\frac{\rho^2}{2I_a}$ can be included as a term in the vibrational Hamiltonian as it does not affect the rotational energy levels. The third term is due to the coriolis interaction on the rotation. The first three terms constitute the rotational Hamiltonian of a symmetric top molecule.

The energy levels for the rotational Hamiltonian are given by

$$F(J, K, \ell_i) = B\ J\ (J + 1) + (A - B)\ K^2 \mp 2A\zeta_i \ell_i K$$

where ℓ_i is a quantum number and ζ_i is the zeta constant which can vary $-1 \leq \zeta \leq 1$; the zeta constant is introduced because the angular momentum about the top axis generated by a vibration will not in general be an integral multiple of $h/2\pi$ because it is only necessary that the sum of vibrational and pure rotational angular momenta be quantized about this axis.

It has been shown[50] that

$$\ell_i = V_i,\ V_i - 2,\ \ldots,\ -V_i.$$

For the first vibrational level $\ell_i = \pm 1$ and so the correction to the energy level is $\mp 2A\zeta_i K$. The degeneracy of the energy levels is removed and the splitting increases linearly with K.

Allen and Cross[51] have shown that the level $\ell_i = +1$ is the lower and that the selection rule is such that the transition $\Delta K = +1$ is from the ground state to the $\ell_i = +1$ level while the transition $\Delta K = -1$ is to the $\ell_i = -1$ level.

The sequence of Q branches may readily be derived as

$$\nu_Q^{sub} = \nu_o + \left[A''(1 - 2\zeta_i) - B'\right] \pm 2\left\{A'(1 - \zeta_i) - B'\right\} K'' + (\alpha_A - \alpha_B) K''^2 \pm 4 D_K K^3 \qquad V.14$$

where $\nu_o = \nu_i + \alpha_B J''(J'' + 1)$. The spacing of the Q branches is now $2\left[A'(1 - \zeta) - B'\right]$ rather than $2(A' - B')$. Since ζ_i is different for each vibration, the spacing will differ for the various bands in the spectrum.

5.6 Free Internal Rotation in Symmetric Top Molecules

In molecules of the type X_3MMY_3 or $X_3MC \equiv CMY_3$, each end can rotate against the other end of the molecule subject to a low enough barrier of rotation around the MM axis.

The former type of molecules have quite large barriers to internal rotation but the latter type have barriers that are very close to zero, if not actually zero. The latter type of molecules are examples of free internal rotors.

In molecules of type $XM_3C = CMY_3$ it has been observed that the vibrational spectrum consists of a series of Q branches where the splitting

is similar in size to that of a rigid rotor consisting of only one of the two tops, e.g. in methyl silyl acetylene the perpendicular CH vibrations have Q branch splittings similar to those in methyl chloride. This is not expected as the rotational constant A is much smaller in the former case than in the latter.

The Hamiltonian of a free internal rotor of type

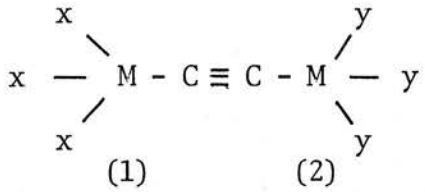

is given by

$$\mathcal{H} = \frac{(P_x - \rho_x)^2}{2I_{xx}} + \frac{(P_y - \rho_y)^2}{2I_{yy}} + \frac{(P_{z_1} - \rho_1)^2}{2I_{z_1}} + \frac{(P_{z_2} - \rho_2)^2}{2I_{z_2}}$$

where P_{z_1}, P_{z_2} are the components of total angular momentum about ends (1) and (2) respectively; ρ_1, ρ_2 are the vibrational angular momenta associated with ends 1 and 2.

The energy levels given by this Hamiltonian for a symmetric top molecule are

$$F(J, K, \ell_i) = B\,J(J+1) - B\,(K_1 + K_2)^2 + A_1K_1^2 + A_2K_2^2$$

$$\mp 2A\zeta_i\ell_iK_{1,2}$$

where K_1, K_2 are the quantum numbers associated with the components of angular momentum about the top axis for ends (1) and (2) respectively. $K_{1,2}$ will be either K_1 or K_2 depending on whether the i^{th} vibration being excited is a vibration in end 1 or 2.

If the vibration studied is associated with end 1, then the selection rules for a perpendicular band are

$$\Delta J = 0, \pm 1; \ \Delta K_1 = \Delta K = \pm 1; \ \Delta K_2 = 0; \ \ell_i = \pm 1.$$

The positions of the Q branches are given by

$$\nu_Q = \nu_o + \left[A_1' (1 - 2\zeta_i) - B'\right] \pm 2 \left[A_1' (1 - \zeta) - B'\right] K_1$$

$$+ (\alpha_A - \alpha_B) K_1^2 \mp 2B' K_2 + (\alpha_A - \alpha_B) K_2^2 \qquad \text{V.15}$$

The Q branches will have a separation of $2\left[A_1' (1 - \zeta_i) - B\right]$ because this is by far the largest term. This is exactly the same splitting as a rotor consisting only of end (1).

In this case, however, each Q branch will be split by 2B' as shown in figure 5.7. The centre of each bunch of Q branches will be when $K_2 = 0$. The centre of each Q branch series reduces to that of a single rotor. Similarly when the vibration excited is associated with end (2), the Q branches occur in bunches at intervals $2\left[A_2' (1 - \zeta_i) - B'\right]$, each bunch consisting of lines separated by 2B'.

5.7 Analysis of Perpendicular Bands

Unless the structure of a parallel band can be analysed, there is no way of calculating the rotational constant B for a symmetric

figure 5.7 A Perpendicular Band of an Internal Rotor

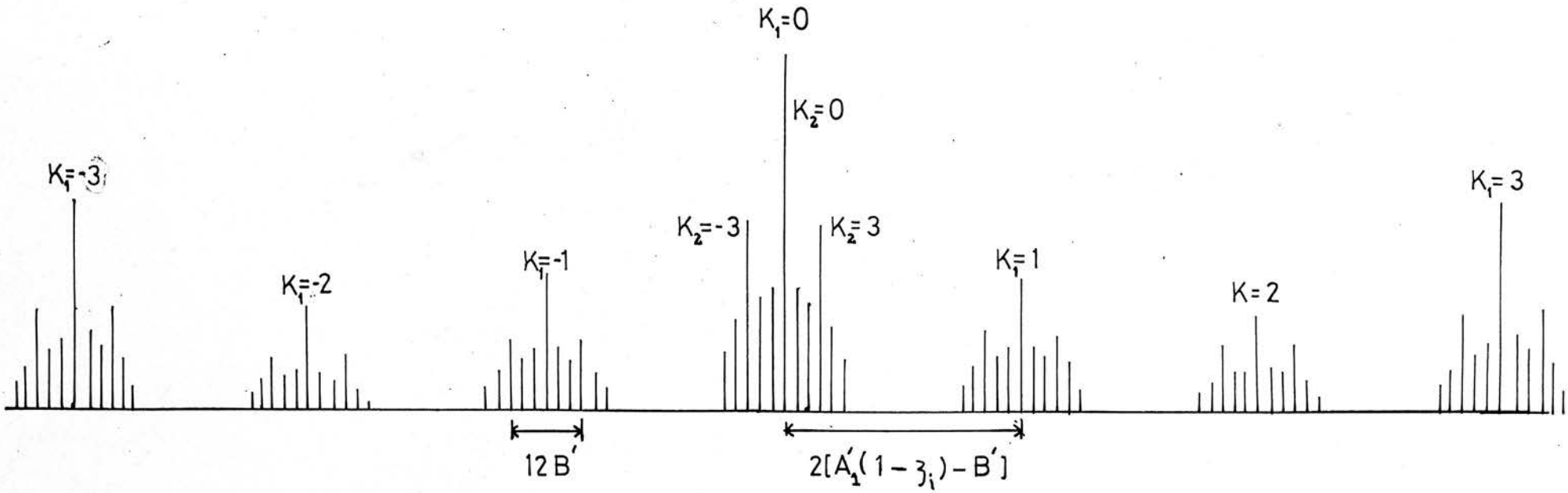

top molecule solely from vibrational spectra. Generally B is too small to cause resolution of the separate lines in the P and R branches of a band. Values of B, however, can be obtained from microwave data and in suitable cases, the change in B with vibrational state can also be observed.

If microwave data is not available, a value of B can be obtained either by use of bond lengths and bond angles from electron diffraction studies to calculate the moment of inertia of the molecule and hence B or by comparison with similar known structures. The electron diffraction data does not yield a value of B for the ground state, but an average value over all occupied states and as such is not as accurate as microwave determination of B. The smaller the value of B compared to A, the more accurate these last two methods become, converging towards the microwave value.

The determination of A is more difficult. It can be determined by microwave only as long as there are sufficient isotopic species to work out the complete structure of the molecule: this is rarely the case. In symmetric top molecules the structure is determined from the microwave spectra of the symmetric top and isotopic species that are slightly asymmetric using Costain's method[52].

The determination of A can under favourable circumstances be achieved using the perpendicular bands in the infra red and raman spectrum. The spacing between successive Q branches as given by equations V.14 and V.15 is $2[A'(1 - \zeta_i) - B']$ for the i^{th} vibrational mode. So long as $B << A$ which it usually is in symmetric top hydrides then a reasonable value of A' can be determined. A' and ζ_i can be found individually as long as the overtone can also be studied.

Jones[53] first used this method in the analysis of perpendicular bands.

The 1st overtone of a degenerate vibration of a molecule with C_{3V} symmetry has a_1 + e components, i.e. it should exhibit a parallel and a perpendicular band in the spectrum. It has been shown[54] that the perpendicular component should have a zeta constant equal to minus twice the ground state value, i.e. $\zeta_{2i} = -2\zeta_i$.

The coriolis constants can also be written for combinations as well. Thus from $\nu_i(e)$; $\zeta_{2\nu_i} = -2\zeta_i$

$$\nu_i(e),\ \nu_j(e);\ \zeta_{(\nu_i + \nu_j)} = -\zeta_i + \zeta_j$$

$$\nu_i(e),\ \nu_j(a_1);\ \zeta(\nu_i + \nu_j) = +\zeta_i$$

$$\nu_i(e);\ \zeta_{3\nu_i} = +\zeta_i$$

For a fundamental and its overtone, the linear and quadratic coefficients of K in the perpendicular bands are

$$[A'(1 - \zeta_i) - B'] \text{ and } [(A' - A'') - (B' - B'')]$$

for the fundamental, and

$$[A^o(1 + 2\zeta_i) - B^o] \text{ and } [(A^o - A'') - B^o - B'']$$

for the overtone, where ^{o} denotes values in the second excited state. If B << A then $B' = B^o = B$. If B has been determined, A^o, A', A'', ζ_i can be evaluated from experimental data. Since A and B vary with the excited state, it is expected that A_ζ will vary in a similar fashion. This treatment neglects the variation of A_ζ with the excited state.

Johnston and Dennison[54] were the first to point out that the sum of the zeta constants for all vibrations of a given symmetry class is independent of the molecular force field and that the sum is a simple function of the rotational constants. This was later shown to hold quite generally[55].

By using the zeta constants obtained by analysis of infra red data and the sum rule, the size of those zeta constants whose bands cannot be analysed directly can be estimated.

In silyl acetylene, for example, the zeta sum value is

$$\sum_i \zeta_i = \frac{B''}{2A''} + 2 \sim 2.02.$$

$\zeta_6 + \zeta_7 + \zeta_8$ was measured at 0.12; thus $\zeta_{10} + \zeta_9 = 1.90$. Even though ν_{10} and ν_9 possessed no fine structure, ζ_{10} and ζ_9 could be estimated using this method.

The following chapter is concerned with the analysis of perpendicular bands of some silyl and germyl acetylenes. The values of B used were, in the main, determined from electron diffraction parameters. Where this was not possible, reasonable bond lengths were assumed. The ground state value of A, A'' was obtained from observation of the MH stretch and its overtone. Subsequent bands were analysed using this value of A''.

CHAPTER 6

Analysis of Perpendicular Bands of Some Silyl and Germyl Acetylenes

6.1 Analysis of the Perpendicular Bands of the Silyl and Germyl Halo Acetylenes

The position of the Q branches in a perpendicular band are governed by the equation V.14.

$$\nu_K^{sub} = \nu_o + [A'(1 - 2\zeta_i) - B'] \pm 2[A'(1 - \zeta_i) - B'] K$$

$$+ [(A' - A'') - (B' - B'')] K^2 \pm 4D_K K^3$$

when ν_K^{sub} is the observed frequency of the sub-band;

ν_o is the band origin as defined in equation V.14;

A',B',A'',B'' are the rotational constants for the upper and lower states respectively;

ζ_i is the zeta constant for the i^{th} normal mode, and

D_K is a centrifugal distortion constant.

Since the centrifugal distortion constants D_K, D_{JK} and D_J are all small compared to A or B, terms containing them have been omitted from the linear and quadratic coefficients of K.

The observed frequencies can be fitted to a polynomial expression as long as the centre of each band is known. Fortunately, the intensities of the P_{Q_K} and R_{Q_K} sub-bands are approximately the same. Moreover, sub-bands having a value of K equal to 0, ± 3, ± 6, . . . , $\pm 3N$ are more intense than the other sub-bands giving rise to a "strong-weak-weak" pattern. This variation in intensity is due to the effect of nuclear spin on the populations of the different rotational states. In general, it is easy to assign values of K to the different frequencies, unless the observed progression is short or overlaps with

another band, when it is often difficult to assign unique values of K. If this problem arises, sets of coefficients are given for all the probable band centres.

The polynomial expression to which the Q branch frequencies are fitted is of type

$$\nu_K^{sub} = a_o + a_1K + a_2K^2 + \ldots + a_nK^n$$

where $n \leq 4$. The constants a_2, a_3, and a_4 tend to be very much smaller than a_1 or a_o with the result that frequencies can be fitted by a least squares linear regression procedure. The largest F value (see Appendix A) obtained for the five orders of regression was taken as the best overall fit to the set of frequencies. The standard deviations of the coefficients and the overall fit to the frequencies were also computed enabling a reasonable estimate of standard deviations in the derived rotational constants and zeta constants to be made.

The perpendicular bands of silyl chloro- and deutero silyl chloro-acetylene

Of the five perpendicular fundamentals in silyl chloro-acetylene, only three possess the expected Q sub-band progression. These three modes are those associated with the silyl group: ν_6, ν_7 and ν_8. In addition to these modes certain overtones and combinations also possess this fine structure.

The 4300 cm^{-1} region in the infra red spectrum had a band with resolved fine structure (figure 6.1). This band clearly is associated in some way with the silyl stretch, ν_6. The possible overtones and combinations occurring in this region are:

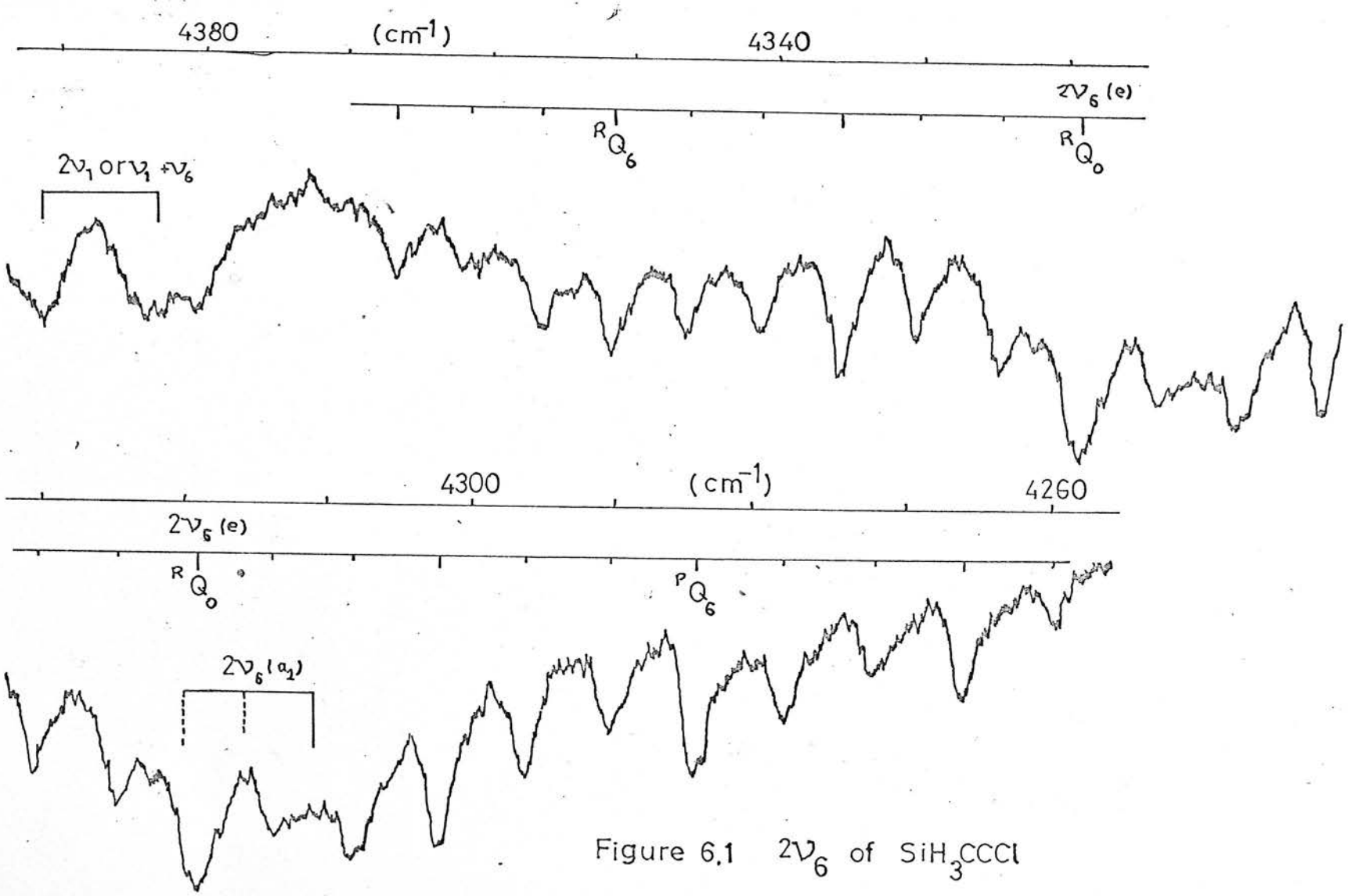

Figure 6.1 $2\nu_6$ of SiH_3CCCl

$2\nu_1$	a_1
$2\nu_2$	a_1
$\nu_1 + \nu_2$	a_1
$2\nu_6$	$a_1 + e$
$\nu_1 + \nu_6$	e
$\nu_2 + \nu_6$	e

The last three bands are the only perpendicular bands; $2\nu_6$ will have a zeta constant of $-2\zeta_6$, while $\nu_1 + \nu_6$ and $\nu_2 + \nu_6$ will have zeta constants of $+\zeta_6$. Reasonable values of ζ_6 and A'' are obtained only when this band is assigned to $2\nu_6$.

A progression is resolved between 1300-1500 cm^{-1} centred to high frequency of a parallel band. These two bands are clearly parallel and perpendicular components of the same band and are assigned to the overtone $2\nu_8$ $(a_1 + e)$.

Another progression is found to the high frequency side of the two broad bands around 1880 cm^{-1}. These are associated with the silyl deformations ν_3 and ν_7 and possibly with the skeletal stretch, ν_4. The possible combinations and overtones are

$2\nu_3$	a_1
$2\nu_4$	a_1
$\nu_3 + \nu_4$	a_1

...cont.

$2\nu_7$	$a_1 + e$
$\nu_3 + \nu_7$	e
$\nu_4 + \nu_7$	e

Unfortunately only a few members of this progression were observed with the result that A'' and ζ could not be determined with sufficient accuracy to assign this band uniquely. In silyl acetylene[2], this band was resolved and assigned to $2\nu_7$. This seems to be the most likely assignment considering that this band is also observed in the silyl halides[56]. In all these cases, reasonable values of A'' and ζ_7 were obtained only where the band was assigned to $2\nu_7$.

The region between 3050 cm^{-1} and 3150 cm^{-1} shows a progression overlapping with at least three parallel bands (figure 6.2). This is a complex region of the spectrum involving possible combinations of six fundamentals. These combinations, with their expected frequencies are

$\nu_1 + \nu_3$	a_1	3132 cm^{-1}
$\nu_1 + \nu_4$	a_1	3110 cm^{-1}
$\nu_2 + \nu_3$	a_1	3103 cm^{-1}
$\nu_2 + \nu_4$	a_1	3081 cm^{-1}
$\nu_6 + \nu_3$	e	3134 cm^{-1}
$\nu_6 + \nu_4$	e	3112 cm^{-1}
$\nu_6 + \nu_7$	$a_1 + e$	3145 cm^{-1}
$\nu_7 + \nu_1$	e	3143 cm^{-1}
$\nu_7 + \nu_2$	e	3114 cm^{-1}

Figure 6.2 The 3100 cm^{-1} Region of the IR Spectrum of SiH_3CCCl

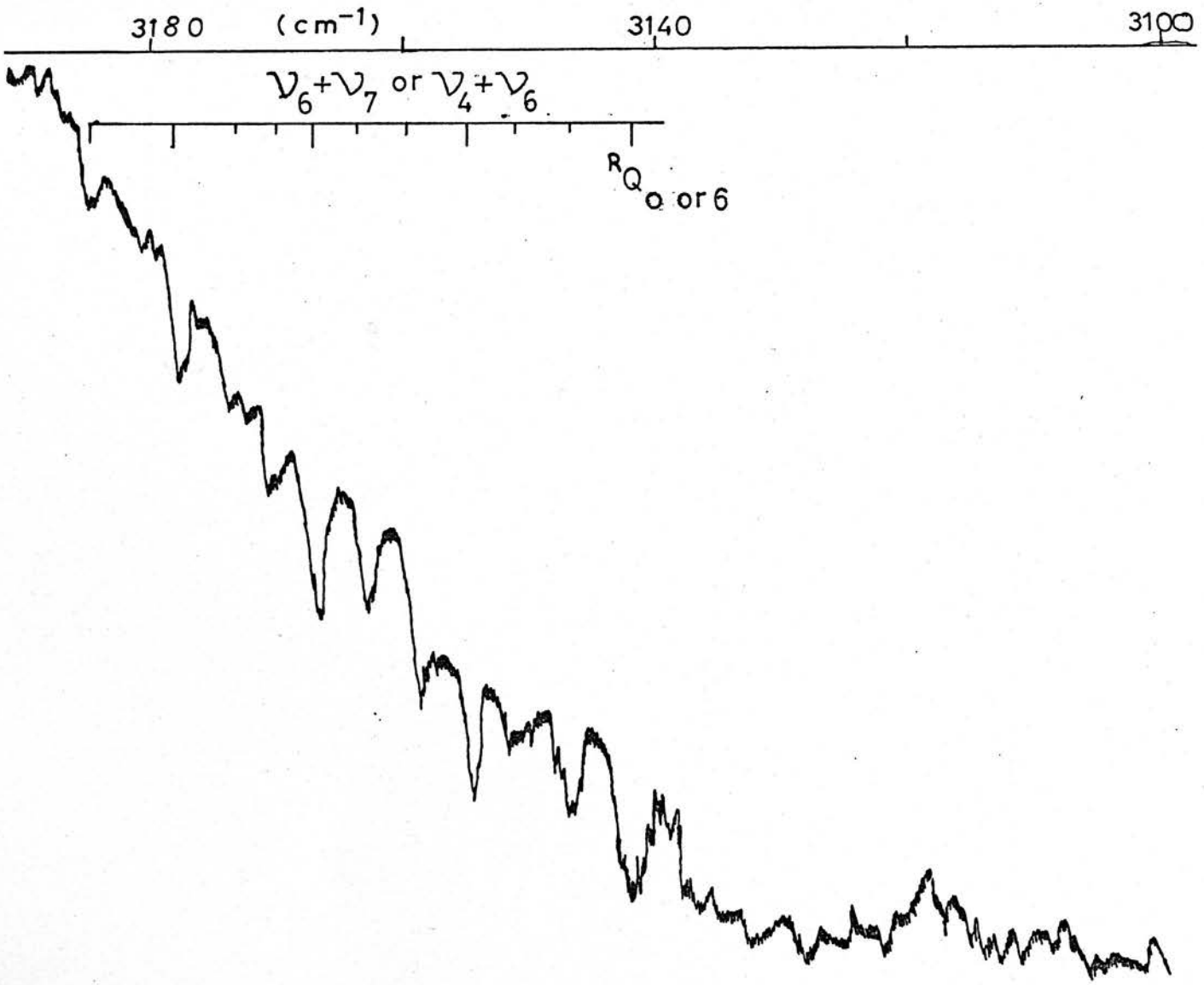

The three parallel bands observed occur at 3082 cm^{-1}, 3107 cm^{-1} and 3129 cm^{-1} corresponding to $\nu_2 + \nu_4$, $\nu_1 + \nu_4$ and $\nu_1 + \nu_3$ respectively. The "strong" Q branches of the perpendicular band occur at 3142.3 cm^{-1}, 3128.6 cm^{-1} and 3113.2 cm^{-1} which could be assigned to $\nu_6 + \nu_7$ or $\nu_7 + \nu_1$, $\nu_6 + \nu_3$, and $\nu_6 + \nu_4$ or $\nu_7 + \nu_2$ respectively. The polynomials found by curve fitting have relatively high standard deviations suggesting that either a strong perturbation is affecting the rotational levels or the observed frequencies form a composite progression, the components of which could not be separated. For this reason the zeta constants were not used to calculate the ground state rotational constant but were calculated assuming the value of A" calculated from other overtones or combinations.

A second weak progression was observed, during the analysis of ν_7 (figure 6.3), to high frequency of each Q branch of ν_7 above 985 cm^{-1} and extending to 1055 cm^{-1}. The centre of this secondary band is not at all clear. There are a number of combinations that occur over this region including the possibility of difference bands with the lowest bending mode. The combinations possible are

$\nu_4 + \nu_{10}$	e
$\nu_8 + \nu_9$	$a_1 + e$
$\nu_7 + \nu_{10} - \nu_{10}$	$a_1 + 3e$
$\nu_3 + \nu_{10} - \nu_{10}$	$a_1 + e$
$2\nu_8 - \nu_9$	$a_1 + e$

If the band is due to $\nu_7 + \nu_{10} - \nu_{10}$, the band centre, ν_o^{sub} of the

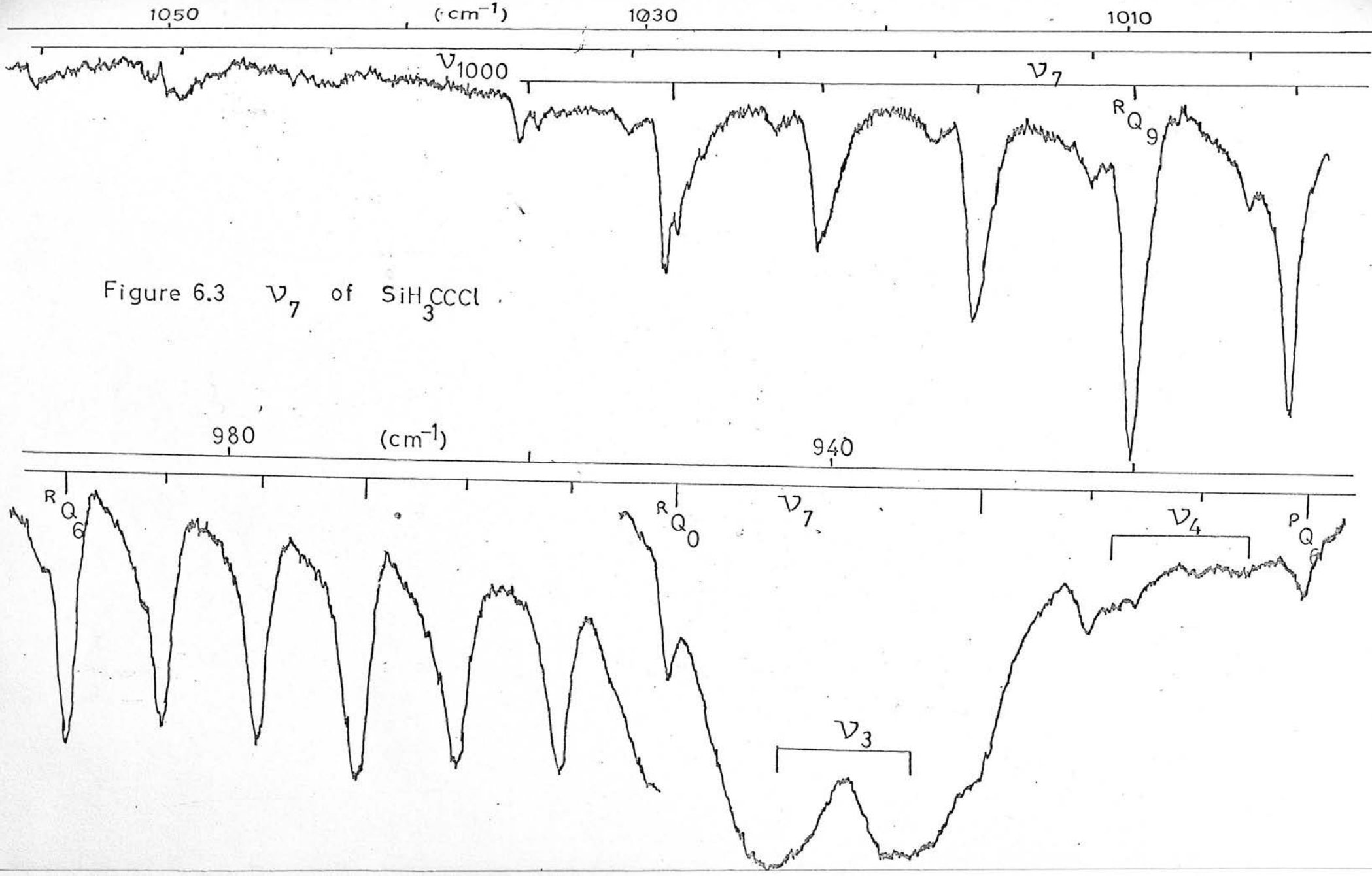

Figure 6.3 ν_7 of SiH_3CCCl .

progression would be expected about 950 cm^{-1} and the zeta constant would be ζ_{10} or $-(\zeta_7 + 2\zeta_{10})$ depending on whether the transition involved the a_1 or e component of the upper level respectively. $\nu_8 + \nu_9$ on the other hand is expected at 1030 cm^{-1} with a zeta constant of $-(\zeta_8 + \zeta_9)$. $\nu_4 + \nu_{10}$ is expected at 1040 cm^{-1} with a zeta constant of ζ_{10}. $\nu_3 + \nu_{10} - \nu_{10}$ is expected around 940 cm^{-1} with a zeta constant of 0. $2\nu_8 - \nu_9$ is expected at 1014 cm^{-1} with a zeta constant of ζ_9 or $-(2\zeta_8 + \zeta_9)$ depending on whether the a_1 or e component of $2\nu_8$ is involved in the transition.

ν_8 is a band where ν_o^{sub} can be either at 683.3 cm^{-1} or 694.7 cm^{-1} although the gas phase raman spectrum suggests the former frequency. This frequency also gives a similar value for A'' to that derived from ν_6 and $2\nu_6$.

The frequencies of the observed Q branches are given in table 6.1 together with the frequencies calculated from the polynomial coefficients and the difference between observed and calculated frequencies. The polynomial fitted to the observed frequencies and the standard deviations are given for each band. The majority of the standard deviations for the overall fit are in the region 0.1 to 0.3 cm^{-1} although the deviation of 0.5 cm^{-1} for $2\nu_7$ is due to poor definition of the band rather than a perturbation of the rotational levels.

The derived molecular constants for each band are given in table 6.2. ν_o^{sub}, the observed band origin, is equivalent to the intercept of the polynomial. $[A'(1 - \zeta_i) - B']$ is derived from the coefficient of K, $[(A' - A'') - (B' - B'')]$ is the coefficient of K^2. The rotational constants A'' and A', the zeta constant, ζ_i and the band origin, ν_o can be obtained from the derived molecular constants

Table 6.I

Q Branch Frequencies of SiH_3CCCl and SiD_3CCCl

SC---NU=6

K	Y(OBS)	Y(CALC)	Y(OBS)-Y(CALC)
19	2293.30	2293.66	-.36
18	2288.80	2288.79	.01
17	2283.95	2283.88	.07
16	2279.00	2278.93	.07
15	2274.05	2273.95	.10
14	2269.00	2268.94	.06
13	2264.10	2263.89	.21
12	2258.85	2258.81	.04
11	2253.75	2253.69	.06
10	2248.65	2248.54	.11
9	2243.45	2243.35	.10
8	2237.95	2238.13	-.18
7	2232.80	2232.87	-.07
6	2227.65	2227.58	.07
5	2222.30	2222.25	.05
4	2216.80	2216.89	-.09
3	2211.40	2211.50	-.10
2	2206.05	2206.07	-.02
1	2200.50	2200.61	-.11
0	2195.20	2195.11	.09
-1	2189.60	2189.58	.02
-2	2184.30	2184.01	.29
-3	2178.40	2178.41	-.01
-4	2172.75	2172.77	-.02
-5	2167.00	2167.10	-.10
-6	2161.40	2161.39	.01
-7	2155.60	2155.65	-.05
-8	2150.00	2149.88	.12
-9	2143.85	2144.07	-.22
-10	2138.35	2138.23	.12
-11	2132.30	2132.35	-.05
-12	2126.20	2126.43	-.23
-13	2120.45	2120.49	-.04
-14	2114.50	2114.50	-.00
-15	2108.35	2108.49	-.14
-16	2102.50	2102.44	.06
-17	2096.55	2096.35	.20
-18	2090.35	2090.23	.12
-19	2084.50	2084.08	.42
-20	2078.05	2077.89	.16
-21	2071.20	2071.66	-.46

S.D. = 0.15 cm^{-1}

SC---NU-7

K	Y(OBS)	Y(CALC)	Y(OBS)-Y(CALC)
13	1035.00	1035.12	-.12
12	1029.05	1029.01	.04
11	1022.90	1022.82	.08
10	1016.50	1016.57	-.07
9	1010.15	1010.25	-.10
8	1003.95	1003.86	.09
7	997.45	997.41	.04
6	990.80	990.89	-.09
5	984.34	984.32	.02
4	977.85	977.70	.16
3	971.20	971.01	.19
2	964.50	964.28	.22
1	957.70	957.50	.20
0	950.30	950.67	-.36
-1	*	943.79	*
-2	*	936.87	*
-3	929.80	929.91	-.11
-4	922.65	922.91	-.26
-5	915.70	915.88	-.18
-6	908.55	908.81	-.26
-7	901.70	901.72	-.02
-8	894.50	894.59	-.09
-9	887.55	887.43	.12
-10	880.30	880.26	.04
-11	873.45	873.06	.39
-12	866.25	865.83	.42
-13	858.80	858.60	.20
-14	851.40	851.34	.06
-15	843.50	844.08	-.58

S.D. = 0.25 cm^{-1}

SC---NU-8

K	Y(OBS)	Y(CALC)	Y(OBS)-Y(CALC)
22	771.20	771.26	-.06
21	767.00	767.06	-.06
20	762.50	762.88	-.38
19	758.75	758.72	.03
18	754.90	754.57	.33
17	750.50	750.43	.07
16	746.35	746.32	.03
15	742.25	742.22	.03
14	738.30	738.14	.16
13	733.90	734.08	-.18
12	729.65	730.04	-.39
11	725.95	726.02	-.07
10	722.05	722.03	.02
9	718.00	718.05	-.05
8	714.20	714.10	.10
7	710.30	710.17	.13
6	706.30	706.26	.04
5	702.40	702.38	.02
4	698.65	698.52	.13
3	694.70	694.69	.01
2	690.85	690.89	-.04
1	687.05	687.11	-.06
0	683.25	683.36	-.11
-1	679.55	679.64	-.09
-2	675.80	675.94	-.14
-3	672.05	672.28	-.23
-4	*	668.64	*
-5	665.15	665.04	.11
-6	661.50	661.47	.03
-7	657.95	657.93	.02
-8	654.10	654.43	-.33
-9	650.90	650.95	-.05
-10	647.70	647.51	.19
-11	644.15	644.11	.04
-12	640.75	640.74	.01
-13	637.45	637.41	.04
-14	634.20	634.11	.09
-15	*	630.85	*
-16	628.15	627.63	.52
-17	624.65	624.45	.20
-18	621.35	621.30	.05
-19	618.00	618.20	-.20
-20	614.75	615.14	-.39

S.D. = 0.20 cm^{-1} (ν_o = 683)

= 0.21 cm^{-1} (ν_o = 694)

SC---2NU-6

K	Y(OBS)	Y(CALC)	Y(OBS)-Y(CALC)
12	4380.30	4380.69	-.39
11	4376.55	4375.97	.58
10	4371.00	4371.18	-.18
9	4366.25	4366.31	-.06
8	4361.40	4361.37	.03
7	4356.45	4356.36	.09
6	4351.20	4351.27	-.07
5	4346.15	4346.11	.04
4	4341.15	4340.87	.27
3	4335.70	4335.57	.13
2	4330.35	4330.19	.16
1	4324.55	4324.74	-.19
0	4319.10	4319.21	-.11
-1	4313.65	4313.61	.04
-2	4308.20	4307.94	.26
-3	4302.35	4302.20	.16
-4	4296.30	4296.38	-.08
-5	4290.25	4290.48	-.23
-6	4284.40	4284.52	-.12
-7	4278.45	4278.48	-.03
-8	4272.05	4272.37	-.32
-9	4266.05	4266.18	-.13
-10	4259.90	4259.93	-.03
-11	4253.75	4253.59	.16
-12	4247.70	4247.19	.51
-13	4241.60	4240.71	.89
-14	4233.60	4234.16	-.56
-15	4227.30	4227.54	-.23

S.D. = 0.30 cm^{-1}

-2NU-7

K	Y(OBS)	Y(CALC)	Y(OBS)-Y(CALC)
9	1947.50	1948.56	-1.06
8	1942.60	1941.96	.64
7	1935.90	1935.37	.53
6	1928.90	1928.77	.13
5	1922.70	1922.18	.02
4	1915.80	1915.58	.22
3	1908.90	1908.99	-.09
2	1902.10	1902.39	-.39
1	*	1895.79	*
0	*	1889.20	*

S.D. = 0.58 cm^{-1}

-2NU-8

K	Y(OBS)	Y(CALC)	Y(OBS)-Y(CALC)
12	1491.80	1492.39	-.59
11	*	1482.27	*
10	1472.50	1472.20	.30
9	1462.20	1462.17	.03
8	1452.10	1451.80	.30
7	1442.50	1442.28	.22
6	1432.30	1432.41	-.11
5	1422.80	1422.58	.22
4	1412.70	1412.81	-.11
3	1403.00	1403.09	-.09
2	1393.70	1393.41	.29
1	*	1383.79	*
0	*	1374.21	*
1	*	1364.69	*
2	*	1355.21	*
-3	1345.80	1345.79	.01
-4	1336.30	1336.41	-.11
-5	1326.70	1327.08	-.38
-6	1317.60	1317.81	-.21
-7	1308.50	1308.58	-.08
-8	1299.30	1299.40	-.10
-9	1290.10	1290.28	-.18
-10	1281.40	1281.20	.20
-11	1272.60	1272.17	.43

S.D. = 0.29 cm^{-1}

C-NU -1ØØØ

K	Y(OBS)	Y(CALC)	Y(OBS)-Y(CALC)
7	1Ø55.2Ø	1Ø55.24	-.Ø4
6	1Ø49.35	1Ø49.22	.13
5	1Ø43.1Ø	1Ø43.13	-.Ø3
4	*	1Ø36.98	*
3	1Ø3Ø.75	1Ø3Ø.77	-.Ø2
2	1Ø24.55	1Ø24.5Ø	.Ø5
1	1Ø18.2Ø	1Ø18.17	.Ø3
Ø	1Ø11.8Ø	1Ø11.77	.Ø3
-1	1ØØ5.3Ø	1ØØ5.31	-.Ø1
-2	998.85	998.79	.Ø6
-3	992.25	992.21	.Ø4
-4	985.55	985.57	-.Ø2

S.D. = 0.06 cm^{-1}

C-NU-31ØØ

K	Y(OBS)	Y(CALC)	Y(OBS)-Y(CALC)
17	3184.9Ø	3184.9Ø	.ØØ
16	*	3181.32	*
15	3177.85	3177.72	.14
14	3173.8Ø	3174.Ø8	-.28
13	3170.35	3170.4Ø	-.Ø5
12	3166.95	3166.67	.28
11	3163.ØØ	3162.86	.14
1Ø	3158.9Ø	3158.98	-.Ø8
9	3154.8Ø	3155.ØØ	-.2Ø
8	3150.85	3150.93	-.Ø8
7	3147.ØØ	3146.73	.27
6	3142.25	3142.41	-.16
5	*	3137.95	*
4	3133.4Ø	3133.35	.Ø5
3	3128.6Ø	3128.58	.Ø2
2	3123.6Ø	3123.63	-.Ø3
1	*	3118.51	*
Ø	3113.2Ø	3113.18	.Ø2
-1	*	3107.65	*
-2	*	3101.89	*
-3	3095.9Ø	3095.91	-.Ø1

S.D. = 0.25 cm^{-1}

NU 6

K	Y(OBS)	Y(CALC)	Y(OBS)-Y(CALC)
18	1647.50	1647.65	-.15
17	*	1645.30	*
16	1643.00	1642.93	.07
15	1640.60	1640.56	.04
14	1638.20	1638.17	.03
13	1635.80	1635.77	.03
12	1633.30	1633.35	-.05
11	1630.90	1630.93	-.03
10	1628.40	1628.49	-.09
9	1626.00	1626.04	-.04
8	1623.60	1623.58	.02
7	1621.40	1621.11	.29
6	1618.60	1618.62	-.02
5	1616.10	1616.13	-.03
4	1613.70	1613.62	.08
3	1611.10	1611.10	.00
2	1608.50	1608.56	-.06
1	1606.10	1606.02	.08
0	1603.40	1603.46	-.06
-1	1601.00	1600.90	.10
-2	1598.40	1598.32	.08
-3	1595.70	1595.72	-.02
-4	1593.50	1593.12	.38
-5	1590.20	1590.50	-.30
-6	1587.50	1587.87	-.37
-7	*	1585.23	*
-8	*	1582.58	*
-9	*	1579.92	*
-10	*	1577.24	*
-11	*	1574.55	*
-12	*	1571.86	*
-13	*	1569.14	*
-14	*	1566.42	*
-15	1563.00	1563.08	-.08
-16	1560.80	1560.94	-.14
-17	1558.10	1558.18	-.08
-18	1555.90	1555.41	.49
-19	1552.50	1552.62	-.12

S.D. = 0.18 cm^{-1}

20 -NU-7

K	Y(OBS)	Y(CALC)	Y(OBS)-Y(CALC)
13	729.00	728.87	.13
12	724.50	724.34	.16
11	719.65	719.92	-.27
10	715.45	715.60	-.15
9	711.30	711.37	-.07
8	707.40	707.22	.18
7	*	703.16	*
6	*	699.17	*
5	*	695.25	*
4	*	691.39	*
3	*	687.60	*
2	*	683.85	*
1	*	680.16	*
0	*	676.51	*
1	*	672.89	*
2	*	669.31	*
- 3	665.80	665.75	.05
- 4	662.20	662.21	-.01
- 5	658.75	658.69	.06
- 6	655.27	655.17	.10
- 7	651.70	651.66	.04
- 8	648.15	648.15	-.00
- 9	644.60	644.63	-.03
-10	641.05	641.10	-.05
-11	637.50	637.55	-.05
-12	633.85	633.98	-.13
-13	630.30	630.38	-.08
-14	626.80	626.74	.06
-15	623.20	623.07	.13

S.D. = 0.16 cm^{-1}

Table 6.2 Molecular Constants for SiH_3CCCl and SiD_3CCCl

Band	ν_0^{sub}	$[A'(I-\zeta_i)-B']$	$[(A'-A'')-(B'-B'')]$
SiH_3CCCl	(cm^{-1})	(cm^{-1})	(cm^{-1})
ν_6	2195.1	2.758(1)	-0.0173(2)
ν_7	950.7	3.427(7)	-0.0225(8)
ν_8	683.4	1.868(3)	0.0141(2)
	694.7	1.909(3)	0.0132(3)
$2\nu_6$	4319.2	2.781(4)	-0.037(1)
$2\nu_7$	1889.2	3.297(5)	-
$2\nu_8$	1374.2	4.775(5)	0.027(2)
ν_{1000}	992.2	3.307(9)	-0.031(2)
	1011.5	3.314(4)	-0.031(2)
ν_{3100}	3113.2	2.71(2)	-0.087(6)
	3138.6	2.428(7)	-0.010(1)
SiD_3CCCl			
ν_6	1603.5	1.281(2)	-0.0060(3)
ν_7	665.8	1.774(7)	0.0102(7)
	676.5	1.817(7)	0.0184(8)

Note: Numbers in brackets indicate standard deviations.

and are given in table 6.3; the standard deviations being shown in brackets. B', calculated from the electron diffraction data, was taken as 0.0444 cm^{-1} and (B' - B'') was assumed to be negligible.

When derived from ν_6 and $2\nu_6$, A'' equals 2.8338 cm^{-1} but is 2.8614 cm^{-1} when derived from ν_8 and $2\nu_8$. The electron diffraction structure predicts a value of A of 2.777 cm^{-1} but this is not a reliable value because the positions of the hydrogen atoms are not well defined and because A found by this method is a time averaged value which is a function of all the occupied states.

It is reasonable, however, to assume that the value of A'' lies in the region 2.830 cm^{-1} to 2.862 cm^{-1}. The ground state value of A derived from ν_6 and $2\nu_6$ was used throughout the analysis. The reasons for this were twofold; ζ_6 is expected to be close to zero and therefore uncertainties in A'' and ζ_6 are minimised and $2\nu_6$ was the only overtone with enough structure to allow a reasonable determination of A'' in the other molecules studied.

The zeta constants for the fundamentals ν_6, ν_7, ν_8 are of a similar magnitude and sign to their counterparts in silyl acetylene[2]. Although fine structure was not observed in ν_9 or ν_{10}, $\zeta_9 + \zeta_{10}$ can be estimated from the zeta sum rule[57]. Thus,

$$\sum_{6}^{10} \zeta_i = \frac{B''}{2A''} + 2 = 2.008; \quad \zeta_6 + \zeta_7 + \zeta_8 = 0.099(4)$$

hence $\zeta_9 + \zeta_{10} = 1.91$. Both ζ_9 and ζ_{10} are nearly equal to 1, similar to values for other acetylenes[2,70].

Table 6.3 Rotational and Zeta Constants of SiH_3CCCl and SiD_3CCCl

Band	ν_0 (cm^{-1})	A'' (cm^{-1})	A' (cm^{-1})	ζ_i
SiH_3CCCl				
ν_6	2I92.4	2.834(2)	2.8I7(2)	0.005(2)
ν_7	946.6	2.834(2)	2.8II(2)	-0.235(3)
ν_8	682.4	2.86I(3)	2.876(3)	0.335(2)
	693.7	2.889(3)	2.902(3)	0.327(2)
	682.4	2.834(2)	2.848(2)	0.328(2)
	693.7	2.834(2)	2.847(2)	0.3I4(2)
$2\nu_6$	43I5.9	2.834(2)	2.797(2)	-0.0I0(3)
$2\nu_7$	I885.4	2.834(2)	2.83(2)	-0.I8(3)
$2\nu_8$	I367.5	2.86I(3)	2.886(3)	-0.670(4)
	I367.5	2.889(3)	2.9I4(3)	-0.654(4)
	I367.5	2.834(2)	2.859(2)	-0.686(4)
ν_{1000}	988.4	2.834(2)	2.803(2)	-0.I96(4)
	I007.8	2.834(2)	2.803(2)	-0.I62(3)
ν_{3100}	3II0.4	2.834(2)	2.729(8)	-0.0I(I)
	3I25.4	2.834(2)	2.747(4)	0.I00(4)
SiD_3CCCl				
ν_6	I602.3	I.4I7(2)	I.4II(2)	0.062(2)
ν_7	663.6	I.4I7(2)	I.427(2)	-0.272(6)
	674.3	I.4I7(2)	I.435(2)	-0.295(5)

The zeta constants can help in the assignments of resolved overtones or combinations. The band at 1300 cm^{-1} is $2\nu_8$. The band at 1900 cm^{-1}, on the other hand, is unlikely to be $2\nu_7$, because the zeta constant has a value nearer to ζ_7 than to $-2\zeta_7$ suggesting that $\nu_3 + \nu_7$ or $\nu_4 + \nu_7$ are more reasonable assignments. This might well be a false conclusion however, due to the rather large standard deviation for this band.

The band in the 3100 cm^{-1} region has a zeta constant approximately equal to zero if the band centre is taken as 3111 cm^{-1}, about 0.1 if the band centre is taken as 3128 cm^{-1} and about 0.2 if the centre is taken as 3143 cm^{-1}. The variation of zeta with change in the band centre is approximately linear hence the value of the zeta constants for the band at 3143 cm^{-1} can be estimated by extrapolation. This band can be assigned to one of two vibrations, either $\nu_4 + \nu_6$, with an expected band centre around 3112 cm^{-1} and a zeta constant of $\zeta_6(0.05)$, or $\nu_6 + \nu_7$ with an expected band centre around 3145 cm^{-1} and a zeta constant of $-(\zeta_6 + \zeta_7)$ equal to 0.24.

The weaker progression in the ν_7 region has a zeta constant of -0.23 when ν_o^{sub} is at 972 cm^{-1} increasing to -0.16 when ν_o^{sub} at 1011 cm^{-1}, assuming that the transition involves a non-degenerate and a degenerate level. The observed zeta constants are not in the required range for any of the expected bands. $\nu_7 + \nu_{10} - \nu_{10}$ and $2\nu_8 - \nu_9$ could also involve transitions between degenerate levels. As a result, the equation V.14 has to be modified. See Appendix B. $2\nu_8 - \nu_9$ is not consistent with the observed data but $\nu_7 + \nu_{10} - \nu_{10}$ has a calculated zeta constant in the region of -5 with a standard deviation of approximately 1.4. The expected value is -1.5. The latter band seems the more likely assignment.

Progressions were observed for two fundamentals of the deuterated species. The Q branch frequencies of ν_6 and ν_7 are given in table 6.1. The exact centre of ν_7 is in doubt due to overlap with a strong parallel band. The derived molecular constants are given in table 6.2 and the rotational constants in table 6.3. B, derived from the electron diffraction data for silyl chloro-acetylene, was calculated as 0.0420 cm^{-1}, assuming that no change in the SiH bond length occurred when the hydrogen atoms were replaced by deuterium.

A'' was assumed to be half of the value found for silyl chloro-acetylene because the mass around the top axis has doubled and because deuterium substitution shortens the SiH bond length by about 0.002 Å at most.

The zeta constants are larger in magnitude than in the non-deuterated acetylene. This is not surprising because the magnitude of the zeta constant is dependent on the mass of the atoms in the vibration concerned.

The perpendicular bands of silyl bromo-acetylene

Only progressions on the silyl modes ν_6, ν_7 and ν_8 were resolved at moderate pressure in a 10 cm cell. Overtones and combinations were not studied because of lack of material. As a result, no internal means for establishing a unique value of A'' could be used. However, observation of silyl compounds have shown that the zeta constant has a value between zero and 0.01 for the silyl stretch. A reasonable estimate for ζ_6 in silyl bromo-acetylene is thus 0.005. B can be obtained using bond distances obtained from electron diffraction[58] and microwave data of related compounds: here B has a

value of 0.0299 cm^{-1}. A'' can be estimated using these parameters.

The Q branch frequencies observed, are given in table 6.4 and the derived molecular constants in table 6.5.

The silyl stretch, ν_6 possesses a progression of Q branches which are partly obscured by the other silyl stretch, ν_1 and the acetylenic stretch, ν_2. The analysis of this band yields a value of A'' equal to 2.835 cm^{-1}. Variation of ζ_6 between 0.000 and 0.010 alters A'' from 2.815 cm^{-1} to 2.855 cm^{-1}. The molecular constants together with those of other bands are given in table 6.6.

The silyl deformation, ν_7 consists of a very strong progression, as is shown in figure 6.4, slightly offset to the high side of ν_3. The centre of the progression is at 949.7 cm^{-1}. Analysis of this band gives a zeta constant of -0.227 which is similar to that obtained for the same mode in silyl chloro-acetylene and silyl acetylene[2]. The second vibrational band as found in silyl chloro-acetylene was not observed.

The silyl rock, ν_8 consists of a progression between 630 cm^{-1} and 750 cm^{-1} as is shown in figure 6.5. The centre of this band has a more complicated structure, resembling the overlap of Q branches of two perpendicular bands. When the frequency is plotted against the quantum number K as shown in figure 6.6, the curve deviates asymptotally from the expected line about K = -1. This type of deviation is consistent with Fermi resonance with another vibration. The affected levels (K = -5 to K = +2) were omitted in the analysis of this band.

The zeta constant for this band was calculated to be 0.317 which is consistent with zeta constants for the corresponding band

Table 6.4

Q branch Frequencies of SiH_3CCBr

K	Y(OBS)	Y(CALC)	Y(OBS)-Y(CALC)
18	2289.35	2289.33	.02
17	2284.45	2284.38	.07
16	2279.55	2279.39	.16
15	2274.30	2274.36	-.06
14	2269.30	2269.31	-.01
13	2264.10	2264.22	-.12
12	2259.25	2259.09	.16
11	2253.90	2253.93	-.03
10	2248.80	2248.74	.06
9	2243.45	2243.52	-.07
8	2238.30	2238.26	.04
7	2232.80	2232.96	-.16
6	2227.65	2227.64	.01
5	2222.15	2222.27	-.12
4	2216.60	2216.88	-.28
3	2211.40	2211.45	-.05
2	2205.90	2205.99	-.09
1	2200.10	2200.49	-.39
0	2195.00	2194.96	.04
-1	2189.40	2189.40	.00
-2	2184.20	2183.80	.40
-3	2178.15	2178.17	-.02
-4	2172.40	2172.50	-.10
-5	2166.60	2166.80	-.20
-6	2160.85	2161.07	-.22
-7	*	2155.30	*
-8	2149.45	2149.50	-.05
-9	2143.85	2143.67	.18
-10	*	2137.80	*
-11	*	2131.90	*
-12	2126.00	2125.96	.04
-13	2120.05	2119.99	.06
-14	2114.20	2113.99	.21
-15	2107.85	2107.95	-.10
-16	2101.85	2101.88	-.03
-17	2095.55	2095.77	-.22
-18	2089.70	2089.64	.06

S.D. = 0.26 cm^{-1}

NU-7

K	Y(OBS)	Y(CALC)	Y(OBS)-Y(CALC)
12	1028.55	1028.42	.13
11	1022.75	1022.67	.08
10	1015.95	1015.87	.08
9	1009.50	1009.51	-.01
8	1003.25	1003.10	.15
7	996.75	996.63	.12
6	990.20	990.10	.10
5	983.70	983.52	.18
4	977.05	976.89	.16
3	970.50	970.20	.30
2	963.80	963.45	.35
1	956.85	956.65	.20
0	949.70	949.80	-.10
-1	942.70	942.89	-.19
-2	*	935.92	*
-3	*	928.90	*
-4	921.75	921.83	-.08
-5	914.75	914.70	.05
-6	907.70	907.51	.19
-7	900.50	900.27	.23
-8	893.25	892.98	.27
-9	885.85	885.63	.22
-10	877.95	878.22	-.27
-11	871.05	870.76	.29

S.D. = 0.18 cm^{-1}

NU-8

K	Y(OBS)		Y(CALC)	Y(OBS)-Y(CALC)	
16	745.85	.00	745.76	.09	.00
15	741.90	.00	741.82	.08	.00
14	737.75	.00	737.86	-.11	.00
13	733.90	.00	733.90	.00	.00
12	729.85	.00	729.92	-.07	.00
11	725.80	.00	725.9[illegible]	-.1[illegible]	.00
10	721.95	.00	721.97	-.02	.00
9	718.00	.00	718.00	.00	.00
8	714.15	.00	714.02	.13	.00
7	710.05	.00	710.06	-.01	.01
6	706.10	.00	706.10	-.0[illegible]	.00
5	702.15	.00	702.16	-.01	.00
4	698.30	.00	698.23	.07	.00
3	694.45	.00	694.32	.13	.00
2	690.70	.00	690.43	.27	.00
1	687.25	.00	686.56	.69	.00
0	683.85	679.10	682.71	1.14	-3.61
-1	680.80	677.65	678.89	1.91	-1.24
-2	.00	674.30	675.11	.00	-.81
-3	.00	670.90	671.35	.00	-.45
-4	.00	667.60	667.63	.00	-.03
-5	.00	663.85	663.95	.00	-.10
-6	.00	660.20	660.31	.00	-.11
-7	.00	656.60	656.72	.00	-.12
-8	.00	653.20	653.17	.00	.03
-9	.00	649.95	649.67	.00	.28
-10	.00	646.35	646.22	.00	.13
-11	.00	642.75	642.82	.00	-.07
-12	.00	639.25	639.48	.00	-.23
-13	.00	636.20	636.21	.00	-.01

S.D. = 0.14 cm^{-1}

Table 6.5 Molecular Constants of SiH_3CCBr

Band	ν_0^{sub} (cm^{-1})	$[A'(I-\zeta_i)-B']$ (cm^{-1})	$[(A'-A'')-(B'-B'')]$ (cm^{-1})
ν_6	2195.0	2.774(2)	-0.0169(4)
ν_7	956.8	3.414(3)	-0.0276(9)
ν_8	682.7	1.916(4)	0.0139(5)

Table 6.6 Rotational and Zeta Constants of SiH_3CCBr

Band	ν_0 (cm^{-1})	A'' (cm^{-1})	A' (cm^{-1})	ζ_i
ν_6	2192.2	2.835(9)	2.818(9)	0.005(9)
ν_7	952.7	2.835(9)	2.808(9)	-0.26(1)
ν_8	681.7	2.835(9)	2.849(9)	0.32(1)

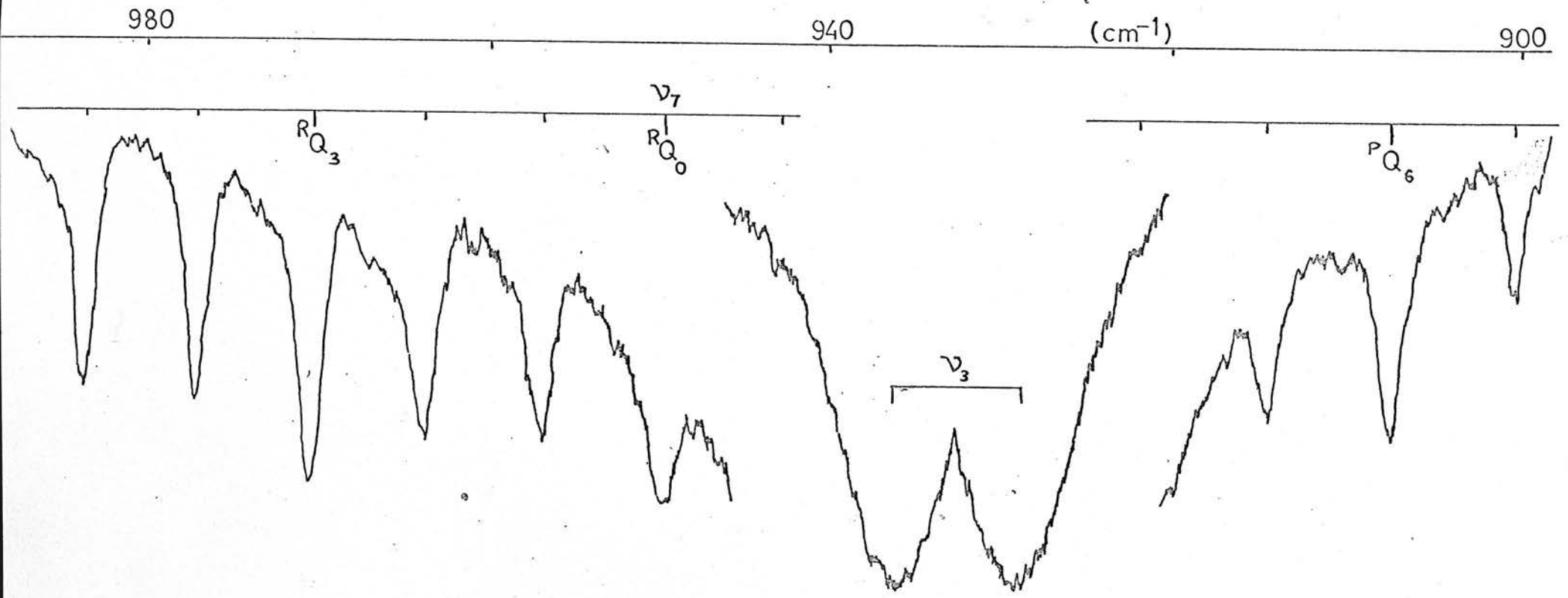

Figure 6.4 ν_7 of SiH_3CCBr

Figure 6.5 ν_8 of SiH_3CCBr

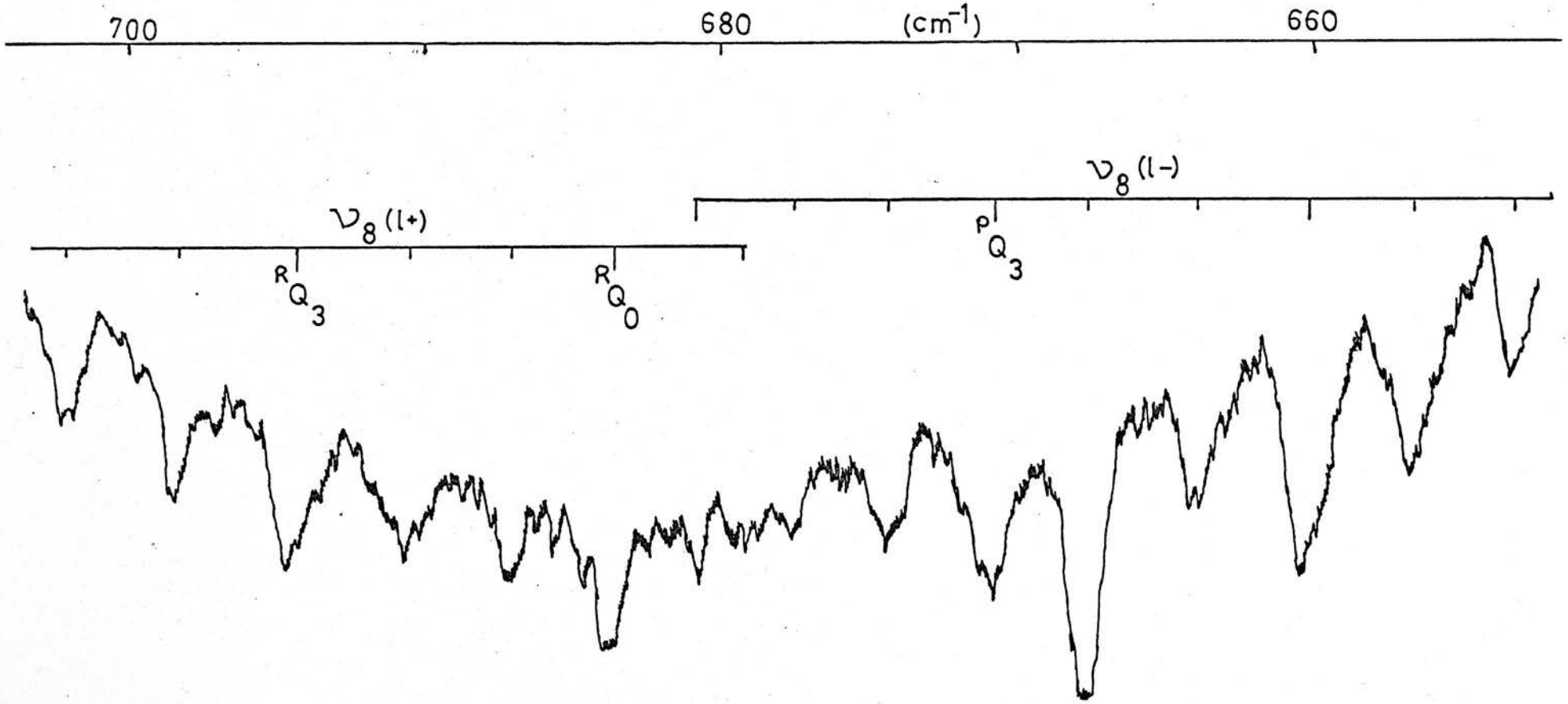

figure 6.6 ν_8 of SiH_3CCBr

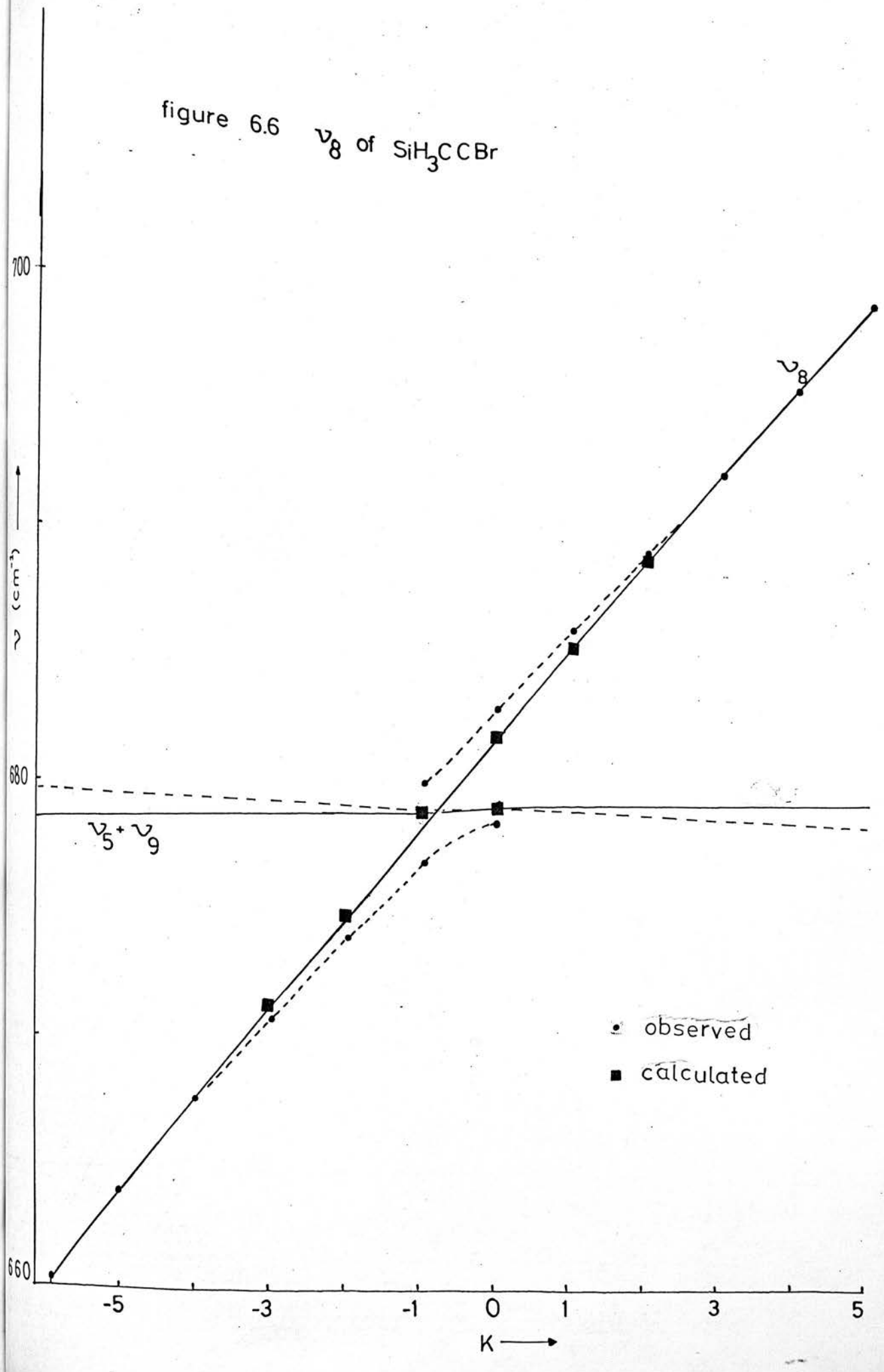

of other molecules. The zeta constant, for ν_9 and ν_{10} can be estimated using the zeta sum rule.

$$\sum_{6}^{10} \zeta_i = \frac{B''}{2A''} + 2 = 2.005; \quad \zeta_6 + \zeta_7 + \zeta_8 = 0.095$$

therefore $\zeta_9 + \zeta_{10} = 1.91$, thus ζ_9 and ζ_{10} lie between 0.9 and 1.0.

Fermi rotational perturbations occur when two vibrational states of the same symmetry species lie close in energy to each other. At the same time the rotational constants for each vibration have to be such that the unperturbed rotational levels intersect when plotted as a function of the rotational quantum number. A further restriction is that only levels with the same K, J and ℓ values can interact. Thus only levels in the immediate vicinity of the curve intersection are heavily perturbed and the magnitude is dependent on the energy difference at the point of intersection.

The magnitude is also in accord with first order perturbation theory since the perturbation function w_{ij} is given by

$$w_{ij} = \langle \psi_i^o | w | \psi_j^o \rangle$$

where ψ_i^o, ψ_j^o are zero approximation eigenfunctions of the perturbing levels and w is a function of anharmonic terms in the potential energy. The intersecting levels repel one another by a factor f where

$$f = \frac{1}{2} \left(4(w_{ij}^2 + \delta^2)^{\frac{1}{2}} \pm \delta\right) \qquad \text{VI.1}$$

where δ is the separation between the two unperturbed levels. w_{ij} is independent of J and K.

ν_8, occurring at 680 cm^{-1}, in silyl bromo-acetylene has e symmetry. The only vibrational state of the same symmetry occurring near this frequency is $\nu_5 + \nu_9$. The band origin, ν_o calculated from the rotational constants of ν_8 is at 681.64 cm^{-1}. The unperturbed energy levels for ν_8 can be calculated using the values of A', ζ_8, ν_o and B derived from analysis of the band. These levels are tabulated in table 6.7. $\nu_5 + \nu_9$ should be observed at 688.9 cm^{-1} assuming no anharmonicity. The zeta constant for this band is ζ_9 which has been taken as 0.95. A' was assumed equivalent to the ground state value of 2.835 cm^{-1} although it might deviate from this value by as much as 0.04 cm^{-1}. The calculated energy levels of $\nu_5 + \nu_9$ are also given in table 6.7.

The ℓ^+ energy levels give rise to the ^RQ branches of ν_8 and $\nu_5 + \nu_9$ while the ℓ^- energy levels give rise to the ^PQ branches. As can be seen from table 6.7, the unperturbed terms cross in the ℓ^+ states when K is between 2 and 3 so that the Q branches most affected would be the $^RQ_1$ and $^RQ_2$ branches. In fact, the $^PQ_1$ branch is the most perturbed. If the origin of $\nu_5 + \nu_9$ is moved by about 10 cm^{-1}, the perturbation will occur in the observed position as is shown by figure 6.7 where the energies of ν_8 and $\nu_5 + \nu_9$ are plotted against J, K.

One interesting feature of figure 6.6 is the existence of two energies with a K quantum number of zero. Since this level does not have different levels corresponding to ℓ^+ and ℓ^-, it cannot be split into two components. The second peak must appear for another reason.

Table 6.7. Energy Levels of ν_8 and $\nu_5 + \nu_9$ in SiH_3CCBr

	ν_8		$\nu_5 + \nu_9$	
J,K	ℓ+	ℓ−	ℓ+	ℓ−
0	681.6		688.9	
1	682.7	686.3	686.4	697.2
2	689.4	696.7	689.5	711.1
3	701.9	712.7	698.3	730.7
4	720.1	734.5	712.8	755.9
5	743.9	762.0	733.0	786.9
6	773.5	795.2	758.8	823.5
7	808.8	834.1	790.3	865.7
8	849.7	878.6	827.5	913.7
9	896.4	928.9	870.3	967.3
10	948.7	984.9	918.8	1026.6
11	1006.8	1046.5	973.0	1091.5
12	1070.5	1113.9	1032.9	1162.1

Figure 6.7 Energy Levels of ν_8 and $\nu_5 + \nu_9$ in SiH_3CCBr

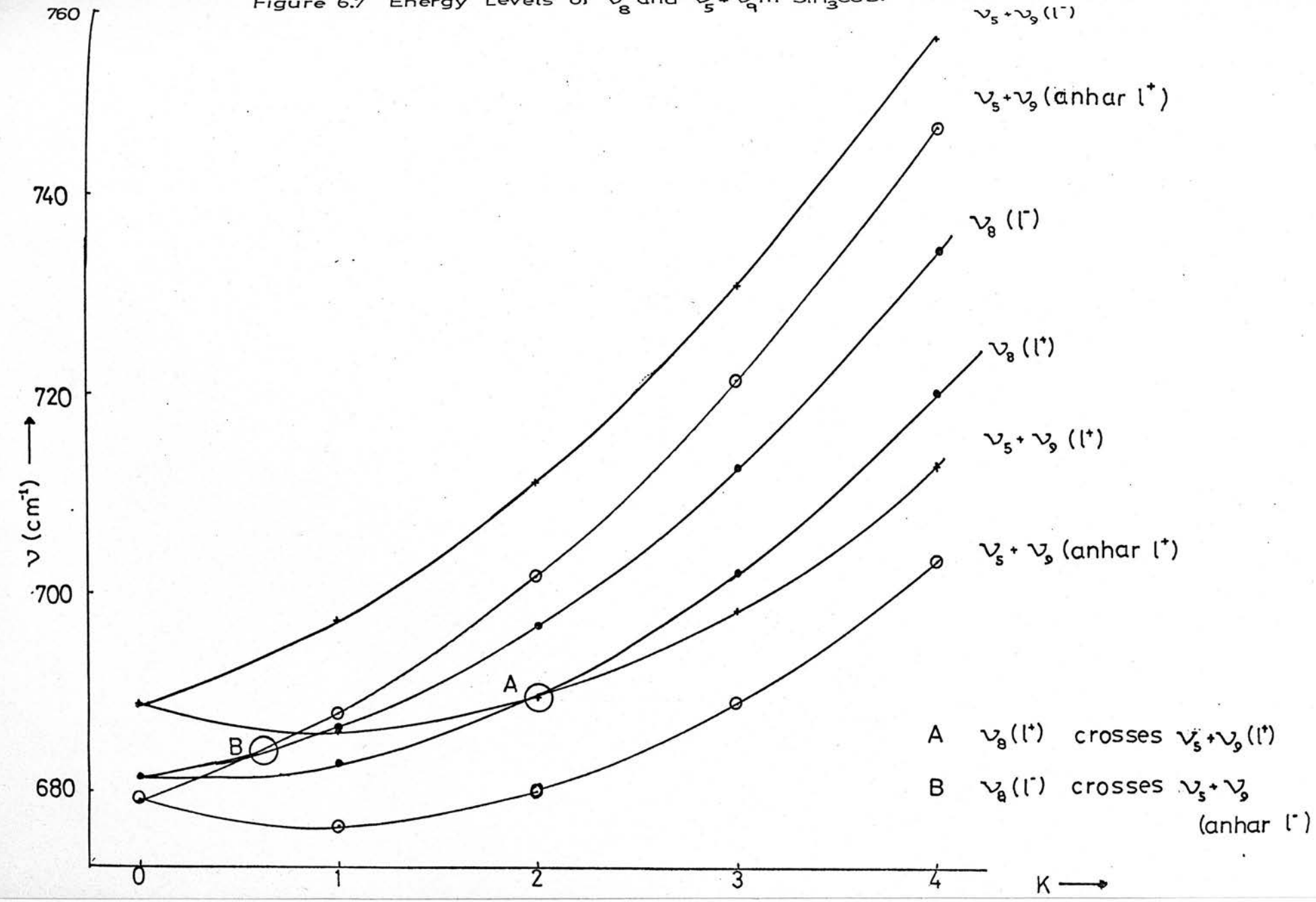

The K = 0 levels of ν_8 and $\nu_5 + \nu_9$ interact and are quite heavily perturbed. One consequence of this is that the intensity of the interacting levels will be effected. The transition moment (T.M.), which governs the intensity, is governed by the equation

$$\text{T.M.} = \langle \Psi_L | d | \Psi_U \rangle$$

where d is the dipole moment operator and Ψ_L, Ψ_U are the upper and lower eigenfunctions involved in the transition. Now Ψ_L is the same for both ν_8 and $\nu_5 + \nu_9$ and Ψ_U has some of the characteristics of the other perturbing level in it. As a result, the closer the two unperturbed energy levels, the nearer in intensity the two perturbed levels will become. It seems plausible that one ^RQ_o branch belongs to ν_8 and the other to $\nu_5 + \nu_9$. A similar mechanism involving the two (K_1, ℓ^-) energy levels produces two $^PQ_1$ branches. In principle, at least, the energy levels could be indirectly observed through such a perturbation. The estimated line of $\nu_5 + \nu_9$ is given as the dashed line in figure 6.6. This line was estimated by calculating an average value of w_{ij} from equation VI.1 and using ρ and δ values from table 6.4.

The slope of this line is approximately 0.048 cm^{-1}, which using a value A'' = 2.835, gives a value of the zeta constant $\zeta_{5,9} = 0.98$. This zeta constant is equivalent to ζ_9 and is very close to the value expected from the zeta sum rule.

The perpendicular bands of germyl chloro-acetylene

Three fundamentals show rotational fine structure: the three germyl vibrations ν_6, ν_7 and ν_8. In addition to these bands there

are several overtones and combinations that have fine structure.

The overtone of ν_6 was observed in the 4100 cm^{-1} region of the spectrum. Although there are several states which could be assigned to this band only $2\nu_6$ is likely for the same reasons as those given in the assignment of $2\nu_6$ in silyl chloro-acetylene.

There is evidence of a progression around 1700 cm^{-1} but this band is not well resolved and has been partly obscured by atmospheric water in the transfer optics of the long path cell which could not be eliminated satisfactorily.

The 2900 cm^{-1} to 3100 cm^{-1} region has a progression starting at about 2900 cm^{-1} and dying about 3010 cm^{-1}. Another progression appears from 3055 cm^{-1} to 3072 cm^{-1}. There is the possibility that this is a single progression because the frequencies when plotted against an integer seem to correlate, even to the point of matching the "strong-weak-weak" pattern (figure 6.8). It does seem more likely, however, that they are two different progressions. The bands in this region of the spectrum are:-

$\nu_1 + \nu_3$	a_1	2949 cm^{-1}
$\nu_1 + \nu_4$	a_1	3004 cm^{-1}
$\nu_1 + \nu_7$	e	3004 cm^{-1}
$\nu_2 + \nu_3$	a_1	3005 cm^{-1}
$\nu_2 + \nu_4$	a_1	3060 cm^{-1}
$\nu_2 + \nu_7$	e	3060 cm^{-1}
$\nu_6 + \nu_3$	e	2953 cm^{-1}
$\nu_6 + \nu_4$	e	3008 cm^{-1}
$\nu_6 + \nu_7$	$a_1 + e$	3008 cm^{-1}

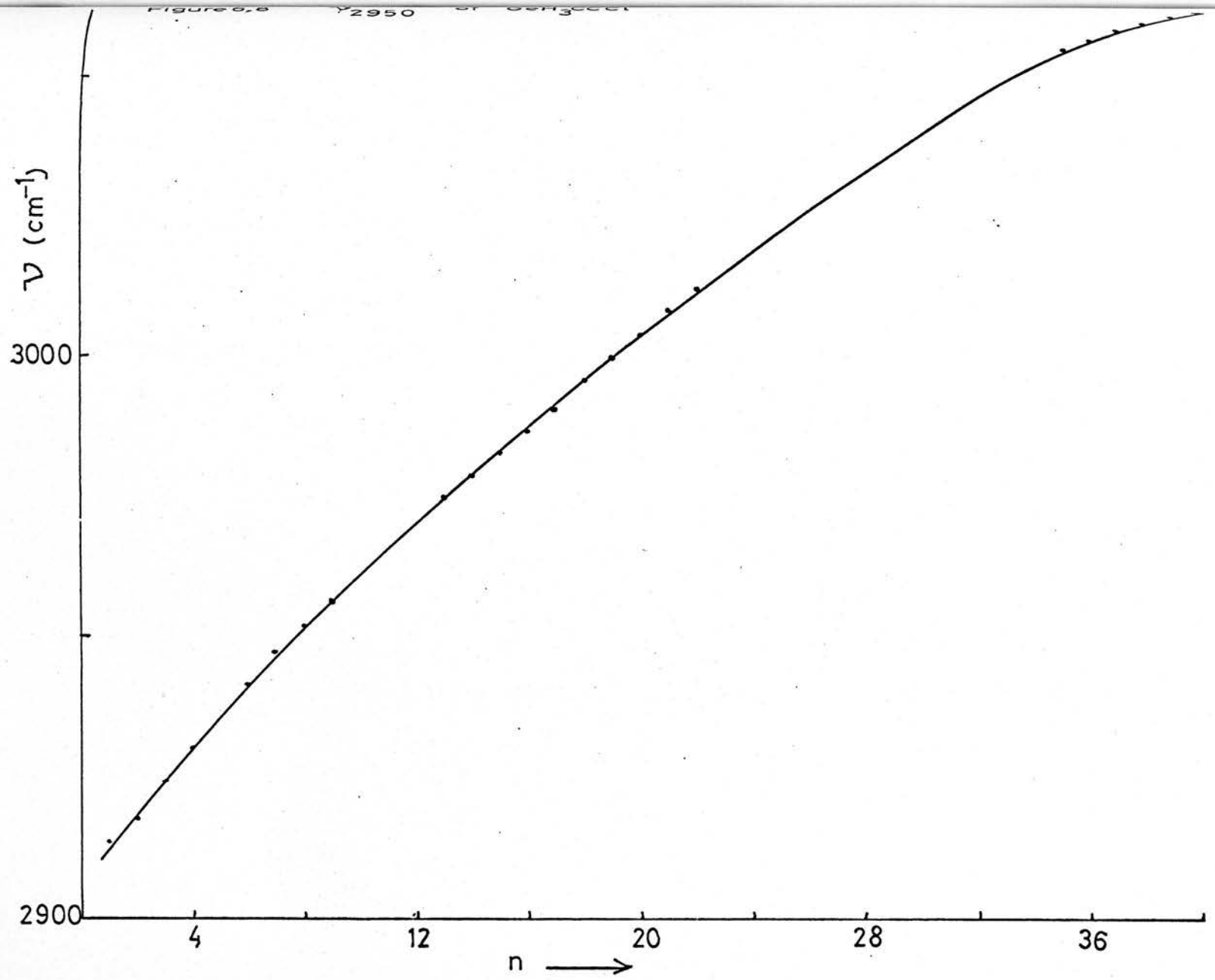
ν (cm⁻¹)
3000
2900
4
12
20
28
36
n

The upper progression is centred on 3060 cm^{-1} so that its assignment is $\nu_2 + \nu_7$ and it should possess a zeta constant of ζ_7. The lower progression could be centred on a number of peaks ranging from 2947 cm^{-1} to 2999 cm^{-1}. Each gives a different zeta value so that a reliable value of the zeta constant could distinguish the most probable bands. The zeta constants, however, have not been determined with sufficient accuracy to allow a definite assignment of this band. The most likely candidate, however, is $\nu_6 + \nu_7$ because the zeta constant of 0.19 is of the same order as that expected for this band (0.24).

The centres of ν_6 and ν_8 (figure 6.9) are clearly defined from the intensities of the Q branches. The centre of ν_7 (figure 4.6) cannot be defined solely from the intensities of the Q branches: overlap with the neighbouring skeletal stretch, ν_4 and the other germyl deformation, ν_3 masks the true intensity pattern. One of the two contenders can be eliminated on detailed analysis of this band due to the presence of a perturbation affecting the energy levels of this band.

The Q branches of all the observed bands are given in table 6.8 and the derived molecular constants from regression analysis are given in table 6.9. The constants obtained for ν_6 and $2\nu_6$ were used to find the ground state value of the rotation constant A''. The rotational constant, B was taken as 0.0287 cm^{-1} calculated from the electron diffraction data in chapter 3. A'' was found to be 2.765 cm^{-1} which is similar to that observed in other C_{3V} germyl compounds[61,62]. This value of A'' was used to obtain the rotational constants and zeta constants of the other bands. These are given in

Table 6.8

Q Branch Frequencies of GeH_3CCCl

GC---NU-6

K	Y(OBS)	Y(CALC)	Y(OBS)-Y(CALC)
18	2213.55	2213.75	-.20
17	2208.75	2208.88	-.13
16	2203.80	2203.97	-.17
15	2198.90	2199.02	-.12
14	2194.05	2194.03	.02
13	2188.90	2189.01	-.11
12	2184.20	2183.95	.25
11	*	2178.85	*
10	2173.60	2173.72	-.12
9	2168.65	2168.54	.11
8	2163.85	2163.33	.52
7	2158.35	2158.08	.27
6	2153.05	2152.80	.25
5	2147.60	2147.48	.12
4	2142.20	2142.12	.08
3	2136.70	2136.72	-.02
2	2131.35	2131.28	.07
1	2125.75	2125.81	-.06
0	2120.65	2120.30	.35
-1	2114.45	2114.75	-.30
-2	2109.65	2109.17	.48
-3	2103.40	2103.54	-.14
-4	2097.75	2097.88	-.13
-5	2092.05	2092.19	-.14
-6	2086.25	2086.45	-.20
-7	2080.40	2080.68	-.28
-8	2074.60	2074.87	-.27
-9	2068.76	2069.02	-.26
-10	2062.85	2063.13	-.28
-11	2057.05	2057.21	-.16
-12	2051.20	2051.25	-.05
-13	2045.20	2045.25	-.05
-14	2039.25	2039.22	.03
-15	2033.25	2033.15	.10
-16	2027.20	2027.04	.16
-17	2021.10	2020.89	.21
-18	2015.05	2014.70	.35

S.D. = 0.25 cm^{-1}

GC===NU=7

K	Y(OBS)	Y(CALC)	Y(OBS)-Y(CALC)
18	996.85	990.14	6.71
17	990.90	984.91	5.99
16	985.35	979.63	5.72
15	979.75	974.30	5.45
14	973.95	968.91	5.04
13	968.20	963.46	4.74
12	962.70	957.96	4.74
11	*	952.40	*
10	*	946.78	*
9	940.80	941.12	-.32
8	935.50	935.39	.11
7	929.80	929.61	.19
6	923.90	923.77	.13
5	917.95	917.88	.07
4	912.10	911.94	.16
3	905.95	905.93	.02
2	899.95	899.87	.08
1	893.65	893.76	-.11
0	887.30	887.59	-.29
- 1	881.60	881.37	.23
- 2	874.80	875.09	-.29
- 3	868.55	868.75	-.20
- 4	862.30	862.36	-.06
- 5	855.80	855.91	-.11
- 6	849.50	849.41	.09
- 7	*	842.85	*
- 8	*	836.23	*
- 9	*	829.56	*
-10	*	822.84	*
-11	816.20	816.06	.14
-12	809.60	809.22	.38
-13	802.75	802.33	.42
-14	795.40	795.38	.02
-15	787.75	788.38	-.63

S.D. = 0.26 cm^{-1}

GC---NU-8

K	Y(OBS)	Y(CALC)	Y(OBS)-Y(CALC)
12	666.05	666.16	-.11
11	662.25	662.48	-.23
10	658.80	658.82	-.02
9	655.30	655.20	.10
8	651.65	651.60	.05
7	648.10	648.04	.06
6	644.60	644.50	.10
5	641.00	641.00	.00
4	637.65	637.52	.13
3	634.25	634.08	.17
2	630.70	630.66	.04
1	627.40	627.27	.13
0	624.00	623.91	.09
-1	620.45	620.59	-.14
-2	617.30	617.29	.01
-3	613.95	614.02	-.07
-4	610.70	610.78	-.08
-5	607.55	607.57	-.02
-6	604.25	604.39	-.14
-7	601.35	601.24	.11
-8	598.15	598.12	.03
-9	594.95	595.03	-.08
-10	591.85	591.97	-.12
-11	588.90	588.94	-.04
-12	585.85	585.94	-.09
-13	582.80	582.97	-.17
-14	579.95	580.02	-.07
-15	577.20	577.11	.09
-16	574.50	574.23	.27
-17	571.45	571.38	.07
-18	568.55	568.55	-.00

S.D. = 0.15 cm^{-1}

GC---2NU=6

K	Y(OBS)	Y(CALC)	Y(OBS)-Y(CALC)
12	4225.85	4225.63	.22
11	4221.80	4221.34	.46
10	4216.55	4216.98	-.43
9	4212.70	4212.53	.17
8	4207.80	4208.01	-.21
7	4203.40	4203.41	-.01
6	4198.85	4198.73	.12
5	4193.80	4193.96	-.16
4	4189.20	4189.12	.07
3	4184.10	4184.21	-.11
2	4179.05	4179.21	-.16
1	4173.80	4174.14	-.34
0	4168.90	4168.98	-.09
-1	4163.45	4163.75	-.30
-2	4158.90	4158.44	.46
-3	4153.10	4153.05	.05
-4	4147.75	4147.57	.18
-5	4141.70	4142.03	-.33
-6	4136.70	4136.40	.30
-7	4131.30	4130.69	.61
-8	4125.05	4124.91	.14
-9	4119.10	4119.04	.06
-10	4113.00	4113.10	-.10
-11	4107.15	4107.07	.07
-12	4101.00	4100.97	.03
-13	4094.95	4094.80	.15
-14	4088.20	4088.54	-.34
-15	4082.05	4082.20	-.15

S.D. = 0.28 cm^{-1}

GC--NU-295

K	Y(OBS)	Y(CALC)	Y(OBS)-Y(CALC)
15	3011.70	3012.00	-.30
14	3008.00	3007.74	.26
13	3003.90	3003.55	.35
12	2999.30	2999.40	-.10
11	2995.70	2995.29	.41
10	2990.65	2991.19	-.54
9	2986.90	2987.09	-.19
8	2982.70	2982.96	-.26
7	2978.85	2978.79	.06
6	2975.10	2974.56	.54
5	2969.70	2970.26	-.56
4	*	2965.85	*
3	*	2961.33	*
2	2956.75	2956.68	.07
1	2952.15	2951.87	.28
0	2947.45	2946.90	.55
-1	2941.90	2941.74	.16
2	*	2936.37	*
-3	2930.30	2930.77	-.47
-4	2924.70	2924.93	-.23
-5	2917.90	2918.83	-.93
-6	2913.40	2912.46	.94

S.D. = 0.51 cm^{-1}

Table 6.9 Molecular Constants of GeH_3CCCl

Band	ν_0^{sub} (cm^{-1})	$[A'(I-\zeta_i)-B']$ (cm^{-1})	$[(A'-A'')-(B'-B'')]$ (cm^{-1})
ν_6	2120.3	2.765(2)	-0.0187(4)
ν_7	868.8	3.182(4)	-0.028(1)
	887.6	3.099(5)	-0.028(1)
ν_8	624.9	1.671(2)	0.0148(4)
$2\nu_6$	4169.0	2.597($4\frac{1}{4}$	-0.0395(9)
ν_{3060}	3060.3	2.46(2)	-
ν_{2970}	2999.4	2.06(4)	0.02(2)
	2987.1	2.06(2)	-0.012(8)
	2974.6	2.13(2)	-0.039(2)
	2961.3	2.29(2)	-0.067(4)
	2946.9	2.53(2)	-0.094(8)

Table 6.10 Rotational and Zeta Constants of GeH_3CCCl

Band	ν_0 (cm^{-1})	A'' (cm^{-1})	A' (cm^{-1})	ζ_i
ν_6	2117.5	2.763(2)	2.744(2)	-0.018(2)
ν_7	865.1	2.763(2)	2.735(2)	-0.174(3)
	884.1	2.763(2)	2.735(2)	-0.144(3)
ν_8	624.3	2.763(2)	2.778(2)	0.388(1)
$2\nu_6$	4166.5	2.763(2)	2.723(2)	0.036(2)
ν_{3060}		2.763(2)	2.763(2)	0.54(1)
ν_{2970}	2998.0	2.763(2)	2.78(2)	0.25(2)
	2985.7	2.763(2)	2.751(8)	0.242(9)
	2973.0	2.763(2)	2.724(4)	0.206(9)
	2959.4	2.763(3)	2.696(5)	0.139(9)
	2944.5	2.763(2)	2.669(9)	0.04(1)

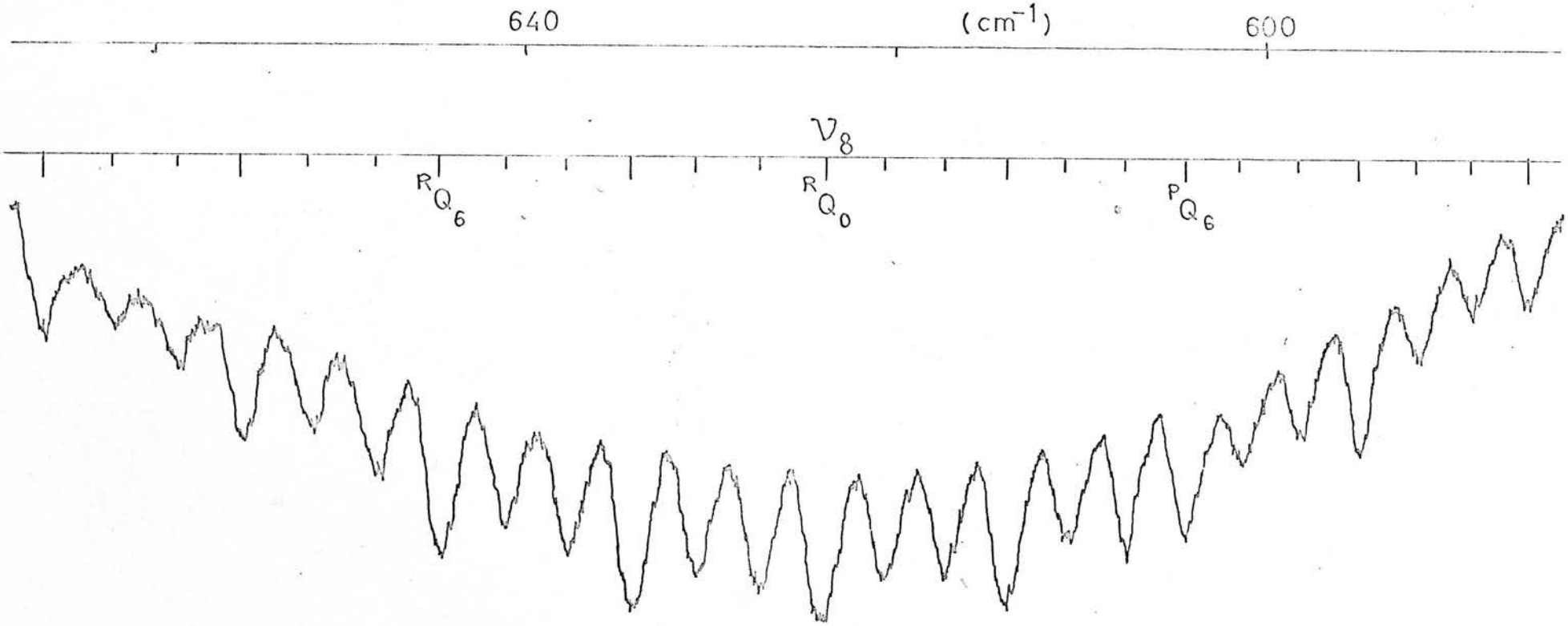

Figure 6.9 ν_8 of GeH_3CCCl

table 6.10. ζ_6 is -0.018 and ζ_7 is either -0.17 or -0.14 depending on whether the band centre is at 868 cm^{-1} or at 884 cm^{-1}. (As will be shown later, the band centre is at 884 cm^{-1}). Both of these zeta constants are in good agreement with other germyl compounds studied. ζ_8, however has a value almost double that expected from other compounds being about 0.38 rather than 0.2. It is not clear why this should be although underlying "hot" bands could affect the precision of the fit.

ζ_9 and ζ_{10} although not resolved, can be estimated as previously for the silyl compounds, from the zeta sum rule.

$$\sum_{6}^{10} \zeta_i = \frac{B''}{2A''} + 2 \simeq 2.00; \quad \zeta_6 + \zeta_7 + \zeta_8 = 0.2276$$

thus $\zeta_9 + \zeta_{10} = 1.77$.

This sum is somewhat less than that found in the silyl acetylenes although the average value of ζ_9 or ζ_{10} is still large at 0.89. The large value of ζ_8 obviously plays a part in lowering the value for the deformations compared to the silyl compounds.

There is a discontinuity in the progression of ν_7, between $^{R}Q_9$ and $^{R}Q_{12}$ (taking $^{R}Q_o$ as 888 cm^{-1}). Unlike ν_8 in silyl bromo-acetylene. where the perturbed levels occur only in the region of the discontinuity, the levels above $^{R}Q_{12}$ are all perturbed while those below $^{R}Q_9$ are unaffected. This type of perturbation is known as a coriolis perturbation.

A coriolis perturbation is produced between any two vibrational states for which the direct products of the symmetry species contain

the species of a rotation[63,64]. The unperturbed term curves must also intersect. This type of interaction is second or higher order because it is an interaction between two different vibrations through coriolis forces. Coriolis interaction produces a shift in the energy of levels from their normal position near the point of intersection of the term curves. This shift does not revert to zero even for large J and K values even though the differences in energy between interacting levels can be fairly large because the interaction increases with increasing K values.

Figure 6.10 shows the perturbed region of ν_7. The assignments of the Q branches are indicated in the figure. Since the interacting vibration must be close in energy to ν_7, the possible perturbing levels are ν_3 and ν_4. Both of these vibrations are of a different symmetry to ν_7, and so they cannot interact by Fermi resonance. Nielsen[64] has shown that fundamentals can interact by a second order coriolis mechanism and that the interaction does become negligible between levels at the point of intersection of the curves when ΔK between the levels is greater than one.

The energy levels of ν_7, ν_3 and ν_4 are given in table 6.11. Those of ν_7 were calculated using the molecular constants in table 6.10. $^{R}Q_{o}$ was taken as 888 cm^{-1} and 861 cm^{-1} because these were the most likely band origins. A'' was assumed for the upper state parameters of ν_3 and ν_4. This value is not expected to differ more than 0.02 from the true value and this does not alter the energy levels significantly.

When the Q branch frequencies are plotted against an arbitrary integer, two distinct curves are obtained with a discontinuity of

Table 6.11. Energy Levels of ν_7, ν_3 and ν_4 in GeH_3CCCl

J,K	$\nu_7(Q^o+864.4\ cm^{-1})$		$\nu_7(Q^o=887.4\ cm^{-1})$		ν_3	ν_4
	ℓ+	ℓ-	ℓ+	ℓ-		
0	864.9		883.9		832.9	888.0
1	868.6	866.7	887.4	885.9	835.7	890.8
2	877.8	874.0	896.5	893.3	844.0	899.1
3	892.5	886.7	911.0	906.2	857.9	913.0
4	912.6	905.0	930.9	924.6	877.2	932.3
5	938.2	928.7	956.3	948.5	902.1	957.2
6	969.2	957.8	987.2	977.8	932.5	987.6
7	1005.8	992.5	1023.6	1012.6	968.5	1023.6
8	1047.8	1032.6	1065.4	1052.9	1010.0	1065.1
9	1095.2	1078.1	1112.8	1098.6	1057.0	1112.1
10	1148.2	1129.2	1165.5	1149.8	1109.5	1164.6
11	1206.6	1185.7	1223.8	1206.5	1167.5	1222.6
12	1270.5	1247.7	1287.5	1268.7	1231.1	1286.2
13	1339.8	1315.1	1356.7	1336.3	1300.2	1355.3
14	1414.7	1388.1	1431.3	1409.4	1376.8	1429.9
15	1495.0	1466.4	1511.5	1487.9	1455.0	1510.1

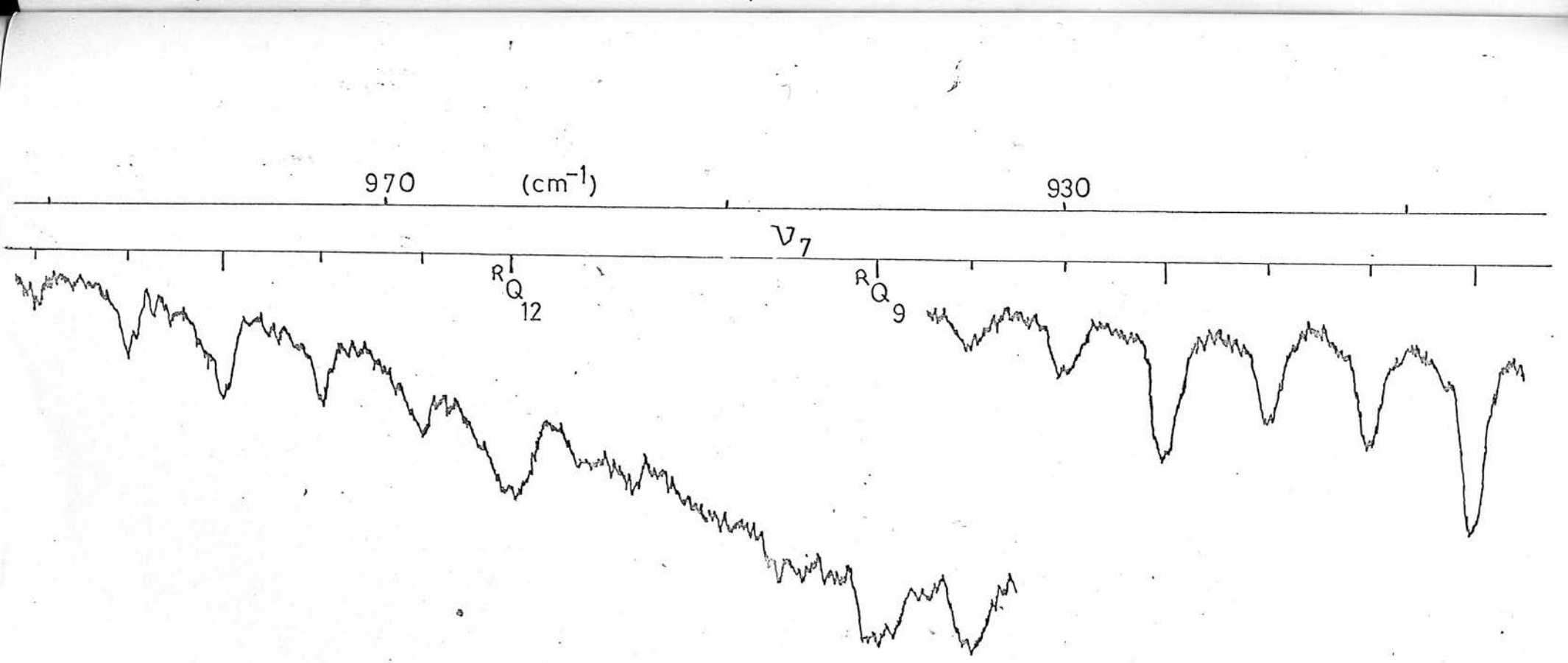

Figure 6.10 Perturbed Region of ν_7 in GeH_3CCCl

the order of 5 cm^{-1} occurring between $^{R}Q_{9}$ and $^{R}Q_{12}$. The ℓ^{+} energy levels of ν_7 give rise to the ^{R}Q branches and so the interacting levels of ν_3 or ν_4 must cross these ℓ^{+} levels. As can be seen from figure 6.11 which is a diagram of the energy levels of ν_7, ν_3 and ν_4 the only crossing that takes place occurs between the ℓ^{-} levels of ν_7 and ν_3. The ℓ^{-} level of ν_7 when the band origin is 864.9 cm^{-1} intersects ν_3 between K = 4 and 5. When the origin is taken as 883.9 cm^{-1}, the ℓ^{-} levels intersect ν_3 between K = 6 and 7. Interaction between ν_7 and ν_3 does not explain the appearance of the pertubation at $^{R}Q_{9}$ and $^{R}Q_{12}$. This is defintely of the coriolis type, because the pertubation does not tend to zero on moving above $^{R}Q_{9}$ but remains approximately constant.

6.2 Analysis of the Perpendicular Bands of Disilyl and Digermyl Acetylenes

Disilyl and digermyl acetylenes are internal rotors. The centres of each Q branch in a particular band are governed by equation V.15 because the secondary structure on each Q branch is not resolved.

$$\nu_o^{sub} = \nu_o + [A(1 - 2\zeta) - B] \pm 2 [A(1 - \zeta) - B] K$$

$$+ (\alpha_A - \alpha_B) K^2 \pm 4 D_K K^3.$$

The intensities of the $^{P}Q_{K}$, $^{R}Q_{K}$ sub-bands are similar and the sub-bands follow the "strong-weak-weak" pattern observed for the rigid rotor.

figure 6.11 Energy Levels of ν_7 Region GeH_3CCCl

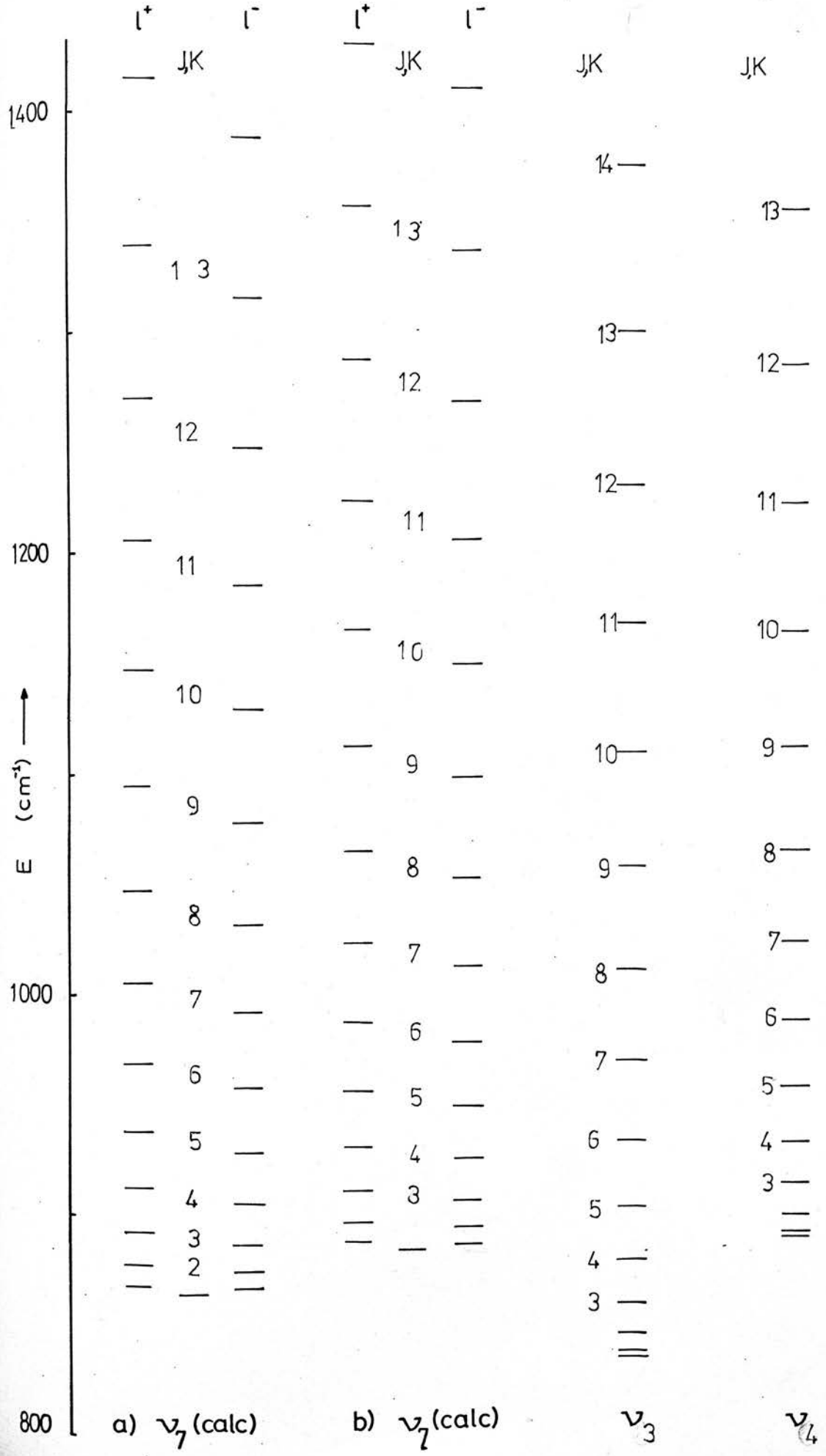

One problem encountered in the analysis of these two compounds is that the band occurring at about 4300 cm^{-1} and 4150 cm^{-1} in the silyl and germyl acetylenes respectively is a combination of the two MH degenerate stretches, ν_8 and ν_{12}. ν_{12} is observed in the infra red, but ν_8 is not because of the mutual exclusion principle. Consequently A'' and ζ_{12} cannot be obtained independently without observation of ν_8. In the analysis of the two species, ζ_8 has been assumed equivalent to ζ_{12}. This is not so unreasonable because both zeta constants are expected to be close to zero. Certainly the value of A'' so obtained is more accurate than a value obtained from electron diffraction data.

The perpendicular bands of disilyl acetylene

Disilyl acetylene has eight degenerate fundamental modes of vibration of which four, ν_8 to ν_{11} inclusive, are infra red inactive. Of the other four, ν_{12},ν_{13} and ν_{14} show resolved rotational fine structure. The overtones of these vibrations are inactive with the result that only combinations are observed. Progressions are observed in the 4300 cm^{-1}, 3100 cm^{-1} and 1300 cm^{-1} regions in addition to the fundamentals.

The progression at 4300 cm^{-1} has $^{R}Q_o$ at 4319.1 cm^{-1} to higher frequency of a strong parallel band. The two bands are probably the parallel and perpendicular components of one band. The possible combinations for this region are

$\nu_1 + \nu_5$	a_{2u}
$\nu_2 + \nu_5$	a_{2u}
$\nu_5 + \nu_8$	e_u

...cont.

$\nu_1 + \nu_{12}$	e_u
$\nu_2 + \nu_{12}$	e_u
$\nu_8 + \nu_{12}$	$a_{2u} + e_u$

The last four bands could all be responsible for the observed progression but $\nu_8 + \nu_{12}$ is the only band that gives reasonable values for the rotational and zeta constants.

The progression with $^{R}Q_o$ at 1372 cm^{-1} could be due to two bands, $\nu_4 + \nu_{13}$ or $\nu_{10} + \nu_{14}$. This band is to higher frequency of a strong parallel band, again suggesting parallel and perpendicular components of one band. $\nu_{10} + \nu_{14}$ is the most likely assignment for this reason and because the expected zeta constant, $-(\zeta_{10} + \zeta_{14})$ is more consistent with the observed zeta constant (-0.506); $\nu_4 + \nu_{13}$ has a zeta constant of ζ_{13} (-0.2).

The frequency of ν_{10}, which was not observed in the raman spectrum, can be estimated from the position of this combination; the anharmonicity in such a calculation being ignored. The frequency deduced is either 679 cm^{-1} or 691 cm^{-1} depending on where the centre of ν_{14} is. Either value is considerably higher than the frequency deduced by Lord[4].

The progression at 3100 cm^{-1} could be centred on several different frequencies. This region has a similar structure to the corresponding region in silyl chloro-acetylene, consisting of several parallel bands with the perpendicular band. The low standard deviation from regression analysis suggests that this progression belongs to one band rather than a complex mixture of different progressions. The possible combinations are

$\nu_1 + \nu_6$	a_{2u}	3111 cm^{-1}
$\nu_2 + \nu_6$	a_{2u}	3053 cm^{-1}
$\nu_5 + \nu_3$	a_{2u}	3135 cm^{-1}
$\nu_1 + \nu_{13}$	e_u	3146 cm^{-1}
$\nu_2 + \nu_{13}$	e_u	3087 cm^{-1}
$\nu_3 + \nu_{12}$	e_u	3139 cm^{-1}
$\nu_5 + \nu_9$	e_u	3136 cm^{-1}
$\nu_6 + \nu_8$	e_u	3108 cm^{-1}
$\nu_8 + \nu_{13}$	$a_{2u} + e_u$	3142 cm^{-1}
$\nu_{12} + \nu_9$	$a_{2u} + e_u$	3142 cm^{-1}

$^{R}Q_o$ can occur at 3142 cm^{-1}, 3127 cm^{-1} or 3112 cm^{-1} suggesting that the band is either $\nu_6 + \nu_8$ at 3112 cm^{-1} or $\nu_8 + \nu_{13}$, $\nu_{12} + \nu_9$ at 3142 cm^{-1}. The zeta constants obtained do not help in the assignment.

The centres of ν_{12} and ν_{13} are readily assigned to the frequencies 2194.8 cm^{-1} and 947.9 cm^{-1} respectively. ν_{14}, however, is not so clear cut; the $^{R}Q_o$ being at either 684 cm^{-1} or 694 cm^{-1}.

The Q branch frequencies for all the observed bands are given in table 6.12 and the derived molecular constants are given in table 6.13.

Reasonable coefficients were obtained for $\nu_8 + \nu_{12}$ only when the Q branches between 4395 cm^{-1} and 4422 cm^{-1} were discarded. Standard deviations in the order of 1 cm^{-1} were obtained if these levels were included suggesting either the presence of a second progression or a perturbed band.

Table 6.I2

Q Branch Frequencies of SiH_3CCSiH_3

SISI---NU=02

K	Y(OBS)	Y(CALC)	Y(OBS)-Y(CALC)
20	2297.70	2297.68	.02
19	2292.75	2292.98	-.23
18	2288.30	2288.22	.08
17	2283.55	2283.42	.13
16	2278.45	2278.57	-.12
15	2274.00	2273.67	.33
14	2268.80	2268.72	.08
13	2263.65	2263.72	-.07
12	2258.80	2258.68	.12
11	2253.50	2253.59	-.09
10	2248.50	2248.46	.04
9	2243.35	2243.29	.06
8	2237.90	2238.07	-.17
7	2232.80	2232.81	-.01
6	2227.65	2227.51	.14
5	2222.10	2222.18	-.07
4	2216.70	2216.80	-.10
3	2211.40	2211.38	.02
2	2205.85	2205.93	-.08
1	2200.05	2200.44	-.39
0	2194.80	2194.91	-.11
-1	2189.35	2189.35	-.00
-2	2184.05	2183.76	.29
-3	2178.60	2178.13	.47
-4	2172.55	2172.47	.08
-5	2166.70	2166.78	-.08
-6	2160.95	2161.06	-.11
-7	2155.35	2155.31	.04
-8	2149.65	2149.53	.12
-9	2143.75	2143.72	.03
-10	2138.20	2137.89	.31
-11	2132.00	2132.03	-.03
-12	2125.95	2126.14	-.19
-13	2120.20	2120.23	-.03
-14	2114.35	2114.30	.05
-15	2108.35	2108.34	.01
-16	2102.20	2102.36	-.16
-17	2096.35	2096.36	-.01
-18	2090.10	2090.34	-.24
-19	2084.15	2084.30	-.15
-20	2078.55	2078.24	.31
-21	2072.25	2072.16	.09

S.D. = 0.19 cm^{-1}

SISI---NU=13

K	Y(OBS)		Y(CALC)	Y(OBS)-Y(CALC)	
15	1046.75	.00	1047.35	-.60	.00
14	1041.20	.00	1041.18	.02	.00
13	1035.35	.00	1034.95	.40	.00
12	1029.45	.00	1028.66	.79	.00
11	1023.65	.00	1022.30	1.35	.00
10	1017.60	1013.70	1015.88	1.72	-2.18
9	1013.45	1007.95	1009.39	4.06	-1.44
8	.00	1001.95	1002.84	.00	-.89
7	.00	995.45	996.23	.00	-.78
6	.00	989.25	989.55	.00	-.30
5	.00	982.70	982.81	.00	-.11
4	.00	976.00	976.01	.00	-.01
3	.00	969.40	969.14	.00	.26
2	.00	962.60	962.21	.00	.39
1	.00	955.65	955.22	.00	.43
0	.00	947.85	948.16	.00	-.31
-1	.00	940.85	941.04	.00	-.19
-2	.00	933.90	933.86	.00	.04
-3	*	*	926.61	*	*
-4	*	*	919.30	*	*
-5	*	*	911.93	*	*
-6	.00	890.75	904.49	.00	-13.74
-7	.00	882.95	896.99	.00	-14.04
-8	.00	875.30	889.42	.00	-14.12
-9	.00	868.30	881.80	.00	-13.50
-10	.00	860.70	874.11	.00	-13.41

S.D. = 0.46 cm^{-1}

SISI---NU=14

K	Y(OBS)		Y(CALC)	Y(OBS)-Y(CALC)	
14	748.30	.00	748.55	-.25	.00
13	745.25	.00	744.85	.40	.00
12	741.20	.00	741.08	.12	.00
11	737.05	.00	737.26	-.21	.00
10	733.15	.00	733.38	-.23	.00
9	729.45	.00	729.47	-.02	.00
8	725.65	.00	725.53	.12	.00
7	721.70	.00	721.58	.12	.00
6	718.40	.00	717.61	.79	.00
5	714.45	.00	713.65	.80	.00
4	710.75	703.10	709.69	1.06	-6.59
3	707.50	701.05	705.74	1.76	-4.69
2	704.30	698.25	701.82	2.48	-3.57
1	701.55	696.30	697.93	3.62	-1.62
0	699.60	692.95	694.06	5.54	-1.11
-1	.00	689.85	690.23	.00	-.38
-2	.00	686.50	686.44	.00	.06
-3	.00	682.50	682.70	.00	-.20
-4	.00	678.95	679.00	.00	-.05
-5	.00	675.25	675.35	.00	-.10
-6	.00	671.75	671.74	.00	.01
-7	.00	668.00	668.19	.00	-.19
-8	.00	664.65	664.68	.00	-.03
-9	.00	661.35	661.23	.00	.12
-10	.00	658.05	657.82	.00	.23
-11	.00	654.55	654.45	.00	.10
-12	.00	651.15	651.13	.00	.02
-13	.00	648.05	647.84	.00	.21
-14	.00	644.45	644.59	.00	-.14
-15	.00	641.20	641.37	.00	-.17
-16	.00	638.20	638.18	.00	.02
-17	.00	634.85	635.00	.00	-.15
-18	.00	631.55	631.84	.00	-.29
-19	.00	629.20	628.68	.00	.52
-20	.00	625.30	625.52	.00	-.22
-21	.00	622.40	622.35	.00	.05

S.D. = 0.15 cm^{-1} (ν_o = 694)

= 0 25 cm^{-1} (ν_o = 682)

(1S)---NU -8 +12

K	Y(OBS)	Y(CAL.)	Y(OBS)-Y(CAL.)
18	4421.95	4406.57	15.38
17	4417.15	4402.34	14.80
16	4411.80	4398.03	13.77
15	4406.45	4393.66	12.79
14	4400.90	4389.20	11.70
13	4395.55	4384.67	10.88
12	*	4380.06	*
11	*	4375.38	*
10	*	4370.62	*
9	4365.80	4365.79	.01
8	4360.90	4360.88	.02
7	4355.75	4355.89	-.14
6	4350.90	4350.84	.06
5	4345.85	4345.70	.15
4	4340.30	4340.49	-.19
3	4335.35	4335.20	.15
2	4329.75	4329.84	-.09
1	4324.00	4324.41	-.41
0	4319.10	4318.89	.21
-1	4313.30	4313.30	-.00
-2	4308.65	4307.64	1.01
-3	4302.05	4301.90	.15
-4	4296.45	4296.09	.36
-5	4290.00	4290.20	-.20
-6	4283.85	4284.23	-.38
-7	4278.05	4278.19	-.14
-8	4271.75	4272.07	-.32
-9	4265.50	4265.88	-.38
-10	4259.55	4259.61	-.06
-11	4253.15	4253.27	-.12
-12	4246.95	4246.85	.10
-13	4240.85	4240.36	.49
-14	4234.20	4233.79	.41

S.D. = 0.33 cm^{-1}

SISI---NU-10 + 14

K	Y(OBS)	Y(CALC)	Y(OBS)-Y(CALC)
11	1483.00	1482.91	.09
10	*	1472.83	*
9	1462.60	1462.74	-.14
8	*	1452.65	*
7	1442.50	1442.57	-.07
6	1432.40	1432.51	-.11
5	1422.70	1422.48	.22
4	1412.40	1412.48	-.08
3	1402.60	1402.53	.07
2	1392.90	1392.62	.28
1	1382.70	1382.78	-.08
0	*	1373.01	*
1	*	1363.32	*
2	*	1353.71	*
3	*	1344.20	*
- 4	1334.00	1334.79	-.79
- 5	1325.80	1325.49	.31
- 6	1316.50	1316.32	.18
- 7	1307.60	1307.27	.33
8	*	1298.36	*
- 9	1289.40	1289.59	-.19

$$S.D. = 0.34\ cm^{-1}$$

SISI --NU-3100

K	Y(OBS)	Y(CALC)	Y(OBS)-Y(CALC)
10	3161.50	3161.63	-.13
9	3156.90	3156.75	.15
8	3151.75	3151.84	-.09
7	*	3146.92	*
6	3142.05	3141.99	.06
5	3137.00	3137.03	-.03
4	3132.35	3132.06	.29
3	3127.05	3127.08	-.03
2	3122.05	3122.08	-.03
1	3116.85	3117.06	-.21
0	*	3112.02	*
1	*	3106.97	*
2	*	3101.90	*
3	*	3096.81	*
- 4	3091.95	3091.71	.24
- 5	3086.65	3086.59	.06
- 6	3081.50	3081.46	.04

$$S.D. = 0.16\ cm^{-1}\ (\nu_o = 3112)$$

$$= 0.14\ cm^{-1}\ (\nu_o = 3142)$$

Table 6.I3 Molecular Constants of SiH_3CCSiH_3

Band	ν_0^{sub} (cm^{-1})	$[A'(1-\zeta_i)-B']$ (cm^{-1})	$[(A'-A'')-(B'-B'')]$ (cm^{-1})
ν_{12}	2I94.9	2.77I(3)	-0.0I74(2)
ν_{13}	948.2	3.54(4)	-0.032(5)
ν_{14}	694.I	I.923(4)	0.0I82(9)
	682.7	I.86I(7)	0.023(2)
$\nu_8 + \nu_{12}$	43I8.9	2.775(6)	-0.038(I)
$\nu_{10} + \nu_{14}$	I373.0	4.87(2)	0.039(4)
ν_{4400}	4406.5	2.69(2)	-0.06(2)
ν_{3100}	3II2.0	2.524(6)	-0.008(2)
	3I27.I	2.497(5)	-0.008(2)
	3I42.0	2.472(9)	-0.008(2)

Table 6.I4 Rotational and Zeta Constants of SiH_3CCSiH_3

Band	ν_0 (cm^{-1})	A'' (cm^{-1})	A' (cm^{-1})	ζ_i
ν_{12}	2I95.8	2.840(3)	2.823(3)	0.003(3)
ν_{13}	943.8	2.840(3)	2.808(6)	-0.28(2)
ν_{14}	68I.8	2.840(3)	2.863(3)	0.335(3)
	693.0	2.840(3)	2.858(3)	0.3I2(3)
$\nu_8 + \nu_{12}$	43I6.I	2.840(3)	2.802(3)	-0.006(4)
$\nu_{10} + \nu_{14}$	I366.I	2.840(3)	2.879(5)	-0.7I(I)
ν_{4400}	4403.8	2.840(3)	2.78(2)	0.02(3)
ν_{3100}	3I09.8	2.840(3)	2.832(4)	0.094(4)
	3I24.6	2.840(3)	2.832(3)	0.I03(4)
	3I39.8	2.840(3)	2.832(3)	0.II2(4)

Analysis of ν_{12} and $\nu_8 + \nu_{12}$ gave a value of A'' equal to 2.8400 cm^{-1} and ζ_{12} as 0.0027. B was assumed to be 0.0431 cm^{-1} calculated from the electron diffraction data. The zeta constant obtained will be an average value for ζ_{12} and ζ_8, and is consistent with zeta constants of other silyl stretching modes. All rotational and zeta constants are given in table 6.14.

The ^RQ branches of $\nu_8 + \nu_{12}$ are observed up to $^RQ_9$ where they overlap with a strong parallel band at 4384 cm^{-1} which could be assigned to $\nu_1 + \nu_5$, $\nu_5 + \nu_8$ or $\nu_1 + \nu_{12}$. Above this band fine structure reappears but a plot of branch frequency against K shows two distinct curves (figure 6.12). The question now arises as to whether $\nu_8 + \nu_{12}$ has been perturbed by close lying rotational states or does the upper state belong to the perpendicular bands, $\nu_5 + \nu_8$ or $\nu_1 + \nu_{12}$? Analysis of the upper portion of the curve yields a zeta constant of between 0.00 and 0.10 suggesting that the band is either $\nu_5 + \nu_8$ or $\nu_1 + \nu_{12}$ because the zeta constant for $\nu_8 + \nu_{12}$ should be less than zero. Further support for this type of assignment is that any band crossing the unperturbed levels of $\nu_8 + \nu_{12}$ between $^RQ_9$ and $^RQ_{12}$ would have to have a band origin at about 4314.7 cm^{-1}. The only band visible at this frequency is in fact centred on 4316 cm^{-1}, being the parallel component of $\nu_8 + \nu_{12}$. This question, however, cannot be settled convincingly without better data.

A similar situation occurred with the analysis of the silyl rock, ν_{14} where Q branches between $^RQ_6$ and $^PQ_3$ were discarded in order to obtain a reasonable fit to a polynomial on analysis. This suggests the presence of Fermi resonance with another band because the higher ^PQ and ^RQ branches fitted to a polynomial expression.

Figure 6.12 $\nu_8 + \nu_{12}$ of SiH_3CCSiH_3

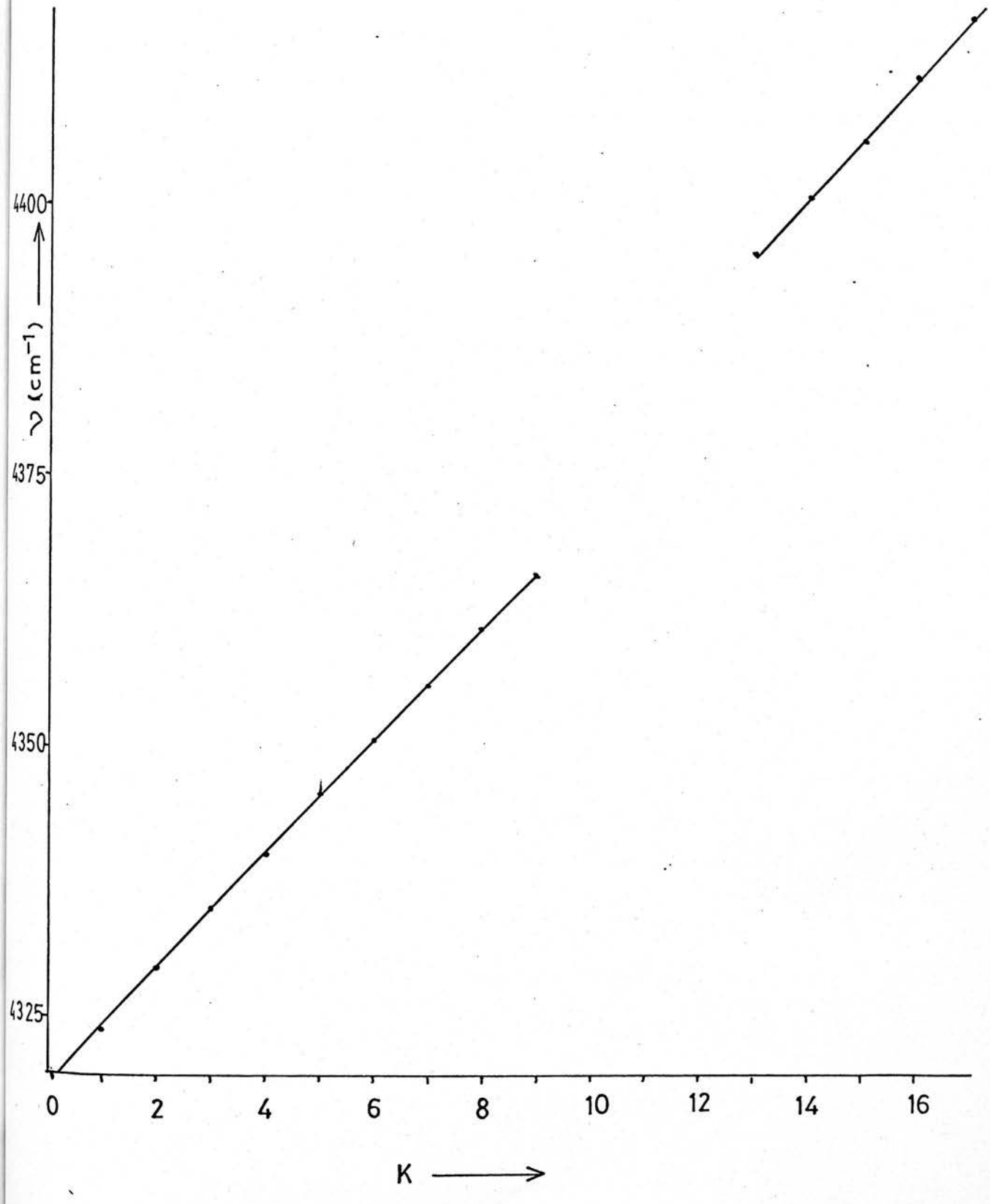

The zeta constant obtained for ν_{14}, being either 0.334 or 0.312 depending on whether the centre of the band is at 680.8 cm^{-1} or 692.1 cm^{-1}, is in keeping with that of a silyl rock. The values of ζ_{14} and A' calculated allow the energy levels to be calculated.

The possible vibrations involved in Fermi resonance are; ν_{10} with ν_o in the region of 692 cm^{-1} or 679 cm^{-1}, taking ν_{14} at ν_o = 680.8 cm^{-1} or 692.1 cm^{-1} respectively; or $\nu_4 + \nu_{11}$ with ν_o in the region of 704 cm^{-1}. ζ_{10} will be similar in magnitude to ζ_{14}. Analysis of $\nu_{10} + \nu_{14}$ gives a value of $-(\zeta_{10} + \zeta_{14})$. The value of ζ_{10} obtained has been used to calculate the energy levels of ν_{10} assuming A' is equivalent to A''. $\nu_4 + \nu_{11}$ should have a zeta constant of ζ_{11}, which will be close to 0.9 from analogy with bending modes in other acetylenes. The energy levels of $\nu_4 + \nu_{11}$ were calculated using this value for the zeta constant and A' equivalent to A''.

The energy levels of ν_{14}, ν_{10} and $\nu_4 + \nu_{11}$ are given in table 6.15. The energy levels of ν_{10} and ν_{14} do not cross when their respective origins are at 679 cm^{-1} and 692 cm^{-1}, but they appear to cross around K = 22 or 23 when their origins are 692 cm^{-1} and 680.8 cm^{-1} respectively. The most perturbed energy levels are when K is 2 or 3 (i.e. the $^{R}Q_1$ or $^{R}Q_2$ branches are the most perturbed in the spectrum). If ν_{10} is the perturbing vibration, then the origin has to be about 681 cm^{-1} which places $\nu_{10} + \nu_{14}$ at 1362 cm^{-1}. The centre of this band actually occurs at a higher frequency. It is unlikely that $\nu_{10} + \nu_{14}$ has a negative anharmonicity and so ν_{10} is probably not the cause of the perturbation in ν_{14}.

The ℓ^+ energy levels of the other band, $\nu_4 + \nu_{11}$ cross those of ν_{14} between J, K = 6 or 7 when the origin of ν_{14} is taken as 680.8 cm^{-1}

Table 6.I5 Energy Levels in SiH_3CCSiH_3

J,K	ν_{14} $\ell+$	$\ell-$	ν_{14} $\ell+$	$\ell-$	ν_{10} $\ell+$	ν_{10} $\ell+$	$\nu_4+\nu_{11}$ $\ell+$
0	682		693		692	679	704
I	683	687	694	698	700	680	70I
2	689	697	70I	708	7I2	686	707
3	702	7I3	7I4	724	730	699	7I3
4	720	735	732	745	754	7I6	728
5	744	763	756	774	783	740	748
6	774	797	786	807	8I8	769	773
7	809	836	82I	846	859	804	805
8	850	88I	862	89I	905	845	843
9	807	93I	909	94I	957	89I	885
IO	949	988	96I	997	IOI5	943	934
II	I008	I050	I020	I059	I078	I00I	988
I2	I072	III8	I084	II27	II47	I064	I048

and between J, K = 3 or 4 when the origin is at 692.1 cm^{-1}. An anharmonicity of 4 cm^{-1} is required to move the point of intersection to the desired point in the latter assignment and an anharmonicity of 10 cm^{-1} is required in the former assignment. This combination is the most likely candidate for the cause of the perturbation in ν_{14}.

The Q branches in the midst of the perturbation appear to be split and less intense (figure 6.13) similar to that observed in ν_8 of silyl bromo-acetylene. Analysis of this region using equation VI.1 gives the position of the perturbing levels of $\nu_4 + \nu_{11}$ or ν_{10}, and hence the approximate value of the zeta constant. The Q branches of disilyl acetylene for this mode are plotted together with the perturbing level in figure 6.14. Zeta for the perturbing level was found to be 0.73. This is too high to be ν_{10} but is not that unreasonable a value for $\nu_4 + \nu_{11}$.

The Q branch frequencies of the silyl deformation, ν_{13} when plotted against K (figure 6.15) shows the presence of two discontinuities. The one occurring between $^RQ_9$ and $^RQ_{10}$ looks like a Fermi type interaction with another vibration. It is not clear whether the Q branch at 890.7 cm^{-1} belongs to $^PQ_6$ or $^PQ_9$, but in either case the second discontinuity occurs between this band and $^PQ_3$. There are not enough resolved Q branches in this second region to tell whether the latter discontinuity is due to Fermi or coriolis interaction with another vibration.

The unperturbed levels between $^PQ_3$ and $^RQ_{15}$ were used to obtain the molecular constants. This band has a higher standard deviation because of the presence of the perturbations, the effects of which cannot be wholely eliminated. The zeta constant obtained was -0.277,

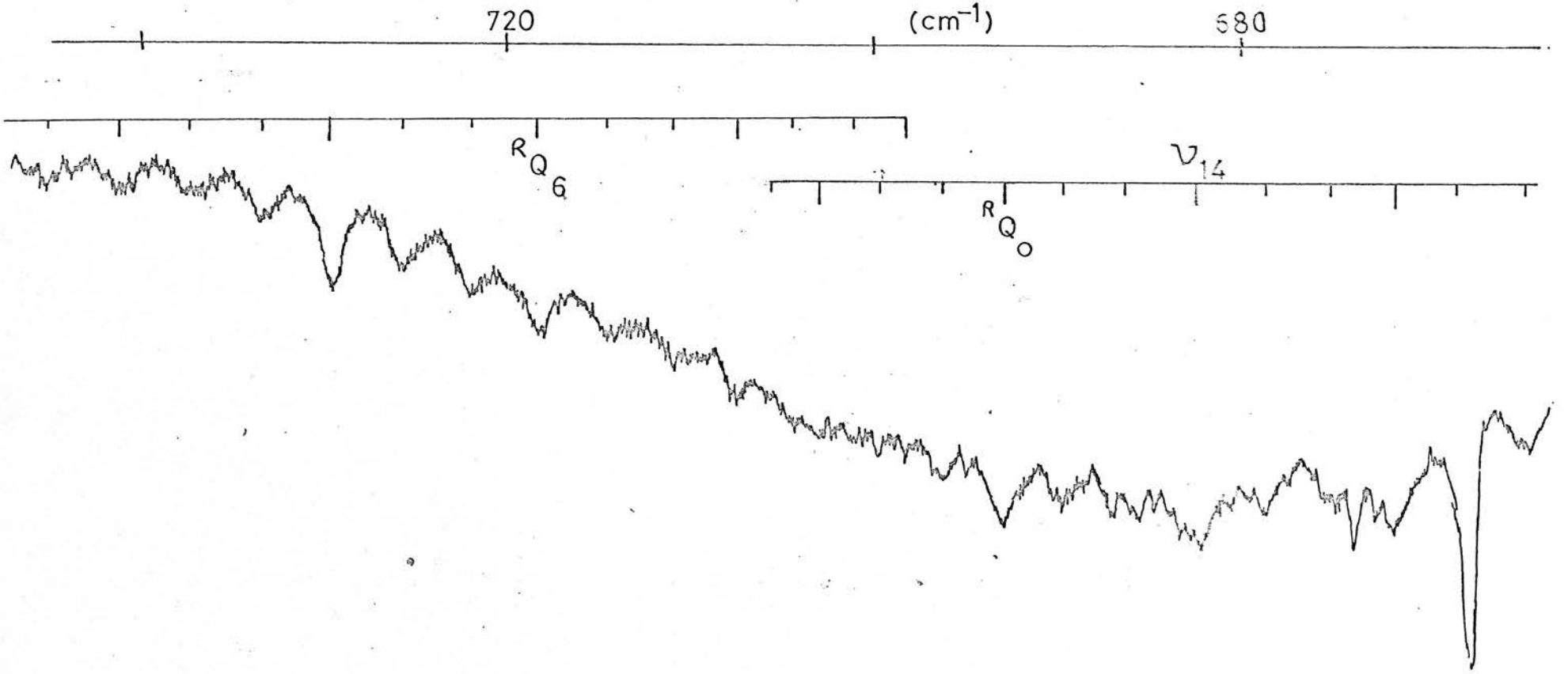

Figure 6.13 ν_{14} of SiH_3CCSiH_3

figure 6.14 ν_{14} of SiH_3CCSiH_3

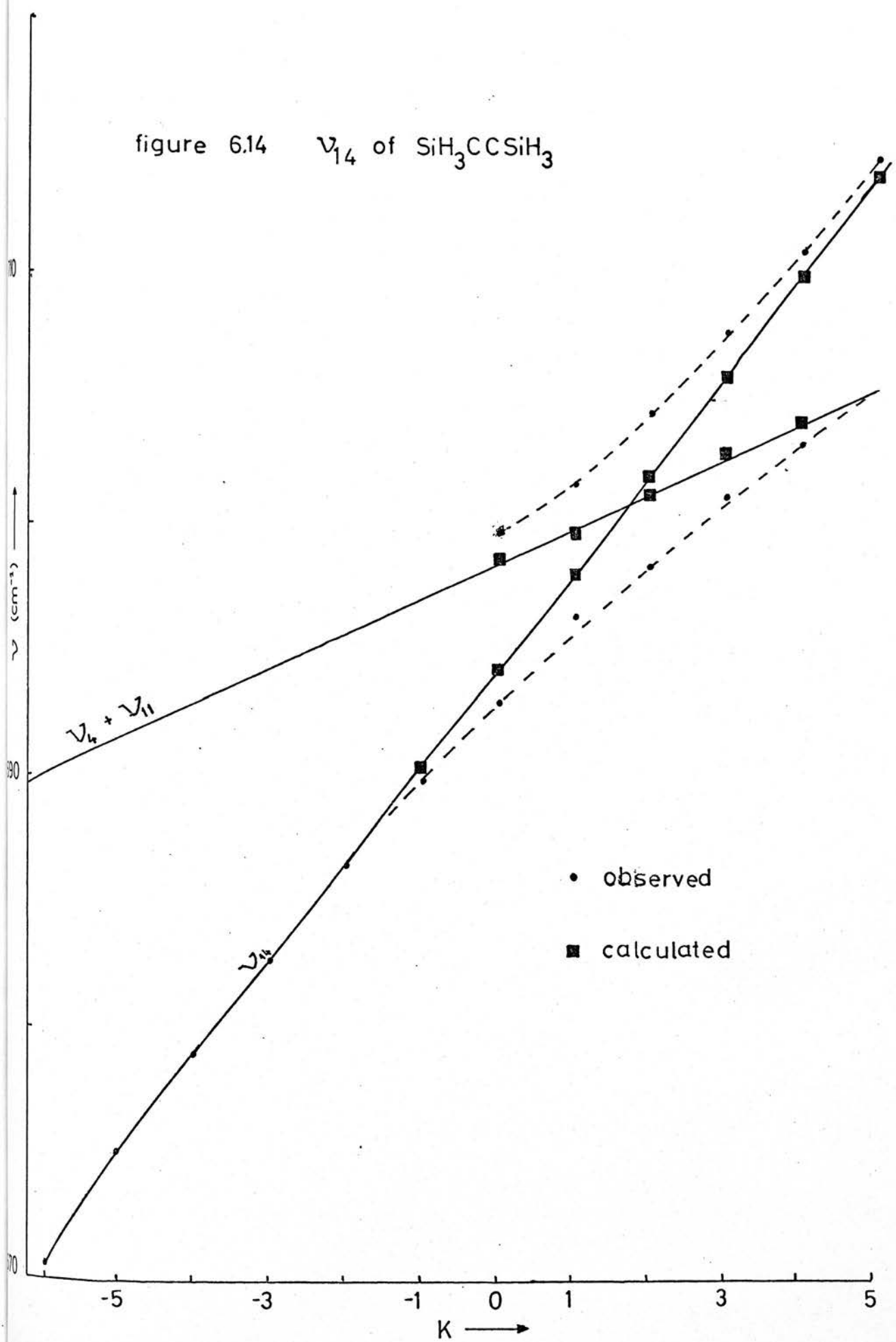

Figure 6.15 ν_{13} of SiH_3CCSiH_3

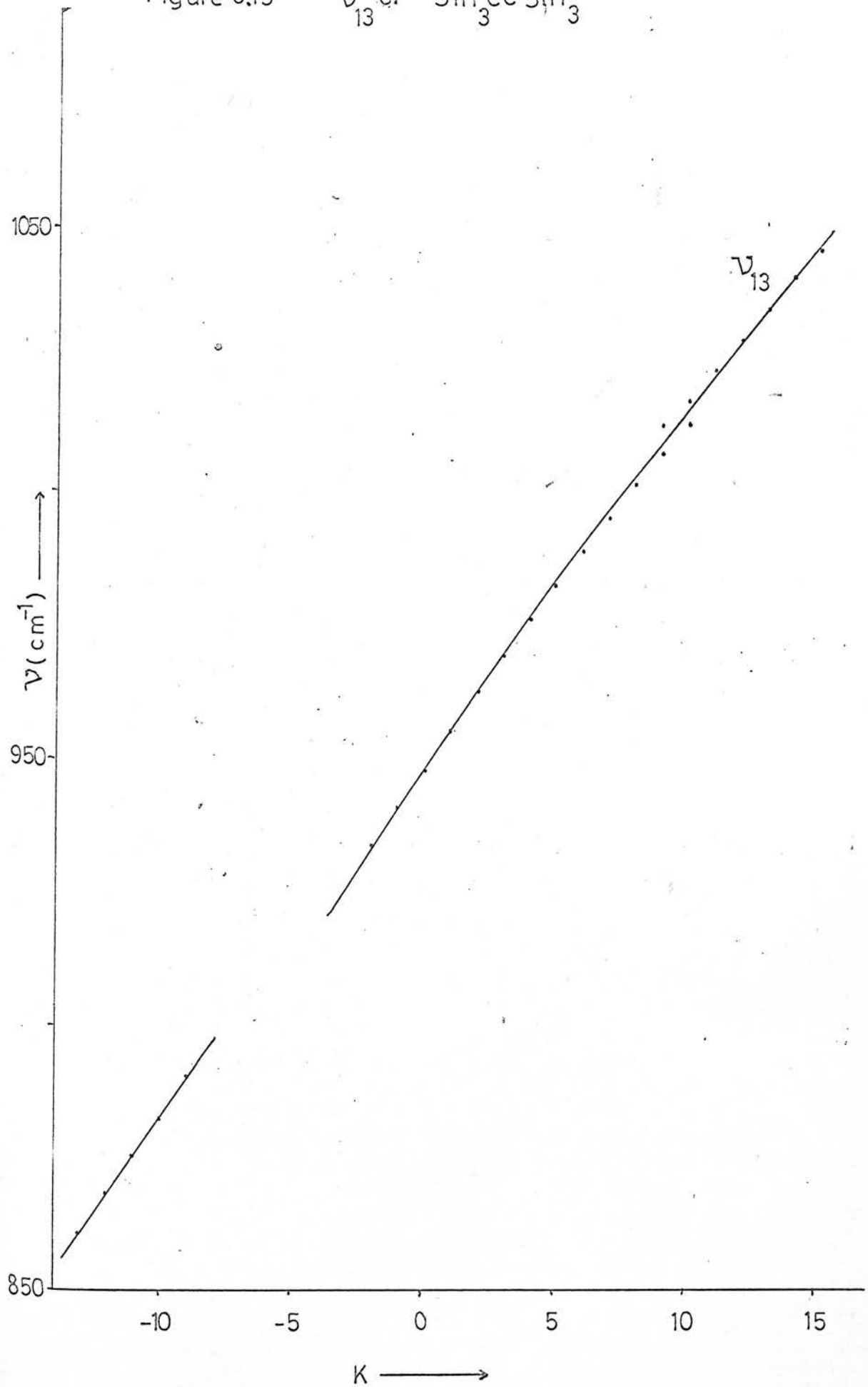

which although rather large, is in keeping with other observed zeta constants.

The discontinuity at the $^{R}Q_{10}$ branch could be caused by interaction with five different vibrations of which three would interact by Fermi resonance. These are $\nu_{11} + \nu_{14}$, $\nu_3 + \nu_{15}$ and $\nu_9 + \nu_{15}$. The energy levels of ν_{13} were calculated from the values of A' and ζ_{13} determined from the analysis of ν_{13}. In all three interacting bands, A' was assumed to be 2.84 cm^{-1}. The zeta constants were assumed to be $-(\zeta_{11} + \zeta_{14})$, ζ_{15} and $-(\zeta_9 + \zeta_{15})$ respectively. The energy levels of the ℓ^+ states are given in table 6.16.

The ℓ^+ energy levels of $\nu_{11} + \nu_{14}$ cross those of ν_{13} at K = 5. This point of intersection is insensitive over a wide range of parameters of $\nu_{11} + \nu_{14}$. The ℓ^+ energy levels of $\nu_3 + \nu_5$ cross those of ν_{13} at K = 15 and those of $\nu_9 + \nu_{15}$ cross at K = 16, both of which are rather high.

It is interesting to note that $\nu_6 + \nu_{15}$ crosses ν_{13} at $^{R}Q_{11}$ which is close to that observed. This band, however, cannot give rise to Fermi resonance.

The second discontinuity could be caused by one (or more) of four bands; ν_9, ν_3 and $\nu_7 + \nu_{15}$ by a coriolis mechanism or $2\nu_4 + \nu_{15}$ by a Fermi mechanism. The energy levels of the ℓ^- states of these bands are also given in table 6.16. ν_9 and ν_3 cross ν_{13} and $^{P}Q_{15}$ and $^{R}Q_2$ respectively. A slight adjustment in any of the variables used in calculating the energy levels could cause the ℓ^- energy levels to interact between the K = 4 and 10 levels. $\nu_7 + \nu_{15}$ and $2\nu_4 + \nu_{15}$ would perturb the $^{P}Q_8$ and $^{P}Q_5$ bands respectively and so could equally be responsible for the observed discontinuity.

Table 6.I6 Energy Levels in SiH_3CCSiH_3

J,K	ν_{13} $\ell+$	$\ell-$	$\nu_{11}+\nu_{14}$ $\ell+$	$\ell+$	$\nu_3+\nu_{15}$ $\ell+$	$\nu_6+\nu_{15}$ $\ell+$	ν_3	ν_9 $\ell-$	$\nu_7+\nu_{15}$ $\ell-$	$\nu_4+\nu_{15}$ $\ell-$
0	944		979	985	I048	I0I5	946	933	9II	924
I	948	946	967	978	I046	I0I3	948	937	9I9	932
2	958	952	972	983	I049	I0I7	957	942	933	946
3	974	965	979	999	I059	I026	972	955	952	965
4	996	984	993	I004	I073	I04I	992	974	978	990
5	I023	I008	I0I2	I023	I094	I06I	I0I7	999	I008	I02I
6	I056	I038	I037	I048	III9	I087	I049	I029	I034	I047
7	I095	I073	I068	I079	II52	III9	I086	I065	I087	I099
8	II39	III4	II04	III5	II89	II57	II28	II07	II34	II47
9	II97	II69	II46	II58	I232	II90	II76	II55	II88	I200
I0	I245	I2I4	II94	I206	I28I	II90	I230	I209	I247	I278
II	I306	I272	I248	I259	I336	I303	I290	I268	I3II	I324
I2	I374	I336	I308	I3I9	I396	I363	I356	I333	I382	I397
I3	I447	I406	I373	I384	I462	I429	I427	I404	I458	I47I
I4	I525	I482	I444	I455	I534	I50I	I503	I480	I540	I552
I5	I609	I563	I52I	I537	I6II	I578	I586	I563	I628	I640

The number of possible perturbing levels would account for the high standard deviations of the constants obtained from analysis. This band would certainly be worth studying in more detail so long as the resolution could be greatly improved.

The perpendicular bands of digermyl acetylene

Digermyl acetylene has four infra red active fundamentals similar to disilyl acetylene. Only ν_{12}, ν_{13} (figure 6.16) and ν_{14} have Q branches. In addition to these three bands, Q branches were observed in 4100 cm^{-1}, 2950 cm^{-1} and 1200 cm^{-1} regions of the spectrum. The progression at 4100 cm^{-1} has a band centred on 4163 cm^{-1} to higher frequency of a parallel band. This latter band is probably the parallel component of $\nu_8 + \nu_{12}$; the former band being the perpendicular component (figure 6.17).

Similarly the 1200 cm^{-1} region has a strong parallel band to lower frequency of the perpendicular band at 1255 cm^{-1}. These two bands can be assigned to $\nu_{10} + \nu_{14}$ because this is the only combination that is expected in this region.

The 2950 cm^{-1} region has a progression between 2914 cm^{-1} and 2954 cm^{-1}. This is to low frequency of a series of combination bands. Unlike the other molecules studied, no distinct Q branches could be seen to the high frequency. The bands expected in this region are

$\nu_1 + \nu_6$	a_{2u}	2963 cm^{-1}
$\nu_2 + \nu_6$	a_{2u}	2947 cm^{-1}
$\nu_3 + \nu_5$	a_{2u}	2949 cm^{-1}

...continued

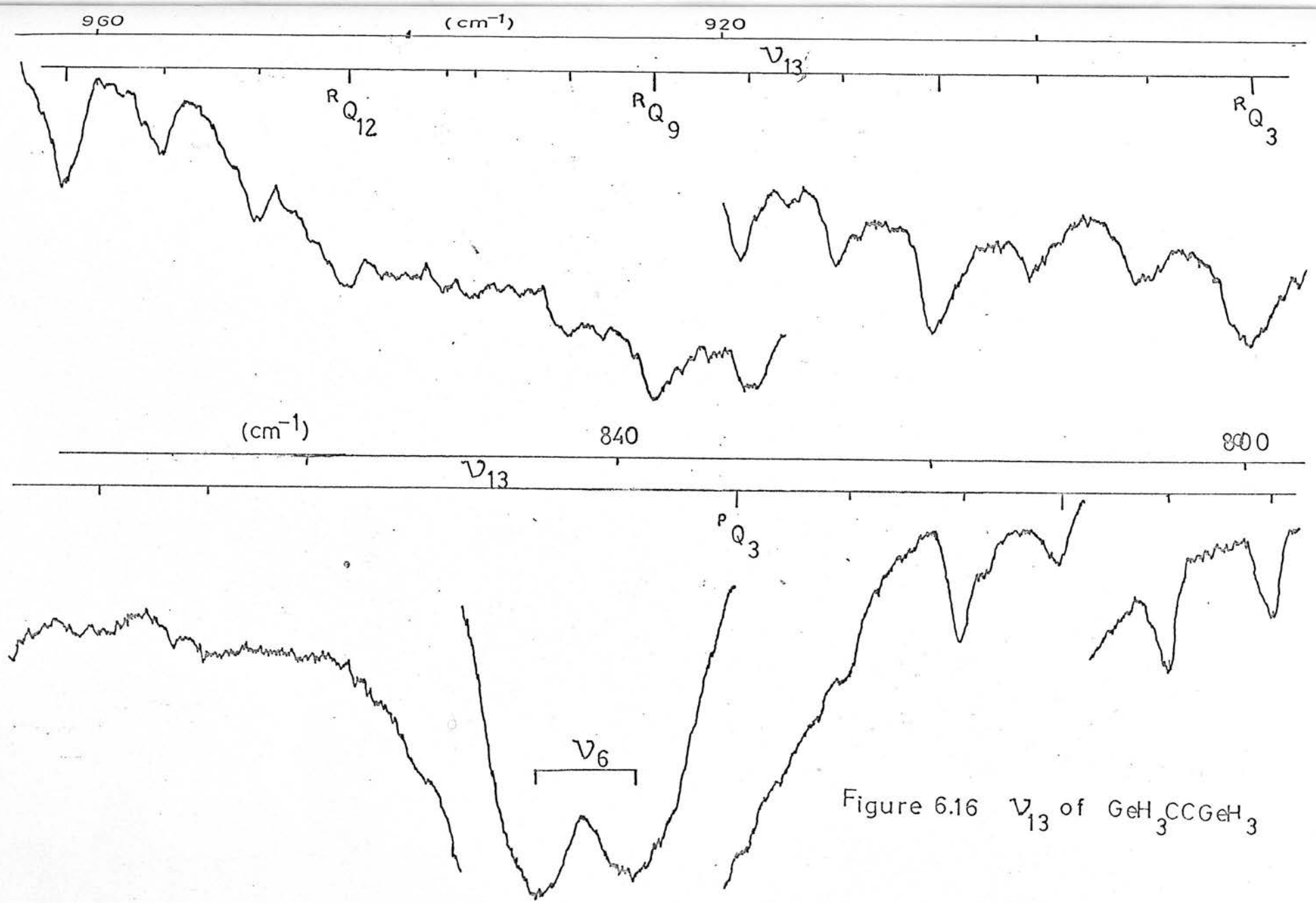

Figure 6.16 ν_{13} of GeH_3CCGeH_3

figure 6.17 $\nu_8 + \nu_{12}$ of GeH_3CCGeH_3

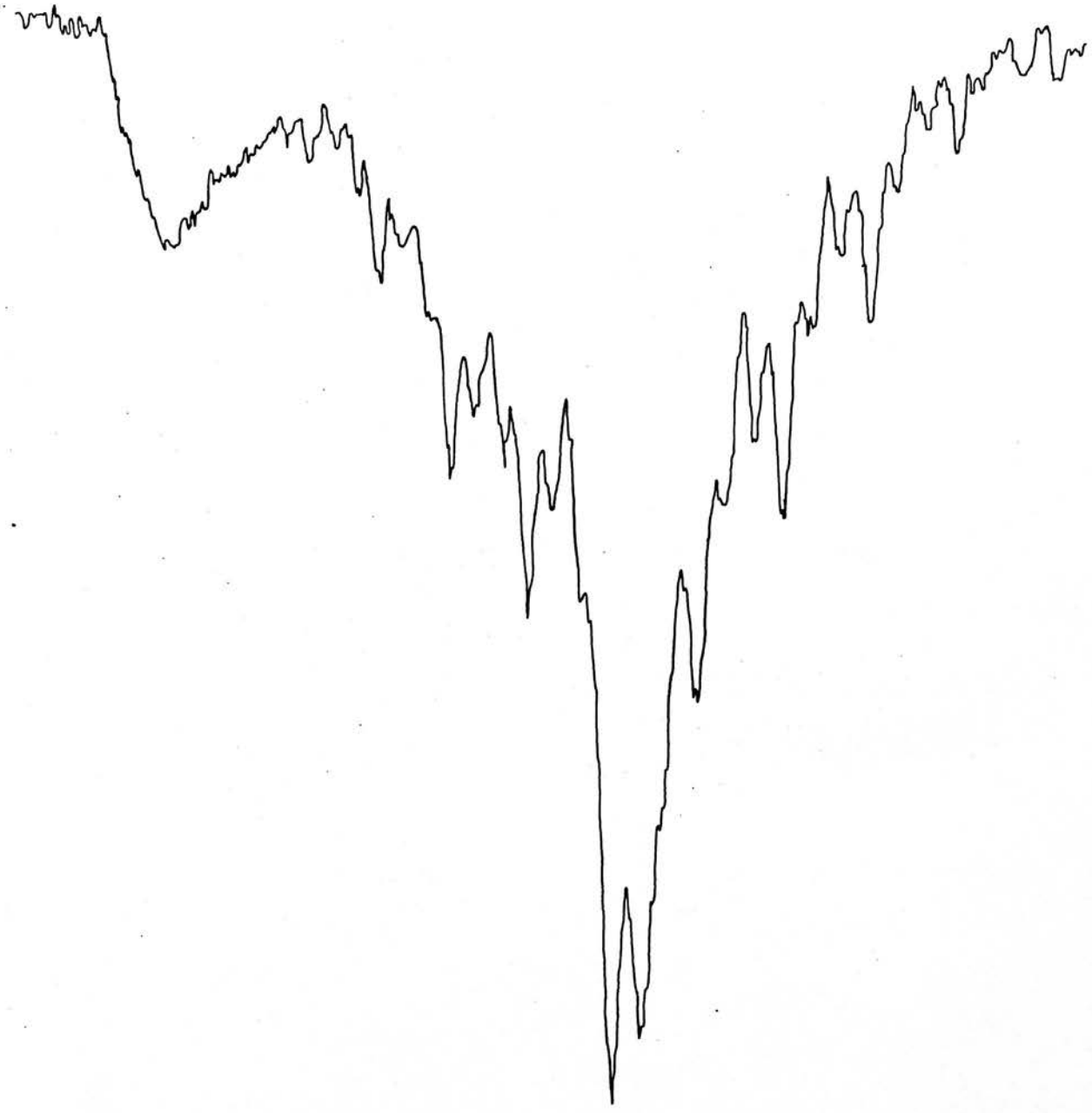

$\nu_6 + \nu_8$	e_u	2947 cm^{-1}
$\nu_1 + \nu_{13}$	e_u	3027 or 3007 cm^{-1}
$\nu_2 + \nu_{13}$	e_u	3011 or 2991 cm^{-1}
$\nu_5 + \nu_9$	e_u	2990 cm^{-1}
$\nu_3 + \nu_{12}$	e_u	2961 cm^{-1}
$\nu_8 + \nu_{13}$	$a_{2u} + e_u$	3011 or 2991 cm^{-1}
$\nu_{12} + \nu_9$	$a_{2u} + e_u$	2993 cm^{-1}

The most likely assignments, taking into account the "strong-weak-weak" pattern, are $\nu_1 + \nu_{13}$ at 3007 cm^{-1}, $\nu_5 + \nu_9$, $\nu_2 + \nu_{13}$ or $\nu_8 + \nu_{13}$ at 2987 cm^{-1} and $\nu_3 + \nu_{12}$ or $\nu_3 + \nu_5$ at 2953 cm^{-1}. The band with ${}^{R}Q_o$ at 2953 cm^{-1} has a similar zeta constant to ζ_{12} or ζ_8, suggesting that this progression belonged to $\nu_3 + \nu_{12}$.

The observed frequencies of the Q branches are given in table 6.17 and the derived molecular constants in table 6.18. A'' was calculated using the derived molecular constants of ν_{12} and $\nu_8 + \nu_{12}$, assuming that ζ_8 is equivalent to ζ_{12}. The value of B used was 0.0167 cm^{-1}, being calculated from the electron diffraction data. A'' was found to be 2.769 cm^{-1} in agreement with values for other germyl stretches. This value of A'' was used to calculate the rotational and zeta constants of other bands. These are given in table 6.19.

The zeta constants found for ν_{12} and ν_{13} are in good agreement with other germyl compounds. ν_{14} on the other hand is 0.405 which is consistent with that obtained for germyl chloro-acetylene but does not agree with those obtained for the germyl halides[61].

Table 6.I7

Q Branch Frequencies of GeH_3CCGeH_3

---NU-12

K	Y(OBS)	Y(CALC)	Y(OBS)-Y(CALC)
21	2225.40	2225.39	.01
20	2220.65	2220.60	.04
19	2215.65	2215.78	-.13
18	2210.90	2210.91	-.01
17	2206.15	2206.00	.15
16	2201.85	2201.04	-.19
15	2196.35	2196.05	.30
14	2191.20	2191.01	.19
13	2185.80	2185.93	-.13
12	2180.75	2180.81	-.06
11	2175.65	2175.65	-.00
10	2170.45	2170.46	-.01
9	2165.20	2165.22	-.02
8	2160.05	2159.95	.10
7	2154.40	2154.64	-.24
6	2149.40	2149.29	.11
5	2143.95	2143.91	.04
4	2138.30	2138.49	-.19
3	2133.05	2133.04	.01
2	2127.65	2127.55	.10
1	2121.75	2122.03	-.28
0	*	2116.48	*
1	*	2110.89	*
-2	2105.90	2105.27	.63
-3	2099.65	2099.62	.03
-4	2094.05	2093.94	.11
-5	2088.10	2088.22	-.12
-6	2082.45	2082.48	-.03
-7	2076.95	2076.71	.24
-8	2070.75	2070.91	-.16
-9	2065.00	2065.08	-.08
-10	2059.35	2059.23	.12
-11	2053.20	2053.34	-.14
-12	2047.25	2047.43	-.18
-13	2041.65	2041.50	.15
-14	2035.55	2035.54	.01
-15	2029.30	2029.55	-.25
-16	2023.60	2023.54	.06
-17	2017.60	2017.51	.09
-18	2011.50	2011.45	.05
-19	2005.50	2005.37	.13
-20	1999.40	1999.27	.13
-21	1992.85	1993.15	-.30
-22	1987.15	1987.01	.14
-23	1980.75	1980.84	-.09
-24	1974.75	1974.66	.09

S.D. = 0.07 cm^{-1}

F---NU-13

K	Y(OBS)		Y(CALC)	Y(OBS)-Y(CALC)	
21	1015.25	.00	1015.17	.08	.00
20	1009.45	.00	1009.39	.06	.00
19	1003.60	.00	1003.58	.02	.00
18	997.70	.00	997.73	-.03	.00
17	991.65	.00	991.85	-.20	.00
16	985.80	.00	985.93	-.13	.00
15	980.30	.00	979.97	.33	.00
14	974.30	.00	973.98	.32	.00
13	967.25	.00	967.96	-.71	.00
12	961.90	.00	961.90	.00	.00
11	956.20	.00	955.80	.40	.00
10	949.55	.00	949.67	-.12	.00
9	944.05	941.40	943.50	.55	-2.10
8	937.95	936.15	937.30	.65	-1.15
7	933.20	929.80	931.06	2.14	-1.26
6	928.05	924.15	924.79	3.26	-.64
5	.00	918.30	918.48	.00	-.18
4	.00	912.30	912.14	.00	.16
3	.00	905.80	905.76	.00	.04
2	.00	900.15	899.35	.00	.79
1	.00	892.95	892.90	.00	.05
0	.00	886.20	886.42	.00	-.22
-1	.00	880.20	879.90	.00	.30
-2	.00	873.75	873.35	.00	.40
-3	.00	866.05	866.76	.00	-.71
-4	*	*	860.13	*	*
-5	*	*	853.47	*	*
-6	*	*	846.78	*	*
-7	*	*	840.04	*	*
-8	*	*	833.28	*	*
-9	.00	831.65	826.48	.00	5.17
-10	.00	825.20	819.64	.00	5.56
-11	.00	817.90	812.77	.00	5.13
-12	.00	811.70	805.86	.00	5.84
-13	.00	805.35	798.92	.00	6.43
-14	.00	798.50	791.94	.00	6.56
-15	.00	791.85	784.93	.00	6.92
-16	.00	785.35	777.88	.00	7.47
-17	.00	778.00	770.80	.00	7.20
-18	.00	771.35	763.68	.00	7.67

S.D. = 0.40 cm^{-1} (ν_o = 886)

= 0 39 cm^{-1} (ν_o = 906)

GEGE---NU=14

K	Y(OBS)	Y(CALC)	Y(OBS)-Y(CALC)
13	668.55	668.75	-.20
12	665.35	665.14	.21
11	661.60	661.56	.04
10	657.90	658.00	-.10
9	654.35	654.47	-.12
8	650.85	650.97	-.12
7	647.40	647.49	-.09
6	644.05	644.04	.01
5	640.70	640.62	.08
4	637.35	637.23	.12
3	634.10	633.86	.24
2	630.65	630.51	.14
1	627.15	627.20	-.05
0	624.20	623.91	.29
- 1	620.75	620.65	.10
- 2	617.20	617.41	-.21
- 3	614.30	614.20	.10
- 4	611.00	611.02	-.02
- 5	607.80	607.86	-.06
- 6	604.70	604.73	-.03
- 7	601.60	601.63	-.03
- 8	598.55	598.55	.00
- 9	595.35	595.50	-.15
-10	592.30	592.48	-.18
-11	589.25	589.48	-.23
-12	586.55	586.51	.04
-13	583.50	583.56	-.06
-14	580.75	580.65	.10
-15	577.65	577.76	-.11
-16	574.95	574.89	.06
-17	*	572.06	*
-18	569.50	569.24	.26

S.D. = 0.17 cm^{-1}

GEGE---NU=8 + 12

K	Y(OBS)	Y(CALC)	Y(OBS)-Y(CALC)
12	4220.05	4219.65	.40
11	4215.40	4215.37	.03
10	4210.80	4211.00	-.20
9	4206.95	4206.54	.41
8	4202.15	4202.01	.14
7	4197.20	4197.40	-.20
6	4192.55	4192.70	-.15
5	4187.75	4187.93	-.18
4	4182.75	4183.07	-.32
3	4178.10	4178.13	-.03
2	4173.10	4173.11	-.01
1	4167.70	4168.00	-.30
0	4162.95	4162.82	.12
- 1	4156.90	4157.56	-.66
- 2	*	4152.21	*
- 3	4147.00	4146.79	.21
- 4	4141.50	4141.28	.22
- 5	4136.00	4135.69	.31
- 6	4130.10	4130.02	.09
- 7	4124.80	4124.26	.54
- 8	4118.45	4118.43	.02
- 9	4112.80	4112.51	.29
-10	4107.10	4106.52	.59
-11	4100.25	4100.44	-.19
-12	4094.25	4094.28	-.03
-13	4087.75	4088.04	-.29
-14	4081.45	4081.72	-.27
-15	4075.30	4075.32	-.02
-16	4068.80	4068.83	-.03

S.D. = 0.30 cm^{-1}

GEGE---NU=10+ 14

K	Y(OBS)	Y(CALC)	Y(OBS)-Y(CALC)
3	1283.80	1284.28	-.48
2	1274.50	1274.63	-.13
1	1265.80	1265.04	.76
0	*	1255.49	*
-1	*	1246.00	*
-2	*	1236.56	*
-3	1227.80	1227.17	.63
-4	1217.80	1217.83	-.03
-5	1208.20	1208.54	-.34
-6	1199.00	1199.31	-.31
-7	1189.90	1190.12	-.22
-8	1181.10	1180.99	.11
-9	1171.70	1171.91	-.21
-10	1163.10	1162.88	.22
-11	1154.30	1153.90	.40
-12	1144.80	1144.97	-.17

S.D. = 0.45 cm^{-1}

GEGE---NU=2950

K	Y(OBS)	Y(CALC)	Y(OBS)-Y(CALC)
0	2953.70	2953.92	-.22
-1	2948.60	2948.24	.36
-2	*	2942.57	*
-3	2936.80	2936.89	-.09
-4	2931.20	2931.22	-.02
-5	2925.50	2925.55	-.05
-6	2919.80	2919.87	-.07
-7	2914.30	2914.20	.10

S D = 0 20 cm^{-1}

Table 6.I8 Molecular Constants of GeH_3CCGeH_3

Band	ν_0^{sub} (cm^{-1})	$[A'(I-\zeta_i)-B']$ (cm^{-1})	$[(A'-A'')-(B'-B'')]$ (cm^{-1})
ν_{12}	2II6.5	2.785(I)	-0.0I635(8)
ν_{13}	886.4	3.25(2)	-0.0I8(2)
	905.8	3.20(I)	-0.0I8(2)
ν_{14}	623.9	I.638(2)	0.0I33(4)
$\nu_8 + \nu_{12}$	4I62.8	2.6I2(4)	-0.0407(9)
$\nu_{10} + \nu_{14}$	I255.5	4.76(3)	0.026(6)
ν_{2950}	2953.9	2.83(2)	-

Table 6.I9 Rotational and Zeta Constants of GeH_3CCGeH_3

Band	ν_0 (cm^{-1})	A'' (cm^{-1})	A' (cm^{-1})	ζ_i
ν_{12}	2II3.6	2.769(I)	2.752(I)	-0.0I8(2)
ν_{13}	883.2	2.769(I)	2.75I(2)	-0.I88(7)
	902.6	2.769(I)	2.75I(2)	-0.I69(5)
ν_{14}	623.4	2.769(I)	2.782(2)	0.405(I)
$\nu_8 + \nu_{12}$	4I60.3	2.769(I)	2.728(I)	0.036(2)
$\nu_{10} + \nu_{14}$	I248.8	2.769(I)	2.794(6)	-0.7I(I)
ν_{2950}	295I.0	2.769(I)	2.769(2)	-0.03(2)

ν_{13} in digermyl acetylene has two discontinuities similar to disilyl acetylene. One occurs, as can be seen from figure 6.16, around the $^{R}Q_{5}$ branch, the other between $^{P}Q_{5}$ and $^{P}Q_{9}$, assuming that the band origin of ν_{13} is at 902.6 cm^{-1} rather than 883.2 cm^{-1}. If the band origin is at 883.2 cm^{-1}, then the two perturbations occur at $^{R}Q_{8}$ and between $^{P}Q_{2}$ and $^{P}Q_{6}$ respectively. The energy levels of ν_{13} were calculated using the constants found by analysis of the band. Since the origin is not well defined, both series of energy levels are given in table 6.20, together with those of the probable perturbing bands. The energy levels of ν_{3} and ν_{6} do not cross those of ν_{13} and so are not included in table 6.20. $\nu_{3} + \nu_{15}$ and $\nu_{7} + \nu_{11}$ have zeta constants of +0.9 corresponding to ζ_{15} and ζ_{11} respectively. $\nu_{11} + \nu_{14}$ and $\nu_{10} + \nu_{11}$ have zeta constants of -1.2 corresponding to $-(\zeta_{11} + \zeta_{14})$ and $-(\zeta_{10} + \zeta_{11})$ respectively and ν_{9} has a zeta constant of -0.14 similar to that of other germyl deformations. The ground state rotation constant, A'' was used to calculate the energy levels of these bands.

The ℓ^{+} energy levels of $\nu_{3} + \nu_{15}$ and $\nu_{7} + \nu_{11}$ cross ℓ^{+} levels of ν_{13}; the K = 5 levels being the most perturbed when the origin of ν_{13} is at 902.6 cm^{-1}; the K = 9 and K = 7 levels in the two respective bands when the origin of ν_{13} is at 883.2 cm^{-1}. This is similar to that observed. This perturbation, however, is of the Fermi type and as a result can be due to $\nu_{3} + \nu_{15}$ or $\nu_{7} + \nu_{11}$. Figure 6.16 shows that some additional bands are just resolved in this region of the spectrum, similar to those observed on the silyl rock of silyl bromo-acetylene and disilyl acetylene. The additional bands belong to the perturbing mode. Consequently the frequencies of the bands

Table 6.20. Energy Levels of ν_{13}, $\nu_{11} + \nu_{14}$, $\nu_{11} + \nu_{10}$, ν_9, $\nu_7 + \nu_{11}$ and $\nu_3 + \nu_{15}$ in GeH_3CCGeH_3

J,K	ν_{13}		ν_{13}		$\nu_{11} + \nu_{14}$(or ν_{10})		ν_9	$\nu_7 + \nu_{11}$	$\nu_3 + \nu_{15}$
	ℓ+	ℓ−	ℓ+	ℓ−	ℓ+	ℓ−	ℓ−	ℓ+	ℓ+
0	883.2		902.6		902.0		876.1	927.0	935.0
1	887.0	884.9	906.3	904.4	911.5	898.1	878.1	924.8	932.8
2	896.3	892.2	915.5	911.8	926.4	899.8	885.1	928.1	936.1
3	911.1	904.9	930.2	924.6	946.9	907.0	898.7	937.0	945.0
4	931.4	923.4	950.4	943.0	972.9	919.8	917.4	951.4	959.4
5	957.2	946.9	976.1	966.8	1004.2	938.1	941.5	971.4	979.4
6	988.5	976.1	1007.2	996.2			971.2	996.9	1004.9
7	1025.3	1010.9	1043.9	1031.0			1006.4	1027.4	1035.9
8	1067.6	1051.1	1086.1	1071.3			1047.2	1064.5	1072.5
9	1115.5	1096.9	1133.8	1117.2			1093.5	1106.5	1114.5
10	1168.8	1148.1	1187.1	1168.5			1145.4	1154.2	1162.2
11	1227.6	1204.9	1245.8	1225.4			1202.7	1207.4	1215.4
12	1291.9	1267.2	1310.0	1287.7			1265.7	1262.1	1274.1
13	1361.7	1334.9	1379.7	1355.6			1334.1	1330.3	1338.3
14	1437.1	1408.2	1454.9	1429.0			1408.1	1410.1	1418.1
15	1517.9	1486.9	1535.6	1507.8			1487.6	1475.2	1483.2

can be plotted against an integer and the zeta constant of the perturbing level can be determined. The observed bands can be arranged in two different ways, both giving the appearance of a Fermi perturbation. The zeta constants found were 0.10 and 1.06 respectively. The latter diagram is shown in figure 6.17a. The former value does not agree with that of any band occurring in this region but the latter value is near to that expected for a skeletal deformation and would confirm the cause of this perturbation as $\nu_3 + \nu_{15}$ or $\nu_7 + \nu_{11}$.

The lower perturbation could be caused by ν_9, only if the origin of ν_{13} is at 883.2 cm^{-1}. Since this band has similar rotational constants and zeta constants to ν_{13}, slight adjustment in any of the parameters could greatly affect the point of intersection of the two curves. $\nu_{11} + \nu_{14}$ (or ν_{10}) could also be responsible for this perturbation because the energy levels intersect with those of ν_{13} when either origin is used. This perturbation would occur at ${}^{R}Q_{o}$ and ${}^{P}Q_{4}$ if the origins are at 902.6 cm^{-1} and 883.2 cm^{-1} respectively. The latter point corresponds to that observed. As a result, the most likely band origin is 883.2 cm^{-1}. The upper perturbation is caused by $\nu_3 + \nu_{15}$, and the lower perturbation by either $\nu_{11} + \nu_{14}$ or $\nu_{10} + \nu_{14}$.

6.3 Analysis of the Perpendicular Bands of Silyl and Germyl Perfluoromethyl Acetylenes

Molecules of type MH_3CCCF_3, M = Si, Ge have eight perpendicular modes, all of which are infra red active. These molecules can be treated as free internal rotors. Since the subsidiary splitting on each Q branch is not resolved, the Q branch separation is also given

figure 6.17a ν_{13} of GeH_3CCGeH_3

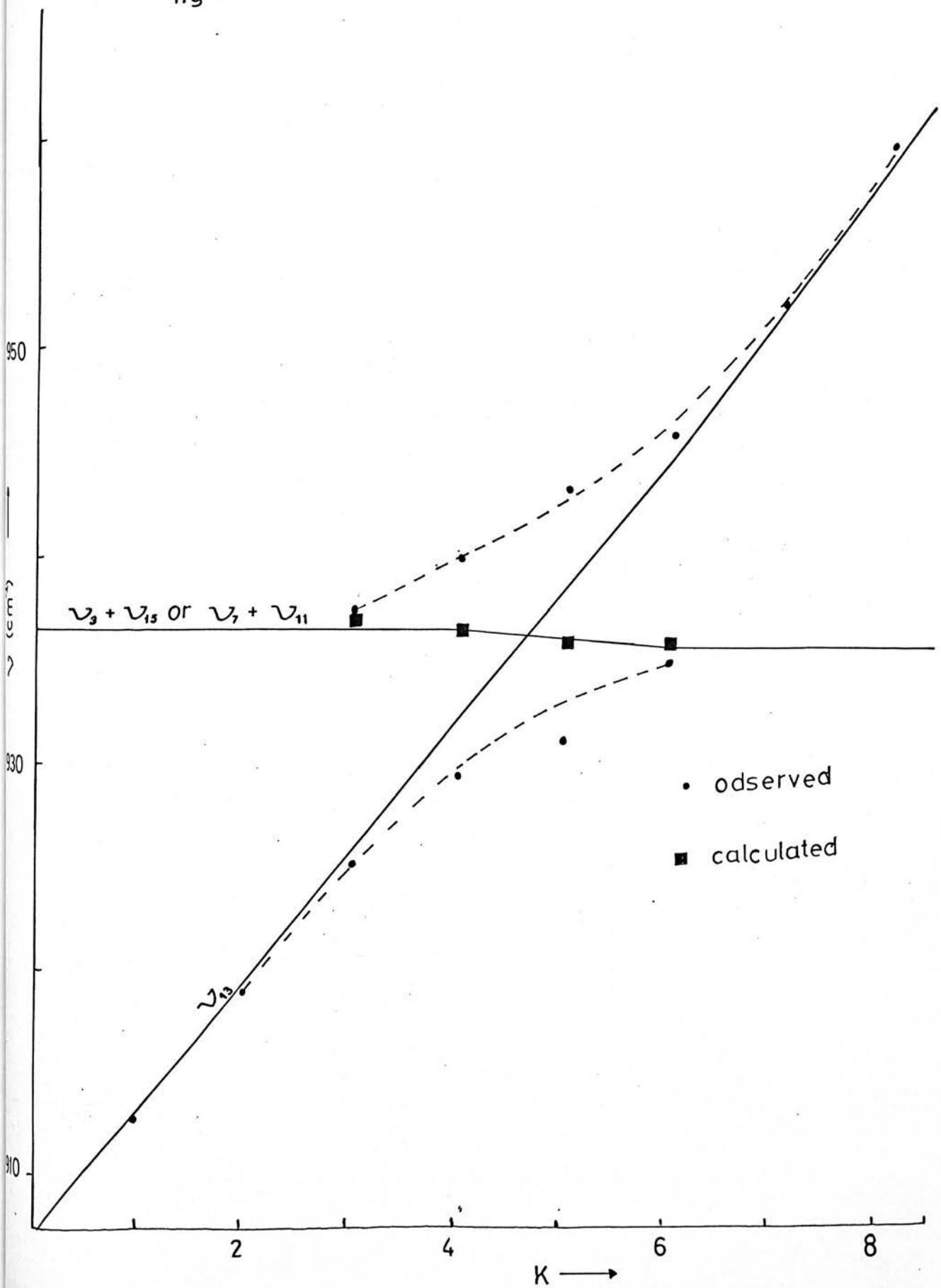

by equation V.15.

$$\nu_o^{sub} = \nu_o + [A'(1 - 2\zeta_i) - B] \pm 2[A'(1 - \zeta) - B] K$$

$$+ [(A' - A'') - (B' - B'')] K^2 \pm 4 D_K K^3$$

The perpendicular bands of silyl perfluoromethyl acetylene

Q branches are observed on the three perpendicular fundamentals associated with the silyl group, ν_8, ν_{10} and ν_{11}. Microwave studies of a number of CF_3 compounds have shown that the rotational constant A for rotation about the C_3 axis has a value of A = 0.19 cm^{-1}. The Q branch splitting for a CF_3 mode would be in the order 0.15 cm^{-1}. In this molecule, each Q branch will be further split into bands 0.06 cm^{-1} apart; the net result being a broad unresolved band.

Q branches were also observed in the 4300 cm^{-1}, 1850 cm^{-1} and 3100 cm^{-1} regions. Strong fundamentals associated with the CF stretching modes were observed in the 1300 cm^{-1} region and as a result the overtone $2\nu_{11}$ was not observed.

The overtones and combinations occurring in the 4300 cm^{-1} region are

$2\nu_1$	a_1
$\nu_1 + \nu_2$	a_1
$2\nu_2$	a_1
$\nu_1 + \nu_8$	e

...cont.

$\nu_2 + \nu_8$	e
$2\nu_8$	$a_1 + e$

Reasonable values of ζ_8 and A'' were obtained only if the observed Q branches were assigned to the overtone $2\nu_8$.

The possible bands in the 1850 cm^{-1} region are

$2\nu_4$	a_1
$\nu_4 + \nu_{10}$	e
$2\nu_{10}$	$e + a_1$

The Q branches were only fitted to a 1st order polynomial because the use of a 2nd order polynomial did not improve the fit. This still enables an estimate for the zeta constant to be calculated. The zeta constant suggested that this band is $2\nu_{10}$ rather than $\nu_4 + \nu_{10}$.

Q branches observed in the 3100 cm^{-1} region appear to follow no distinct pattern, which made it impossible to analyse. The possible combinations are

$\nu_1 + \nu_4$	a_1
$\nu_2 + \nu_4$	a_1
$\nu_1 + \nu_{10}$	e
$\nu_2 + \nu_{10}$	e
$\nu_4 + \nu_8$	e
$\nu_8 + \nu_{10}$	$a_1 + e$

It is probable that more than one progression is visible leading to the indistinct pattern observed.

The Q branch frequencies of this molecule are listed in table 6.21 and the derived molecular constants in table 6.22. The spectrum of ν_8 is shown in figure 6.18 as it is a particularly striking band showing overlap of ν_8 with the PQR band of ν_2.

The ground state value of the rotation constant, A'' obtained from ν_8 and $2\nu_8$, was A'' = 2.8111 cm^{-1}. This was derived using a value of B = 0.0301 cm^{-1} obtained from electron diffraction data. The zeta constant of 0.005 is similar to that of other silyl stretches. The constants for the other bands, given in table 6.23, were derived using this value of A''.

The centre of the silyl rock, ν_{11} was not well defined, being at either 681.4 cm^{-1} or 692.6 cm^{-1}. There was no perturbation observed, affecting the Q branch frequencies of this band. The zeta constants were similar to those of other silyl rocks.

The Q branches of the silyl deformation, ν_{10}, formed more than one curve when the frequencies were plotted against K (figure 6.19). Perturbations occurred at $^{R}Q_{10}$ and $^{R}Q_{2}$. The bands between $^{P}Q_{15}$ and $^{R}Q_{o}$ were used to obtain the parameters of this mode. The frequencies did not fit a second order polynomial and as a result, the zeta constant was estimated using the ground state rotational constant, A''. The energy levels of this band are given in table 6.24 together with those of the probable perturbing bands. The energy levels of ν_4, ν_5, $2\nu_{13}$ and $\nu_{12} + \nu_{14}$ are not included because they do not intersect with those of ν_{10}.

The only band that could cause the perturbation at $^{R}Q_{10}$ (figure 6.20) is $\nu_4 + \nu_{15}$; the most perturbed band being predicted

Table 6.2I

Q Branch Frequencies of SiH_3CCCF_3

SICF---NU -8

K	Y(OBS)	Y(CALC)	Y(OBS)-Y(CALC)
18	2303.40	2302.89	.51
17	*	2298.00	*
16	2292.80	2293.07	-.27
15	2288.50	2288.10	.40
14	2282.30	2283.10	-.80
13	2277.70	2278.07	-.37
12	2273.10	2273.00	.10
11	2267.90	2267.90	.00
10	2262.60	2262.76	-.16
9	2257.80	2257.59	.21
8	2252.80	2252.38	.42
7	2247.10	2247.14	-.04
6	2242.30	2241.86	.44
5	2236.60	2236.55	.05
4	2230.80	2231.21	-.41
3	2225.80	2225.83	-.03
2	2220.40	2220.42	-.02
1	2214.80	2214.97	-.17
0	2209.20	2209.49	-.29
-1	*	2203.97	*
-2	*	2198.42	*
-3	2193.40	2192.83	.57
-4	2187.80	2187.21	.59
-5	2181.60	2181.55	.05
-6	2175.60	2175.86	-.26
-7	2169.90	2170.14	-.24
-8	2164.40	2164.38	.02
-9	2158.30	2158.58	-.28
-10	2153.00	2152.76	.24
-11	2147.00	2146.89	.11
-12	2140.80	2141.00	-.20
-13	2134.80	2135.06	-.26
-14	2129.20	2129.10	.10
-15	2122.90	2123.10	-.20
-16	*	2117.06	*
-17	2111.50	2110.99	.51
-18	2104.70	2104.89	-.19

S.D. = 0.36 cm^{-1}

CF---NU--10

K	Y(OBS)		Y(CALC)	Y(OBS)-Y(CALC)	
15	1045.55	.00	1053.32	-7.77	.00
14	1039.20	.00	1046.39	-7.19	.00
13	1032.70	.00	1039.46	-6.76	.00
12	1026.60	.00	1032.54	-5.94	.00
11	1020.40	1012.10	1025.61	-5.21	-13.51
10	1014.45	1008.45	1018.68	-4.23	-10.23
9	.00	1003.40	1011.76	.00	-8.36
8	.00	997.85	1004.83	.00	-6.98
7	.00	991.55	997.90	.00	-6.35
6	.00	985.15	990.97	.00	-5.82
5	.00	977.85	984.05	.00	-6.20
4	.00	970.40	977.12	.00	-6.72
3	.00	963.20	970.19	.00	-6.99
2	*	*	963.27	*	*
1	*	*	956.34	*	*
0	.00	949.90	949.41	.00	.49
-1	.00	941.85	942.49	.00	-.64
-2	*	*	935.56	*	*
-3	*	*	928.63	*	*
-4	*	*	921.70	*	*
-5	*	*	914.78	*	*
-6	.00	908.55	907.85	.00	.73
-7	.00	901.15	900.92	.00	.23
-8	.00	894.10	894.00	.00	.10
-9	.00	886.80	887.07	.00	-.27
-10	.00	879.80	880.14	.00	-.34
-11	.00	872.75	873.22	.00	-.47
-12	.00	865.95	866.29	.00	-.34
-13	.00	859.00	859.36	.00	-.36
-14	.00	852.20	852.43	.00	-.23
-15	.00	846.65	845.51	.00	1.14

S.D. = 0.56 cm^{-1}

SICF---NU-11

K	Y(OBS)	Y(CALC)	Y(OBS)-Y(CALC)
15	740.60	740.69	-.09
14	736.35	736.50	-.15
13	732.40	732.34	.06
12	728.15	728.22	-.07
11	724.15	724.13	.02
10	720.00	720.08	-.08
9	716.20	716.06	.14
8	712.20	712.08	.12
7	708.15	708.13	.02
6	704.40	704.21	.19
5	700.45	700.33	.12
4	697.15	696.48	.67
3	692.65	692.67	-.02
2	*	688.89	*
1	685.00	685.15	-.15
0	681.20	681.44	-.24
-1	677.75	677.76	-.01
-2	673.20	674.12	-.92
-3	670.45	670.51	-.06
-4	666.70	666.94	-.24
-5	663.20	663.41	-.21
-6	660.20	659.90	.30
-7	656.30	656.43	-.13
-8	653.30	653.00	.30
-9	650.00	649.60	.40
-10	646.50	646.23	.27
-11	642.90	642.90	-.00
-12	639.60	639.61	-.01
-13	636.40	636.35	.05
-14	633.20	633.12	.08
-15	629.60	629.93	-.32

SD = 0.30 cm^{-1}

2NU-8

K	Y(OBS)	Y(CALC)	Y(OBS)-Y(CALC)
13	4415.40	4415.46	-.06
12	4409.40	4409.63	-.23
11	4404.40	4404.1	.39
10	4399.20	4398.56	.64
9	4393.00	4393.23	-.23
8	4387.40	4387.99	-.59
7	4382.00	4382.0	-.00
6	4377.70	4377.65	.05
5	4372.40	4372.49	-.09
4	4367.20	4367.30	-.11
3	4362.10	4362.07	.03
2	4356.90	4356.78	.12
1	4351.60	4351.41	.20
0	4346.50	4345.94	.56
-1	4340.60	4340.37	.23
-2	4334.60	4334.70	-.10
-3	4328.80	4328.92	-.12
-4	4322.90	4323.02	-.12
-5	4316.60	4317.02	-.42
-6	4310.00	4310.02	-.02
-7	4304.80	4304.73	.07
-8	4298.20	4298.45	-.25
-9	4292.20	4292.11	.09
-10	4286.30	4285.72	.58
-11	4279.00	4279.30	-.30
-12	4272.70	4272.88	-.18
-13	4266.80	4266.49	.31
-14	4260.40	4260.15	.25
-15	4253.60	4253.89	-.29

S.D. = 0.32 cm^{-1}

Table 6.22 Molecular constants of SiH_3CCCF_3

Band	ν_0^{sub} (cm^{-I})	[A'(I-ζ_1)-B'] (cm^{-I})	[(A'-A'')-(B'-B'')] (cm^{-I})
ν_8	2209.5	2.750(3)	-0.0I73(7)
ν_{10}	949.4	3.46(2)	-
ν_{12}	68I.4	I.846(4)	0.0I75(8)
	692.7	I.898(4)	0.0I72(8)
$2\nu_8$	4345.I	2.757(9)	-0.05I(3)
$2\nu_{10}$	I86I.6	I.56(2)	-
	I87I.4	I.56(2)	-

Table 6.23 Rotational and Zeta Constants of SiH_3CCCF_3

Band	ν_0 (cm^{-I})	A'' (cm^{-I})	A' (cm^{-I})	ζ_i
ν_8	2206.8	2.8II(4)	2.794(4)	0.005(4)
ν_{10}	945.2	2.8II(4)	2.79(2)	-0.25(I)
ν_{12}	680.5	2.8II(5)	2.828(4)	0.337(3)
	690.0	2.8II(4)	2.828(4)	0.3I8(3)
$2\nu_8$	4342.4	2.8II(4)	2.76I(5)	-0.0I0(6)
$2\nu_{10}$	I86I.2	2.8II(4)	2.834(9)	0.42(2)
	I870.8	2.8II(4)	2.834(9)	0.40(3)

Table 6.24 Energy Levels of ν_{10}, $\nu_4 + \nu_{15}$, $\nu_5 + \nu_{15}$, $\nu_6 + \nu_{14}$, $\nu_{11} + \nu_{14}$ in SiH_3CCCF_3

J,K	ν_{10} ℓ^+	ν_{10} ℓ^-	$\nu_4 + \nu_{15}$ ℓ^+	$\nu_5 + \nu_{15}$ ℓ^-	$\nu_6 + \nu_{14}$ ℓ^+	$\nu_{11} + \nu_{14}$ ℓ^-
0	945.9		IOI3.0	962.0	94I.0	92I.0
I	950.2	947.4	IOIO.4	959.4	938.2	930.6
2	960.0	954.5	IOI3.5	962.5	952.I	945.6
3	975.4	967.2	IO22.2	97I.2	97I.6	966.6
4	996.5	985.6	IO36.5	985.5	996.7	993.I
5	IO23.2	IOO9.2	IO56.4	IOO5.4	IO27.4	IO25.I
6	IO55.5	IO39.I	IO82.0	IO3I.0	IO63.8	IO62.8
7	IO93.5	IO74.3	III3.2	IO62.2	II05.7	II06.2
8	II37.0	III5.2	II50.0	IO99.0	II53.3	II55.I
9	II86.2	II6I.2	II92.4	II4I.4	I206.5	I209.7
IO	I24I.0	I2I3.7	I240.4	II89.4	I265.4	I269.8
II	I30I.4	I27I.4	I294.I	I243.I	I329.8	I335.7
I2	I367.5	I334.7	I353.4	I302.4	I399.9	I402.4
I3	I439.2	I403.7	I4I8.3	I367.3	I475.6	I484.3
I4	I5I6.5	I478.2	I488.8	I437.8	I557.0	I566.8
I5	I599.4	I558.4	I565.0	I5I4.0	I643.9	I655.0

figure 6.18 ν_8 of SiH_3CCCF_3

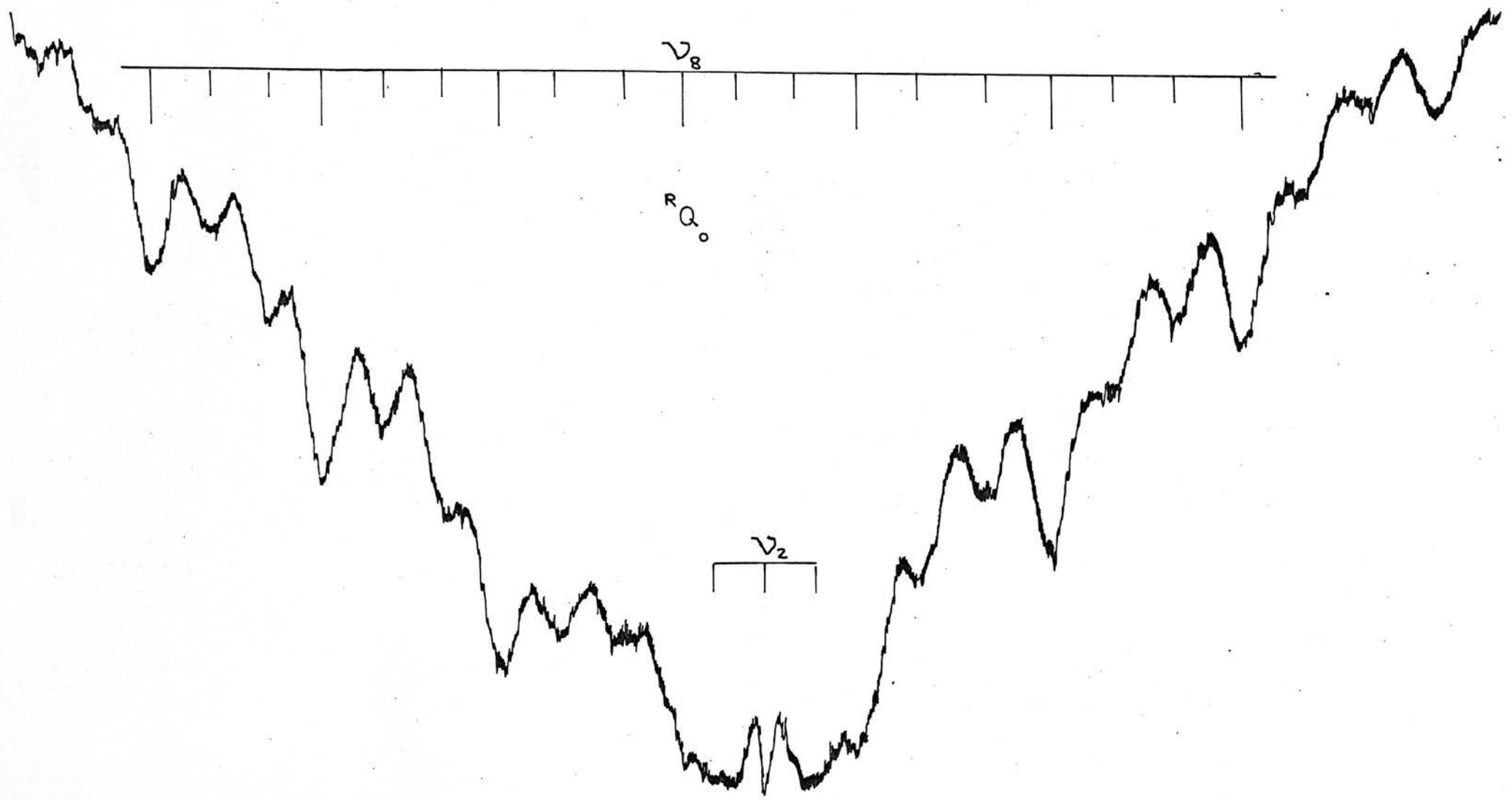

figure 6.19 ν_{10} of SiH_3CCCF_3

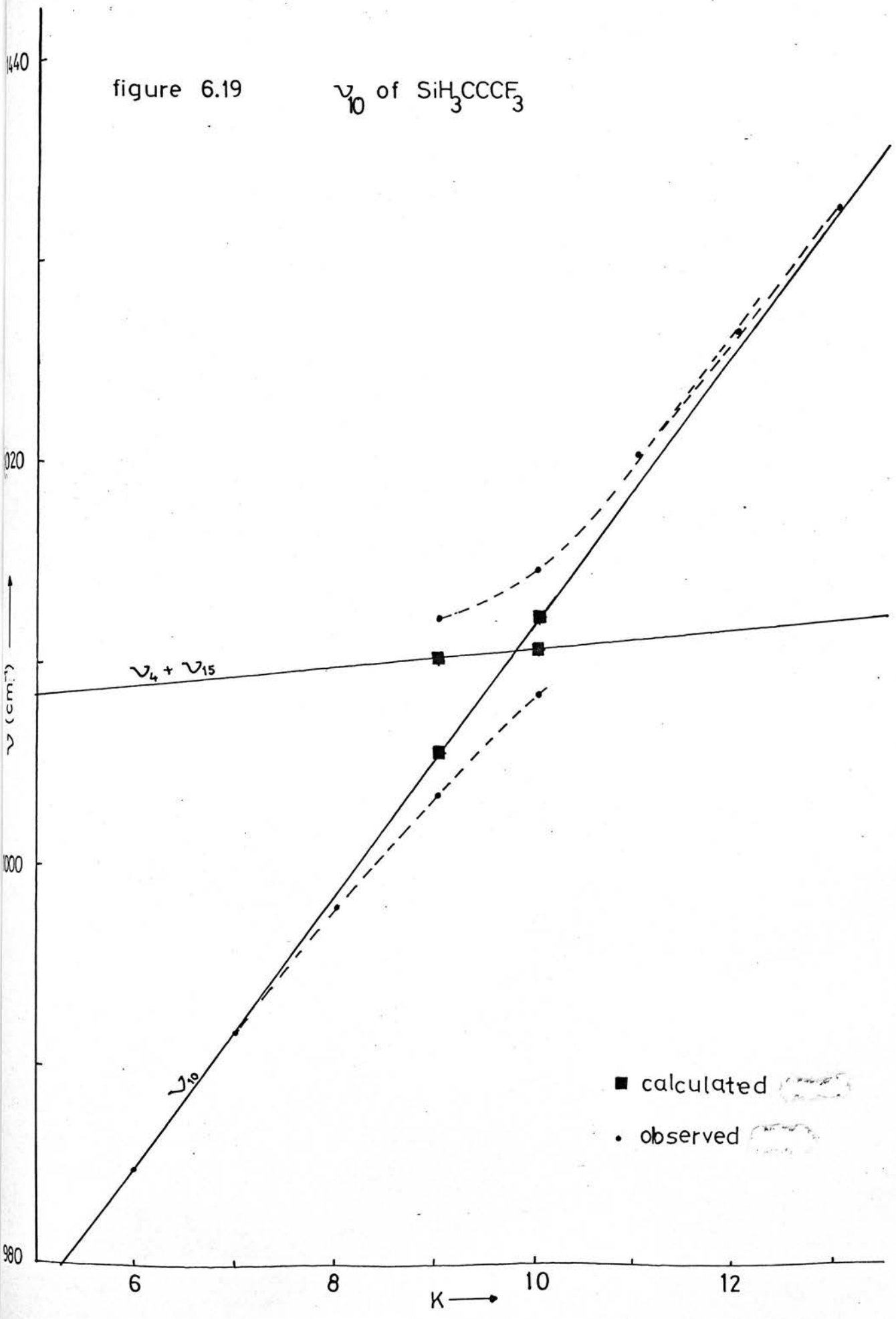

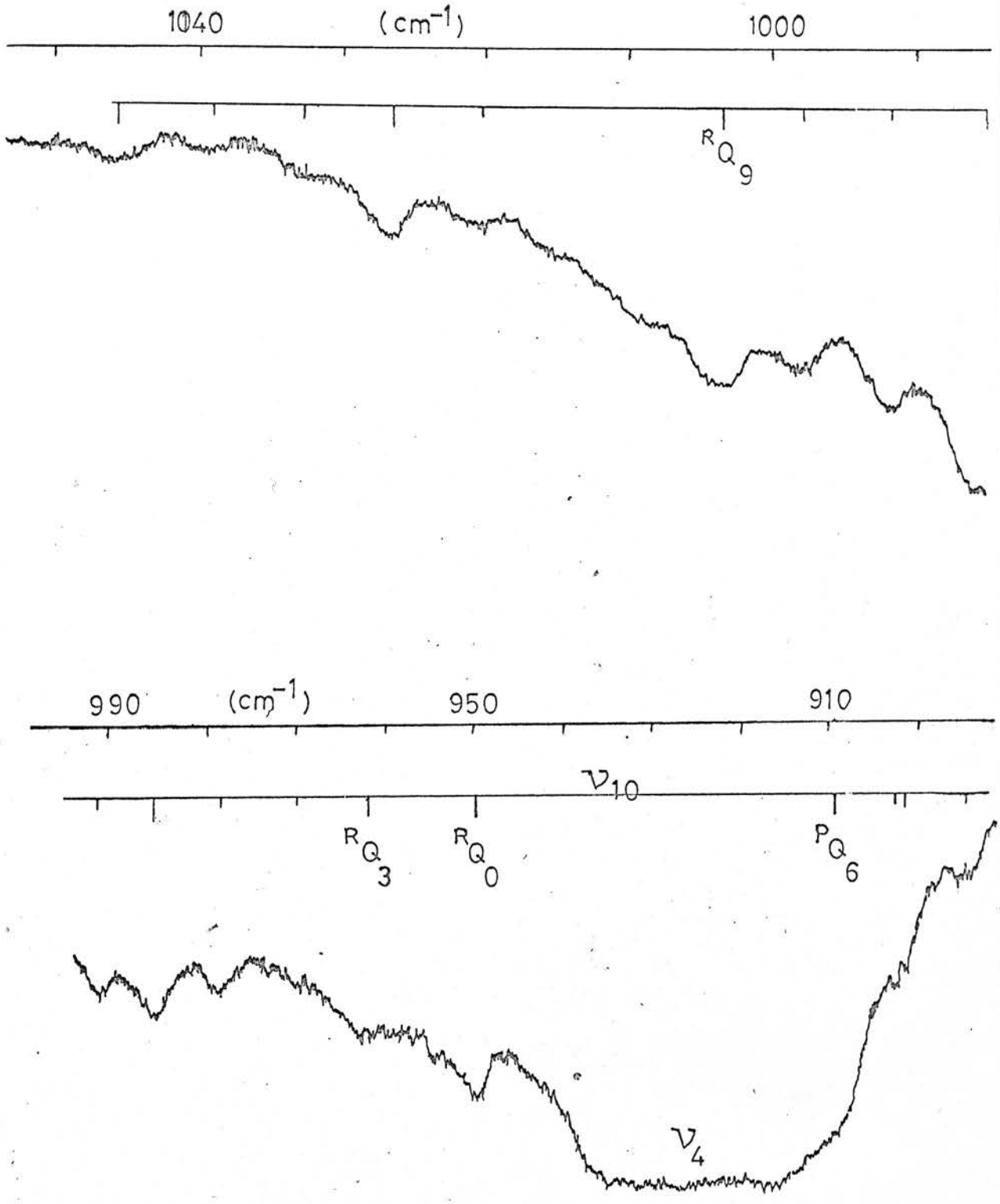

Figure 6.20 ν_{10} of SiH_3CCCF_3

as $^{R}Q_{9}$. Since two of the observed bands belong to the perturbing level, the zeta constant could be estimated. A value of 0.91 was obtained which is of the correct magnitude for $\nu_4 + \nu_{15}$.

There are four bands that could cause the perturbation at $^{R}Q_{2}$: $\nu_5 + \nu_{15}$, $\nu_6 + \nu_{14}$, $\nu_{11} + \nu_{14}$ and $\nu_7 + \nu_{12}$. The energy levels of $\nu_5 + \nu_{15}$ and $\nu_6 + \nu_{14}$ were calculated using a zeta constant of 0.9, equivalent to ζ_{15} and ζ_{14} respectively. $\nu_{11} + \nu_{14}$ has a zeta constant of $-(\zeta_{11} + \zeta_{14})$ which was taken as -1.2 and $\nu_7 + \nu_{12}$ has a zeta constant of ζ_{12}. The zeta constant for a CF_3 deformation has been found to be about -0.8[53]. This value has been used but the actual value could be quite different in this molecule, which in turn would affect the point of intersection of the energy levels. The correct position of the perturbation is predicted for $\nu_5 + \nu_{15}$ although $\nu_{11} + \nu_{14}$ is also close by at $^{R}Q_{4}$.

The perpendicular bands of germyl and deutero-germyl perfluoromethyl acetylene

The three fundamentals associated with the germyl group, ν_8, ν_{10} and ν_{11} have resolved Q branches. In addition, progressions were observed in the 4100 cm^{-1} region, corresponding to the overtone $2\nu_8$, and the 3000 cm^{-1} region. The Q branches in this latter region were not resolved satisfactorily enough for analysis of the band.

Q branches were observed on the germyl deformation, ν_{10} in deutero-germyl perfluoromethyl acetylene. The germyl stretch, ν_8 in this molecule were not resolved properly.

The Q branches of both compounds are given in table 6.25 and the derived molecular constants in table 6.26. ν_8 and $2\nu_8$ give a value of the rotational constant, A'' = 2.750 cm^{-1} and a zeta constant,

Table 6.25

Q Branch Frequencies of GeH_3CCCF_3 and GeD_3CCCF_3

GECF---NU=8

K	Y(OBS)	Y(CALC)	Y(OBS)-Y(CALC)
16	2217.00	2217.36	-.36
15	2212.10	2212.40	-.30
14	2207.40	2207.41	-.01
13	2202.40	2202.38	.02
12	2197.60	2197.31	.29
11	2192.35	2192.21	.14
10	2187.25	2187.08	.17
9	2182.20	2181.91	.29
8	2176.80	2176.71	.09
7	2171.55	2171.48	.07
6	2166.25	2166.21	.04
5	2161.00	2160.90	.10
4	2155.40	2155.56	-.16
3	2150.25	2150.19	.06
2	2144.90	2144.78	.12
1	2139.10	2139.34	-.24
0	2133.55	2133.86	-.31
-1	2128.35	2128.35	-.00
-2	2123.35	2122.81	.54
-3	2117.40	2117.23	.17
-4	2111.20	2111.62	-.42
-5	2105.95	2105.97	-.02
-6	2100.20	2100.29	-.09
-7	2094.45	2094.57	-.12
-8	2088.65	2088.82	-.17
-9	2082.80	2083.03	-.23
-10	2077.05	2077.21	-.16
-11	2071.05	2071.36	-.31
-12	2065.40	2065.47	-.07
-13	2059.50	2059.55	-.05
-14	2053.45	2053.59	-.14
-15	2047.45	2047.60	-.15
-16	2041.55	2041.57	-.02
-17	2035.50	2035.51	-.01
-18	2029.55	2029.42	.13
-19	2023.35	2023.29	.06

S.D. = 0.28 cm^{-1}

6 CF---NU-1

K	Y(OBS)		Y(CAL)	Y(OBS)-Y(CAL)	
23	988.10	.00	987.86	.24	.00
22	982.15	.00	982.02	.13	.00
21	975.99	.00	976.19	-.21	.00
20	970.05	.00	970.28	-.23	.00
19	964.15	.00	964.38	-.23	.00
18	958.45	.00	958.46	-.01	.00
17	952.40	.00	952.52	-.12	.00
16	946.65	.00	946.58	.07	.00
15	941.00	930.30	940.58	.42	-1.28
14	.00	934.05	934.58	.00	-.53
13	.00	927.65	928.55	.00	-.91
12	.00	921.55	922.51	.00	-.96
11	.00	915.70	916.44	.00	-.74
10	.00	910.00	910.36	.00	-.36
9	*	*	904.24	*	*
8	*	*	898.13	*	*
7	.00	894.15	891.98	.00	2.17
6	.00	887.55	885.81	.00	1.74
5	.00	881.50	879.62	.00	1.88
4	.00	873.35	873.41	.00	-.06
3	*	*	867.18	*	*
2	*	*	860.93	*	*
1	.00	855.85	854.66	.00	1.19
0	.00	849.20	848.37	.00	.83
-1	.00	842.30	842.06	.00	.24
-2	.00	835.25	835.73	.00	-.48
-3	*	*	829.37	*	*
-4	*	*	823.00	*	*
-5	*	*	816.60	*	*
-6	*	*	810.19	*	*
-7	.00	803.65	803.75	.00	-.10
-8	.00	797.35	797.30	.00	.05
-9	.00	790.50	790.82	.00	-.32
-10	.00	784.55	784.32	.00	.23
-11	.00	777.85	777.80	.00	.05
-12	.00	771.30	771.26	.00	.04

S.D. = 0.24 cm^{-1} (ν_o = 848)

= 0.27 cm^{-1} (ν_o = 867)

GECF---NU=11

K	Y(OBS)	Y(CALC)	Y(OBS)-Y(CALC)
17	684.90	685.16	-.26
16	681.55	681.42	.13
15	678.00	677.69	.31
14	*	673.97	*
13	670.20	670.27	-.07
12	666.85	666.61	.24
11	662.85	662.98	-.13
10	659.30	659.39	-.09
9	655.85	655.86	-.01
8	652.35	652.38	-.03
7	649.05	648.96	.09
6	645.60	645.60	-.00
5	642.10	642.31	-.21
4	639.10	639.08	.02
3	636.10	635.91	.19
2	632.90	632.82	.08
1	629.75	629.78	-.03
0	626.85	626.81	.04
-1	624.00	623.90	.10
-2	621.05	621.05	.00
-3	617.80	618.24	-.44
-4	614.95	615.49	-.54
5	*	612.78	*
6	*	610.10	*
7	*	607.45	*
-8	605.65	604.82	.83
-9	602.80	602.19	.61
-10	599.90	599.57	.33
-11	596.70	596.93	-.23
-12	593.85	594.28	-.43
-13	591.60	591.58	.02
-14	588.45	588.84	-.39
-15	585.75	586.04	-.29
-16	583.20	583.16	.04
-17	580.35	580.18	.17
-18	577.35	577.10	.25

S.D. = 0.32 cm^{-1}

GECF---2NU=8

K	Y(OBS)	Y(CALC)	Y(OBS)-Y(CALC)
9	4240.40	4240.24	.16
8	*	4235.49	*
7	4230.80	4230.69	.11
6	4225.90	4225.82	.08
5	4220.90	4220.89	.01
4	4215.60	4215.89	-.29
3	4210.50	4210.84	-.34
2	4205.80	4205.72	.08
1	*	4200.54	*
0	4195.00	4195.30	-.30
1	*	4189.99	*
2	*	4184.62	*
-3	4179.20	4179.19	.01
-4	4174.40	4173.70	.70
-5	4168.60	4168.14	.46
-6	4162.70	4162.52	.18
-7	4156.40	4156.84	-.44
-8	4151.10	4151.09	.01
-9	4145.00	4145.29	-.29
-10	4139.30	4139.42	-.12
-11	4133.40	4133.48	-.09
-12	4127.70	4127.49	.21

S.D. = 0.30 cm^{-1}

DECF-D- -NU-1

K	Y(OBS)	Y(CALC)	Y(OBS)-Y(CALC)
10	654.30	654.53	-.23
9	651.20	651.27	-.07
8	648.15	648.06	.09
7	645.00	644.88	.12
6	641.85	641.74	.11
5	639.10	638.64	.46
4	635.70	635.57	.13
3	632.25	632.54	-.29
2	629.55	629.56	-.01
1	626.20	626.60	-.40
0	623.65	623.69	-.04
- 1	620.85	620.82	.03
- 2	617.75	617.98	-.23
- 3	615.40	615.18	.22
- 4	612.55	612.42	.13

S.D. = 0.24 cm^{-1}

Table 6.26 Molecular Constants of GeH_3CCCF_3 and GeD_3CCCF_3

Band	ν_0^{sub}	$[A'(I-\zeta_i)-B']$	$[(A'-A'')-(B'-B'')]$
GeH_3CCCF_3	(cm^{-1})	(cm^{-1})	(cm^{-1})
ν_8	2133.9	2.742(2)	-0.0172(5)
ν_{10}	848.4	3.150(5)	-0.0103(9)
	867.2	3.120(3)	-0.0103(9)
ν_{12}	618.0	1.43(1)	0.026(1)
	629.6	1.506(8)	0.026(1)
$2\nu_8$	4195.3	2.637	-0.0313
GeD_3CCCF_3			
ν_{10}	623.7	1.45(1)	0.0119(4)

Table 6.27 Rotational and Zeta Constants of GeH_3CCCF_3 and GeD_3CCF_3

Band	ν_0 (cm^{-1})	A'' (cm^{-1})	A' (cm^{-1})	ζ_i
GeH_3CCCF_3				
ν_8	2131.1	2.750(3)	2.733(3)	-0.012(4)
ν_{10}	844.9	2.750(3)	2.740(4)	-0.145(3)
	863.6	2.750(3)	2.740(4)	-0.156(2)
ν_{11}	617.7	2.750(3)	2.779(4)	0.459(3)
	626.6	2.750(3)	2.780(4)	0.465(3)
$2\nu_8$	4192.7	2.750(3)	2.719(4)	0.023(6)
GeD_3CCCF_3				
ν_{10}	622.7	1.375(3)	1.394(5)	-0.048(8)

ζ_8 = -0.0116, both of which are in keeping with other germyl compounds. The rotational and zeta constants are given in table 6.27 and were derived using the value of A'' above. B was calculated using reasonable bond lengths for this molecule.

The germyl rock, ν_{11} contains a slight anomoly. The polynomial for the whole band gives a standard deviation of 0.33 cm^{-1}, while the polynomial when branches between $^{P}Q_1$ and $^{P}Q_{11}$ are left out, reduced this standard deviation to 0.20 cm^{-1}. It would appear that there is a slight Fermi perturbation in this region of the spectrum; a plot of Q branch frequencies against K would tend to confirm this view (figure 6.21). The probable interfering vibrations are ν_{12} and ν_6, of which only ν_{12} is of the correct symmetry for Fermi resonance.

The energy levels of ν_{11}, ν_{12} and ν_6 are given in table 6.28. The rotational and zeta constants determined from the polynomial coefficients were used for calculating the energy levels of ν_{11}. A'' was used to calculate the energy levels of ν_{12} and ν_6, and ζ_{12} was taken as -0.8, similar to that in other CF_3 deformations.[54]

The ℓ^- energy levels of ν_6 cross the ℓ^- levels of ν_{11} between K = 11 and 12. This would mean that the $^{P}Q_{10}$ branch is the most perturbed level. The ℓ^+ energy levels of ν_{12} and ν_{11} cross when K = 1. A slight adjustment of about 5 cm^{-1} in the origin of ν_{12} would move this point of interaction to the $^{P}Q_2$ band. If this perturbation is of the Fermi type, it must be due to ν_{12}, although a weak coriolis perturbation between ν_6 and ν_{11} cannot be excluded.

Two perturbations affect the Q branch frequencies of ν_{10}. Both appear to be Fermi interactions because the best polynomial fit to the frequencies is obtained when only the outer Q branches are

Table 6.28 Energy Levels of $\nu_{11}, \nu_6, \nu_{12}$ in GeH_3CCCF_3-

J,K	ν_{11} ℓ^+	ν_{11} ℓ^-	ν_6	ν_{12} ℓ^+	ν_{12} ℓ^-
0	626.5		660.0	6I5.0	
I	623.7	63I.8	662.8	622.7	6I2.8
2	632.5	642.8	67I.0	635.9	6I6.I
3	643.9	659.2	684.8	654.7	625.0
4	660.8	68I.2	704.I	678.9	639.3
5	683.3	708.8	728.8	708.6	659.I
6	7II.3	742.0	759.I	743.8	684.4
7	744.9	780.6	794.9	784.5	7I5.2
8	784.I	824.9	836.2	830.8	75I.6
9	828.8	874.7	882.9	882.5	793.6
I0	879.0	930.I	935.2	939.7	840.7
II	934.8	99I.0	993.0	I002.4	893.5
I2	996.2	I057.5	I056.2	I070.6	95I.8
I3	I063.I	II29.5	II52.0	II44.4	I0I5.7
I4	II35.6	I207.I	II99.3	I223.6	I085.0
I5	I2I3.7	I290.3	I279.I	I308.3	II59.8

figure 6.21 ν_{11} of GeH_3CCCF_3

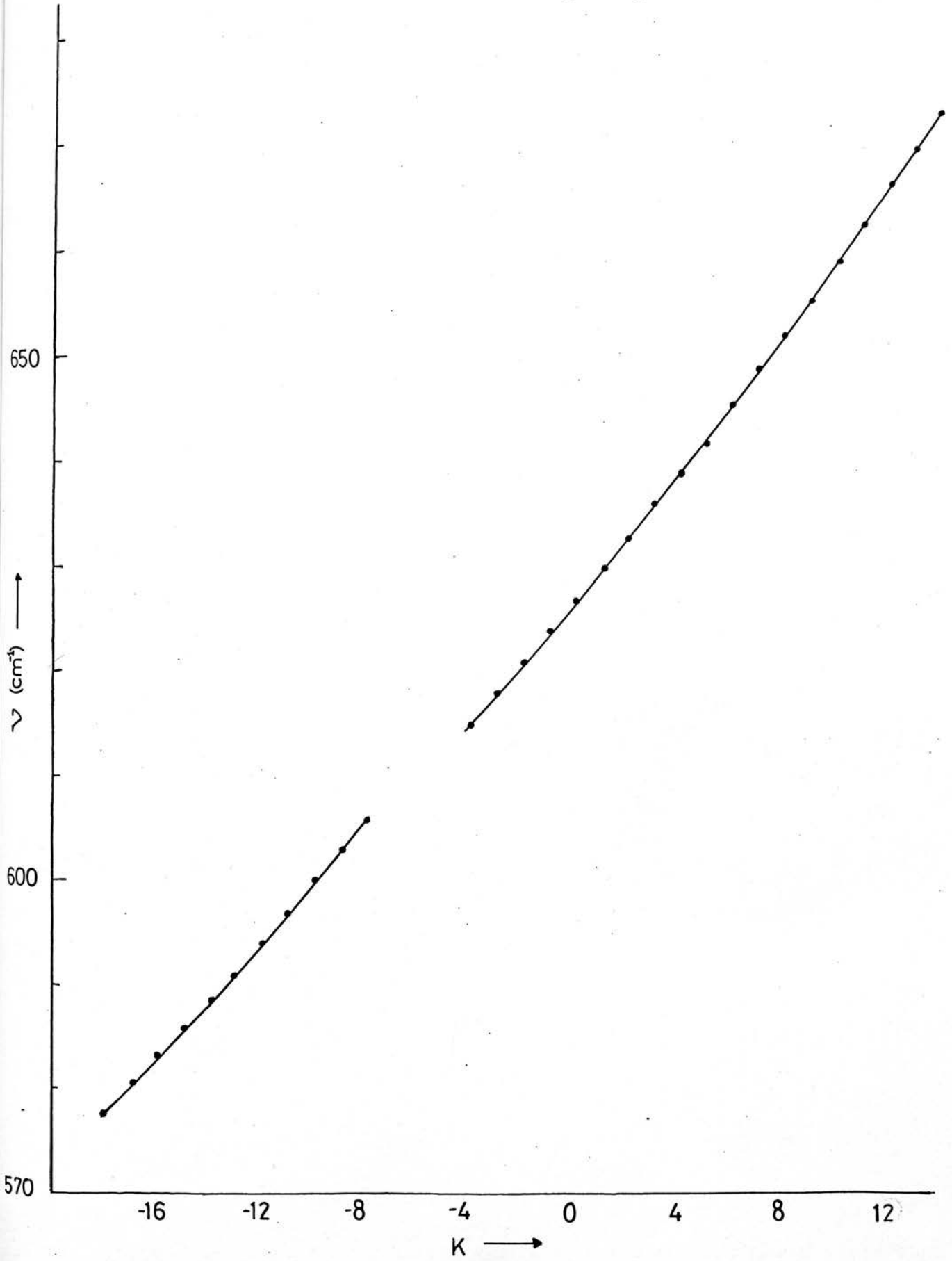

considered. The centre of ν_{10} is at 848.4 cm^{-1} or 867.2 cm^{-1}, the latter band being hidden under ν_5 at 862 cm^{-1} (figure 6.22). The zeta constants obtained for the two frequencies were -0.145 and -0.156 respectively, both of which are similar to those of other germyl deformations.

The two perturbations occur at $^{R}Q_8$ and $^{R}Q_{15}$ if the $^{R}Q_o$ branch of ν_{10} is at 848.4 cm^{-1}, or at $^{R}Q_5$ and $^{R}Q_{12}$ if at 867.2 cm^{-1}. The energy levels of four bands intersect those of ν_{10}: $\nu_6 + \nu_{14}$, $\nu_4 + \nu_{15}$, $\nu_7 + \nu_{11}$ and $\nu_{12} + \nu_{14}$. The energy levels of these bands, calculated using A'' and their expected zeta constants, together with ν_{10} are given in table 6.29.

The upper perturbation is due to either $\nu_4 + \nu_{15}$ or $\nu_3 + \nu_{11}$ depending on whether the origin of ν_{10} is at 863.6 cm^{-1} or 844.8 cm^{-1} respectively. The lower perturbation could be due to $\nu_6 + \nu_{14}$ because the ℓ^+ energy levels cross those of ν_{10} in the correct region using either band origin for ν_{10}. The ℓ^+ energy levels of $\nu_{12} + \nu_{14}$ cross those of ν_{10} at K = 6 if ν_{10} is taken as 844.8 cm^{-1}, but this is using a zeta constant of zero. The value of this constant is probably closer to -0.1 which would move the most perturbed branch towards the $^{R}Q_8$ branch.

Q branches are observed on the germyl deformation, ν_{10} in the deutero germyl perfluoromethyl acetylene. The centre of the Q branches is at 623.7 cm^{-1}, which gives a zeta constant of -0.048, assuming A'' was half that of the germyl acetylene. This is rather low in magnitude for a germyl deformation.

Table 6.29 Energy Levels In GeH_3CCCF_3

J,K	ν_{10}		ν_{10}		$\nu_6 + \nu_{14}$	$\nu_4 + \nu_{15}$	$\nu_7 + \nu_{11}$	$\nu_{12} + \nu_{14}$
	ℓ +	ℓ +	ℓ −	ℓ −	ℓ +	ℓ +	ℓ +	ℓ +
0	845		864		894	9I4	892	849
I	848	847	867	866	89I	9I2	892	852
2	857	854	876	873	895	9I5	898	860
3	872	867	89I	886	904	924	909	874
4	892	885	9II	904	9I8	939	926	893
5	9I8	9IO	937	928	938	959	949	9I8
6	949	940	968	958	964	984	977	949
7	986	950	IOO5	993	985	IOO5	IOOO	985
8	IO28	IOI5	IO47	IO33	IO32	IO52	IO49	IO26
9	IO75	IO6I	IO95	IO79	IO73	IO94	IO94	IO73
IO	II29	III3	II49	II3I	II2I	II4I	II44	II26
II	II87	II69	I207	II88	II74	II94	I200	II84
I2	I25I	I232	I27I	I250	I233	I253	I26I	I248
I3	I32I	I300	I34I	I3I8	I297	I3I7	I338	I3I6

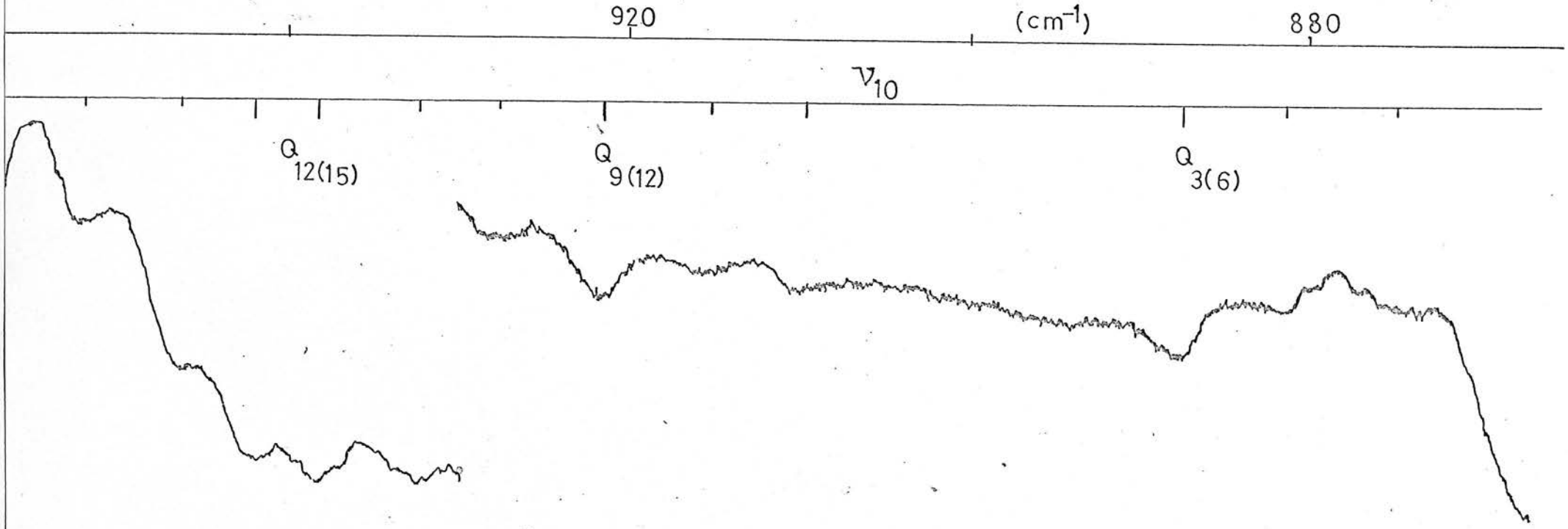

Figure 6.22 Perturbed Region of ν_{10} in GeH_3CCCF_3

6.4 Discussion

The molecular parameters of those compounds discussed in this chapter together with those of some related compounds are given in table 6.30. The distance of the H atoms from the molecular axis, D, is constant for the two series of compounds; the silyl and germyl acetylenes. MH bond lengths have not been determined with enough accuracy to determine how the HMH angle varies within the groups.

The zeta constants for the MH stretch and MH deformation in general do not differ significantly from those obtained for the silyl and germyl halides. Those of the MH_3 rocks, on the other hand, appear to be practically double those of the corresponding group IV halides. The reason for this is not clear, although it must be associated with the zeta constants of the skeletal bending modes, which are not present in the halides. The zeta constants of the bending modes are of the order of +1. Values derived from the zeta sum rule or from observation of a perturbing level are of similar magnitude. Values of these zeta constants derived from the zeta sum rule or from observation of a perturbing level are less than +1. It is likely that interaction between the group IV rock and the skeletal bending modes would mix the zeta constants for the vibrations as well, with the result that the zeta constant of the rock increases in value while that of the skeletal deformation decreases.

It would be interesting to investigate some of the perturbations studied in more detail, but this would only be worthwhile with an instrument capable of much better resolution. Similarly the individual Q branches of the free internal rotors should, at higher resolution, possess fine structure and so yield useful information concerning the interaction of the two rotating groups.

Table 6.30. Molecular Parameters of Some Silyl and Germyl Acetylenes

Compound	B(cm^{-1})	A'' (cm^{-1})	I_a ($x10^{-40}$ g/cm^2)	D(Å)[a]	$\zeta(\nu_{MH})$	$\zeta(\delta_{MH})$	$\zeta(\rho_{MH_3})$	ζ[b]
SiH_3CCH[c]	0.161	2.826	9.913	1.405	0.0024	-0.217	0.337	0.96[d]
SiH_3CCCl	0.0444	2.834	9.988	1.404	0.0051	-0.235	0.328 0.314	0.96[d]
SiH_3CCBr	0.0299	2.835	9.988	1.403	0.005	-0.26	0.32	0.98,[d] 0.96
SiH_3CCCH_3[e]	0.072[f]	2.84[g]	9.86	-	0.00	-0.21 -0.23	0.34	-
SiH_3CCSiH_3	0.0431	2.840	9.863	1.402	0.0029	-0.28	0.335 0.312	0.73
SiH_3CCCF_3	0.0301	2.811	9.963	1.407	0.0049	-0.25	0.337 0.318	0.91
SiD_3CCCl	0.0420	1.417	-	1.404	0.062	-0.272 -0.295	-	-
SiD_3CCCH_3[h]	0.058[f]	1.44	-	-	0.01	-0.12	0.48	-
GeH_3CCH[i]	0.1196[j]	2.698[j]	10.38	1.43	-0.052	-0.266	0.364	0.98[d]

...continued

Table 6.30 (Continued)

Compound	B(cm^{-1})	A'' (cm^{-1})	I_a($x10^{-40}$ g/cm^2)	D(Å)[a]	$\zeta(\nu_{MH})$	$\zeta(\delta_{MH})$	$\zeta(\rho_{MH_3})$	ζ[b]
GeH_3CCCl	0.0287	2.765	10.13	1.421	-0.0179	-0.174 -0.144	0.388	0.89[d]
GeH_3CCGeH_3	0.0767	2.769	10.12	1.420	-0.0182	-0.188 -0.169	0.405	1.06
GeH_3CCCF_3	0.0181	2.750	10.18	1.425	-0.0116	-0.156 -0.145	0.465	-
GeD_3CCH[i]	-	1.349	-	-	-	-0.248	-	-
GeD_3CCCF_3	0.0162	1.375	-	1.425	-	-0.05	-	-

a) 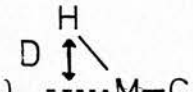

b) zeta constants of skeletal deformation.

c) reference 2.

d) from zeta sum rule.

e) reference 5.

f) assumed from 'normal' bond distances.

g) assumed.

h) reference 85.

i) reference 3.

j) from microwave studies.

One problem encountered in the analysis of the bands was that the zeta constants in combinations or overtones were assumed to be exact multiples of the fundamental values. Use of raman spectra could overcome this problem. With the advent of powerful lasers, high resolution gas phase raman spectra are readily obtained. Since the selection rules for perpendicular bands involve $\Delta K = \pm 1$ and $\Delta K = \pm 2$, A'' and zeta can be obtained for each band. Studies of overtones and combinations as well as fundamentals, would allow the variation of the zeta constant to be studied.

It would be interesting to study the remaining members of the halo-acetylenes. These could be prepared from the lithium or sodium salts, similar to that outlined in chapter 1.

APPENDIX A

Experimental

Experimental

General Experimental Methods

All volatile compounds were prepared and handled in a conventional Pyrex glass vacuum system with greased taps. When working at raised temperatures Apiezon T was used to grease the joints instead of the normal Apiezon N or L. Quantities of condensable materials were measured in calibrated volumes using a glass spiral gauge to measure pressures. Volatile compounds were purified by trap to trap distillation until they were tensiometrically homogeneous and their purity was checked by IR spectroscopy.

Low resolution IR spectra were recorded using a Perkin-Elmer 457 double beam grating spectrometer (range 4000-250 cm^{-1}) and for high resolution work a Perkin Elmer 225 double beam grating spectrometer was employed (range 4000-200 cm^{-1}). Vapour phase spectra were recorded using a 10 cm glass cell with potassium bromide or caesium iodide windows. Vibrational overtones were observed using a 3 litre, long path cell with White optics. Prolonged use of this cell inevitably caused some decomposition of the gas but this did not interfere with the observation and measurement of particular bands in the infra red spectrum.

Records of spectra recorded on the Perkin-Elmer 225 spectrometer were linear in frequency. Calibration marks were inserted on the output at regular intervals, either manually or automatically depending on the chart recorder used. Frequencies of absorption bands were measured relative to these calibrations. All random errors in this procedure were taken into account when the frequencies were fitted

to a polynomial by a least squares regression procedure.

Calibration was effected by repeating the above procedure with a series of standard compounds covering the desired frequency range. In this way a set of calibration charts was plotted to give the correction to any frequency. The calibration was checked from time to time but was found not to alter significantly. A very accurate absolute frequency cannot be claimed, however, because each spectrum was not calibrated individually; the accuracy being within 0.3 cm^{-1}. The high resolution work was extremely accurate because this relied on differences between frequencies rather than absolute frequencies.

A computer program using standard library routines of regression analysis was used to fit the observed frequencies to a polynomial. The F value, which is a measure of the significance of the fit to the polynomial, was used as a basis for deciding which order of polynomial was the most significant: increasing F value gives a better fit over the previous order of polynomial. The computer program gives an honest estimate of the standard deviation of the points about the calculated curve, and of the standard deviations in the coefficients of the polynomial. The standard deviations in the molecular parameters were calculated from the standard deviation of the polynomial coefficients, making use of well known variance formulae.

Far infra red spectra were recorded on a Beckman IR 720 Fourier transform spectrometer (range 10-450 cm^{-1}) using a medium pressure mercury lamp as a source and a golay detector. 10 cm and 1 m gas cells, using polythene windows, were employed for recording spectra. The windows were attached with Apiezon Q to prevent seepage of the sample when the cell was placed under vacuum.

Raman spectra of liquid samples were recorded on a Cary 83 raman spectrophotometer using an argon laser as source. Gas phase spectra and accurate frequency measurements were recorded on the Spex raman spectrophotometer at Glasgow University; an argon laser was employed as source. Liquid samples were sealed in capillary tubes and gas phase samples were contained in a glass cell with Brewster windows.

The Spex raman spectrophotometer printed calibration marks at regular intervals and bands were measured relative to these. Calibration of the instrument was relative to carbon tetrachloride.

Ultra violet spectra were recorded using a Unicam SP 800 spectrophotometer; 10 cm gas cells with spectrocil quartz windows were employed to record spectra.

Photoelectron spectra were recorded using a Perkin-Elmer PS16 spectrometer with He I (58.4 nm) excitation. Calibration was relative to the $^{3}P_{3/2}$ line of the argon ion.

Electron diffraction photographic intensities were recorded on the Balzer's KD.G2 gas diffraction apparatus at the University of Manchester Institute of Science and Technology. Plate distances from the nozzle were set at 1000, 500 and 250 mm. Values of the wavelength used (0.056600 $\pm$ 0.000030 Å) were obtained by direct measurement of the accelerating voltage. The data was obtained in digital format by the use of a Joyce-Loebl automatic microdensitometer. The overall procedure was calculated using benzene.

The data reduction and least-squares refinement programmes were developed from Cambridge programmes[65,66]. The latter was derived from that described by Hedberg[67]. Refinements were carried out on the

calculated molecular intensity data, the intensity expression being given by

$$I_{calc}(s) = \sum_{ij} G_{ij} \sin|s(r_{ij} - K_{ij}s^2)| \exp|-\mu_{ij}^2 s^2/2|/sr_{ij}$$

The values of G_{ij} were calculated as a function of s from the complex scattering factors of Schafer, Yates and Bonham[68]. All the amplitudes, μ_{ij}, may be refined but the interatomic distances were defined in terms of a minimum set of distances and angles so that self-consistancy was maintained. The anharmonicities, K_{ij}, were not refined but were calculated[69] from values of approximate amplitudes using the relationship $K_{ij} = a_{ij}\mu_{ij}^4/6$. The anharmonic constant was normally fixed at 2 for bonded distances and zero for nonbonded distances. In the analysis of electron diffraction data, care must be taken to ensure that correlation between adjacent data points does not give rise to unrealistic estimates of random error[70]. Allowance for correlation has been made in two ways: a) Intensity data used is interpolated at fairly wide intervals, usually 0.4, 0.2 and 0.1 s units for the 250, 500 and 1000 mm intensity data sets respectively, b) An off-diagonal weight matrix was used. For a camera height k, where data extends from s_{min} to s_{max}, two points s_1 and s_2 were chosen by inspection. The elements of the weight matrix are then given by:-

$$w_{ii} = (s_i - s_{min})/(s_1 - s_{min}) \text{ for } s_{min} \leq s_i \leq s_1$$

$$w_{ii} = 1 \qquad s_1 \leq s_i \leq s_2$$

$$w_{ii} = (s_{max} - s_i)/(s_{max} - s_2) \text{ for } s_2 \leq s_i \leq s_{max}$$

$$w_{ij} = 0 \qquad i \neq j \pm 1$$

$$w_{ij} = -0.5\ (w_{ii} + w_{jj})\ (\tfrac{P}{h})_k \qquad i = j \pm 1$$

where $(\frac{P}{h})_k$ is the correlation parameter for k calculated by the method used in reference 7.

Nuclear magnetic resonance spectra were either recorded on a Varian Associates HA 100 spectrometer or a Varian Associates XL 100 spectrometer. All ppm were measured relative to tetramethyl silane (TMS) as standard. (+ppm indicates resonance to high frequency of standard).

Preparation of starting materials

Compound	Method	Reference
SiH_3Br	$PhSiCl_3 + AlH_4$ then HBr	71
SiH_3Cl	$SiH_3Br + HgCl_2$ (streaming)	72
GeH_4	$GeO_2 + BH_4^-$	73
GeH_3Br	GeH_4 + HBr then $AlBr_3$	74
GeH_3Cl	$GeH_3Br + HgCl_2$ (streaming)	-
$HCCCF_3$	$Zn/Cu + CHCl_2CCl_2CF_3$	75

All other compounds were commercially produced. Purities were checked spectroscopically.

Solvents were purified as follows:-

TMS	distilled and found adequately pure
deuterochloroform	as for TMS
ammonia	warmed to 209K with sodium wire then distilled
diethyl ether	dried over sodium wire

APPENDIX B

Appendix B.

When transitions occur between degenerate vibrational levels both upper and lower states have energies that are a function of the zeta constants of the two respective states. Normally only the upper state is degenerate. Transition between degenerate states have a parallel and perpendicular component of the oscillating dipole moment. For the parallel component, $+\ell \longleftrightarrow +\ell$ and $-\ell \leftrightarrow -\ell$ so that the sub-bands are given by

$$\nu_o^{sub} = \nu_o + (\alpha_A - \alpha_B)\, K^2 \mp 2[A'\zeta_i' - A''\zeta_i'']\, K$$

The splitting of the Q branches would be small as long as $\zeta_i' \sim \zeta_i''$ as would occur in a "hot" band of type $\nu_j + \nu_i - \nu_i$, ν_j being a non-degenerate and ν_i being a degenerate vibration. If, however, $\zeta_i' \sim \zeta_i''$ as occurs in the example when ν_j is degenerate, then the splitting can be very large.

For the perpendicular component, $-\ell \longleftrightarrow +\ell$ for $\Delta K = +1$ and $+\ell \quad -\ell$ for $\Delta K = -1$, the sub-bands are given by

$$\nu_o^{sub} = \nu_o + [A'(1 + 2\zeta_i') - B'] \pm 2[(A' - B')$$

$$+ (A'\zeta_i' - A''\zeta_i'')]\, K + [\alpha_A - \alpha_B]\, K^2$$

where the upper sign is due to the R branches. This is very similar to an ordinary perpendicular band but the spacing is

$2[A(1 + \zeta_i' - \zeta_i'') - B]$ rather than $2[A(1 - \zeta_i) - B]$.

REFERENCES

1) D.W.W. Anderson, Ph.D. Thesis, Edinburgh University, 1973.

2) E.A.V. Ebsworth, S.G. Frankiss, W.J. Jones, J. Mol. Spec. 13, 9, 1964.

3) R.W. Lovejoy, D.R. Baker, J. Chem. Phys. 46, 658, 1967.

4) R.C. Lord, D.W. Mayo, H.E. Opitz, J.S. Peake, Spectrochim. Acta 12, 147, 1958.

5) D.W. Robinson, R.B. Reeves, J. Chem. Phys. 37, 2625, 1962.

6) G.R. Hunt, M. Kent-Wilson, J. Chem. Phys. 34, 1301, 1961.

7) E. Kloster-Jensen, Tetr. 27, 33, 1971.

8) A.G. Meister, J. Chem. Phys. 16, 950, 1948.

9) E. Kloster-Jensen, E. Heilbronner, Helvetica Chim. Acta, 53, 1073, 1970.

10) E. Kloster-Jensen, E. Heilbronner, Helvetica Chim. Acta 53 331, 1970.

11) W. Ensslin, H. Bock, G. Becker, J. Amer. Chem. Soc., 96, 2757, 1974.

12) S.D. Worley, Chem. Rev., 71, 295, 1971.

13) E. Lindholm, C. Fridh, L. Asbrink, Disc. Far. Soc., 54, 127, 1973.

14) T. Koopmans, Physica, 1, 104, 1934.

15) G.E. Moore, Atomic Energy Levels, National Bureau of Standards, Washington, D.C.

16) S. Cradock, Unpublished results.

17) S. Cradock, R.A. Whiteford, J. Chem. Soc., Faraday Trans. II, 68, 281, 1972.

18) S. Cradock, J. Chem. Phys., 55, 980, 1971.

19) E. Hielbronner, V. Hornung, E. Kloster-Jensen, J.P. Mailer, J. Amer. Chem. Soc., 96, 4252, 1974.

20) R. Thompson, P.A. Warsop, Trans. Far. Soc., 65, 2806, 1969.

21) R. Thompson, P.A. Warsop, Trans. Far. Soc., 66, 1871, 1970.

22) C.F. Thomas, E.J. Sherrard, J. Sheriden, Trans. Far. Soc., 51, 619, 1955.

23) W. Airey, C. Glidewell, A.G. Robiette, G.M. Sheldrick, J. Mol. Struct., 8, 435, 1971.

24) R. Varma, K.S. Buckton, J. Chem. Phys., 46, 1565, 1967.

25) E.C. Thomas, V.W. Laurie, J. Chem. Phys., 44, 2602, 1966.

26) S.J. Cyvin, 'Amplitudes of Vibration', Elsevier, Holland, 1968.

27) V. Daverajan, S.J. Cyvin, Aust. J. Chem. 25, 1387, 1972.

28) W. Zeil, J. Haase, N. Dakkouri, Disc. Far. Soc., 47, 149, 1969.

29) B. Beagley, J.J. Monaghan, T.G. Hewitt, J. Mol. Struct., 8, 401, 1971.

30) A.G. Robiette, Specialist Periodic Report; Molecular Structure by Diffraction Methods, Vol. 1, Ch. 4, pp. 160-197.

31) D.P. Brown, Ph.D. Thesis, U.M.I.S.T., 1971.

32) K.I. Karakida, K. Kuchitsu, Inorg. Chem. Acta 13, 113, 1975.

33) D.H. Christensen, T. Stroyer-Hansen, P. K. Laboe, E. Kloster-Jensen, E.E. Tucker, Spectro. Chim. Acta., 28A, 939, 1972.

34) A.G. Meister, J. Chem. Phys., 16, 950, 1948.

35) W.R. Angus, C.R. Bailey, J.B. Hale, C.K. Ingold, A.H. Leckie, C.G. Raisin, J.W. Thompson, C.L. Wilson, J. Chem. Soc., 971, 1936.

36) J.K. Brown, N. Sheppard, Spectro. Chim. Acta., 23A, 129, 1967.

37) S.L. Gerhart, D.M. Dennison, Phys. Rev., 43, 197, 1933.

38) G.R. Hunt, M.K. Wilson, J. Chem. Phys., 34, 1301, 1961.

39) H.C. Longuet-Higgins, Mol. Phys., 6, 445, 1963.

40) E.C. Tuazon, W.G. Fatily, J. Chem. Phys., 53, 3178, 1970.

41) R.J.H. Clark, O.H. Ellestad, Mol. Phys., 30, 1899, 1975.

42) B. Wojtkowiah, R. Queigne, Comptes Rendus, B262, 486, 1966.

43) H.O. Pritchard, H.A. Skinner, Chem. Rev. 55, 745, 1955.

66) B. Beagley, A.G. Robiette, G.M. Sheldrick, J. Chem. Soc. (A), 3002, 1968.

67) K. Hedberg, M.I. Wasaki, Acta. Cryst., 17, 529, 1964.

68) L. Schafer, A.C. Yates, R.A. Bonham, J. Chem. Phys., 55, 3055, 1971.

69) K. Kuctutsu, L.S. Bartell, J. Chem. Phys., 35, 1945, 1961.

70) Y. Murato, Y. Morino, Acta. Cryst., 20, 605, 1965.

71) G. Fritz, D. Kummer, Z. Anorg. Chem., 308, 105, 1961.

72) G.M. Sheldrick, Ph.D. Thesis, Cambridge, 1966.

73) W.L. Jolly, J. Amer. Chem. Soc., 83, 335, 1961.

74) L.M. Dennis, P.R. Judy, J. Amer. Chem. Soc., 51, 2321, 1929.

75) D.W.W. Anderson, Ph.D. Thesis, Edinburgh University, 1973.

76) L.J. Nugent, D.E. Mann, D.R. Lide, J. Chem. Phys., 36, 965, 1962.

77) J.N. Shoolery, J. Chem. Phys., 19, 1364, 1951.

78) A. Almenningen, O. Bastiansen, T. Munthe-Kaas, Acta. Chem. Scand., 10, 261, 1956.

79) J.K. Tyler, J. Sheridan, Trans. Far. Soc., 59, 2661, 1963.

80) C.C. Costain, J. Chem. Phys., 23, 2037, 1955.

81) J. Haase, W. Steingross, W. Zeil, Z. Naturforsch, A22, 195.

82) A. Bjoerseth, K.M. Marstokk, J. Mol. Struct., 13, 191, 1972.

83) M. Tanimota, K. Kuchitsu, Y. Morino, Bull. Chem. Soc., Japan, 42, 2519, 1969.

84) A. Bjorseth, E. Kloser-Jensen, K.M. Marstokk, H. Mollendal, J. Mol. Struct., 6, 181, 1970.

85) D.W. Robinson, R.B. Reeves, J. Chem. Phys., 41, 1699, 1964.

44) J.K. Brown, N. Sheppard, Spectro. Chim. Acta., 23A, 129, 1967.

45) D.R.J. Boyd, H.W. Thompson, Trans. Far. Soc., 48, 493, 1952.

46) M. Born, R. Oppenheimer, Ann. Physik, 84, 457, 1927.

47) D.R.J. Boyd, H.C. Longuet-Higgins, Proc. Roy. Soc., A213, 55, 1952.

48) E. Teller, Hand-Und. Jahrb. d. Chem. Phys. 9II, 43, 1934.

49) M. Johnston, D.M. Dennison, Phys. Revs., 48, 868, 1935.

50) G. Hertzberg, "The Infra-red and Raman Spectra of Polyatomic Molecules", Van Nostrad, New York, 1945, p. 405.

51) H.E. Allen, P.L. Cross, "Molecular Vibration-Rotations", Wiley, New York, 1963, p. 55.

52) C.C. Costain, J. Chem. Phys., 29, 864, 1958.

53) E.A.V. Ebsworth, S.G. Frankiss, W.J. Jones, J. Mol. Spectr., 13, 9, 1964.

54) M. Johnston, D.M. Dennison, Phys. Revs., 48, 868, 1935.

55) L.F. Thomas, E.J. Sherrard, J. Sheridan, Trans. Far. Soc., 51, 623, 1955.

56) A.G. Robiette, Ph.D. Thesis, Cambridge University, 1961.

57) A.R. Mochel, A. Bjorseth, C.O. Britt, J.E. Boggs, J. Mol. Spectra., 48, 107, 1973.

58) A. Almenningen, I. Hargittai, E. Kloser-Jensen, R. Stocevik, Acta. Chem. Scand., 24, 3463, 1970.

59) H. Jones, W.L. Owen, J. Sheridan, Nature, 213, 175, 1967.

60) J. Sheridan, W. Gordy, J. Chem. Phys. 20, 736, 1952.

61) K.H. Rhee, M.K. Wilson, J. Chem. Phys. 43, 333, 1965.

62) R.W. Lovejoy, D.R. Baker, J. Chem. Phys., 46, 658, 1967.

63) H.A. Jahn, Phys. Rev., 56, 680, 1939.

64) H.H. Nielson, 'Handbuck der Physika', edited by S. Flugge, (Springer-Verlog, Berlin 1959), Vol. 37, Part I, p. 173.

65) D.W.H. Rankin, A.G. Robiette, G.M. Sheldrick, W.S. Sheldrick, B.J. Aylett, I.A. Ellis, J.J. Monaghan, J. Chem. Soc. (A), 1224, 1969.